CRCLEME
Cooperative Research Centre for
Landscape Evolution & Mineral Exploration

CSIRO
EXPLORATION
AND MINING

AMIRA
Australian Mineral Industries Research Association Limited ACN 004 448 266

OPEN FILE
REPORT
SERIES

LATERITE GEOCHEMISTRY IN THE CSIRO-AGE DATABASE FOR THE WILUNA REGION

(Duketon, Kingston, Sir Samuel, Wiluna sheets)

E.C. Grunsky

CRC LEME OPEN FILE REPORT 27

December 1998

(CSIRO Division of Exploration Geoscience Report 154R, 1990.
Second impression 1998)

AMIRA
Australian Mineral Industries Research Association Limited ACN 004 448 266

CRCLEME
Cooperative Research Centre for Landscape Evolution & Mineral Exploration

CSIRO
EXPLORATION AND MINING

LATERITE GEOCHEMISTRY IN THE CSIRO-AGE DATABASE FOR THE WILUNA REGION (Duketon, Kingston, Sir Samuel, Wiluna sheets)

E.C. Grunsky

CRC LEME OPEN FILE REPORT 27

December 1998

(CSIRO Division of Exploration Geoscience Report 154R, 1990.
Second impression 1998)

CRC LEME is an unincorporated joint venture between The Australian National University, University of Canberra, Australian Geological Survey Organisation and CSIRO Exploration and Mining
Headquarters: CRC LEME c/o CSIRO Exploration and Mining, Private Bag, PO Wembley, Western Australia, 6014

RESEARCH ARISING FROM CSIRO/AMIRA REGOLITH GEOCHEMISTRY PROJECTS 1987-1993

In 1987, CSIRO commenced a series of multi-client research projects in regolith geology and geochemistry which were sponsored by companies in the Australian mining industry, through the Australian Mineral Industries Research Association Limited (AMIRA). The initial research program, "Exploration for concealed gold deposits, Yilgarn Block, Western Australia" (1987-1993) had the aim of developing improved geological, geochemical and geophysical methods for mineral exploration that would facilitate the location of blind, buried or deeply weathered gold deposits. The program included the following projects:

P240: Laterite geochemistry for detecting concealed mineral deposits (1987-1991). Leader: Dr R.E. Smith.
Its scope was development of methods for sampling and interpretation of multi-element laterite geochemistry data and application of multi-element techniques to gold and polymetallic mineral exploration in weathered terrain. The project emphasised viewing laterite geochemical dispersion patterns in their regolith-landform context at local and district scales. It was supported by 30 companies.

P241: Gold and associated elements in the regolith - dispersion processes and implications for exploration (1987-1991). Leader: Dr C.R.M. Butt.
The project investigated the distribution of ore and indicator elements in the regolith. It included studies of the mineralogical and geochemical characteristics of weathered ore deposits and wall rocks, and the chemical controls on element dispersion and concentration during regolith evolution. This was to increase the effectiveness of geochemical exploration in weathered terrain through improved understanding of weathering processes. It was supported by 26 companies.

These projects represented "an opportunity for the mineral industry to participate in a multi-disciplinary program of geoscience research aimed at developing new geological, geochemical and geophysical methods for exploration in deeply weathered Archaean terrains". This initiative recognised the unique opportunities, created by exploration and open-cut mining, to conduct detailed studies of the weathered zone, with particular emphasis on the near-surface expression of gold mineralisation. The skills of existing and specially recruited research staff from the Floreat Park and North Ryde laboratories (of the then Divisions of Minerals and Geochemistry, and Mineral Physics and Mineralogy, subsequently Exploration Geoscience and later Exploration and Mining) were integrated to form a task force with expertise in geology, mineralogy, geochemistry and geophysics. Several staff participated in more than one project. Following completion of the original projects, two continuation projects were developed.

P240A: Geochemical exploration in complex lateritic environments of the Yilgarn Craton, Western Australia (1991-1993). Leaders: Drs R.E. Smith and R.R. Anand.
The approach of viewing geochemical dispersion within a well-controlled and well-understood regolith-landform and bedrock framework at detailed and district scales continued. In this extension, focus was particularly on areas of transported cover and on more complex lateritic environments typified by the Kalgoorlie regional study. This was supported by 17 companies.

P241A: Gold and associated elements in the regolith - dispersion processes and implications for exploration. Leader: Dr. C.R.M. Butt.
The significance of gold mobilisation under present-day conditions, particularly the important relationship with pedogenic carbonate, was investigated further. In addition, attention was focussed on the recognition of primary lithologies from their weathered equivalents. This project was supported by 14 companies.

Although the confidentiality periods of the research reports have expired, the last in December 1994, they have not been made public until now. Publishing the reports through the CRC LEME Report Series is seen as an appropriate means of doing this. By making available the results of the research and the authors' interpretations, it is hoped that the reports will provide source data for future research and be useful for teaching. CRC LEME acknowledges the Australian Mineral Industries Research Association and CSIRO Division of Exploration and Mining for authorisation to publish these reports. It is intended that publication of the reports will be a substantial additional factor in transferring technology to aid the Australian Mineral Industry.

This report (CRC LEME Open File Report 27) is a Second impression (second printing) of CSIRO, Division of Exploration Geoscience Restricted Report 154R, first issued in 1990, which formed part of the CSIRO/AMIRA Project P240.

Copies of this publication can be obtained from:
The Publication Officer, c/- CRC LEME, CSIRO Exploration and Mining, PMB, Wembley, WA 6014, Australia. Information on other publications in this series may be obtained from the above or from http://leme.anu.edu.au/
Cataloguing-in-Publication:
Grunsky, E.C.
Laterite geochemistry in the CSIRO-AGE Database for the Wiluna Region (Duketon, Kingston, Sir Samuel, Wiluna sheets)
ISBN 0 642 28243 9
1. Geochemistry 2. Chemical weathering 3. Weathering - Western Australia.
I. Title
CRC LEME Open File Report 27.
ISSN 1329-4768

PROJECT LEADER'S PREFACE

R. E. Smith, 15 December 1990

During the period 1980 to mid-1986, phases of testing the use of relatively wide-spaced sampling for laterite geochemistry in mineral exploration of the Yilgarn Block were carried out. These followed on from the CSIRO orientation studies on the Golden Grove (volcanogenic base metal sulphide) and Greenbushes (rare metal pegmatite) deposits. Sample coverage of the Yilgarn Block in these trials largely followed the strategy and tactics of the companies in the AGE joint venture with regard to ground availability, exploration potential, and the feasibility of follow up exploration. The CSIRO Laterite Geochemistry Group provided a research component for these trials, by guiding the scientific parameters including the fundamentals of sampling, data presentation, and data interpretation.

The priorities for sampling are shown in the figure below. These priorities initially were the most important factors in choosing terrain for sampling.

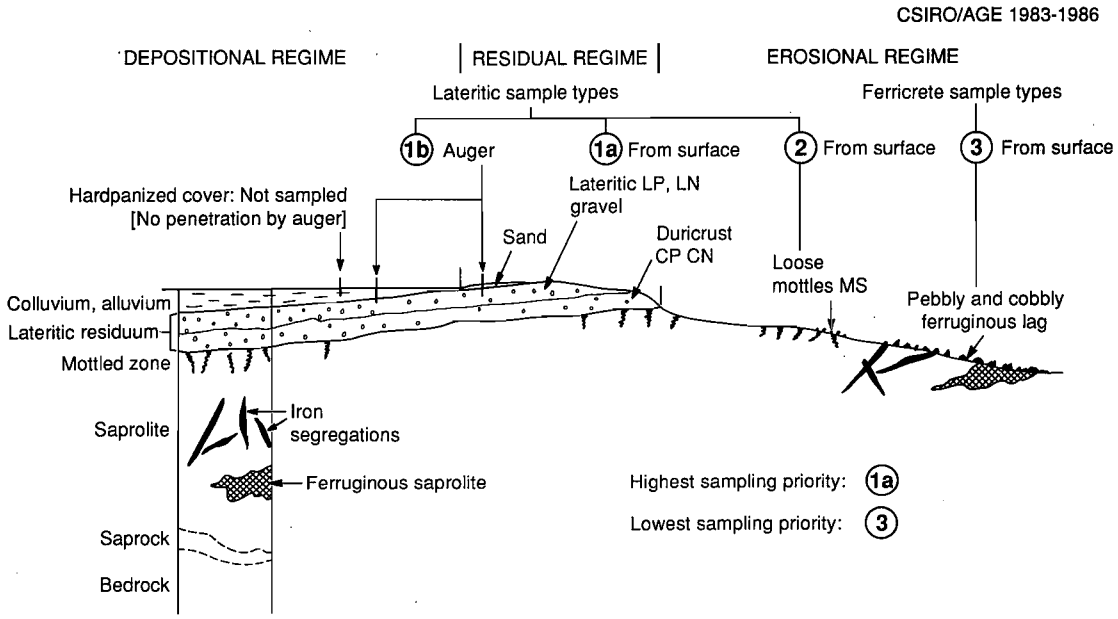

Terminology CSIRO/AGE 1983-1986 Sample type	Code	Equivalent Classification CSIRO/AMIRA 1989 Codes
Lateritic Types		
Loose Pisoliths	LP	LT102
Loose Nodules	LN	LT104
Cemented Pisoliths	CP	LT202, LT212
Cemented Nodules	CN	LT204, LT214
Vermiform Laterite	VL	LT231
Plinthite	PN	
Mottled Zone Scree	MS	LG105
Ferricrete Types		
Massive Ferricrete	MF	IS101, IS102, IS103 IS201, IS301, Some LT229
Ferricrete Fragments	FF	LG201, LG203, LG206
Cemented Pebbly Ferricrete	PF	Some LT228
Ferricrete Pellets	PE	LG201
Re-cemented Fe-rich Colluvium	RC	
Miscellaneous Types		
Ooliths Loose	OL	
Lateritized Rock	LR	
Gossan	GS	
Calareous Nodules	CC	
Other	OT	

It should be noted that in the AGE reconnaissance stage, it was not generally feasible to sample through areas of hardpanized colluvium to reach buried laterite profiles. Hand augering was not successful in such areas, nor was drilling using a light trailer-mounted auger rig where access allowed. Thus there are large gaps within the AGE sampling that can now be effectively explored using to advantage the findings of the current Laterite Geochemistry Project.

Besides generating numerous geochemical anomalies, the testing of which will continue for years to come, the CSIRO/AGE database provides knowledge of backgrounds, regional variation. and element levels in laterite tied, where feasible, to gross bedrock type. Such information thus complements that arising from the Laterite Geochemistry Project's orientation areas and is of relevance both to research and exploration.

TABLE OF CONTENTS

Page

Page

Diskette

5.25" Diskette (in back pocket)

Diskette: WILUNA.SDF Wiluna-Kingston-Duketon-Sir Samuel Geochemical Data

ABSTRACT

A multi-element geochemical study has been carried out on laterite and ferricrete samples that cover parts fo the greenstone belts and portions of the granitoid/gneiss terrain of the DUKETON, KINGSTON, SIR SAMUEL, and WILUNA 1:250 000 map sheets. The report presents a summay of the data and a provisional interpretation of selected parts of the data. The data used in this study are contained in the accompanying diskette (in the back pocket).

The sampling arose as part of a combined research programme between CSIRO and an experimental exploration programme (the AGE Joint Venture Programme) during the period 1983 to 1986. The database which was used for the study is composed of predominantly supracrustal metavolcanic and metasedimentary rocks over four supracrustal sequences; the Duketon, Dingo Range, Lake Violet-Milrose-Yandal, and Wiluna-Mt. Keith-Perseverance-Agnew greenstone belts.

Laterite and ferricrete are both abundant materials in this area. The laterites are predominantly composed of loose nodules and mottled zone scree and number 272 samples. The ferricrete materials are mostly massive and fragments of ferricrete, numbering 174 samples. Fifty samples of lateritized rock are also included in the database but were not included in the interpretation.

A total of 496 samples were analyzed for 30 elements. Summary statistics, histograms, and maps of the percentile classes are presented for selected elements in laterites. Several numerically-based procedures were applied for the purposes of outlining regional trends and detecting areas of relatively-high abundances of selected elements (anomalies). Numerical techniques included the use of principal components analysis, ranking of individual elements, ranking of CHI-6*X, PEG-4, and NUMCHI indices, and multivariate ranking of selected chalcophile elements (X^2 plots).

The resulting ranked scores of these techniques have been plotted on maps and scatter plots. The most anomalous samples tend to occur as outliers when these methods are applied. The results of these applications confirm the presence of some broad regional geochemical trends which are related to bedrock lithologies and possible regional alteration processes.

The dominant geochemical features are:

- Several multi-element associations with Au have been noted in the Rose Hills, Milrose, and several localities in the Duketon greenstone belt.

- Several Au anomalies occur in the Rose Hills, Milrose, southeast corner of the WILUNA sheet, and in the southern part of the Duketon greenstone belt on the DUKETON sheet.

- Several individual elements (Bi, Mo, Sn, W, Ag, Nb, Se) indicate that the Rose Hills, Milrose, and Biddy Well areas are the most favourable areas for exploration on the WILUNA sheet and the Quongdong Well, Urarey Well, Christmas Well (Erlistoun), and Swanson Hill areas are the most favourable on the DUKETON sheet.

- Regional, geochemical features that are characteristic of the greenstone belts are defined by higher relative abundances of Cr, Mn, V, Zn, Ni, Co, and Fe_2O_3. Geochemical features, characteristic of the marginal granitoid/gneiss terrain, are defined by higher relative abundances of Nb, Ga, Mo, and Pb.

The data and results presented in this report may provide sufficient information for a selective and cost efficient exploration programme.

1.0 INTRODUCTION

The report summarizes the results of the progress of an on-going project to assess the geochemistry of laterites and associated ferruginous materials for the purposes of developing and improving exploration concepts, sampling strategies, and isolation of potentially-mineralized areas. The report presents the results of reconnaissance-scale laterite geochemistry on the WILUNA, KINGSTON, DUKETON, and SIR SAMUEL 1:250,000 map sheets. The sampling was carried out in the 1983-1986 period as part of an application feasibility test of laterite geochemistry for mineral exploration. This work was collaborated between the AGE Joint Venture (Greenbushes Ltd., St. Joe Minerals, and later Sons of Gwalia, NL) and the Multi-element Geochemistry Group, CSIRO.

This report is produced in a format similar to that of the previous Exploration Geoscience Reports 2R, Southern Murchison region; 68R, Northern Murchison region, and 121R, Central Yilgarn region; (Grunsky *et al.*, 1988, 1989; Grunsky, 1990).

Regional geochemical databases have been developed for a variety of uses in several countries. One of their ultimate aims has been to define geochemical provinces in which the bedrock sequences contain anomalous populations of specific elements that can be related to zones of mineralization.

The results of this report are part of a reconnaissance-scale survey that resulted in a geochemical database. The database contains samples that cover wide areas of the Yilgarn Block of Western Australia, and forms part of the foundations for on-going research into the use of laterite geochemistry in mineral exploration. The project has focused on the sampling and analysis of the laterite cover and other residual materials that are extensively, but variably, developed throughout the Yilgarn Block. Sampling within this area covers some migmatitic and granitoid terrain. The strategy was to provide multi-element information within felsic and gneissic terrains. This information provides a set of reference groups with which unknown samples may be compared.

1.1 Concept and scope

The research objectives of establishing a regional geochemical database were:

- to provide knowledge of regional variations in laterite geochemistry which may be due to regional changes in climate or landform characteristics;
- to establish the types of variation in laterite composition encountered in areas away from orientation studies about specific ore deposits;
- to relate laterite composition to both regional and local geological variation;
- to test and further develop the most efficient sampling strategies that will allow cost-effective exploration.

Further discussions on the philosophy and strategy of developing a multi-element geochemical database for the Yilgarn block have been discussed by Smith (1987).

1.2 Background to the study

Primary and secondary haloes can develop, persist, or be greatly enhanced in size through the development of laterite profiles as documented by Smith *et al.* (1979) who found kilometre-scale chalcophile element haloes in the pisolitic laterite cover associated with the Golden Grove Cu-Zn orebodies. These haloes can occur locally, as well as occurring in a consistent and contiguous manner within greenstone areas. Smith *et al.* (1989) have outlined a number of "chalcophile corridors" within the Yilgarn block and propose that these areas have significantly-higher economic potential.

These observations, together with those of Mazzucchelli and James (1966) and Zeegers *et al.* (1981), provided the rationale for sampling various laterite materials and analyzing a suite of chalcophile and associated elements as well as additional indicator elements. By concisely defining the geochemical characteristics of the various laterite materials, it is expected that better control can be established on classifying the characteristics of unknown suites of samples with the ability to recognize geochemical anomalies that may be associated with mineralization.

The geological map of the area is shown in Figure 1. Some of the more significant localities are shown on the map for reference purposes with the subsequent maps of this report.

The area forms part of the Archaean Yilgarn Block which is composed of synformal arcuate sequences of metamorphosed supracrustal volcanic and sedimentary assemblages intruded by felsic plutons. Most of the area is dominated by large expanses of gneissic terrain which represent assimilated plutonic and supracrustal rocks.

The region was sampled using a 3-km triangular grid with selected follow-up sampling at a spacing of 1 km and 300 m. A variety of laterite materials was sampled and classified as to the type of sample. Most samples belong to one of two groups consisting of either laterite or ferricrete materials. The most common forms of the laterites are nodular or pisolitic. The ferricrete material is typically Fe-rich, rubbly, or pebbly lag from partly truncated profiles. The sampling media are discussed below.

2.0 CLIMATE AND PHYSIOGRAPHY

The climate of the area is semi-arid with hot summers and cool winters. Temperatures range from 22°C - 36°C in January with frequent highs of >40°C to 6°C - 18°C in July. Rainfall is variable but averages 215 mm per year with most rain falling in the cooler months of April-September although cyclonic systems can cause heavy falls in the summer months.

The area shows only slight topographic variation (430 - 650 m), with the exception of the resistant bedrock that forms prominent hills. In the WILUNA sheet, the prominant BIF is a major drainage divide. Granitoid outcrops are commonly bounded by breakaways where the lateritic profile is being actively eroded. Elongate sheets of valley calcrete outline fossil trunk valleys that represent a paleodrainage system on an older plateau surface (Elias and Bunting, 1982). Bunting (1980) subdivided the physiography of the Kingston area into degradational areas, intermediate areas, and aggradational areas. Degradational areas include regions of high relief (hills, breakaways). Intermediate areas are composed of sheet-wash plains, valley floors, and eolian sand plains. Aggradational areas are composed of the infillings of trunk drainages (salt lakes) in the Cretaceous-Tertiary paleodrainage system.

Erosion of the greenstone belts has resulted in elongate hills with laterite capping near the tops. Their height is dependent upon the nature of the underlying bedrock. Banded iron formation (BIF) resists weathering and often underlies the larger hills.

3.0 GEOLOGICAL SETTING AND MINERALIZATION

3.1 Regional Geology

Much of the discussion on the regional geology and mineralization has been synthesized from reports of the Geological Survey of Western Australia by Elias and Bunting (1982), Bunting (1980), Bunting and Chin (1979), and Bunting and Williams (1979). The more recent Memoir 3 of the Geological Survey of Western Australia (1990) provides a regional perspective of these areas within the Eastern Goldfields Province. Griffin (1990) discusses the regional geology of the Eastern Goldfields Province which includes the Wiluna area. Most of the area is Archean in age; however, Proterozoic rocks cover most of the KINGSTON sheet in the northeast, and a small portion of the western part of the WILUNA sheet. The Proterozoic rocks will not be discussed in this report.

The area is underlain by early supracrustal rocks, "greenstones", and surrounding felsic intrusive stocks and batholiths with enclaves of gneissic material of Archaean age. The supracrustal areas are comprised of predominantly mafic volcanics overlain by later felsic volcanic and sedimentary sequences that have been deformed, metamorphosed, and intruded by later post-kinematic plutons. Late stage faulting has occurred throughout the preserved greenstone belts. Many Au deposits have a proximity to these large scale fault systems. The felsic plutonic rocks are chiefly composed of orthoclase-bearing tonalite that has been commonly referred to as adamellite. The IUGS subcommission on the Systematics of Igneous Rocks recommends that this term be avoided and the term "monzogranite" be substituted (LeMaitre, 1989:40)

Four arcuate greenstone belts occur within the area, surrounded by monzogranite-tonalite and gneiss terrain. The most easterly greenstone belt, the *Duketon belt*, occurs in the DUKETON-KINGSTON sheets and trends north-westerly to north-easterly. North and west of the Duketon belt is the *Mt. Eureka-Dingo Range belt* located at the junction of the WILUNA, KINGSTON, DUKETON, and SIR SAMUEL sheets. West of the Mt. Eureka-Dingo Range belt is the *Lake Violet-Milrose-Yandal greenstone belt* within the WILUNA and SIR SAMUEL sheets. The furthest westward greenstone belt of the area is the *Wiluna-Mt. Keith-Perseverance-Agnew greenstone belt* which occurs in the western parts of the WILUNA and SIR SAMUEL sheets.

Duketon Greenstone Belt

Two volcanic cycles have been recognized within this greenstone belt. Bunting and Chin (1979) describe the succession as comprising two mafic and two felsic volcanic-clastic sequences.

The lower mafic sequence is composed of amphibolite with high-magnesium basalt near the base and BIF towards the top. The overlying sequence is predominantly clastic and comprised of fine-grained metasediments with interbedded chert.

The upper mafic sequence consists of metabasalt at the eastern side of the Erlistoun syncline and metadolerite on the western side of the syncline. The youngest rocks are the felsic volcanics situated in the core of the syncline.

Serpentinized extrusive and intrusive ultramafic rocks are common to both sequences. The mafic extrusive rocks are typically metamorphosed, fine-grained, and featureless. With increasing metamorphic grade, a well-defined foliation develops. Mineral assemblages that typify the mafic volcanics are hornblende-plagioclase-quartz, clinopyroxene-quartz-epdidote-carbonate-feldspar, epidote-feldspar-actinolite-prehnite. Mafic intrusive rocks are generally concordant bodies within the volcanic stratigraphy. Felsic volcanic rocks are composed chiefly of felsic lavas, porphyry, and pyroclastics.

The clastic sediments are contained within two distinct zones; 1) North Pinnacle-Bandy Hill-Hootanui, and 2) Russell Hill-German Well. The sediments are composed of black shales, fine-grained tuffaceous sediments, conglomerate, and greywacke.

Granitoid rocks range from granite to granodiorite in composition. Granitic rocks with well-developed gneissic structures occur marginally to the greenstone belt.

Laterite and ferricrete sampling was carried out primarily in the DUKETON sheet with only a few samples collected within the KINGSTON sheet.

Mt. Eureka-Dingo Range Belt

The Mt. Eureka-Dingo Range Belt is predominantly a mafic volcanic sequence. The dominant mafic rock type is high-magnesium basalt with interbedded BIF, chert, shale, felsic volcanics, and ultramafic intrusive rocks (Griffin, 1990; Bunting and Williams, 1979; Elias and Bunting, 1982; Bunting and Chin, 1979). Poorly-exposed tuffs and shales occur at the top of the sequence. The succession has been interpreted to be folded into a broad anticlinal structure (Bunting and Williams, 1979).

Laterite and ferricrete sampling was carried out only in the southeast part of the WILUNA sheet.

Lake Violet-Milrose-Yandal Belt

This greenstone belt is generally, poorly exposed. In the northern part of the belt, in the WILUNA sheet, the sequence is a sedimentary-felsic volcanic succession composed of BIF, volcaniclastics, felsic tuffaceous rocks, shales, and argillites (Elias and Bunting, 1982). The eastern part of the sequence, bounded by the Celia Lineament, is poorly exposed, but has been interpreted to be comprised of ultramafic rocks, schistose metasediments/felsic volcanics, and amphibolitized mafic metavolcanics. The central part of the belt is composed of a sequence of mafic volcanic flows that have been metamorphosed to amphibolite facies.

The southern extension of the supracrustal sequence is known as the Yandal belt and is comprised of a thick mafic sequence overlain by the Spring Well felsic volcanic complex (Bunting and Williams, 1979). The

rocks are dacite to rhyodacite in composition. The fragmental rocks are interpreted to be ignimbritic with associated coarse tuff breccias.

Laterite and ferricrete sampling have been carried out in the WILUNA sheet. The extension of the belt (Yandal) into the SIR SAMUEL sheet has not been sampled.

Wiluna-Mt. Keith-Perseverance-Agnew Greenstone Belt

The belt is comprised of two sequences of supracrustal rocks separated by the Perseverance Fault that extends along the length of the belt.

East of the Perseverance Fault, the sequence is comprised of a lower sequence of ultramafic and mafic volcanic rocks overlain by felsic volcanics and sedimentary rocks (Elias and Bunting, 1982). These rocks are of relatively low metamorphic grade (prehnite-pumpellyite to greenschist) and lack a strong penetrative fabric. The Mount Keith ultramafic intrusive occurs in the felsic volcanic-sedimentary assemblage. The mafic volcanics are predominantly komatiitic basalt with intercalated felsic volcanics. Tholeiitic volcanics overly the ultramafic sequence. The felsic volcanic rocks are tuffaceous grading from fine-grained granular textured tuff to coarse-grained tuff breccias. The sequence grades northwesterly into felsic wackes and volcaniclastic sediments. The Mount Keith ultramafic intrusive is comprised of an elongate, narrow intrusion extending for about 200 km along the Agnew-Wiluna supracrustal belt. It is a significant host for nickel sulphide ore bodies.

To the south, in the SIR SAMUEL sheet area, the sequence is comprised of a lower mafic/ultramafic sequence overlain by feldspathic sediments and conglomerate grading upwards into fine-grained pelitic rocks (Bunting and Williams, 1979). This lower sequence is in turn overlain by pillowed mafic volcanics. Anastomosing faults in the Kathleen Valley and Mt. Roberts areas obscure the relationships of the supracrustal rocks.

West of the Perseverance Fault, the supracrustal sequence is comprised of amphibolite facies BIF, ultramafic rocks, and amphibolitic basalt. The supracrustal rocks take on gneissic characteristics. The fabrics and metamorphic characteristics between the successions on either side of the Perseverance Fault suggest that the sequences have significantly different histories and there is no direct evidence to suggest that the two sequences are genetically related.

The laterite profile is buried beneath extensive lake and colluvium deposits. No laterite sampling was carried out in this greenstone belt.

Gneissic Rocks

Gneissic rocks occur flanking the west side of the Lake Violet-Milrose-Yandal belt, the west side of the Wiluna-Mt. Keith-Perseverance-Agnew belt, and the west side of the Duketon belt. Typically, the gneisses are quartzo-feldspathic in composition with small amounts of biotite or hornblende, granite to granodiorite in composition. Paragneiss has been noted within the succession, but it is not considered to be a major component. Most the gneisses are believed to be orthogneiss and the gneissosity trends in a north-northwesterly direction (Elias and Bunting, 1982; Bunting and Williams, 1979; Bunting and Chin, 1979). West of the Agnew area, the gneiss contains granoblastic garnet and diopside indicating that metamorphism attained upper amphibolite facies. East of the Perseverance Fault, much of the gneiss is well banded and may be paragneiss. The gneissic rocks adjacent to the western edge of the Yandal belt are primarily orthogneiss with amphibolitic inclusions.

Granitoid Rocks

Most of the granitoid rocks occur as composite batholiths with compositions ranging from biotite granite, tonalite, and granodiorite. Alkalic granitoid rocks occur east of the Lake Violet-Milrose-Yandal belt (Elias and Bunting, 1982). The tonalitic and granodioritic rocks are commonly medium- to coarse-grained and equigranular. Porphyritic granite, monzonite, and tonalite commonly contain microcline phenocrysts. Almost all granitoid rocks show varying degrees of alteration which include degradation of plagioclase, biotite, and muscovite.

Bunting and Williams (1979) have subdivided the Dingo Range, Lake Violet-Milrose-Yandal, and Wiluna-Mt. Keith-Perseverance-Agnew belts into four tectonic zones with distinct granitoid characteristics.

In zone 1, west of the Wiluna-Mt. Keith-Perseverance-Agnew belt, the granitoids are principally a large batholith of tonalite with varying degrees of grain size and porphyritic phases. It is part of a post-tectonic event that forms a continuous marginal zone of batholiths along the western edge of the Wiluna-Mt. Keith-Perseverance-Agnew belt extending southerly through the Leonora-Menzies-Kalgoorlie-Lake Johnstone areas. The second zone separates the eastern and western parts of the Wiluna-Mt. Keith-Perseverance-Agnew belt. This zone is primarily a plagioclase-rich tonalite that grades locally into granodiorite containing microcline phenocrysts. The third zone divides the Lake Violet-Milrose-Yandal belt from the Wiluna-Mt. Keith-Perseverance-Agnew belt and is predominantly a large tonalite batholith with varying grain sizes and porphyritic phases. Small ellipsoidal plutons of granodiorite, tonalite, porphyritic granite, and quartz monzonite have intruded the Lake Violet-Milrose-Yandal greenstone sequence. The fourth zone extends eastward from the Celia lineament. It is comprised of a large batholith of tonalite with local phases of other granitoid rocks. Flourite has been noted in the Mt. Boreas tonalite.

3.2 Mineralization

Gold

The nature and distribution of Au deposits have been summarized by a number of researchers and agencies (Groves, 1988; Hickman and Watkins, 1988).

Gold deposits and production have been concentrated primarily in the Wiluna-Mt. Keith-Perseverance-Agnew belt with smaller Au deposits and prospects in the Lake Violet-Milrose-Yandal and Duketon belts. Many of the larger Au deposits are associated with the Perseverance Fault.

In the WILUNA area, there have been two significant gold producers, the Moonlight Wiluna and Wiluna Gold mines. The area has produced over 56,000 kg of Au and 312 kg of Ag. In the SIR SAMUEL area, more than 12,613 kg of Au and 441 kg of Ag have been recovered primarily from the Sir Samuel, Yellow Aster, and Bellevue deposits. In the DUKETON area, more than 1,186 kg of Au and 1 kg of Ag were recovered from the Duketon-Hootanui and Erlistoun areas. In the KINGSTON area, Au production has been minor in the Duketon belt. Only 2kg of Au have been produced.

Base Metals

Reserves of 263 Mt of Ni averaging 0.6% have been outlined in the Mt. Keith ultramafic intrusion (Marston, 1984:67). The mineralization occurs as disseminated sulphides within serpentinized dunite-olivinite. Several other disseminated Ni sulphide bodies occur along the Mt. Keith intrusion, including the Charterhall, Betheno prospects, and the Honeymoon Well prospects (10 Mt averaging 1.1% Ni). Several other smaller prospects occur along the intrusion.

Copper was mined in the Kathleen Valley area from 1908 to 1966. A total of 435 t of copper ore was mined from pyrite-chalcopyrite-quartz veins with varying amounts of Au and Ag. Secondary enrichment to malachite, azurite, chrysocolla, oxides, bornite, chalcocite, and covellite occur within the ore zones.

Other Commodities

Arsenic from arsenopyrite and Sb from stibnite were produced as a by-product of gold recovery at the Moonlight Wiluna and Wiluna Gold mines. Up to 1947, 3,923 tonnes of Sb and 39,710 tonnes of As were produced.

Tin was mined from a cassiterite bearing lepidolite-albite pegmatite close to Kathleen Valley, and 0.4 km southwest of the Sir Samuel townsite. Tin production for the period 1945-53 was 0.2 tonnes.

Corundum was mined (55 t of ore) from an area 1 km south-southeast of Mount Mann in 1952. It occurs as a massive granular deposit intermixed with andalusite.

Tungsten was mined from Moriarty's Mine 5 km north-northwest of Kathleen, where 23.87 kg of WO_3 were extracted from scheelite.

Uranium (carnotite) has been noted in calcrete within channels of the saline paleodrainage system into Lake Way (WILUNA sheet). Work carried out by Delhi International Oil in 1978 indicated reserves of 6800 t

of U_3O_8 with an average grade of 0.5 kg/t. In the SIR SAMUEL area, 30 Mt of U_3O_8 with an average grade of 0.15% have been outlined in the Yeelirrie area.

4.0 THE SAMPLING PROGRAMME

4.0.1 SAMPLING

A 3-km spaced triangular sampling grid was used over most of the sampled area, with limitations caused by the distribution of access roads, the extent of erosional dissection of the laterite cover, the extent of cover by younger alluvium/colluvium, and the extent of mining and other land tenements. Various follow-up and fill-in samples were also taken, usually closing the sample spacing to 1 km, in some cases to 330 m; the locations of follow-up sampling is obvious in the plots showing sample sites, for example at 1:250,000 scale or more detailed. Figures 2, 3, and 4 show the distribution of the samples collected throughout the area according to the two major sample groups, the laterite (Figures 2a,b) and the ferricrete materials (Figures 3a,b). The figures are subdivided into "Regional (R)" samples (Figures 2a, 3a) and "Follow-up (F2/F3)" samples (Figures 2b, 3b). Figure 4 shows the distribution of Lateritized Rock (LR) samples collected throughout the area.

The database is composed of samples collected from all three phases of the study. Samples that are labelled "R" in the description field (see Appendix 1) are those initially collected at the 3-km spacing regional scale. Samples labelled "F2" are those collected during follow-up work at the 1-km spacing interval, and samples labelled "F3" are those samples collected at less than 1-km spacing from additional follow-up work after the F2 samples were collected. The number of samples for each type is:

R	Regional Samples	211
F2	Follow-up Phase 2	244
F3	Follow-up Phase 3	41
Total		496

Not all of the greenstone areas have been sampled. Areas that were not included in the sampling programme are the: Yandal, Dingo Range, Mt. Fisher, and Wiluna-Mt. Keith-Perseverance-Agnew greenstone belts. These areas are covered by extensive areas of colluvium and sand.

The strategy was to sample the cemented pisolitic laterite blanket and/or the loose laterite pisoliths which had been released from the duricrust by natural disaggregation. Lateritic nodules and pisoliths in the range of 1-cm to 2-cm diameter were sought in order to avoid the possibility of skewing the sample characteristics if very coarse material were collected and to aid sample preparation by providing suitable feed for the disk grinding stage (avoiding coarse crushing). Sampling was typically carried out over a 10-metre radius in order to suppress any unforeseen local variation. A 1-kg sample was collected for crushing, grinding and analysis of an aliquot. A separate 1-kg sample was collected for permanent reference. Other sample types were collected where the prime media were not available. A breakdown of the number of samples collected is given in Table 1. Where available, 1:50,000 photomosaics were used in selecting sample sites and for recording the locations. Each sample was assigned AMG coordinates.

The classification used in this report is the scheme adopted during the AGE study of 1983-1986. A more comprehensive and, in due course, genetic classification scheme is currently under development within the CSIRO/AMIRA Laterite Geochemistry Project. The most recent terminology and classification can be found in Anand *et al.* (1989) in which the terminology and classification of laterite and ferruginous materials have been expanded. The terms used in this report follow the older terms that are general enough to be considered useful for the purposes of a regional study. Correlation between the older and current schemes is given in Table 1.

Table 1. Sample Type, Abbreviation, and Number of Samples.

Sample type	Code	Number of Samples	Equivalent Classification CSIRO/AMIRA 1989 Codes (Anand et al, 1989)
Lateritic Types			
Loose Pisoliths	LP	4	LT102
Cemented Pisoliths	CP	0	LT202, LT212
Loose Nodules	LN	152	LT104
Cemented Nodules	CN	1	LT204, LT214
Vermiform Laterite	VL	0	LT231
Plinthite	PN	2	
Mottled Zone Scree	MS	113	LG105
TOTAL		272	
Ferricrete Types			
Massive Ferricrete	MF	73	IS101, IS102, IS103, IS201, IS301, Some LT229
Ferricrete Fragments	FF	94	LG201, LG203, LG206
Cemented Pebbly Ferricrete	PF	0	Some LG228
Ferricrete Pellets	PE	7	LG201
Re-cemented Fe-rich Colluvium	RC	0	
TOTAL		174	
Miscellaneous Types			
Ooliths Loose	OL	0	
Lateritized Rock	LR	50	
TOTAL		50	
GRAND TOTAL		496	

4.0.2 SAMPLE TYPES

I LATERITE SAMPLE TYPES

Samples belonging to the laterite family often occurring geomorphically above breakaways (i.e. a relatively complete laterite profile):

Loose Pisoliths (LP) and Cemented Pisoliths (CP) - Ferruginous particles with high sphericity, 2 mm to 3 cm in diameter, and a concretionary Fe-rich or Fe-bearing coating. Internal concentric banding is common. This sample type commonly forms a blanket deposit, whether loose or cemented, up to a few metres in thickness. Also forms redistributed colluvium.

Loose Nodular Laterite (LN) Cemented Nodular Laterite (CN) - Ferruginous particles with low sphericity but rounded. Commonly 1 to 4 cm across and a goethitic cutan (skin). Lateritic nodules and pisoliths form a continuous series and commonly occur together.

Vermiform or Vermicular Laterite (VL) - Iron-rich cemented mottled zone saprolite containing sinuous worm-like tunnels, holes or clay zones. May contain spaced pisoliths, nodules, or sporadic rock fragments.

Plinthite (PN) - Grit cemented by goethite, with visible quartz grains. Plinthite fragments do not have a concretionary goethite cutan.

Mottled Zone Scree (MS) - Loose, locally-derived scree or float derived from Fe-rich mottles within the lateritic weathering profile.

II FERRICRETE SAMPLE TYPES

Samples belonging to the ferricrete family typically occurring in situations where the nodular/pisolitic laterite has been removed by erosion, but stripping has not cut deeply into saprolite. These include:

Massive Ferricrete (MF) - Iron-rich material lacking pisolith- nodule texture, commonly has a botryoidal texture.

Ferricrete Fragments (FF) - Rounded fragments of Fe-rich material often showing relict internal structure but have no Fe-rich concretionary skin.

Cemented Pebbly Ferricrete (PF) - Dense black Fe-rich material with pebbly texture and irregular shape. This type normally occurs at the top of a full laterite profile.

Ferricrete Pellets (PE) - Particles of Fe-rich material with moderate to high sphericity, up to 1.5 cm across and no Fe-rich concretionary skin.

Recemented Fe-rich Colluvium (RC) - Fe-rich angular to sub-rounded rock fragments in a fine Fe-rich matrix.

III OTHER CATEGORIES

Loose Ooliths (OL) - Ferruginous particles with high sphericity <2 mm in size with a definite concretionary Fe-rich coating. Commonly they are black or very dark brown. These may occur in soil, as surface lag or may be cemented. They do not form blanket deposits.

Lateritized Rock (LR) - Saprolite that is enriched in Fe-bearing weathering minerals; goethite and hematite.

Figures 2a and 2b show the distribution of the laterite sample materials (LN, LP, CN, CP, MS, PN) and Figures 3a and 3b show the distribution of the ferricrete materials (FF, MF, PF, RC, PE). Sampling of ferricretes is more widespread in the northern part of the area, whilst sampling of loose nodules dominates the southern part of the area.

4.0.3 SAMPLE PREPARATION

The samples were prepared using non-metallic sample preparation methods described by Smith *et al.* (1987:256). Oversized material from 1 kg samples was reduced to minus 8 mm by crushing between zirconia plates in an automated hydraulic press. The crushed oversized material, together with the direct feed material, was then fed to an epoxy-resin lined disc grinder with alumina plates and further reduced to minus 1 mm. Final milling was done in an agate or alumina mill. Cleaning of the equipment was performed by a combination of air- and sand-blasting and the passage of a quartz blank.

4.1 Analytical Methods

A total 496 samples were analyzed by Amdel Ltd. (Adelaide) for 24 elements. An additional 7 elements were analyzed by the CSIRO analytical facilities on 40% of the samples. Gold was analyzed by Analabs (Perth). The methods of analysis are outlined in Table 2. Tin and Bi were analyzed by two methods because of their perceived importance in laterite geochemistry and to provide a consistent gauge of confidence in the results. The following elements have been analyzed by the methods outlined in Table 2: SiO_2, Fe_2O_3, MgO, CaO, TiO_2, Au, Mn, Cr, V, Cu, Pb, Zn, Ni, Co, As, Sb, Bi1, Bi2, Mo, Ag, Sn1, Sn2, Ge, Ga, W, Ba, Zr, Nb, Ta, Se,

and Be. Additional elements may be analyzed later on. Only Bi2 and Sn2 have been used in this report. *All references to these two elements have been made with respect to Bi2 and Sn2.* The data on the accompanying diskette contain Bi1, Bi2, Sn1, and Sn2. Appendix 1 indicates the format of the data.

Samples analyzed by CSIRO were carried out on an Inductively Coupled Plasma Spectrometer (ICP) using a lithium metaborate fusion dissolved in nitric acid. Gold was analyzed by Analabs Laboratories using Atomic Absorption Spectroscopy (Graphite Furnace) after aqua-regia dissolution of 50 g of sample pulp.

4.1.1 ANALYTICAL QUALITY CONTROL

Each batch of samples submitted for analysis contained three control samples that represent a spectrum of multi-element values. These control samples were submitted in a scrambled numerical sequence. The samples were also subjected to replicate analysis both by the CSIRO analytical facilities and by an independent laboratory. Problems of between-batch variation could usually be detected by examination of maps of the plotted data. If any clustering or unusual patterns were noted, the duplicated samples were submitted for assay.

5.0 DATA PRESENTATION AND ANALYSIS

The geochemical data that accompany this report are contained on a 5.25" floppy diskette which can be found in the back pocket of the report. Appendix 1 provides the details regarding the format of the data.

A summary of the multi-element geochemical data is listed in Tables 3-5. The Tables list the number of samples analyzed for each element, the 1, 5, 10, 25, 50, 75, 90, 95, and 99th percentiles, minimum, maximum, mode, mean values, and the standard deviation.

The Tables list the summary statistics for the following groups of data:

Table 3a: Summary Statistics for the Wiluna area, all Regional (R) samples for **Lateritic** materials (LN, LP, CN, CP, PN, VL, MS).

Table 3b: Summary Statistics for the Wiluna area, all Follow-up (F2/F3) samples for **Lateritic** materials (LN, LP, CN, CP, PN, VL, MS).

Table 4a: Summary Statistics for the Wiluna area, all Regional (R) samples for **Ferricrete** materials (MF, FF, PF, PE ,RC).

Table 4b: Summary Statistics for the Wiluna area, all Follow-up (F2/F3) samples for **Ferricrete** materials (MF, FF, PF, PE ,RC).

Table 5: Summary Statistics for the Wiluna area, all Regional (R) and Follow-up (F2/F3) samples for **Lateritized Rock** (LR).

Materials which were classified as loose nodules (LN), loose pisoliths (LP), cemented nodules (CN), cemented pisoliths (CP), plinthite (PN), vermicular laterite (VL), and mottled zone scree (MS) are generally known to be compatible sample media and were therefore grouped together. These samples, placed in the laterite family, total 272, and their statistics are shown in Tables 3a,b, Similarly, samples of the ferricrete categories, ferricrete fragments (FF), massive ferricrete (MF), cemented pebbly ferricrete (PF), and re-cemented Fe-rich colluvium (RC) were grouped together, totalling 174 samples, and their statistics are listed in Table 4a,b. Lateritized rock (LR) tends to have geochemical characteristics that are distinct from both the lateritic and ferricrete materials. Thus, samples that fall into the Lateritized Rock category are distinct and the statistics of this group are shown in Table 5. The Wiluna region tends to show a near equal distribution of both lateritic and ferricrete materials. This contrasts with the distribution of these two major sample media types in the Murchison Province (Grunsky *et al.*, 1988; Grunsky *et al.*, 1989) and the Southern Cross greenstone belt (Grunsky, 1990).

Table 2
Analytical Methods and Lower Limits of Detection

Element	Reported as	Detection Limit	Laboratory	Analysis Method	Digestion Method
SiO2	WT%	0.5	CSIRO	ICP	FS
Al2O3	WT%	0.5	CSIRO	ICP	FS
Fe2O3	WT%	0.1	AMDEL	AAS	HF
MgO	WT%	0.05	CSIRO	ICP	FS
CaO	WT%	0.05	CSIRO	ICP	FS
TiO2	WT%	0.003	CSIRO	ICP	FS
Mn	PPM	5	AMDEL	AAS	HF
Cr	PPM	5	AMDEL	XRF	
V	PPM	10	AMDEL	XRF	
Cu	PPM	2	AMDEL	AAS	HF
Pb	PPM	4	AMDEL	XRF	
Zn	PPM	2	AMDEL	AAS	HF
Ni	PPM	5	AMDEL	AAS	HF
Co	PPM	5	AMDEL	AAS	HF
As	PPM	2	AMDEL	XRF	
Sb	PPM	2	AMDEL	XRF	
Bi1	PPM	1	AMDEL	OES	
Bi2	PPM	1	AMDEL	XRF	
Mo	PPM	2	AMDEL	XRF	
Ag	PPM	0.1	AMDEL	OES	
Sn1	PPM	1	AMDEL	OES	
Sn2	PPM	1	AMDEL	XRF	
Ge	PPM	1	AMDEL	OES	
Ga	PPM	1	AMDEL	OES	
W	PPM	10	AMDEL	XRF	
Ba	PPM	100	CSIRO	ICP	FS
Zr	PPM	50	CSIRO	ICP	FS
Nb	PPM	4	AMDEL	XRF	
Ta	PPM	3	AMDEL	XRF	
Se	PPM	1	AMDEL	XRF	
Be	PPM	1	AMDEL	OES	
Au	PPB	1	ANALABS	Carbon Rod Aqua Regia	

Legend:		
	AAS	Atomic Absorption Spectroscopy
	XRF	X-ray Flouresence
	ICP FS	Inductively Coupled Plasma Fusion
	OES	Optical Emmission Spectroscopy

Many samples were analyzed for elements whose values were below the detection limit. In these cases, the value of the variable was set to one third of the detection limit as the default minimum value. Subsequent statistical and numerical procedures used this minimum value. As mentioned above, not all samples have been analysed for the full set of elements, at this stage. In such cases, for calculations of statistics the number of samples used to compute the statistic was reduced. The number of samples used for the calculations of the statistics of each element is indicated in the Tables.

Examination of the Tables is useful in making preliminary assessments about the data. The first part of each table provides insight as to how the values of data are distributed over the range of the data. By scanning the values over the range of percentiles, the nature of the distribution of the data can be quickly observed. Elements with highly skewed distribution (e.g. Au) tend to have similar concentrations over the range of percentiles, increasing rapidly at the 90, 95, and 99 percentile rankings. More normally-distributed elements (e.g. V) show a more uniform change in abundance with increasing percentile levels. Samples that occur in the upper percentile range (>95th percentile) are usually of interest in an exploration programme. It is these "high" or "anomalous" values that may be indicative of a mineralized zone whose chemistry is unlike that of the regional geochemical patterns.

The 50th percentile gives the abundance value of the midpoint of the distribution of samples and can be quite different from the arithmetic mean of the sample population. This 50th percentile value is recommended for estimating the central value of a distribution. The Tables also list minimum, maximum, median, mode,

mean, and standard deviation for each element. Normally-distributed populations tend to have similar values for the median, mode, and mean. The standard deviation gives an estimate of the range of the data around the arithmetic mean. Initially, the regional samples were not analyzed for SiO_2, Al_2O_3, MgO, CaO, and TiO_2. Subsequent follow-up sampling included analysis for these elements. Thus these major oxide elements are omitted from Tables 3a and 4b.

Comparison of Tables 3 and 4 clearly shows significant differences of chemistry between the two populations of laterites and ferricretes over the entire area. Examination of Tables 3a with 4a shows that the chemistry between the regional samples ("R") varies between the two media. The lateritic samples have greater median abundances for Cr, V, Ni, As, Ge, Ga, Nb, Se, and Au. The ferricrete materials of Table 4a show greater median abundances for Fe_2O_3, Mn, Cu, Ni, Zn, and Co. The follow-up samples (F2/F3) in Tables 3b and 4b exhibit similar patterns. Table 5 shows characteristics of materials that are different relative to the lateritic or ferricrete sample media. Relative to the abundances in Tables 3a, 3b (Laterites, "R" samples) the lateritized rock (LR) samples show a relative decrease in SiO_2, Al_2O_3, TiO_2, Cr, and V. A relative increase is observed with Mn, Cu, As and Ba. It is unclear whether these differences are the result of different host rock lithologies, the lateritic weathering process or a combination of the two.

Statistical tests involving the t-test (testing the similarities of the means) and the F-test (testing the similarities of variances) have not been carried out because many of the frequency distributions are non-normal and any statistical inferences may be misleading. Procedures exist for transforming the data into more normal-like distributions for subsequent statistical inferences (e.g., power transformations, see Smith *et al.*, 1984); however, such a task is beyond the scope of this report.

Barium must be interpreted with caution as the method of sample preparation (from alumina disks) adds an average of about 100 ppm of Ba, because of an impurity in the alumina, depending on the hardness of the sample.

Bismuth and Sn include two methods of analysis one by OES and the other by XRF. Both methods confirm consistency of the results.

5.1 Histograms

Histograms of the data were plotted for selected elements of specific sample types. These plots are shown in Figures 5 - 29. The histograms were computed using 40 class divisions based on the minimum and maximum values of the variables. For presentation purposes, the minimum and maximum values were truncated at the mean ± three standard deviations. Above each histogram is a box and whisker plot that shows the median (50th percentile), left hinge (25th percentile), right hinge (75th percentile) and range (minimum and maximum values) of the data. Each histogram also lists these values in a numerical form at the right-hand side of the figure.

The presentation of the data is similar to previous reports (Grunsky *et al.*, 1988, 1989). Each figure is comprised of two histograms. Figures 5a-29a show histograms of the lateritic materials and Figures 5b-29b show histograms of the ferricrete materials.

A visual comparison of the histograms yields the following observations:

- **Fe_2O_3**: Abundances are higher in the ferricretes relative to the laterites as shown in Figures 5a,b.
- **Ag**: The range and median values (Figure 6a,b) are similar for both sample media.
- **Mn**: Ferricrete materials have a greater range of abundances than the laterites (Figure 7a,b). The median value of the ferricretes is significantly higher than that of the laterites.
- **Cr**: Both sample media show a similar range of abundances; however, the lateritic samples display a greater median abundance level (Figure 8a,b). The Cr abundance of the lateritic materials tends to reflect the original host rock lithology.

- **V**: The lateritic materials show a greater median and range of abundances relative to the ferricrete materials (Figure 9a,b).

- **Cu**: Both materials show a similar range of abundances (Figure 10a,b). The laterites display a bimodal distribution with peaks at 100 and 200 ppm. The ferricretes show a polymodal distribution with peaks at 100, 200, and 350 ppm. These peaks may be due to original host rock differences, mineralization, and/or weathering effects.

- **Pb**: Both laterites and ferricretes show similar ranges and median abundances (Figure 11a,b).

- For many of the elements, the ferricrete materials display a greater range of abundances and higher median abundance relative to the lateritic materials. The lateritic abundances generally reflect the underlying host rock lithologies with the exception of the tails of the distribution which may reflect secondary processes related to alteration or mineralization. The ferricrete materials have a more complex history and the range of abundances can reflect both the original host rock lithology and subsequent weathering. Distributions that exhibit these characteristics were noted for **Zn** (Figure 12a,b), **Ni** (Figure 13a,b), **Co** (Figure 14a,b), **As** (Figure 15a,b), and **Ba** (Figure 23a,b).

- The following elements all show similar ranges and median abundances for the two sample media. **Sb** (Figure 16a,b), **Bi** (Figure 17a,b), **Mo** (Figure 18a,b), **Sn** (Figure 19a,b), **Ge** (Figure 20a,b), **W** (Figure 22a,b), **Zr** (Figure 24a,b), **Nb** (Figure 25a,b), **Ta** (Figure 26a,b), **Se** (Figure 27a,b), and **Be** (Figure 28a,b)

- **Ga** (Figure 21a,b) displays a distinct difference between the ferricrete and lateritic materials. The media and range of abundances is greater for the lateritic materials

- **Ta** and **Be** (Figures 26a,b, 28a,b) display little variation in abundances and are of limited use. Almost all of the values are less than detection limit; however, where they are elevated they may reflect alteration/mineralization events.

- **Au** (Figure 29a,b) shows a similar median and range of abundances for both sample types.

Some elements exhibit bimodal or polymodal distributions. This usually occurs with elements that reflect underlying lithologies and alteration/mineralizing events. Elements that exhibit these characteristics are SiO_2, Al_2O_3, Fe_2O_3, TiO_2, Ag, Cr, V, Cu, Zn, Ni, As, Sb, Bi, Mo, Sn, W, Zr, and Au. Elements that also show bimodal characteristics related to greenstone lithologies include SiO_2, Al_2O_3, Fe_2O_3, TiO_2, Cr, V, and Zr. Bimodal characteristics occur in areas where there is a greater diversity of lithologies (basalts vs. rhyolites, etc.). These same elements display a more uni-modal distribution in areas where the compositional range of the underlying lithologies (granitoid rocks) is not as diverse.

Most of the elements have non-normal frequency distributions and for many of the histograms of these elements positively skewed values can represent fractionated igneous environments or anomalous values that are potentially associated with various types of mineralization. Some elements, in particular the chalcophile suite (As, Sb, Bi, Se, Pb, Ge, Zn, Cu, Ag), are known to be good pathfinders for both base-metal sulphide mineralization and precious metal mineralization. These elements form the basis for the empirical chalcophile and pegmatophile functions as well as for use in multivariate statistical analysis that have been developed by Smith and Perdrix (1983) and Smith *et al.* (1984).

An analysis of the nature of the causes of the frequency distributions of the elements is beyond the scope of this report. The non-normal nature of the distributions may be due to a mixture of samples from different geological environments, some of which may represent rare occurrences due to mineralization (e.g. As, Sb, Bi, Ag, Au).

5.2 Element maps

Maps of the ranked abundances of most of the elements listed in Table 2 are shown in Figures 30a,b-49a,b. The lateritic materials are shown in Figures 30a-49a and the ferricrete materials are shown in Figures 30b-49b.

Since the sample sites are not distributed uniformly over the map area, methods of data presentation such as contour maps are not appropriate for describing the spatial variation of the data at the scale presented. However, the data can be conveniently presented by using symbols whose sizes are based upon the percentile ranking of the data relative to the ***maximum*** and ***minimum*** values of the data. A commonly-used method of expressing concentrations over irregularly-sampled areas is the expression of each concentration by a symbol whose size is proportional to its magnitude (Howarth, 1983:124). The use of such symbols can be employed to indicate areas that are enriched or depleted. However, caution is advised in the interpretation of these proportionally-sized symbols. Symbol size does not necessarily reflect anomalously low or high values, rather it reflects the maximum and minimum values of the data which may or may not be "anomalous" with respect to zones of mineralization.

The size of the symbols is not a linear function of concentration of the elements. For visual ease and assistance in the recognition of outlier data, the symbol sizes are defined as:

Map Symbol Size = Minimum Symbol Size for Map + Constant Symbol Size * (Percentile/100)^4,

where the percentile is the percentile ranking of the sample for the particular element being considered. This quartic function enhances the size of the symbols for samples in the upper percentile rankings whilst making the samples that fit in the rankings of less than 75 percentile range more equal in size. This non-linear distribution of symbol sizes assists in a faster visual assessment of anomalous values.

5.3 Interpretation of the Geochemical Distributions

Interpretation of the geochemical maps requires some knowledge of the geological processes that have acted upon, or are still acting within an area. Inference about the geological environment can be made from many of the geochemical maps and can assist in refining geological models. Hallberg (1984) has shown that within the saprolitic laterite profile, ratios of TiO_2, Cr, and Zr retain characteristics of the original lithologies. Titanium and Cr ratios commonly outline the mafic volcanic or mafic volcanicly-derived sedimentary assemblages, whilst Zr is useful in outlining the Zr-enriched felsic volcanics. Maps of these elements must be interpreted with caution as the abundances may have been modified by several processes, particularly during weathering. Fractionated igneous rocks tend to show enrichment in Mo, Be, W, Ga, and Sn and laterite geochemistry on a regional scale could be expected to reflect such effects. Birrell and Smith (1984) have previously reviewed chalcophile distributions for selected portions of the Yilgarn block. They recommended that for selected chalcophile elements, samples which rank above the 90th percentile are significant and that the areas from which these samples were taken be considered for follow-up sampling.

Many of the elements reflect the compositions of the underlying lithologies. The elements that most commonly reflect the underlying supracrustal rocks of the greenstone belts include: Fe_2O_3, TiO_2, SiO_2, Cr, Mn, V, Ni, Co, Zr, Cu, Zn, Ga, and Nb. Elements such as SiO_2, Mo, Sn, Pb, Nb, and Se tend to reflect underlying lithologies associated with the felsic granitoid/gneissic terrains which are largely fractionated environments. The effects of weathering processes can be reflected by the abundances of Fe_2O_3, TiO_2, Cr, Mn, V, Ni, and Zr. These elements tend to be residual even after the lateritic material weathers. Thus, the interpretation of some of these elements must be cautiously applied. Other elements such as Cu, Zn, Ga, and Nb can also reflect secondary processes, for example alteration, that are commonly associated with mineralization. Elements such as Ag, As, Sb, Bi, Mo, Sn, W, Se, Ga, and Nb can also reflect environments that are associated with alteration and mineralization. Any one element in itself is not necessarily a good pathfinder associated with an altered/mineralized zone. However, a combination of a selected group of elements may be a suitable means of isolating areas with more mineral potential.

Generally, the laterites are a better sample medium for distinguishing the characteristics of the various geological processes. Ferricretes are also useful, but the geochemical signals are more erratic. Nonetheless, the ferricretes may be the only material available in areas where laterites are missing, and can assist in assessing the geochemical characteristics in a sampling programme. The following descriptions of the elements includes both the laterites and ferricretes except where noted otherwise.

- Iron, **Fe_2O_3** (Figures 30a,b), tends to show a relative increase in abundance in the Lake Violet-Milrose-Yandal belt relative to the Duketon belt in both the lateritic and ferricrete materials. This feature is also demonstrated by **Mn** (Figures 32a,b), **Cr** (Figures 33a,b), **Cu** (Figures 35a,b), **Zn**

(Figures 37a,b), **Ni** (Figures 38a,b), and **Co** (Figures 39a,b). This most probably reflects the expression of the underlying mafic volcanic lithologies. Copper and Zn anomalies are difficult to assess since their abundance levels are also a function of lithology. Besides being economic commodities, they are also ubiquitously associated with alteration zones within bedrock. Thus elevated values must be interpreted cautiously. Methods of anomaly detection for these elements can be assisted by using methods such as those advocated by Smith *et al.* (1984), Stanley and Sinclair (1987), and Garrett (1989).

- Elevated abundances of **Fe_2O_3**, **Mn**, **Pb**, **Zn**, **Ni**, **Co**, **W**, and **Au** in the lateritic materials occur together in the central part of the Dingo Range belt. The nature of this association is not clear; however, it may suggest Au mineralization within a mafic volcanic host lithology.

- Chromium, **Cr** (Figures 33a,b), **Ni** (Figures 38a,b), and **Co** (Figures 39a,b) tend to outline the mafic lithologies in the eastern part of the Duketon belt, the western part of the northern Duketon belt extension, and in the mafic succession within the Lake Violet-Milrose-Yandal belt.

- Vanadium, **V** (Figures 34a,b), shows elevated abundances in the southern part of the Duketon belt and in the southern part of the Lake Violet-Milrose-Yandal belt within the WILUNA sheet. Elevated levels of V correlate with elevated abundances of Fe_2O_3. The ferricrete materials show elevated abundances at isolated localities throughout the study area.

- Copper, **Cu** (Figures 35a,b), **Pb** (Figures 36a,b), and **Zn** (Figures 37a,b) show elevated abundances in the felsic metavolcanic-metasedimentary sequence in the Lake Violet-Milrose-Yandal belt within the WILUNA sheet. The Cu and Zn abundances most probably reflect compositional variation of the volcanic rocks and the elevated Pb abundances may reflect the more fractionated felsic rocks. Lead and Zn show increased levels in the Dingo Range belt situated in the southeast corner of the WILUNA sheet.

- Arsenic, **As** (Figuress 40a,b), and **Sb** (Figures 41a,b) display elevated abundances within the western part of the Lake Violet-Milrose-Yandal belt. Some slightly elevated abundances occur within the Duketon belt.

- Bismuth, **Bi** (Figures 42a,b), **Mo** (Figures 43a,b), **Sn** (Figures 44a,b), and **W** (Figures 46a,b) show elevated abundances within the felsic metavolcanic-metasedimentary sequence in the Rose Hills and Milrose areas of the WILUNA sheet. Similar patterns are also observed east of the Pinjanie and Swanson Hills, the Urarey Well area, and northwest of the Gerry Well area on the DUKETON sheet.

- Silver, **Ag** (Figures 31a,b), displays significant levels northwest of the Gerry Well area on the DUKETON sheet.

- Gallium, **Ga** (Figures 45a,b), shows a relatively even pattern across the area and does not reflect anything noteworthy.

- Niobium, **Nb** (Figures 47a,b), shows elevated abundance levels in the Gerry Well, Urarey Well, and Swanson Hill areas on the DUKETON sheet. Elevated abundances also occur in the Milrose area on the WILUNA sheet

- Selenium, **Se** (Figures 48a,b), shows elevated abundance levels in the Rose Hills area on the WILUNA sheet and a few isolated elevated values in the Tooheys Well and Christmas Well (Erlistoun) area on the DUKETON sheet.

- Gold, **Au** (Figures 49a,b), occurs in elevated abundances in the Deep Well, Snake Well areas, the Rose Hills area, and the southeast part of the WILUNA sheet. Elevated abundances also occur in the Corner Well, King John Well, and Christmas Well (Erlistoun) area on the DUKETON sheet.

5.4 Multivariate data analysis

The usefulness of multivariate data analysis methods applied to geochemical data has been well documented (Howarth and Sinding-Larsen, 1983, Chapter 6). The most commonly used multivariate methods include,

principal components, cluster, factor, regression, and canonical analyses. Multivariate techniques have been specifically applied to Archaean volcanic terrains from which a number of geological processes can be inferred, ranging from primary compositional variation to alteration and associated mineralization (Grunsky, 1986). Multivariate techniques also include empirical techniques such as the chalcophile and pegmatophile indices developed by Smith and Perdrix (1983). Multivariate techniques were applied in previous studies (Grunsky *et al.*, 1988, 1989) and quite clearly outlined multi-element geochemical signatures that could warrant further investigation.

There are some fundamental problems that commonly occur in geochemical databases such as the regional geochemical database that is being compiled for the Yilgarn block.

1) Most elements have a "censored" distribution, meaning that values at less than the detection limit can only be reported as being less than that limit.

2) The data do not occur as normally-distributed abundances.

3) The data have missing values. That is, not every sample has been analysed for the same number of elements.

4) Not every element has been analysed by the same method or the limits of detection of the method have changed over time.

These problems create difficulties when applying mathematical or statistical procedures to the data. Statistical procedures have been devised to deal with all except the last problem. To overcome the problems of censored distributions, procedures have been developed by applying transformations to estimate replacement values for the purposes of statistical calculations by the CSIRO Division of Mathematics and Statistics. Non-normally distributed data can be transformed using standard procedures as outlined by Smith *et al.* (1984). When the data have missing values, several procedures can be applied to estimate replacement values. Most procedures use a multiple regression procedure which estimates the replacement value based on a regression with samples that have complete analyses.

It is beyond the scope of this study to apply and report on all of these procedures. However, one of the more basic procedures can be applied to the data in order to enhance zones of increased abundances, or anomalies. This involves the use of robust estimates of means, correlations and covariances of the data. Because the nature of most of the element distributions is non-normal and positively skewed, the arithmetic means of these distributions tend to be higher than the medians or "true" means of the populations (cf. Histograms, Figures 5-29). Robust statistical procedures determine mean values and subsequent correlations and covariances between the elements based on finding a value of the mean closer to the median of the sample population. Robust procedures were subsequently applied to two procedures used in this report. Principal components analysis has been carried out using robust estimates of the means and correlations for the multivariate populations examined. The use of the Mahalanobis distance as an estimate of whether an unknown sample is anomalous or not is based on a robust estimate of the mean. These procedures are discussed below.

5.5 Geochemical Anomalies

Geochemical anomalies can be defined by a number of techniques. Simple ranking and examination of the extremes of pathfinder and target elements is an effective means of defining anomalies. Tables 6 and 7 provide listings of samples that rank above the 95th percentile. Table 6 lists the samples for the lateritic sample media and Table 7 lists the samples for the ferricrete materials. These Tables can be used to identify anomalous samples that may be associated with various types of mineralization.

Previous work by the Laterite Geochemistry Group of the Division of Exploration Geoscience, CSIRO outlined a number of anomalies associated with element enrichments determined by a number of methods. These methods detected anomalies through:

a) element abundances above known background thresholds,

b) samples in which several elements had elevated abundances above specified percentile levels after the data were ranked,

c) the use of empirical indices, developed from orientation studies, such as the chalcophile index, CHI-6*X, the pegmatophile index, PEG-4, and the NUMCHI index.

Figure 1b and Table 8 show the anomalies that were noted from the initial regional sampling programme. Samples that are associated with these anomalies are noted in the database file that accompanies this report. These anomalies were outlined by a number of empirical procedures including selection by abundances greater than the 95th percentile, ranking of chalcophile elements, CHI-6*X, and PEG-4 indices. In the case of the Wiluna area, only three anomalies were noted.

5.6 Principal Components Analysis

Many of the geochemical patterns that were described above can be determined by the use of systematic and statistical means of data analysis. A fundamental objective in the analysis of data is the extraction of meaningful information from which a reasonable interpretation can be made. As the number of variables increase, the more detail is provided; however, this is at the expense of simplicity of interpretation. There are several good reviews that discuss the basics of multivariate data analysis techniques (e.g. Jöreskog *et al.*, 1976; Howarth and Sinding-Larsen, 1983; Davis, 1986).

In geological applications, and particularly within the study of igneous rocks, the foundation of petrology is based upon the systematic variation of the elements involved in magmatic fractionation. It is already known that the lithogeochemistry of igneous rocks contains a number of chemical variables that will correlate with one another. Because of this, it would be easier to examine just a few critical elements to extract a meaningful interpretation. However, it is not always known which elements are involved in the magmatic process during fractionation of igneous rocks nor is it always known what subsequent alteration or metamorphism has occurred. Thus, there is uncertainty in choosing, a priori, which variables to include in a subsequent data analysis. A way to overcome this uncertainty is to apply some technique of data analysis that will assist in reducing the number of variables based on correlations or covariances of the variables. Techniques such as factor analysis, principal components analysis, and cluster analysis, have been developed in response to these problems.

The objective of principal components analysis is to reduce the number of variables necessary to describe the observed variation within a set of data. This is done by forming linear combinations of the variables (components) that describe the distribution of the data. Ideally, to the geologist, each component might be interpreted as describing a geological process such as differentiation (partial melting, crystal fractionation, etc.), alteration/mineralization (carbonatization, silicification, alkali depletion, metal associations and enrichments, etc.), and weathering processes (bedrock-saprolite-laterite).

A method of principal components analysis known as Simultaneous RQ-Mode Principal Components Analysis (Zhou *et al.*, 1983) was carried out on the correlation matrix of the combined regional ("R") laterite and ("F2/F3") laterite data groups. This is in contrast to separation of the "R" samples from the "F2/F3" samples analyzed in a previous report (Grunsky, 1990). Principal components analysis was carried out separately for the "R" samples and for the "F2/F3" samples. The results of each analysis were essentially the same with similar element relationships expressed in each group. Thus it was decided to include both groups together for further analysis.

The technique of RQ-mode principal components analysis presented here is different from the methods presented in earlier reports (Grunsky *et al.*, 1988, 1989) in that the correlation matrix used to compute the principal components has been derived by robust estimation methods. Robust estimation gives a better estimate of the means and correlations of the variables by down-weighting the influence of anomalous samples.

The complete set of oxides/elements was not used in the analysis. A subset of 19 oxides/elements was chosen for the laterite materials as listed in Table 9. A subset of 18 oxides/elements was chosen for the ferricrete materials as listed in Table 10. Two factors influence the choice of a subset of variables. Firstly, either not all of the samples were analysed for all of the elements (e.g. SiO_2, Al_2O_3, TiO_2, MgO, CaO, Ba, Zr,

etc.) or the elements were of such low abundance levels that it was not considered useful to include them in the analysis (e.g. Bi, Ge, Ta, Be). Secondly, only those samples with non-zero values for all elements were included in the analysis.

Tables 9 and 10 show the results of the principal components analysis. The tables list the element correlations, eigenvalues, the component loadings of the elements, and the contribution (relative significance) that each element makes to each component of the reduced variable space.

The correlation coefficients can be useful in assessing pairs of significant relationships between elements. Correlation coefficients can be tested for their significance by statistical procedures (Student's t-test). In the case of the laterites and the ferricretes of 265 and 162 samples respectively, significant correlation coefficients are defined by absolute correlation coefficient values greater than 0.1013 and 0.1297 at the 95% confidence level respectively. A description of the correlations between the elements would be awkward. The relationships can be expressed best by the examination of the principal component scores in Tables 9 and 10. As well, the relationships can be visually assessed by projecting the principal component scores of the elements and samples on to the principal component axes.

5.6.1 PRINCIPAL COMPONENTS ANALYSIS: LATERITE SAMPLES

A general rule is that eigenvalues (see Table 9) which are greater than 1.0 are considered to be significant components. Thus in Table 9, the first 7 components would be considered worth examining. An exception to this is where components which contribute only a small amount of the overall data variation but contain contributions by economically significant elements. In this case, Au is significant in the 10th component and thus it will be considered as well. The cumulative contribution of the first seven eigenvalues plus the tenth eigenvalue accounts for 68.4% of the data variation.

The relationships between the elements are expressed in Table 9. The principal component scores for the elements indicate the relative associations of the variables. Positive and negative associations between the variables can be observed in the first two columns of the principal component scores in Table 9. The relative contributions of the variables are also shown in Table 9 and indicate the relative amount that each variable contributes to each component. This assists in determining which component is the most significant for each element. For example, much of the Fe_2O_3 variation is accounted for in the first component (>44.6) while the variation of Au is distributed over two components (F5, and F10). A discussion of all of the principal components is not practical for the purpose of this report. Only those components which are considered to be useful for assistance in exploration are discussed here.

Table 9 shows that two groups of elements contribute to the first principal component. This can be seen by examining the relative contributions and the principal component scores of the variables. The first group consists of positively correlated Fe_2O_3, Mn, Cu, Zn, Ni, and Co and the second group consists of samples associated with Ga (V, Ag, Pb, and Nb). The two groups, however, are inversely associated. These two groups most likely represent the differences between the supracrustal lithologies. The more mafic greenstones are associated with Fe_2O_3, Mn, Cu, Zn, Ni, and Co while the felsic volcanic rocks are associated with increased abundances of Ga (Al enrichment). The first component accounts for 19% of the total variation of the data.

The relative contributions to the second component (9.9% of the data variation) are due to variation in Pb, Ag, Sn, Nb, As, Mo V, Mn, Cr, and Au. Lead, Ag, V, Nb, Sn, As, Cr, and Mo are all inversely associated with Au.

Figure 50a shows the samples and elements plotted on to the first two principal component axes. The relationships of the elements noted above can be clearly seen in the diagram. *Each sample is plotted as a small cross and each element is also projected on to the F1-F2 plane. In this way the relationship between the samples and the elements can be graphically displayed.* The figure illustrates the relationships between the mafic and felsic supracrustal rocks by the relative positions of the samples with respect to the elements. The mafic metavolcanics and associated metasedimentary rocks are associated with the relative increases in Cu, Fe_2O_3, Ni, Mn, Zn, and Co. The felsic metavolcanic and metasedimentary rocks show a relative increase in Ga with respect to the other elements. Many of the samples plot along the positive side of the F2 axis and these samples show an association with a relative increase in V, Ag, Pb, Nb, and Sn. This diagram not only indicates which of these samples are relatively enriched in those elements, but it also indicates that it is the

more felsic rocks that have this enrichment. Gold plots along the negative part of the F2 axis with no other associated elements. A few samples plot along the negative side of the F2 axis near to Au. These samples are Au enriched but relatively depleted with respect to the other elements. This indicates that these Au enriched samples have no multi-element associations.

Figure 51a shows a map of the sample scores for the first principal component. Large negative scores (asterisks) and the smaller positive scores (small circles) are associated with Ga enriched (felsic) areas while larger positive scores (circles) are associated with the mafic rocks. Thus the map provides a crude outline of the major compositional variation within the area.

Figure 51b shows a map of the sample scores for the second principal component. The large positive scores are associated with Pb, Ag, Sn, Nb enrichment and the large negative scores are associated with Au. Both the larger positive and negative scores may be potential sites for follow-up exploration. The large positive scores occur in the southeast corner of the WILUNA sheet, the Biddy Well area, and the Rose Hills area on the WILUNA sheet. Large positive scores also occur in the Quongdong Well, east of Duketon, and north west of the Gerry Well area on the DUKETON sheet. Large negative scores, indicating Au enrichment occur in the Christmas Well (Erlistoun) to German Well area along the eastern margin of the Duketon belt. Large negative F2, Au associated, scores occur in Milrose area and the Longreach Well area on the WILUNA sheet.

Table 9 indicates that the fifth component (6.4% of the overall data variation) accounts for a significant amount of Au variation (relative contribution=38.0%). The scores of the elements and the relative contributions indicate that Nb is positively associated with Au, whilst W is inversely associated with Au. Figure 50b shows the samples and elements projected on to the F1-F5 plane. The negative part of the F5 axis shows an association of Au, Nb, and Sn, while the positive side of the axis shows an association with W only. Figure 51c shows a map of the sample scores for the fifth component. Large positive scores indicate relative W enrichment northwest of the Gerry Well area (DUKETON), the southeast corner of the WILUNA sheet, and Biddy Well area (WILUNA). Large negative scores associated with Au-Nb-Sn occur in the German Well and Gerry Well areas (DUKETON), and north of 14 Mile Well (WILUNA).

The sixth principal component accounts for 5.8% of the data variation. Examination of the relative contributions in Table 9 shows that Sb, As, Cr, and Au contribute the most to the component. The principal component scores of Table 9 indicated that Sb, As, Cr, and Au are all negatively correlated. This can be observed visually in Figure 50c where the samples and elements are plotted on to the F1-F6 plane. Samples that plot along the negative part of the F6 axis show a relative increase in Sb with accompanying relative increases in As, Cr, and Au. Figure 51d shows a map of the F6 sample scores. Large negative F6 scores occur in the area west-southwest of Gerry Well (DUKETON sheet), the southeast corner of the WILUNA sheet, and northwest of the Rose Hills area on the WILUNA sheet. These sites suggest that there is a relative enrichment of Sb, As, Cr, and Au in comparison to the rest of the laterite sample population.

The tenth principal component accounts for 4.5% of the data variation. Table 9 shows the relative contributions are most significant for W, Au, and Sn. The component scores of the elements show that they are all positively associated. Figure 50d shows the samples and elements plotted on to the F1-F10 plane. The diagram shows that the samples that plot along the positive side of the F10 axis are enriched in W, Au, and Sn relative to the rest of the sample population. Figure 51e shows the map of the F10 scores. The large positive scores indicate the W-Au-Sn association which occurs in the southeast corner of the WILUNA sheet, the Rose Hills, east of the Deep Well areas on the WILUNA sheet. To a lesser extent the association also occurs in the Mason Hill and Christmas Well (Erlistoun) areas of the DUKETON sheet.

5.6.2 PRINCIPAL COMPONENTS ANALYSIS: FERRICRETE SAMPLES

The results of the principal components analysis applied to the ferricrete data are shown in Table 10. In this analysis the first 8 components account for 75.3% of the data variation. The components that account for significant amounts of Au variation are the seventh, eighth, fifth and second components respectively.

The first component (21.4% of the data variation) is dominated by Co, Zn, Mn, Ga, Fe_2O_3, Ni, Ag, V, and Cr as seen by the relative contributions in Table 10. These elements most probably represent the ferricrete equivalents of the underlying supracrustal lithologies. The principal component scores of the elements

indicate that Co, Zn, Mn, Fe_2O_3, and Ni are all positively associated and are inversely associated with Ga, Ag, V, and Cr.

The second component (15.3% of the data variation) is dominated by As, V, Cr, Sb, Pb, Ag, Mn, Ga, and to a lesser extent Au (relative contributions). The component scores of the elements in Table 10 show that As, Sb, Pb and Au are positively associated and are inversely associated with V, Cr, Ag, and Ga.

Figure 52a shows a plot of the sample and element scores plotted on to the F1-F2 plane. The plot indicates that the Co, Mn, Ni, Fe_2O_3, and Zn association most probably defines the more mafic supracrustal rocks along the F1 axis. The more fractionated felsic rocks are indicated by the samples associated with Ga, Ag, and Sn. Although V and Cr are associated with the more fractionated materials, it is unclear as to their exact relationship with these rocks. The nature of the ferricrete chemistry may rule out the use of Cr or V as indicators of underlying lithological variation. The As, Sb, Pb, and Au association is clearly shown along the negative side of the F2 axis and indicates that the samples that plot in this field of the diagram have an enrichment in As, Sb, Pb, and Au relative to the rest of the sample population.

Figure 53a shows a map of the first principal component scores for the samples. The large positive scores indicate areas of Co, Mn, Ni, Fe_2O_3, and Zn enrichment. These are most probably mafic volcanic rocks that occur in the Duketon belt and the Lake Violet-Milrose-Yandal belt. Figure 53b shows a map of the second principal component scores for the samples. In this map large negative scores (>-0.20) indicate the As, Sb, Pb, Au association and are potential follow-up sites for further exploration. Large negative scores are located primarily in the Rose Hills area of the WILUNA sheet.

The fifth principal component (6.4% of the data variation) is dominated by Mo, Sb, Au, and W. Gold is inversely associated with Mo, Sb, and W as shown in Table 10. Figure 52b shows the scores of the elements plotted on to the F1-F5 plane. Negative F5 scores indicate Mo, Sb, and W enrichment while large positive F5 scores indicate Au enrichment. Figure 53c shows a map of the fifth component scores of the samples. Large negative scores associated with Mo, Sb, and W occur in the Swanson Hill area, and east of Duketon on the DUKETON sheet. Large negative scores also occur in the Rose Hills area on the WILUNA sheet. Large positive scores associated with Au enrichment occur in the Rose Hills area on the WILUNA sheet and in the German Well area of the DUKETON sheet.

The seventh principal component accounts for 5.5% of the data variation and the relative contributions in Table 10 indicate that it is dominated by Au, Mo, W, and Pb and that these are all positively associated with each other. Figure 52c shows the scores of the samples and elements plotted on to the F1-F7 plane. The Au, Mo, W, Pb association is seen along the positive side of the F7 axis. Figure 53d shows the scores of the samples plotted on to the map. Large positive scores (> 0.20) indicate the Au, Mo, W, and Pb association in the Swanson Hill, Urarey Well, east of Duketon, and northwest of Gerry Well on the DUKETON sheet. Large positive scores also occur in the Rose Hills area, Milrose, and Shady Well areas on the WILUNA sheet.

The eighth principal component accounts for 5.0% of the data variation. Table 10 shows the relative contributions of Cu, and Au are the most significant. Both of the elements are positively associated. Figure 52d shows the sample and elements scores plotted on to the F1-F8 plane. Large positive scores can be seen to be associated with Au and Cu. Figure 53e shows the sample scores plotted on to the map. Large positive scores occur in the Corner Well area of the DUKETON sheet, and in several places along the northwest trend and northerly trend of samples in the Lake Violet-Milrose-Yandal belt on the WILUNA sheet.

The application of principal components analysis has shown that there are several multi-element associations with Au. Although these associations occur as distinct principal components, these relationships all occur within the same altered/mineralized areas and thus the components do not necessarily reflect different geological processes, but rather variations in the style of one or two processes.

5.7 Anomaly Recognition by Principal Components Analysis

The results of the principal components analysis, discussed above, can be used as a means for ranking anomalies. Because the method determines factors based on the variance of the data, extreme values of the factors represent samples that are enriched in the linear combinations of elements that comprise that factor.

Tables 11a,b,c,d list the ranked scores for the second, fifth, sixth, and tenth components of the laterite samples, as discussed previously. Only negative scores are ranked for F6, while only positive scores are ranked for F10. Both positive and negative scores are ranked for F2 and F5. Negative scores are ranked in descending order while positive scores are ranked in ascending order.

Tables 12a,b,c,d list the ranked scores for the second, fifth, seventh, and eighth components for the ferricrete samples. Only positive scores are ranked for F7. Both positive and negative scores are ranked for F2, F5, and F8.

Robust principal component scores assist in verifying the atypical nature of some of these "outlier" samples. The areas of highest score-ranking have already been discussed in the section on "Principal Components Analysis". Many of these scores are coincident with high ranking (> 90th percentile) abundances of individual elements (Tables 6 and 7) and the CHI-6*X, PEG-4, and NUMCHI indices (to be discussed in Section 5.8).

5.8 Anomaly Recognition by the CHI-6*X, PEG-4, and NUMCHI Indices

The initial regional samples of **laterites** were selected from the database and were used to calculate the CHI-6*X, PEG-4, and NUMCHI indices as outlined by Smith and Perdrix (1983). These indices are based on the empirical selection of pathfinder elements, from orientation studies, that are combined to produce a "score". The magnitude of the score is directly proportional to the significance of the exploration target. The indices are calculated according to the following formulae:

$$\text{CHI-6*X} = \text{As} + 3.56\text{x}\text{Sb} + 10\text{x}\text{Bi} + 3\text{x}\text{Mo} + 30\text{x}\text{Ag} + 30\text{x}\text{Sn} + 10\text{x}\text{W} + 3.5\text{x}\text{Se},$$

$$\text{PEG-4} = .09\text{x}\text{As} + 1.33\text{x}\text{Sb} + \text{Sn} + 0.14\text{x}\text{Ga} + 0.4\text{x}\text{W} + 0.6\text{x}\text{Nb} + \text{Ta}.$$

CHI-6*X and PEG-4 indices must be interpreted cautiously as these indices can be very large, but the value can be the result of only one anomalous element. A useful adjunct to these indices is the NUMCHI index.

The NUMCHI index is based on an integer accumulation of the presence of a number of elements that exceed a given threshold and is thus a measure of the *number* of anomalous elements that are present.

The following elements and thresholds were used for the NUMCHI index:

Laterites											
Element:	Cu	Pb	Zn	As	Sb	Bi	Mo	Ag	Sn	W	Se
Threshold: (ppm)	265	31	183	101	6	3	4	0.6	4	17	6
Ferricretes											
Element:	Cu	Pb	Zn	As	Sb	Bi	Mo	Ag	Sn	W	Se
Threshold: (ppm)	276	38	695	105	6	4	5	0.2	3	21	6

For a given sample, a cumulative score is obtained by adding 1 for each element that exceeds the threshold. Thus, for this NUMCHI index, a maximum possible score would be 11. The threshold values were chosen as the 90th percentile value for the distributions of the elements. These values were taken from Table 3a (Laterites) and Table 4a (Ferricretes) which provide background values for the "R" (regional) samples that were collected over the area.

These indices are subject to modification which is largely dependent upon the regional background values for which the indices are calculated. These formulae should not be applied without careful consideration of the materials being used, preferably from an orientation study, over the area. Depending upon the commodities being sought, the NUMCHI index can be varied by adding or deleting elements and varying the threshold coefficients.

Laterites

Areas most worthy of further follow-up contain samples that rank in the upper percentile range of any individual index. However, the index must be above the regional background total for the index used. Tables 13a,b list the CHI-6*X and PEG-4 indices for the samples that scored greater than the 90th percentile level for the laterite samples. Table 13c lists the samples for which NUMCHI is greater than 3 (more than 3 anomalous elements). Maps of the anomalous samples are shown in Figures 54a,b,c.

Figure 54a shows the CHI-6*X indices plotted on to the map. Notably large indices occur in the Rose Hills, Milrose, and Biddy Well areas on the WILUNA sheet, and large CHI-6*X values occur in the Quongdong Well, Urarey Well, northwest of Gerry Well, and Corner Well areas on the DUKETON sheet.

Figure 55a shows the PEG-4 indices plotted on to the map. Large PEG-4 indices occur in the same localities as for the CHI-6*X indices.

The NUMCHI indices are plotted on the map in Figure 54c. The indices with values greater than 3 occur in the Rose Hill, Milrose, and Biddy Well areas on the WILUNA sheet, and in the Quongdong Well, Urarey Well, and the Corner Well area on the DUKETON sheet.

Ferricretes

The use of the CHI-6*X and PEG-4 indices on the ferricrete materials may not be as readily interpretable as for the laterite materials for which they were designed. Nonetheless, the indices generated using these materials can still provide a guide-line for follow-up, particularly for samples that rank above the 95th percentile.

Tables 14a,b list the CHI-6*X and PEG-4 indices for the samples that scored greater than the 90th percentile level for the ferricrete samples. Table 14c lists the samples for which NUMCHI is greater than 4 (more than 4 anomalous elements). Figures 55a,b,c show the three indices plotted on to the map.

Figures 55a,b show that the significant CHI-6*X and PEG-4 indices occur primarily in the Rose Hills area on the WILUNA sheet. Figure 55c displays the same feature, where the Rose Hills area contains the greatest number of anomalous elements.

The use of these indices suggests that the most favourable areas for follow-up exploration would be in the Rose Hills, Milrose, and Biddy Well areas on the WILUNA sheet, and in the Quongdong Well, Urarey Well, and the Corner Well area on the DUKETON sheet.

5.9 Anomaly Recognition by the use of X^2 [Chi-Square] Plots

Most anomaly recognition procedures are based upon determining the threshold that distinguishes background from anomalous values. However, the use of multivariate procedures can be useful in determining background from anomalous samples for a set of desired elements.

Garrett (1989, 1990) describes the use of the covariance matrix as a tool for distinguishing background from anomalous sample populations. The covariance matrix contains information on the variability of the elements as well as their inter-relationships. The multi-element data define a hyper-ellipsoid in multidimensional space. In a multivariate normal sample population, most samples fall within a close distance of each other and by definition are part of the background group of samples. However, if outliers are included in the data, the shape of the hyper-ellipsoid that is defined by the covariance matrix changes. The distance of each sample to the centroid of the cloud of points is the Mahalanobis distance.

Outliers can be distinguished from the main background population by determining the Mahalanobis distance of each sample to the group centroid. The distances can be compared to the "expected" distances of a multivariate normal population (cumulative probability with the number of degrees of freedom defined as the number of variables) by the use of chi-square (X^2) values. This procedure *should not be confused* with the CHI-6*X index which uses a suite of chalcophile elements for the calculation of a chalcophile index.

A graphical procedure of plotting the Mahalanobis distances of the observed from the expected allows for the detection of outliers. If the sample population is multivariate normal, then the Chi-square plot is a straight

line. If the population contains outliers, then the observed Mahalanobis distances are greater than the expected chi-square values and the plot becomes non-linear. The procedure was carried out on a selected group of elements of chalcophile affinity, namely: Cu, Zn, Pb, As, Sb, Bi, Mo, Ag, Sn, W, Se, Ga, Nb, and Ta.

Laterites

Table 15 and Figures 56a,b,c show the results of the Chi-square/Mahalanobis Distance procedure.

Figure 56a shows a plot of the Mahalanobis distances vs. theoretical Chi-square distances for 266 laterite samples. The Mahalanobis distances were based on the ordinary sample mean calculated for each of the chalcophile elements. The figure shows that samples having large Mahalanobis distances depart significantly from the expected Chi-square values. This results in the upper samples breaking away from the trend of the main group of data. The original data were then re-ordered based on the Mahalanobis distance from the group mean.

The procedure was then repeated using the re-ordered data. The sample means were then recalculated without the upper 15% of the ranked data (15% trimming of the data). This is a more robust estimate of the element means. The corresponding Mahalanobis distances are thus different. Figure 56b shows the Mahalanobis distances of the 266 samples versus the Chi-square distribution. The anomalous values are even further enhanced by the 15% trim of the data for the estimate of the group mean. Figure 56c shows a plot of this dataset with the upper 15% samples deleted. The sample points lie on a smooth continuous curve. Ideally, the points should define a straight line. This is based on the assumption that the data are multivariate normally distributed. This is not the case for most of the elements which have a skewed distribution. Thus the curved line results from non-normal distributions. The important feature is the *continuity* of the curve. If the curve is continuous then the samples can be assumed to be from a uniform population. Thus the samples identified as departing from the main trend in Figure 56b can be targeted as anomalous samples and their locations require follow-up. These upper samples are identified in Table 15.

Figure 57 shows a map of the Mahalanobis distances based on the 15% trimming of the data. The samples with the large Mahalanobis distances can be interpreted as being anomalous. Anomalous samples are observed in the Rose Hills, Milrose, and Biddy Well areas on the WILUNA sheet, and northwest of Gerry Well, Quongdong Well, Urarey Well, and east of Duketon on the DUKETON sheet.

Ferricretes

Table 16 and Figures 58a,b,c show the results of the Chi-square/Mahalanobis Distance procedure for ferricretes. The same procedure was applied as used in the laterites. Figure 58a shows the Mahalanobis distances versus the Chi-square distribution for the samples using the ordinary estimates of the means. Figure 58b shows the same samples using a 15% trim from the ordered samples derived from Figure 58a, and Figure 58c shows the samples with the upper 15% removed. The patterns of the three graphs are similar to those for the laterites in Figure 56a,b,c. The anomalous samples are clearly identified in Figure 58b. Figure 58c shows a more or less continuous curve for the trimmed ferricrete materials.

Figure 59 shows the map of Mahalanobis distances based on the 15% trimming of the data. The samples with large Mahalanobis distances are anomalous and occur in the Rose Hills, and Milrose areas on the WILUNA sheet, and east of Duketon, Quongdong Well, Urarey Well, and the Gerry Well areas on the DUKETON sheet.

It is important to keep in mind that these anomalies are based on a selected suite of elements (Cu, Zn, Pb, As, Sb, Bi, Mo, Ag, Sn, W, Se, Ga, Nb, Ta) that best reflect chalcophile enrichment and thus, may not reflect other processes that might be investigated. This analysis naturally is biased towards anomalous groups of elements that are likely to be associated within the greenstone sequences.

6.0 DISCUSSION AND CONCLUSIONS

Gold mineralization is commonly associated with an increase in the abundance of a variety of elements, most commonly, As, Sb, W, Mo, B, Ag, Li, Ba, Rb, and Cr in the unweathered profile. As well, Cu, Pb, and Zn can be present in some Au deposits (Groves, 1988; Colvine *et al.*, 1988). However, not all of these elements are present for all types of deposits. Pegmatite associated rare metal deposits can be indicated by enrichment of

Bi, As, Sb, Mo, Sn, Ge, W, Nb, and Au. Any one or combination of these elements can be considered as possible pathfinders to a variety of ore deposits.

The Tables of summary statistics and histograms are a useful means for determining the range and distribution of elemental abundances within the area being investigated. In this particular study, the histograms clearly reflect the bimodal nature of the materials associated with the greenstone and the granitoid areas. The histograms in this study may assist as a basis of comparison between terrains in which the underlying lithologies are uncertain. Statistical procedures, such as those outlined by Smith *et al.* (1984), could be applied to unknown samples which could characterize the affinity with either greenstone or granitoid lithologies. This approach is currently being investigated.

The maps of the elements can be useful for isolating elevated abundances for further follow-up sampling. In particular, Au (Figure 49) abundances are useful for isolating the more obvious areas of potential economic Au. Figure 49 shows that Au values increase primarily in the Rose Hills, Milrose, southeast corner of the WILUNA sheet, and in the southern part of the Duketon belt on the DUKETON sheet.

Several individual elements (Bi, Mo, Sn, W, Ag, Nb, Se) indicate that the Rose Hills, Milrose, and Biddy Well areas are the most favourable areas for exploration on the WILUNA sheet and the Quongdong Well, Urarey Well, Christmas Well (Erlistoun), and Swanson Hill areas are the most favourable on the DUKETON sheet.

Other elements are difficult to assess individually. Since most economic commodities being sought have multi-element geochemical signatures, it makes sense to employ methods that make use of these multi-element characteristics. The results of the principal components analysis, the CHI-6*X, PEG-4, and NUMCHI indices, and Mahalanobis distance methods all show zones that have multi-element enrichment and suggest additional follow-up investigation. Exploration for Au and associated precious metal deposits may be assisted by the use of several of these multi-element methods. The use of the multi-element indices has indicated that the Rose Hills and Milrose areas contain the most significant number of anomalous samples on the WILUNA sheet and several localities within the Duketon greenstone belt, on the DUKETON sheet, are also favourable targets for further exploration.

Previous reports (Grunsky *et al.*, 1988, 1989) suggested the presence of chalcophile corridors within the Murchison belt and other areas in the Yilgarn block (Smith *et al.*, 1989) that define zones of economic mineral potential. The distribution of samples in the area is sufficiently sparse that it would be difficult to infer such a trend.

The data and results presented in this report, plus additional geophysical, lithological, lithogeochemical, and structural data, may provide sufficient information for a selective and cost efficient exploration programme.

7.0 REFERENCES

Anand, R.R., Smith, R.E., Innes, J., Churchward, H.M., Perdrix, J.L. and Grunsky, E.C., 1989. Laterite Types and Associated Ferruginous Materials, Yilgarn Block WA, Terminology, Classification, and Atlas; Chapter 3, *CSIRO Exploration Geoscience Restricted Report 60R.*

Birrell, R.D. and Smith, R.E., 1984. Project C Report, Review of Anomalies, Geochemical Assessment, CSIRO, September 1984, 12 pp.

Bunting, J.A., 1980. KINGSTON, 1:250 000 *Geological Series-Explanatory Notes*, Geological Survey of Western Australia, SG 51-10, 18 pp., accompanied by 1:250 000 Geological Map.

Bunting, J.A. and Williams, S.J., 1979. SIR SAMUEL, 1:250 000 *Geological Series-Explanatory Notes*, Geological Survey of Western Australia, SG 51-13, 40 pp., accompanied by 1:250 000 Geological Map.

Bunting, J.A. and Chin, R.J., 1979. DUKETON, 1:250 000 *Geological Series-Explanatory Notes*, Geological Survey of Western Australia, SG 51-14, 24 pp., accompanied by 1:250 000 Geological Map.

Colvine, A.C. *et al.*, 1988. Archaean Lode Gold Deposits in Ontario; *Ontario Geological Survey Miscellaneous Paper 139*, 136 pp.

Davis, J.C., 1986. *Statistics and Data Analysis in Geology*, John Wiley & Sons Inc., second edition, 646 pp.

Elias, M., and Bunting, J.A., 1982. WILUNA, 1:250 000 *Geological Series-Explanatory Notes*, Geological Survey of Western Australia, SG 51-9, 20 pp., accompanied by 1:250 000 Geological Map.

Garrett, R.G., 1989. The chi-square plot: a tool for multivariate outlier detection, *J. Geochem. Explor.*,. **32**:319-41.

Garrett, R.G., 1990. A Robust Multivariate Procedure with Applications to Geochemical Data. In: Proceedings of the Colloquium on "*Statistical Applications in the Earth Sciences*", Geological Survey of Canada Paper 89-9, pp. 309-318.

Geological Survey of Western Australia, 1990. *Geology and Mineral Resources of Western Australia*: Geological Survey of Western Australia, Memoir 3, 827 pp.

Griffin, T.J., 1990. Eastern Goldfields Province. In: *Geology and Mineral Resources of Western Australia*: Geological Survey of Western Australia, Memoir 3, 77-119.

Groves, D.I. 1988. Gold Mineralization in the Yilgarn Block, Western Australia. In: *Bicentennial Gold 88, Extended Abstracts, Oral Programme*, Geological Society of Australia Inc., Abstracts No. 22, 13-23.

Grunsky, E.C., 1986. Recognition of Alteration in Volcanic Rocks Using Statistical Analysis of Lithogeochemical Data, *J. Geochem. Explor.*, **25**:157-83.

Grunsky, E.C., 1990. Report on Laterite Geochemistry in the CSIRO-AGE Database for the Central Yilgarn Region, *Exploration Geoscience Restricted Report, 121R*, 162 pp., 2 5.25" diskettes.

Grunsky, E.C., Innes, J., Smith, R.E. and Perdrix, J.L., 1988. Report on Laterite Geochemistry in the CSIRO-AGE Database for the Southern Murchison Region, *Exploration Geoscience Restricted Report, 2R*, 92 pp., 1 5.25" diskette.

Grunsky, E.C., Innes, J., Smith, R.E. and Perdrix, J.L., 1989. Report on Laterite Geochemistry in the CSIRO-AGE Database for the Northern Murchison Region, *Exploration Geoscience Restricted Report, 68R*, 148 pp., 1 5.25" diskette.

Hallberg, J.A., 1984. A Geochemical Aid to Igneous Rock Type Identification in Deeply Weathered Terrain, *J. Geochem. Explor.*, **20**:1-8.

Hickman, A.H. and Watkins, K.P., 1988. Gold Mineralization in the Murchison Province, Western Australia. In: *Bicentennial Gold 88, Extended Abstract, Poster Programme*, Vol. 1, Geological Society of Australia Inc., Abstracts No. 23, 23-25.

Howarth, R.J., 1983. Statistics and Data Analysis in Geochemical Prospecting, edited by R.J. Howarth, Vol. 2. In: *Handbook of Exploration Geochemistry*, edited by G.J.S. Govett, Elsevier, 437 pp.

Howarth, R.J. and Sinding-Larsen, 1983. Multivariate Data Analysis, Chapter 6; Statistics and Data Analysis in Geochemical Prospecting, edited by R.J. Howarth, Vol. 2. In: *Handbook of Exploration Geochemistry*, edited by G.J.S. Govett, Elsevier, 437 pp.

Jöreskog, K.G., Klovan, J.E. and Reyment, R.A., 1976. *Geological Factor Analysis*. Elsevier Scientific Publishing Company, New York, 178 pp.

LeMaitre, R.W., 1989. *A Classification of Igneous Rocks and Glossary of Terms*, Recommendations of the International Union of Geological Sciences Subcommission on the Systematics of Igneous Rocks, R.W. LeMaitre, editor, Blackwell Scientific Publications, Melbourne, 193 pp.

Marston, R.J., 1984. Nickel Mineralization in Western Australia, Geological Survey of Western Australia, *Mineral Resources Bulletin 14*, 271 pp.

Mazzucchelli, R.H. and James, C.H., 1966. Arsenic as a guide to gold mineralization in laterite-covered areas of Western Australia., *Trans. Inst. Min. Metall.* Sect, B, **75**:285-94.

Smith, R.E., 1987. Current Research at CSIRO Australia on Multi-element Laterite Geochemistry for Detecting Concealed Mineral Deposits, *Chemical Geology*, **60**:205-11.

Smith, R.E., Moeskops, P.G. and Nickel, E.H., 1979. Multi-element geochemistry at the Golden Grove Cu-Zn-Ag deposit. In: J.E. Glover, D.I. Groves, and R.E. Smith (Editors), *Pathfinder and Multi-element Geochemistry in Mineral Exploration* Univ. W. Australia, Geol. Dept. Extension Service, Publ. 4, 30-41.

Smith, R.E. and Perdrix, J.L. 1983. Pisolitic laterite geochemistry in the Golden Grove massive sulphide district, Western Australia, *J. Geochem. Explor.*, **18**:131-64.

Smith, R.E., Campbell, N.A. and Litchfield, R. 1984. Multivariate Statistical Techniques Applied To Pisolitic Laterite Geochemistry At Golden Grove, Western Australia, *J. Geochem. Explor.*, **22**:193-216.

Smith, R.E., Perdrix, J.L. and Davis, J.M. 1987. Dispersion into Pisolitic Laterite from the Greenbushes Mineralized Sn-Ta Pegmatite System, Western Australia, *J. Geochem. Explor.*, **28**:251-65.

Smith, R.E., Birrell, R.D. and Brigden, J.F.. 1989. The implications to exploration of chalcophile corridors in the Archaean Yilgarn Block, Western Australia, as revealed by laterite geochemistry, *J. Geochem. Explor.*, **32**:169-84.

Stanley, C.R. and Sinclair, A.J., 1987. Anomaly recognition for multi-element geochemical data- A background characterization approach. *J. Geochem. Explor.*, **29**:333-53.

Zeegers, H., Goni, J. and Wilhem, E., 1981. Geochemistry of lateritic profiles over a disseminated Cu-Mo mineralization in Upper Volta (West Africa) - preliminary results. In: M.K. Roychowdhury, B.P. Radhakrishna, R. Vaidyanadhan, P.K. Banerjee and K. Ranganathan (Editors), *Lateritization Processes*. Balkema Publishers, Rotterdam, pp. 359-68.

Zhou, D., Chang, T. and Davis, J.C., 1983. Dual Extraction of R-Mode and Q-Mode Factor Solutions, *Mathematical Geology*, **15**(5):581-606.

APPENDIX 1

Data Format of the Wiluna Database

The data is contained on a double sided high density (360Kb) 5.25" floppy diskette formatted for an IBM PC or compatible computer running under DOS.

The name of the file that contains the data is: WILUNA.SDF

Refer to Table 2 for the meaning of the various element codes.
The data is recorded in ASCII format and each record of the file has the following attributes:

Field ec	Name	Type	Width	Dec	Field	Name	Type	Width	D
1	CONFID	Logical 1			22	ZN	Numeric	6	0
2	SAMPLE	Character	7		23	NI	Numeric	6	0
3	SAMPLETYPE	Character	5		24	CO	Numeric	6	0
4	MAPREF	Character	8		25	AS	Numeric	6	0
5	EASTING	Numeric	6	0	26	SB	Numeric	6	0
6	NORTHING	Numeric	7	0	27	BI1	Numeric	6	0
7	GEOLOGY	Character	5		28	BI2	Numeric	6	0
8	ANOMALY	Character	5		29	MO	Numeric	6	0
9	DESCRIPT	Character	5		30	SN1	Numeric	6	0
10	SIO2	Numeric	6	2	31	SN2	Numeric	6	0
11	AL2O3	Numeric	6	2	32	GE	Numeric	6	0
12	FE2O3	Numeric	6	2	33	GA	Numeric	6	0
13	MGO	Numeric	6	3	34	W	Numeric	6	0
14	CAO	Numeric	6	3	35	BA	Numeric	6	0
15	TIO2	Numeric	6	3	36	ZR	Numeric	6	0
16	AG	Numeric	6	1	37	NB	Numeric	6	0
17	MN	Numeric	6	0	38	TA	Numeric	6	0
18	CR	Numeric	6	0	39	SE	Numeric	6	0
19	V	Numeric	6	0	40	BE	Numeric	6	0
20	CU	Numeric	6	0	41	AU	Numeric	6	0
21	PB	Numeric	6	0					

For the variable, GEOLOGY, the following codes are used to define the geology of the areas where the samples were collected:

AVR - Acid Volcanic Rocks
BIF - Banded Iron Formation
FGM - Foliated Granite and Migmatite
GIR - Granitic Intrusions
LBU - Layered Basic and Ultrabasic Intrusions
MBU - Metabasic and Ultrabasic Rocks
MSR - Metasedimentary Rocks
UMG - Undifferentiated Massive Granitic Rocks

The codes were derived from the geological maps of the Western Australia Geological Survey.

APPENDIX 1 (cont'd)

A FORTRAN 77 format statement would read in the data in the following manner

```
      LOGICAL CONFID
      CHARACTER*5 SAMTYP,GEOL,DESCRIPT,ANOMALY
      CHARACTER*7 SAMPLE
      CHARACTER*8 MAPREF
      REAL*4  EAST,NORTH,
     $     SIO2,AL2O3,FE2O3,MGO,CAO,TIO2,AG,MN,CR,V,CU,PB,
     $     ZN,NI,CO,AS,SB,BI1,BI2,MO,SN1,SN2,GE,GA,W,BA,ZR,
     $     NB,TA,SE,BE,AU
      READ(5,10) CONFID,SAMPLE,SAMTYP,MAPREF,EAST,NORTH,
     $     GEOL,ANOMALY,DESCRIPT,
     $     SIO2,AL2O3,FE2O3,MGO,CAO,TIO2,AG,MN,CR,V,CU,PB,
     $     ZN,NI,CO,AS,SB,BI1,BI2,MO,SN1,SN2,GE,GA,W,BA,ZR,
     $     NB,TA,SE,BE,AU
   10 FORMAT(L1,A7,A5,A8,F6.0,F7.0,3A5,3F6.2,3F6.3,F6.1,25F6.0)
```

Negative values indicate less than detection limit. The detection limit is defined as the absolute value of the quoted value.

Zero values indicate that no analysis was performed for that element.

Table 3a:
Summary statistics for Wiluna Area (Wiluna, Kingston, Duketon, Sir Samuel)

"R" Regional Samples

Sample types:
LP CP LN CN PN VL MS

No. of Samples in Group: 149

Element		Lab	Method	L.L.D.	#Samples	Percentiles								
						1%	5%	10%	25%	50%	75%	90%	95%	99%
Fe203	Wt%	Amdel	AAS-HF	0.1	143	7.15	32.74	36.89	47.75	57.47	65.05	71.20	76.20	85.07
Ag	ppm	Amdel	OES	0.1	143	.03	.03	.03	.03	.03	.20	.60	.80	3.00
Mn	ppm	Amdel	AAS	5.0	143	28.00	43.00	50.00	72.00	126.00	261.00	598.00	836.00	3946.00
Cr	ppm	Amdel	XRF	5.0	143	142.00	265.00	290.00	463.00	682.00	1246.00	2656.00	3720.00	9999.00
V	ppm	Amdel	XRF	10.0	143	3.33	297.00	408.00	638.00	911.00	1319.00	1593.00	2182.00	2567.00
Cu	ppm	Amdel	AA-HF	2.0	143	9.00	20.00	47.00	84.00	123.00	194.00	265.00	315.00	473.00
Pb	ppm	Amdel	XRF	4.0	143	.67	.67	6.00	11.00	18.00	24.00	31.00	39.00	73.00
Zn	ppm	Amdel	AA-HF	2.0	143	14.00	28.00	31.00	38.00	61.00	128.00	183.00	266.00	974.00
Ni	ppm	Amdel	AA-HF	5.0	143	13.00	28.00	36.00	50.00	65.00	97.00	139.00	255.00	1168.00
Co	ppm	Amdel	AA-HF	5.0	143	1.67	1.67	1.67	6.00	13.00	23.00	44.00	98.00	285.00
As	ppm	Analb	XRF	2.0	143	3.00	6.00	8.00	14.00	23.00	47.00	101.00	180.00	987.00
Sb	ppm	Amdel	XRF	2.0	143	.67	.67	.67	.67	.67	4.00	6.00	10.00	24.00
Bi	ppm	Amdel	OES	1.0	143	.33	.33	.33	.33	.33	.33	.33	.33	6.00
Bi	ppm	Amdel	XRF	1.0	143	.33	.33	.33	.33	.33	2.00	3.00	4.00	7.00
Mo	ppm	Amdel	XRF	2.0	143	.67	.67	.67	.67	2.00	3.00	4.00	5.00	15.00
Sn	ppm	Amdel	OES	1.0	143	.33	.33	.33	.33	.33	.33	.33	.33	6.00
Sn	ppm	Amdel	XRF	1.0	143	.33	.33	.33	.33	1.00	3.00	4.00	5.00	7.00
Ge	ppm	Amdel	OES	1.0	143	.33	.33	.33	.33	.33	.33	1.00	1.00	2.00
Ga	ppm	Amdel	OES	1.0	143	.33	3.00	6.00	10.00	15.00	15.00	25.00	25.00	25.00
W	ppm	Amdel	XRF	10.0	143	3.33	3.33	3.33	3.33	3.33	3.33	17.00	18.00	28.00
Nb	ppm	Amdel	XRF	4.0	143	1.33	1.33	1.33	1.33	1.33	4.00	7.00	12.00	50.00
Ta	ppm	Amdel	XRF	3.0	143	1.00	1.00	1.00	1.00	1.00	1.00	3.00	6.00	7.00
Se	ppm	Amdel	XRF	1.0	143	.33	.33	.33	2.00	3.00	5.00	6.00	7.00	10.00
Be	ppm	Amdel	OES	1.0	143	.33	.33	.33	.33	.33	.33	.33	.33	1.00
Au	ppb	Analb	234	1.0	142	1.00	1.00	1.00	2.00	3.00	5.00	14.00	18.00	109.00

Table 3a: (cont'd)
Summary statistics for Wiluna Area (Wiluna, Kingston, Duketon, Sir Samuel)
Laterites
Sample types:
LP CP LN CN PN VL MS

Element		Lab	Method	L.L.D.	#Samples	Minimum	Maximum	Median	Mode	Mean	Std. Dev.
Fe2O3	Wt%	Amdel	AAS-HF	0.1	143	6.29	86.07	56.33	59.77	55.68	14.09
Ag	ppm	Amdel	OES	0.1	143	.03	3.00	.03	.04	.21	.49
Mn	ppm	Amdel	AAS	5.0	143	20.00	4567.00	120.00	48.56	290.68	590.91
Cr	ppm	Amdel	XRF	5.0	143	74.00	9999.00	674.00	456.83	1257.30	1765.09
V	ppm	Amdel	XRF	10.0	143	3.33	2623.00	908.00	798.55	1000.94	535.84
Cu	ppm	Amdel	AA-HF	2.0	143	8.00	508.00	120.00	95.49	146.09	92.62
Pb	ppm	Amdel	XRF	4.0	143	.67	98.00	18.00	18.88	19.08	13.08
Zn	ppm	Amdel	AA-HF	2.0	143	14.00	1170.00	60.00	40.46	107.90	155.38
Ni	ppm	Amdel	AA-HF	5.0	143	8.00	1832.00	65.00	51.23	114.28	207.69
Co	ppm	Amdel	AA-HF	5.0	143	1.67	351.00	12.00	2.15	24.12	43.96
As	ppm	Analb	XRF	2.0	143	.67	2375.00	23.00	12.32	69.31	224.97
Sb	ppm	Amdel	XRF	2.0	143	.67	47.00	.67	.71	2.91	5.07
Bi	ppm	Amdel	OES	1.0	143	.33	15.00	.33	.00	.52	1.35
Bi	ppm	Amdel	XRF	1.0	143	.33	23.00	.33	.35	1.16	2.23
Mo	ppm	Amdel	XRF	2.0	143	.67	16.00	2.00	.69	2.34	2.25
Sn	ppm	Amdel	OES	1.0	143	.33	10.00	.33	.00	.48	1.04
Sn	ppm	Amdel	XRF	1.0	143	.33	7.00	1.00	.36	1.79	1.81
Ge	ppm	Amdel	OES	1.0	143	.33	2.00	.33	.34	.48	.35
Ga	ppm	Amdel	OES	1.0	143	.33	30.00	15.00	15.01	13.42	6.87
W	ppm	Amdel	XRF	10.0	143	3.33	43.00	3.33	3.41	6.55	6.52
Nb	ppm	Amdel	XRF	4.0	143	1.33	60.00	1.33	1.39	3.84	7.55
Ta	ppm	Amdel	XRF	3.0	143	1.00	8.00	1.00	1.02	1.45	1.42
Se	ppm	Amdel	XRF	1.0	143	.33	10.00	3.00	2.03	3.41	2.20
Be	ppm	Amdel	OES	1.0	143	.33	1.00	.33	.00	.36	.13
Au	ppb	Analb	234	1.0	142	.33	232.00	3.00	3.07	7.25	21.70

NOTE: Mode estimated by binning of data: # of bins= 100.
Bin width=(95%ile-minimum value)/100.0

Table 3b: Summary statistics for Wiluna Area (Wiluna, Kingston, Duketon, Sir Samuel)

"F2/F3" Follow-up Samples

Sample types:
LP CP LN CN PN VL MS

No. of Samples in Group: 123

Element		Lab	Method	L.L.D.	#Samples	Percentiles								
						1%	5%	10%	25%	50%	75%	90%	95%	99%
SiO2	Wt%	Csiro	ICP-FS	0.5	48	7.57	10.97	12.21	14.08	16.52	19.90	25.26	28.93	60.21
Al2O3	Wt%	Csiro	ICP-FS	0.5	48	5.60	6.59	8.25	11.43	13.40	16.17	19.06	21.36	23.22
Fe2O3	Wt%	Amdel	AAS-HF	0.1	123	27.74	32.31	39.17	50.04	57.90	64.91	73.92	76.35	82.06
MgO	Wt%	Csrio	ICP-FS	0.05	48	.04	.04	.04	.05	.06	.08	.12	.13	.14
CaO	Wt%	Csiro	ICP-FS	0.05	48	.05	.05	.05	.06	.07	.08	.11	.12	.14
TiO2	Wt%	Csiro	ICP-FS	0.003	48	.37	.40	.41	.61	.82	1.15	1.78	1.99	7.77
Ag	ppm	Amdel	OES	0.1	123	.03	.03	.03	.03	.20	.60	1.00	2.00	3.00
Mn	ppm	Amdel	AAS	5.0	123	31.00	53.00	60.00	113.00	184.00	442.00	1273.00	2049.00	3094.00
Cr	ppm	Amdel	XRF	5.0	123	104.00	227.00	307.00	446.00	795.00	1236.00	2716.00	5375.00	7567.00
V	ppm	Amdel	XRF	10.0	123	13.00	276.00	337.00	639.00	886.00	1234.00	1518.00	1829.00	2092.00
Cu	ppm	Amdel	AA-HF	2.0	123	21.00	42.00	58.00	103.00	141.00	200.00	251.00	299.00	464.00
Pb	ppm	Amdel	XRF	4.0	123	.67	5.00	8.00	13.00	18.00	26.00	41.00	51.00	82.00
Zn	ppm	Amdel	AA-HF	2.0	123	19.00	22.00	25.00	34.00	60.00	146.00	290.00	411.00	692.00
Ni	ppm	Amdel	AA-HF	5.0	123	9.00	17.00	21.00	40.00	69.00	121.00	330.00	420.00	1136.00
Co	ppm	Amdel	AA-HF	5.0	123	1.67	1.67	1.67	8.00	15.00	33.00	98.00	153.00	190.00
As	ppm	Analb	XRF	2.0	123	3.00	7.00	13.00	17.00	34.00	57.00	125.00	283.00	947.00
Sb	ppm	Amdel	XRF	2.0	123	.67	.67	.67	.67	.67	4.00	7.00	9.00	22.00
Bi	ppm	Amdel	OES	1.0	123	.33	.33	.33	.33	.33	.33	.33	.33	1.00
Bi	ppm	Amdel	XRF	1.0	123	.33	.33	.33	.33	.33	.33	2.00	2.00	4.00
Mo	ppm	Amdel	XRF	2.0	123	.67	.67	.67	.67	2.00	3.00	5.00	7.00	10.00
Sn	ppm	Amdel	OES	1.0	123	.33	.33	.33	.33	.33	.33	1.00	1.00	2.00
Sn	ppm	Amdel	XRF	1.0	123	.33	.33	.33	.33	3.00	5.00	6.00	7.00	12.00
Ge	ppm	Amdel	OES	1.0	123	.33	.33	.33	.33	.33	.33	1.00	1.00	2.00
Ga	ppm	Amdel	OES	1.0	123	.33	.33	1.00	5.00	10.00	15.00	30.00	30.00	40.00
W	ppm	Amdel	XRF	10.0	123	3.33	3.33	3.33	3.33	3.33	3.33	15.00	17.00	25.00
Ba	ppm	Csiro	ICP	100.0	48	88.00	98.00	103.00	121.00	157.00	340.00	519.00	752.00	1439.00
Zr	ppm	Csiro	ICP-FS	50.0	48	186.00	192.00	202.00	216.00	231.00	264.00	290.00	316.00	395.00
Nb	ppm	Amdel	XRF	4.0	123	1.33	1.33	1.33	1.33	1.33	5.00	7.00	10.00	16.00
Ta	ppm	Amdel	XRF	3.0	123	1.00	1.00	1.00	1.00	1.00	1.00	1.00	3.00	6.00
Se	ppm	Amdel	XRF	1.0	123	.33	.33	.33	2.00	3.00	4.00	6.00	7.00	8.00
Be	ppm	Amdel	OES	1.0	123	.33	.33	.33	.33	.33	.33	.33	.33	1.00
Au	ppb	Analb	234	1.0	123	.33	.33	.33	.33	1.00	3.00	7.00	12.00	65.00

Table 3b: (cont'd)
Summary statistics for Wiluna Area (Wiluna, Kingston, Duketon, Sir Samuel)

Sample types:
LP CP LN CN PN VL MS

Element		Lab	Method	L.L.D.	#Samples	Minimum	Maximum	Median	Mode	Mean	Std. Dev.
SiO2	Wt%	Csiro	ICP-FS	0.5	48	7.57	60.21	16.31	13.44	18.28	8.80
Al2O3	Wt%	Csiro	ICP-FS	0.5	48	5.60	23.22	13.36	12.93	13.73	3.99
Fe2O3	Wt%	Amdel	AAS-HF	0.1	123	16.87	83.21	57.62	59.99	56.62	12.95
MgO	Wt%	Csrio	ICP-FS	0.05	48	.04	.14	.06	.04	.07	.03
CaO	Wt%	Csiro	ICP-FS	0.05	48	.05	.14	.06	.06	.07	.02
TiO2	Wt%	Csiro	ICP-FS	0.003	48	.37	7.77	.76	.75	1.08	1.10
Ag	ppm	Amdel	OES	0.1	123	.03	4.00	.20	.04	.41	.66
Mn	ppm	Amdel	AAS	5.0	123	25.00	6549.00	182.00	116.08	476.02	816.91
Cr	ppm	Amdel	XRF	5.0	123	66.00	9999.00	777.00	357.99	1267.36	1643.24
V	ppm	Amdel	XRF	10.0	123	3.33	2133.00	877.00	779.24	941.91	459.05
Cu	ppm	Amdel	AA-HF	2.0	123	9.00	1641.00	140.00	109.05	165.08	156.88
Pb	ppm	Amdel	XRF	4.0	123	.67	158.00	18.00	14.01	22.76	19.22
Zn	ppm	Amdel	AA-HF	2.0	123	19.00	869.00	59.00	24.88	122.93	145.98
Ni	ppm	Amdel	AA-HF	5.0	123	1.67	1251.00	68.00	37.23	128.49	189.22
Co	ppm	Amdel	AA-HF	5.0	123	1.67	228.00	14.00	2.42	32.87	45.72
As	ppm	Analb	XRF	2.0	123	.67	1194.00	33.00	16.19	73.15	151.18
Sb	ppm	Amdel	XRF	2.0	123	.67	39.00	.67	.71	2.99	4.76
Bi	ppm	Amdel	OES	1.0	123	.33	20.00	.33	.00	.51	1.77
Bi	ppm	Amdel	XRF	1.0	123	.33	23.00	.33	.34	.78	2.15
Mo	ppm	Amdel	XRF	2.0	123	.67	21.00	2.00	.70	2.52	2.67
Sn	ppm	Amdel	OES	1.0	123	.33	2.00	.33	.34	.43	.29
Sn	ppm	Amdel	XRF	1.0	123	.33	13.00	3.00	.37	3.01	2.67
Ge	ppm	Amdel	OES	1.0	123	.33	2.00	.33	.34	.47	.32
Ga	ppm	Amdel	OES	1.0	123	.33	50.00	10.00	15.02	12.64	10.24
W	ppm	Amdel	XRF	10.0	123	3.33	35.00	3.33	3.40	6.11	5.86
Ba	ppm	Csiro	ICP	100.0	48	88.00	1439.00	152.00	131.16	259.79	254.96
Zr	ppm	Csiro	ICP-FS	50.0	48	186.00	395.00	229.00	220.45	241.38	43.08
Nb	ppm	Amdel	XRF	4.0	123	1.33	20.00	1.33	1.38	3.07	3.50
Ta	ppm	Amdel	XRF	3.0	123	1.00	9.00	1.00	1.01	1.23	1.04
Se	ppm	Amdel	XRF	1.0	123	.33	9.00	3.00	2.97	3.15	2.05
Be	ppm	Amdel	OES	1.0	123	.33	1.00	.33	.00	.35	.10
Au	ppb	Analb	234	1.0	123	.33	140.00	1.00	.98	4.25	14.08

NOTE: Mode estimated by binning of data: # of bins= 100.
Bin width=(95%ile-minimum value)/100.0

Table 4a: Summary statistics for Wiluna Area (Wiluna, Kingston, Duketon, Sir Samuel)

"R" Regional Samples

Sample types:
MF FF PF PE RC

No. of Samples in Group: 51

Element		Lab	Method	L.L.D.	#Samples	Percentiles								
						1%	5%	10%	25%	50%	75%	90%	95%	99%
Fe2O3	Wt%	Amdel	AAS-HF	0.1	41	30.45	64.77	68.91	73.63	76.49	81.06	84.64	86.21	92.07
Ag	ppm	Amdel	OES	0.1	41	.03	.03	.03	.03	.03	.03	.20	.40	.60
Mn	ppm	Amdel	AAS	5.0	41	72.00	146.00	228.00	699.00	2960.00	4055.00	4504.00	5289.00	9342.00
Cr	ppm	Amdel	XRF	5.0	41	35.00	118.00	158.00	189.00	324.00	543.00	867.00	2588.00	9999.00
V	ppm	Amdel	XRF	10.0	41	113.00	234.00	265.00	318.00	481.00	605.00	792.00	936.00	1459.00
Cu	ppm	Amdel	AA-HF	2.0	41	54.00	57.00	72.00	141.00	179.00	227.00	276.00	343.00	470.00
Pb	ppm	Amdel	XRF	4.0	41	.67	.67	.67	6.00	16.00	25.00	38.00	45.00	73.00
Zn	ppm	Amdel	AA-HF	2.0	41	39.00	49.00	72.00	163.00	320.00	446.00	695.00	835.00	893.00
Ni	ppm	Amdel	AA-HF	5.0	41	20.00	47.00	62.00	100.00	203.00	358.00	768.00	847.00	1728.00
Co	ppm	Amdel	AA-HF	5.0	41	1.67	13.00	23.00	51.00	102.00	170.00	270.00	297.00	612.00
As	ppm	Analb	XRF	2.0	41	.67	.67	2.00	5.00	12.00	26.00	105.00	169.00	2232.00
Sb	ppm	Amdel	XRF	2.0	41	.67	.67	.67	.67	.67	.67	6.00	8.00	16.00
Bi	ppm	Amdel	OES	1.0	41	.33	.33	.33	.33	.33	.33	.33	3.00	4.00
Bi	ppm	Amdel	XRF	1.0	41	.33	.33	.33	.33	.33	3.00	4.00	4.00	6.00
Mo	ppm	Amdel	XRF	2.0	41	.67	.67	.67	.67	2.00	4.00	5.00	7.00	16.00
Sn	ppm	Amdel	OES	1.0	41	.33	.33	.33	.33	.33	.33	.33	.33	2.00
Sn	ppm	Amdel	XRF	1.0	41	.33	.33	.33	.33	.33	2.00	3.00	3.00	7.00
Ge	ppm	Amdel	OES	1.0	41	.33	.33	.33	.33	.33	.33	.33	.33	1.00
Ga	ppm	Amdel	OES	1.0	41	.33	.33	.33	.33	2.00	3.00	15.00	15.00	20.00
W	ppm	Amdel	XRF	10.0	41	3.33	3.33	3.33	3.33	3.33	16.00	21.00	23.00	31.00
Nb	ppm	Amdel	XRF	4.0	41	1.33	1.33	1.33	1.33	1.33	1.33	1.33	6.00	8.00
Ta	ppm	Amdel	XRF	3.0	41	1.00	1.00	1.00	1.00	1.00	1.00	4.00	4.00	7.00
Se	ppm	Amdel	XRF	1.0	41	.33	.33	.33	.33	2.00	3.00	6.00	7.00	10.00
Be	ppm	Amdel	OES	1.0	41	.33	.33	.33	.33	.33	.33	.33	.33	1.00
Au	ppb	Analb	234	1.0	39	.33	.33	.33	1.00	2.00	4.00	5.00	8.00	21.00

Table 4a: (cont'd)
Summary statistics for Wiluna Area (Wiluna, Kingston, Duketon, Sir Samuel)

Sample types:
MF FF PF PE RC

Element		Lab	Method	L.L.D.	#Samples	Minimum	Maximum	Median	Mode	Mean	Std. Dev.
Fe2O3	Wt%	Amdel	AAS-HF	0.1	41	30.45	92.07	76.35	79.80	75.67	10.32
Ag	ppm	Amdel	OES	0.1	41	.03	.60	.03	.04	.09	.13
Mn	ppm	Amdel	AAS	5.0	41	72.00	9342.00	2742.00	4480.36	2741.17	1994.04
Cr	ppm	Amdel	XRF	5.0	41	35.00	9999.00	292.00	175.42	822.37	1880.93
V	ppm	Amdel	XRF	10.0	41	113.00	1459.00	439.00	289.94	507.54	256.61
Cu	ppm	Amdel	AA-HF	2.0	41	54.00	470.00	178.00	179.72	186.15	85.90
Pb	ppm	Amdel	XRF	4.0	41	.67	73.00	15.00	.89	18.32	16.13
Zn	ppm	Amdel	AA-HF	2.0	41	39.00	893.00	316.00	42.98	350.05	230.09
Ni	ppm	Amdel	AA-HF	5.0	41	20.00	1728.00	147.00	106.84	308.05	342.00
Co	ppm	Amdel	AA-HF	5.0	41	1.67	612.00	98.00	23.82	129.50	117.11
As	ppm	Analb	XRF	2.0	41	.67	2232.00	11.00	1.51	82.32	347.09
Sb	ppm	Amdel	XRF	2.0	41	.67	16.00	.67	.70	2.14	3.21
Bi	ppm	Amdel	OES	1.0	41	.33	4.00	.33	.35	.62	.91
Bi	ppm	Amdel	XRF	1.0	41	.33	6.00	.33	.35	1.39	1.66
Mo	ppm	Amdel	XRF	2.0	41	.67	16.00	2.00	.70	2.97	2.96
Sn	ppm	Amdel	OES	1.0	41	.33	2.00	.33	.00	.37	.26
Sn	ppm	Amdel	XRF	1.0	41	.33	7.00	.33	.35	1.12	1.51
Ge	ppm	Amdel	OES	1.0	41	.33	1.00	.33	.00	.37	.15
Ga	ppm	Amdel	OES	1.0	41	.33	20.00	1.00	.41	3.89	5.46
W	ppm	Amdel	XRF	10.0	41	3.33	31.00	3.33	3.43	9.76	7.88
Nb	ppm	Amdel	XRF	4.0	41	1.33	8.00	1.33	1.36	1.86	1.68
Ta	ppm	Amdel	XRF	3.0	41	1.00	7.00	1.00	1.01	1.46	1.32
Se	ppm	Amdel	XRF	1.0	41	.33	10.00	1.00	.37	2.29	2.46
Be	ppm	Amdel	OES	1.0	41	.33	1.00	.33	.00	.35	.10
Au	ppb	Analb	234	1.0	39	.33	21.00	2.00	.99	2.84	3.45

NOTE: Mode estimated by binning of data: # of bins= 100.
Bin width=(95%ile-minimum value)/100.0

Table 4b: Summary statistics for Wiluna Area (Wiluna, Kingston, Duketon, Sir Samuel)

"F2/F3" Follow-up Samples

Sample types:
MF FF PF PE RC

No. of Samples in Group: 123

Element		Lab	Method	L.L.D.	#Samples	Percentiles								
						1%	5%	10%	25%	50%	75%	90%	95%	99%
SiO2	Wt%	Csiro	ICP-FS	0.5	71	4.18	4.50	5.32	8.11	11.39	14.80	21.99	25.65	28.82
Al2O3	Wt%	Csiro	ICP-FS	0.5	71	1.20	1.49	1.91	2.71	4.60	6.10	8.31	9.56	12.67
Fe2O3	Wt%	Amdel	AAS-HF	0.1	123	45.46	55.62	58.90	66.34	73.49	78.06	81.78	83.21	88.64
MgO	Wt%	Csrio	ICP-FS	0.05	71	.04	.05	.06	.08	.11	.15	.19	.20	.27
CaO	Wt%	Csiro	ICP-FS	0.05	71	.06	.06	.07	.08	.10	.14	.23	.57	1.39
TiO2	Wt%	Csiro	ICP-FS	0.003	71	.05	.06	.09	.13	.27	.41	.84	1.12	2.66
Ag	ppm	Amdel	OES	0.1	123	.03	.03	.03	.03	.03	.20	.40	.60	2.00
Mn	ppm	Amdel	AAS	5.0	123	79.00	188.00	221.00	393.00	839.00	2430.00	3635.00	4160.00	4824.00
Cr	ppm	Amdel	XRF	5.0	123	80.00	118.00	151.00	218.00	457.00	809.00	1464.00	1963.00	2905.00
V	ppm	Amdel	XRF	10.0	123	25.00	111.00	180.00	321.00	464.00	673.00	954.00	1482.00	1701.00
Cu	ppm	Amdel	AA-HF	2.0	123	34.00	76.00	92.00	135.00	197.00	270.00	340.00	416.00	751.00
Pb	ppm	Amdel	XRF	4.0	123	.67	6.00	12.00	19.00	31.00	47.00	69.00	74.00	165.00
Zn	ppm	Amdel	AA-HF	2.0	123	33.00	50.00	76.00	184.00	361.00	611.00	854.00	919.00	1637.00
Ni	ppm	Amdel	AA-HF	5.0	123	16.00	26.00	40.00	77.00	146.00	312.00	486.00	594.00	1267.00
Co	ppm	Amdel	AA-HF	5.0	123	1.67	8.00	15.00	31.00	59.00	157.00	264.00	284.00	487.00
As	ppm	Analb	XRF	2.0	123	3.00	8.00	11.00	21.00	69.00	190.00	507.00	1161.00	1749.00
Sb	ppm	Amdel	XRF	2.0	123	.67	.67	.67	.67	3.00	6.00	10.00	11.00	21.00
Bi	ppm	Amdel	OES	1.0	123	.33	.33	.33	.33	.33	.33	.33	.33	1.00
Bi	ppm	Amdel	XRF	1.0	123	.33	.33	.33	.33	.33	.33	1.00	3.00	5.00
Mo	ppm	Amdel	XRF	2.0	123	.67	.67	.67	.67	3.00	4.00	4.00	5.00	7.00
Sn	ppm	Amdel	OES	1.0	123	.33	.33	.33	.33	.33	.33	1.00	1.00	2.00
Sn	ppm	Amdel	XRF	1.0	123	.33	.33	.33	.33	2.00	4.00	6.00	6.00	10.00
Ge	ppm	Amdel	OES	1.0	123	.33	.33	.33	.33	.33	.33	.33	1.00	1.00
Ga	ppm	Amdel	OES	1.0	123	.33	.33	.33	.33	1.00	3.00	15.00	15.00	30.00
W	ppm	Amdel	XRF	10.0	123	3.33	3.33	3.33	3.33	3.33	11.00	18.00	21.00	30.00
Ba	ppm	Csiro	ICP	100.0	71	134.00	158.00	238.00	364.00	602.00	1241.00	2438.00	3042.00	8636.00
Zr	ppm	Csiro	ICP-FS	50.0	71	175.00	186.00	196.00	211.00	235.00	249.00	280.00	313.00	468.00
Nb	ppm	Amdel	XRF	4.0	123	1.33	1.33	1.33	1.33	1.33	1.33	1.33	5.00	9.00
Ta	ppm	Amdel	XRF	3.0	123	1.00	1.00	1.00	1.00	1.00	1.00	1.00	3.00	5.00
Se	ppm	Amdel	XRF	1.0	123	.33	.33	.33	.33	2.00	4.00	6.00	7.00	11.00
Be	ppm	Amdel	OES	1.0	123	.33	.33	.33	.33	.33	.33	.33	.33	1.00
Au	ppb	Analb	234	1.0	123	.33	.33	.33	.33	1.00	3.00	7.00	13.00	22.00

Table 4b: (cont'd)
Summary statistics for Wiluna Area (Wiluna, Kingston, Duketon, Sir Samuel)

Sample types:
MF FF PF PE RC

Element		Lab	Method	L.L.D.	#Samples	Minimum	Maximum	Median	Mode	Mean	Std. Dev.
SiO2	Wt%	Csiro	ICP-FS	0.5	71	4.18	28.82	11.38	10.51	12.35	6.14
Al2O3	Wt%	Csiro	ICP-FS	0.5	71	1.20	12.67	4.45	3.50	4.74	2.58
Fe2O3	Wt%	Amdel	AAS-HF	0.1	123	31.17	88.93	73.20	72.54	71.92	9.17
MgO	Wt%	Csrio	ICP-FS	0.05	71	.04	.27	.11	.07	.12	.05
CaO	Wt%	Csiro	ICP-FS	0.05	71	.06	1.39	.10	.07	.17	.23
TiO2	Wt%	Csiro	ICP-FS	0.003	71	.05	2.66	.26	.10	.40	.44
Ag	ppm	Amdel	OES	0.1	123	.03	3.00	.03	.04	.18	.36
Mn	ppm	Amdel	AAS	5.0	123	41.00	5209.00	827.00	432.30	1466.37	1368.29
Cr	ppm	Amdel	XRF	5.0	123	56.00	4167.00	450.00	199.02	642.74	634.26
V	ppm	Amdel	XRF	10.0	123	3.33	1755.00	460.00	321.25	542.90	363.77
Cu	ppm	Amdel	AA-HF	2.0	123	31.00	934.00	197.00	229.27	218.50	131.52
Pb	ppm	Amdel	XRF	4.0	123	.67	189.00	31.00	17.17	37.20	30.12
Zn	ppm	Amdel	AA-HF	2.0	123	20.00	2621.00	355.00	150.35	441.07	356.42
Ni	ppm	Amdel	AA-HF	5.0	123	1.67	1320.00	142.00	140.86	224.46	230.49
Co	ppm	Amdel	AA-HF	5.0	123	1.67	591.00	57.00	39.78	106.50	106.67
As	ppm	Analb	XRF	2.0	123	.67	1994.00	67.00	18.07	208.79	367.24
Sb	ppm	Amdel	XRF	2.0	123	.67	21.00	3.00	.72	4.17	4.41
Bi	ppm	Amdel	OES	1.0	123	.33	1.00	.33	.00	.34	.08
Bi	ppm	Amdel	XRF	1.0	123	.33	5.00	.33	.35	.65	.91
Mo	ppm	Amdel	XRF	2.0	123	.67	8.00	2.00	.69	2.45	1.69
Sn	ppm	Amdel	OES	1.0	123	.33	3.00	.33	.34	.44	.38
Sn	ppm	Amdel	XRF	1.0	123	.33	32.00	2.00	.36	2.50	3.48
Ge	ppm	Amdel	OES	1.0	123	.33	4.00	.33	.34	.42	.38
Ga	ppm	Amdel	OES	1.0	123	.33	30.00	1.00	.41	3.70	6.18
W	ppm	Amdel	XRF	10.0	123	3.33	32.00	3.33	3.42	6.91	6.75
Ba	ppm	Csiro	ICP	100.0	71	134.00	8636.00	597.00	148.54	1055.56	1297.87
Zr	ppm	Csiro	ICP-FS	50.0	71	175.00	468.00	234.00	240.55	236.80	42.07
Nb	ppm	Amdel	XRF	4.0	123	1.33	15.00	1.33	1.35	1.82	1.87
Ta	ppm	Amdel	XRF	3.0	123	1.00	5.00	1.00	1.01	1.19	.74
Se	ppm	Amdel	XRF	1.0	123	.33	23.00	2.00	.37	2.78	2.96
Be	ppm	Amdel	OES	1.0	123	.33	1.00	.33	.00	.36	.12
Au	ppb	Analb	234	1.0	123	.33	186.00	1.00	.40	4.34	16.98

NOTE: Mode estimated by binning of data: # of bins= 100.
Bin width=(95%ile-minimum value)/100.0

Table 5: Summary statistics for Wiluna Area (Wiluna, Kingston, Duketon, Sir Samuel)

"R/F2/F3" Regional and Follow-up Samples

Sample types:
LR

No. of Samples in Group: 50

Element		Lab	Method	L.L.D.	#Samples	Percentiles								
						1%	5%	10%	25%	50%	75%	90%	95%	99%
SiO2	Wt%	Csiro	ICP-FS	0.5	24	5.31	8.94	10.25	15.31	19.45	36.40	41.89	42.98	50.65
Al2O3	Wt%	Csiro	ICP-FS	0.5	24	2.07	3.21	3.35	6.16	6.92	7.79	9.02	10.81	10.98
Fe2O3	Wt%	Amdel	AAS-HF	0.1	50	28.17	33.60	37.60	46.32	60.48	66.91	72.06	76.92	81.49
MgO	Wt%	Csrio	ICP-FS	0.05	24	.04	.05	.06	.09	.11	.14	.19	.20	.27
CaO	Wt%	Csiro	ICP-FS	0.05	24	.06	.06	.06	.08	.09	.17	.25	.32	.64
TiO2	Wt%	Csiro	ICP-FS	0.003	24	.06	.10	.12	.27	.35	.38	.60	.64	.74
Ag	ppm	Amdel	OES	0.1	50	.03	.03	.03	.03	.10	.10	.20	.20	.40
Mn	ppm	Amdel	AAS	5.0	50	54.00	63.00	80.00	127.00	199.00	439.00	903.00	1195.00	4133.00
Cr	ppm	Amdel	XRF	5.0	50	21.00	81.00	133.00	179.00	345.00	766.00	1377.00	2359.00	4562.00
V	ppm	Amdel	XRF	10.0	50	36.00	78.00	135.00	274.00	524.00	729.00	1173.00	1457.00	2479.00
Cu	ppm	Amdel	AA-HF	2.0	50	56.00	70.00	77.00	122.00	180.00	252.00	328.00	348.00	533.00
Pb	ppm	Amdel	XRF	4.0	50	.67	.67	4.00	11.00	19.00	25.00	37.00	52.00	61.00
Zn	ppm	Amdel	AA-HF	2.0	50	37.00	42.00	55.00	73.00	132.00	258.00	392.00	531.00	599.00
Ni	ppm	Amdel	AA-HF	5.0	50	6.00	9.00	33.00	43.00	68.00	141.00	197.00	256.00	593.00
Co	ppm	Amdel	AA-HF	5.0	50	1.67	8.00	9.00	12.00	19.00	36.00	64.00	128.00	262.00
As	ppm	Analb	XRF	2.0	50	.67	2.00	7.00	23.00	49.00	119.00	280.00	419.00	1723.00
Sb	ppm	Amdel	XRF	2.0	50	.67	.67	.67	.67	4.00	6.00	8.00	9.00	12.00
Bi	ppm	Amdel	OES	1.0	50	.33	.33	.33	.33	.33	.33	.33	.33	3.00
Bi	ppm	Amdel	XRF	1.0	50	.33	.33	.33	.33	.33	.33	3.00	4.00	9.00
Mo	ppm	Amdel	XRF	2.0	50	.67	.67	.67	.67	2.00	3.00	5.00	6.00	19.00
Sn	ppm	Amdel	OES	1.0	50	.33	.33	.33	.33	.33	1.00	2.00	2.00	2.00
Sn	ppm	Amdel	XRF	1.0	50	.33	.33	.33	.33	2.00	4.00	6.00	8.00	11.00
Ge	ppm	Amdel	OES	1.0	50	.33	.33	.33	.33	.33	.33	1.00	1.00	1.00
Ga	ppm	Amdel	OES	1.0	50	.33	.33	.33	1.00	6.00	15.00	20.00	20.00	30.00
W	ppm	Amdel	XRF	10.0	50	3.33	3.33	3.33	3.33	3.33	3.33	13.00	18.00	32.00
Ba	ppm	Csiro	ICP	100.0	24	155.00	212.00	232.00	435.00	682.00	1034.00	1549.00	1731.00	2666.00
Zr	ppm	Csiro	ICP-FS	50.0	24	148.00	159.00	174.00	192.00	206.00	214.00	232.00	241.00	246.00
Nb	ppm	Amdel	XRF	4.0	50	1.33	1.33	1.33	1.33	1.33	1.33	6.00	7.00	13.00
Ta	ppm	Amdel	XRF	3.0	50	1.00	1.00	1.00	1.00	1.00	1.00	1.00	9.00	14.00
Se	ppm	Amdel	XRF	1.0	50	.33	.33	.33	.33	2.00	4.00	6.00	7.00	9.00
Be	ppm	Amdel	OES	1.0	50	.33	.33	.33	.33	.33	.33	.33	1.00	2.00
Au	ppb	Analb	234	1.0	50	.33	.33	.33	.33	2.00	3.00	7.00	12.00	124.00

Table 5: (cont'd)
Summary statistics for Wiluna Area (Wiluna, Kingston, Duketon, Sir Samuel)

Sample types:
LR

Element		Lab	Method	L.L.D.	#Samples	Minimum	Maximum	Median	Mode	Mean	Std. Dev.
SiO2	Wt%	Csiro	ICP-FS	0.5	24	5.31	50.65	19.41	19.44	24.69	12.90
Al2O3	Wt%	Csiro	ICP-FS	0.5	24	2.07	10.98	6.82	6.40	6.65	2.14
Fe2O3	Wt%	Amdel	AAS-HF	0.1	50	28.17	81.49	58.62	45.48	56.49	13.67
MgO	Wt%	Csrio	ICP-FS	0.05	24	.04	.27	.11	.09	.12	.05
CaO	Wt%	Csiro	ICP-FS	0.05	24	.06	.64	.09	.08	.14	.12
TiO2	Wt%	Csiro	ICP-FS	0.003	24	.06	.74	.34	.36	.35	.17
Ag	ppm	Amdel	OES	0.1	50	.03	.40	.10	.03	.10	.08
Mn	ppm	Amdel	AAS	5.0	50	54.00	4133.00	192.00	162.40	447.28	798.88
Cr	ppm	Amdel	XRF	5.0	50	21.00	4562.00	331.00	126.21	677.24	889.65
V	ppm	Amdel	XRF	10.0	50	36.00	2479.00	491.00	455.20	586.88	452.55
Cu	ppm	Amdel	AA-HF	2.0	50	56.00	533.00	173.00	162.58	194.84	96.40
Pb	ppm	Amdel	XRF	4.0	50	.67	61.00	19.00	18.89	20.31	14.05
Zn	ppm	Amdel	AA-HF	2.0	50	37.00	599.00	131.00	54.29	183.62	146.26
Ni	ppm	Amdel	AA-HF	5.0	50	6.00	593.00	64.00	42.25	104.14	109.42
Co	ppm	Amdel	AA-HF	5.0	50	1.67	262.00	19.00	8.61	35.51	48.54
As	ppm	Analb	XRF	2.0	50	.67	1723.00	48.00	40.41	146.69	335.33
Sb	ppm	Amdel	XRF	2.0	50	.67	12.00	3.00	.71	3.86	3.25
Bi	ppm	Amdel	OES	1.0	50	.33	3.00	.33	.00	.39	.38
Bi	ppm	Amdel	XRF	1.0	50	.33	9.00	.33	.35	.93	1.59
Mo	ppm	Amdel	XRF	2.0	50	.67	19.00	2.00	.69	2.73	2.84
Sn	ppm	Amdel	OES	1.0	50	.33	2.00	.33	.34	.69	.56
Sn	ppm	Amdel	XRF	1.0	50	.33	11.00	2.00	.37	2.55	2.46
Ge	ppm	Amdel	OES	1.0	50	.33	1.00	.33	.34	.44	.25
Ga	ppm	Amdel	OES	1.0	50	.33	30.00	6.00	.43	7.95	7.78
W	ppm	Amdel	XRF	10.0	50	3.33	32.00	3.33	3.41	6.17	5.92
Ba	ppm	Csiro	ICP	100.0	24	155.00	2666.00	664.00	430.80	804.58	577.70
Zr	ppm	Csiro	ICP-FS	50.0	24	148.00	246.00	206.00	198.68	202.17	23.47
Nb	ppm	Amdel	XRF	4.0	50	1.33	13.00	1.33	1.36	2.65	2.72
Ta	ppm	Amdel	XRF	3.0	50	1.00	14.00	1.00	1.04	1.68	2.47
Se	ppm	Amdel	XRF	1.0	50	.33	9.00	2.00	.37	2.49	2.38
Be	ppm	Amdel	OES	1.0	50	.33	2.00	.33	.34	.41	.28
Au	ppb	Analb	234	1.0	50	.33	124.00	2.00	.39	4.96	17.44

NOTE: Mode estimated by binning of data: # of bins= 100.
Bin width=(95%ile-minimum value)/100.0

Table 6: Ranked Samples > 95th Percentile
Wiluna "R/F2/F3" Samples
(Wiluna, Kingston, Duketon, Sir Samuel)
Laterites LP CP LN CN PN VL MS

Element	Lab	Method	L.L.D.	#Samples
SiO2 Wt%	Csiro	ICP-FS	0.5	48

Sample	Anomaly	Easting	Northing	Value
G06372	WL 02	293050.	7061700.	60.210
G06382	DU 01	430450.	7007950.	48.260
G06373	WL 02	291050.	7057350.	28.930
G06394	DU 01	430600.	7002300.	27.660
G06375	DU 01	428600.	7012400.	25.260
G06396	DU 01	430500.	7001050.	22.900
G06392	DU 01	429200.	7006250.	21.590
G05360	DU 01	429050.	6964750.	21.530
G06399	DU 01	432900.	7013050.	21.050
G06383	DU 01	431400.	7007500.	20.870

Element	Lab	Method	L.L.D.	#Samples
Al2O3 Wt%	Csiro	ICP-FS	0.5	48

Sample	Anomaly	Easting	Northing	Value
G06373	WL 02	291050.	7057350.	23.220
G06375	DU 01	428600.	7012400.	22.020
G05360	DU 01	429050.	6964750.	21.360
G06396	DU 01	430500.	7001050.	21.140
G06392	DU 01	429200.	7006250.	19.060
G06386	DU 01	431550.	7003950.	18.830
G05367	DU 01	431100.	6965500.	17.740
G06387	DU 01	432650.	7002450.	17.440
G05368	DU 01	429450.	6965050.	17.010
G05359	DU 01	433600.	7007700.	16.490

Element	Lab	Method	L.L.D.	#Samples
Fe2O3 Wt%	Amdel	AAS-HF	0.1	266

Sample	Anomaly	Easting	Northing	Value
G06199		349350.	7013550.	86.070
G06200		349350.	7015400.	85.070
G06190	WL 01	270550.	7073950.	83.210
G06193	WL 01	266650.	7075400.	82.060
G06115		439000.	6917100.	82.060
G05718	WL 02	292200.	7043850.	80.350
G03592	WL 01	274900.	7056000.	79.350
G06202		344500.	7017950.	77.630
G06130		449000.	6916650.	77.630
G03577	DU 01	429200.	7004250.	77.200

Element	Lab	Method	L.L.D.	#Samples
MgO Wt%	Csrio	ICP-FS	0.05	48

Sample	Anomaly	Easting	Northing	Value
G06382	DU 01	430450.	7007950.	.144
G06372	WL 02	293050.	7061700.	.144
G06373	WL 02	291050.	7057350.	.130
G06393	DU 01	428400.	7003800.	.119
G05367	DU 01	431100.	6965500.	.117
G06317	WL 01	268850.	7068050.	.108
G05375	DU 01	430700.	6963800.	.106
G06399	DU 01	432900.	7013050.	.103
G06394	DU 01	430600.	7002300.	.093
G06336	WL 01	269850.	7064850.	.078

Element	Lab	Method	L.L.D.	#Samples
CaO Wt%	Csiro	ICP-FS	0.05	48

Sample	Anomaly	Easting	Northing	Value
G06338	WL 02	298000.	7054100.	.138
G06373	WL 02	291050.	7057350.	.127
G06317	WL 01	268850.	7068050.	.120
G06393	DU 01	428400.	7003800.	.115
G06399	DU 01	432900.	7013050.	.106
G05375	DU 01	430700.	6963800.	.104
G05372	DU 01	430150.	6964600.	.100
G05359	DU 01	433600.	7007700.	.090
G06298	WL 01	265650.	7076150.	.084
G06383	DU 01	431400.	7007500.	.078

Element	Lab	Method	L.L.D.	#Samples
TiO2 Wt%	Csiro	ICP-FS	0.003	48

Sample	Anomaly	Easting	Northing	Value
G06364	WL 02	294000.	7061100.	7.770
G05358	DU 01	433750.	7010450.	2.280
G06375	DU 01	428600.	7012400.	1.990
G05375	DU 01	430700.	6963800.	1.930
G06387	DU 01	432650.	7002450.	1.780
G06389	DU 01	432250.	7003500.	1.720
G05359	DU 01	433600.	7007700.	1.590
G05357	DU 01	434000.	7012600.	1.580
G06396	DU 01	430500.	7001050.	1.570
G06394	DU 01	430600.	7002300.	1.470

Element	Lab	Method	L.L.D.	#Samples
Ag ppm	Amdel	OES	0.1	266

Sample	Anomaly	Easting	Northing	Value
G06385	DU 01	430300.	7004900.	4.000
G06605	DU 01	434850.	7007200.	3.000
G03563	DU 01	436100.	7011250.	3.000
G06203		344150.	7023500.	3.000
G06392	DU 01	429200.	7006250.	3.000
G06601	DU 01	436100.	7006600.	2.000
G05748		307600.	7012700.	2.000
G06602	DU 01	434950.	7011400.	2.000
G06182	WL 01	255200.	7078000.	2.000
G06396	DU 01	430500.	7001050.	2.000

Element	Lab	Method	L.L.D.	#Samples
Mn ppm	Amdel	AAS	5.0	266

Sample	Anomaly	Easting	Northing	Value
G06382	DU 01	430450.	7007950.	6549.000
G06200		349350.	7015400.	4567.000
G06199		349350.	7013550.	3946.000
G06183	WL 01	252850.	7078100.	3094.000
G06202		344500.	7017950.	2971.000
G06372	WL 02	293050.	7061700.	2629.000
G06193	WL 01	266650.	7075400.	2544.000
G06184	WL 01	253350.	7080550.	2442.000
G05369	DU 01	429450.	6964100.	2411.000
G06206		324750.	7019850.	2130.000

Element	Lab	Method	L.L.D.	#Samples
Cr	ppm Amdel	XRF	5.0	266

Sample	Anomaly	Easting	Northing	Value
G06136		419350.	6996350.	9999.000
G06137		418400.	6996950.	9999.000
G06194	WL 01	269550.	7075450.	9999.000
G05726		292900.	7039300.	9999.000
G03565	DU 01	438850.	7011550.	9999.000
G06190	WL 01	270550.	7073950.	7567.000
G06192	WL 01	264800.	7077250.	7072.000
G06129		447100.	6918950.	6811.000
G06965		295987.	7076379.	6618.000
G05717	WL 02	294100.	7045850.	6261.000

Element	Lab	Method	L.L.D.	#Samples
V	ppm Amdel	XRF	10.0	266

Sample	Anomaly	Easting	Northing	Value
G03561	DU 01	431400.	7011800.	2623.000
G05726		292900.	7039300.	2567.000
G03541		418800.	6936500.	2330.000
G03592	WL 01	274900.	7056000.	2323.000
G05738		296350.	7026800.	2307.000
G05732		286900.	7032050.	2278.000
G03536		441150.	6931100.	2240.000
G06130		449000.	6916650.	2182.000
G06110		432500.	6909950.	2177.000
G05718	WL 02	292200.	7043850.	2133.000

Element	Lab	Method	L.L.D.	#Samples
Cu	ppm Amdel	AA-HF	2.0	266

Sample	Anomaly	Easting	Northing	Value
G06163	WL 01	276000.	7070500.	1641.000
G03587	WL 01	278900.	7062700.	508.000
G03590	WL 01	280100.	7059200.	473.000
G06164	WL 01	271650.	7072450.	464.000
G03552		43085.	6962100.	452.000
G03524		435850.	6948600.	449.000
G06959	WL 01	275381.	7066337.	432.000
G06550	WL 01	276900.	7065450.	378.000
G06129		447100.	6918950.	367.000
G06181	WL 01	253350.	7074700.	356.000

Element	Lab	Method	L.L.D.	#Samples
Pb	ppm Amdel	XRF	4.0	266

Sample	Anomaly	Easting	Northing	Value
G05701	WL 02	289500.	7059050.	158.000
G06200		349350.	7015400.	98.000
G06181	WL 01	253350.	7074700.	82.000
G06372	WL 02	293050.	7061700.	77.000
G03544		424850.	6935150.	73.000
G05719	WL 02	289850.	7045650.	70.000
G06182	WL 01	255200.	7078000.	64.000
G06174	WL 01	264250.	7070450.	62.000
G06154		289900.	7076600.	53.000
G06163	WL 01	276000.	7070500.	51.000

Element	Lab	Method	L.L.D.	#Samples
Zn	ppm Amdel	AA-HF	2.0	266

Sample	Anomaly	Easting	Northing	Value
G06199		349350.	7013550.	1170.000
G06200		349350.	7015400.	974.000
G06206		324750.	7019850.	934.000
G06183	WL 01	252850.	7078100.	869.000
G06181	WL 01	253350.	7074700.	692.000
G06163	WL 01	276000.	7070500.	665.000
G03578		427550.	7005950.	478.000
G06193	WL 01	266650.	7075400.	477.000
G06175	WL 01	261300.	7070400.	476.000
G05369	DU 01	429450.	6964100.	445.000

Element	Lab	Method	L.L.D.	#Samples
Ni	ppm Amdel	AA-HF	5.0	266

Sample	Anomaly	Easting	Northing	Value
G06171		250450.	7087750.	1832.000
G05367	DU 01	431100.	6965500.	1251.000
G06136		419350.	6996350.	1168.000
G05709	WL 02	288500.	7052250.	1136.000
G06137		418400.	6996950.	1072.000
G06181	WL 01	253350.	7074700.	741.000
G06188	WL 01	269600.	7071450.	678.000
G06206		324750.	7019850.	612.000
G06199		349350.	7013550.	566.000
G06387	DU 01	432650.	7002450.	531.000

Element	Lab	Method	L.L.D.	#Samples
Co	ppm Amdel	AA-HF	5.0	266

Sample	Anomaly	Easting	Northing	Value
G06199		349350.	7013550.	351.000
G06200		349350.	7015400.	285.000
G06183	WL 01	252850.	7078100.	228.000
G05709	WL 02	288500.	7052250.	190.000
G06193	WL 01	266650.	7075400.	188.000
G06553	WL 01	277300.	7059300.	171.000
G06206		324750.	7019850.	160.000
G06175	WL 01	261300.	7070400.	158.000
G06181	WL 01	253350.	7074700.	157.000
G06184	WL 01	253350.	7080550.	153.000

Element	Lab	Method	L.L.D.	#Samples
As	ppm Analb	XRF	2.0	266

Sample	Anomaly	Easting	Northing	Value
G05735		293900.	7025700.	2375.000
G06195	WL 01	261800.	7073950.	1194.000
G03563	DU 01	436100.	7011250.	987.000
G06163	WL 01	276000.	7070500.	947.000
G03590	WL 01	280100.	7059200.	759.000
G06301	WL 01	263100.	7072100.	479.000
G03586	WL 01	275300.	7063700.	417.000
G06174	WL 01	264250.	7070450.	397.000
G06549	WL 01	275700.	7064650.	364.000
G06196	WL 01	262700.	7072100.	339.000

Element	Lab	Method	L.L.D.	#Samples
Sb	ppm Amdel	XRF	2.0	266

Sample	Anomaly	Easting	Northing	Value
G03592	WL 01	274900.	7056000.	47.000
G06174	WL 01	264250.	7070450.	39.000
G03586	WL 01	275300.	7063700.	24.000
G06377	DU 01	429600.	7011500.	22.000
G06104		427650.	6919800.	19.000
G06335	WL 01	270150.	7065950.	19.000
G06195	WL 01	261800.	7073950.	15.000
G03590	WL 01	280100.	7059200.	13.000
G05735		293900.	7025700.	12.000
G03584	WL 01	270850.	7063650.	11.000

Element	Lab	Method	L.L.D.	#Samples
Bi	ppm Amdel	OES	1.0	266

Sample	Anomaly	Easting	Northing	Value
G05360	DU 01	429050.	6964750.	20.000
G03549		427900.	6969950.	15.000
G03527		442200.	6943400.	6.000
G03544		424850.	6935150.	4.000
G03550		427050.	6972100.	1.000
G05364	DU 01	429450.	6967050.	1.000
G05361	DU 01	429450.	6965500.	1.000
G03588	WL 01	282250.	7062600.	1.000
G03554		430650.	6969500.	1.000
G06132		444200.	6918650.	1.000

Element	Lab	Method	L.L.D.	#Samples
Bi	ppm Amdel	XRF	1.0	266

Sample	Anomaly	Easting	Northing	Value
G05360	DU 01	429050.	6964750.	23.000
G03549		427900.	6969950.	23.000
G03527		442200.	6943400.	7.000
G03578		427550.	7005950.	5.000
G05727		292800.	7033700.	5.000
G06970	WL 01	294430.	7061177.	4.000
G06194	WL 01	269550.	7075450.	4.000
G06132		444200.	6918650.	4.000
G06136		419350.	6996350.	4.000
G03588	WL 01	282250.	7062600.	4.000

Element	Lab	Method	L.L.D.	#Samples
Mo	ppm Amdel	XRF	2.0	266

Sample	Anomaly	Easting	Northing	Value
G06163	WL 01	276000.	7070500.	21.000
G03554		430650.	6969500.	16.000
G03527		442200.	6943400.	15.000
G06181	WL 01	253350.	7074700.	10.000
G06203		344150.	7023500.	10.000
G06182	WL 01	255200.	7078000.	9.000
G05360	DU 01	429050.	6964750.	9.000
G05826		293070.	7070820.	9.000
G05369	DU 01	429450.	6964100.	8.000
G06186	WL 01	251650.	7084850.	7.000

Element	Lab	Method	L.L.D.	#Samples
Sn	ppm Amdel	OES	1.0	266

Sample	Anomaly	Easting	Northing	Value
G06141	DU 01	421100.	7005600.	10.000
G06138	DU 01	425200.	7007000.	6.000
G03554		430650.	6969500.	6.000
G05834	WL 01	290962.	7066755.	2.000
G05826		293070.	7070820.	2.000
G06968	WL 01	292918.	7060537.	1.000
G05832	WL 01	290798.	7063273.	1.000
G06965		295987.	7076379.	1.000
G05849		291729.	7074094.	1.000
G05842		296030.	7077149.	1.000

Element	Lab	Method	L.L.D.	#Samples
Sn	ppm Amdel	XRF	1.0	266

Sample	Anomaly	Easting	Northing	Value
G05834	WL 01	290962.	7066755.	13.000
G06377	DU 01	429600.	7011500.	12.000
G05358	DU 01	433750.	7010450.	9.000
G06194	WL 01	269550.	7075450.	8.000
G05832	WL 01	290798.	7063273.	8.000
G06965		295987.	7076379.	8.000
G06969	WL 01	293766.	7061167.	7.000
G05357	DU 01	434000.	7012600.	7.000
G06550	WL 01	276900.	7065450.	7.000
G03554		430650.	6969500.	7.000

Element	Lab	Method	L.L.D.	#Samples
Ge	ppm Amdel	OES	1.0	266

Sample	Anomaly	Easting	Northing	Value
G06104		427650.	6919800.	2.000
G06377	DU 01	429600.	7011500.	2.000
G03561	DU 01	431400.	7011800.	2.000
G03582	WL 01	275400.	7066650.	2.000
G06136		419350.	6996350.	2.000
G06376	DU 01	429050.	7014100.	2.000
G06134	DU 01	424550.	7000550.	1.000
G06103		427650.	6917000.	1.000
G03564	DU 01	436050.	7013400.	1.000
G05748		307600.	7012700.	1.000

Element	Lab	Method	L.L.D.	#Samples
Ga	ppm Amdel	OES	1.0	266

Sample	Anomaly	Easting	Northing	Value
G06599	DU 01	436050.	7012000.	50.000
G06601	DU 01	436100.	7006600.	40.000
G06598	DU 01	437450.	7011700.	40.000
G06595	DU 01	438700.	7010150.	30.000
G06604	DU 01	434850.	7008600.	30.000
G06386	DU 01	431550.	7003950.	30.000
G06607	DU 01	433500.	7005050.	30.000
G05834	WL 01	290962.	7066755.	30.000
G06364	WL 02	294000.	7061100.	30.000
G06603	DU 01	434850.	7010000.	30.000

Element		Lab	Method	L.L.D.	#Samples
W	ppm	Amdel	XRF	10.0	266

Sample	Anomaly	Easting	Northing	Value
G03553		430550.	6959500.	43.000
G05826		293070.	7070820.	35.000
G03538		421500.	6944200.	28.000
G06132		444200.	6918650.	28.000
G03582	WL 01	275400.	7066650.	25.000
G05375	DU 01	430700.	6963800.	25.000
G06361	WL 02	293600.	7060200.	24.000
G05832	WL 01	290798.	7063273.	23.000
G06194	WL 01	269550.	7075450.	21.000
G06199		349350.	7013550.	21.000

Element		Lab	Method	L.L.D.	#Samples
Ba	ppm	Csiro	ICP	100.0	48

Sample	Anomaly	Easting	Northing	Value
G06382	DU 01	430450.	7007950.	1439.000
G06393	DU 01	428400.	7003800.	894.000
G06338	WL 02	298000.	7054100.	752.000
G06372	WL 02	293050.	7061700.	733.000
G06301	WL 01	263100.	7072100.	519.000
G06399	DU 01	432900.	7013050.	501.000
G06336	WL 01	269850.	7064850.	477.000
G05375	DU 01	430700.	6963800.	460.000
G05364	DU 01	429450.	6967050.	382.000
G06373	WL 02	291050.	7057350.	364.000

Element		Lab	Method	L.L.D.	#Samples
Zr	ppm	Csiro	ICP-FS	50.0	48

Sample	Anomaly	Easting	Northing	Value
G05358	DU 01	433750.	7010450.	395.000
G06364	WL 02	294000.	7061100.	378.000
G05357	DU 01	434000.	7012600.	316.000
G05359	DU 01	433600.	7007700.	313.000
G06382	DU 01	430450.	7007950.	290.000
G06959	WL 01	275381.	7066337.	280.000
G06394	DU 01	430600.	7002300.	279.000
G05361	DU 01	429450.	6965500.	272.000
G06284	WL 01	257800.	7074650.	270.000
G06387	DU 01	432650.	7002450.	266.000

Element		Lab	Method	L.L.D.	#Samples
Nb	ppm	Amdel	XRF	3.0	266

Sample	Anomaly	Easting	Northing	Value
G06141	DU 01	421100.	7005600.	60.000
G03554		430650.	6969500.	50.000
G06138	DU 01	425200.	7007000.	36.000
G03527		442200.	6943400.	25.000
G03549		427900.	6969950.	21.000
G05826		293070.	7070820.	20.000
G06607	DU 01	433500.	7005050.	16.000
G06364	WL 02	294000.	7061100.	15.000
G05832	WL 01	290798.	7063273.	14.000
G05842		296030.	7077149.	13.000

Element		Lab	Method	L.L.D.	#Samples
Ta	ppm	Amdel	XRF	3.0	266

Sample	Anomaly	Easting	Northing	Value
G06192	WL 01	264800.	7077250.	9.000
G06201		347400.	7016000.	8.000
G06130		449000.	6916650.	7.000
G05737		295450.	7023750.	7.000
G03561	DU 01	431400.	7011800.	6.000
G05727		292800.	7033700.	6.000
G05826		293070.	7070820.	6.000
G06103		427650.	6917000.	6.000
G03570	DU 01	433850.	7011500.	6.000
G03527		442200.	6943400.	6.000

Element		Lab	Method	L.L.D.	#Samples
Se	ppm	Amdel	XRF	1.0	266

Sample	Anomaly	Easting	Northing	Value
G05733		291250.	7028300.	10.000
G03586	WL 01	275300.	7063700.	10.000
G06119		444157.	6930050.	10.000
G06163	WL 01	276000.	7070500.	9.000
G06182	WL 01	255200.	7078000.	8.000
G06564	WL 01	280100.	7058100.	8.000
G05370	DU 01	430000.	6965050.	8.000
G06115		439000.	6917100.	8.000
G03590	WL 01	280100.	7059200.	8.000
G06399	DU 01	432900.	7013050.	7.000

Element		Lab	Method	L.L.D.	#Samples
Be	ppm	Amdel	OES	1.0	266

Sample	Anomaly	Easting	Northing	Value
G06140	DU 01	423550.	7009150.	1.000
G03527		442200.	6943400.	1.000
G06172	WL 01	266800.	7066800.	1.000
G06167		250400.	7104650.	1.000
G03530		444400.	6938050.	1.000
G03560	DU 01	426950.	7012250.	1.000
G06372	WL 02	293050.	7061700.	1.000
G03572	DU 01	436100.	7008150.	1.000
G06364	WL 02	294000.	7061100.	1.000
G06567		294150.	7051400.	.000

Element		Lab	Method	L.L.D.	#Samples
Au	ppb	Analb	234	1.0	265

Sample	Anomaly	Easting	Northing	Value
G06211		340250.	7027000.	232.000
G06971	WL 01	294104.	7060803.	140.000
G03547		429850.	6964600.	109.000
G06599	DU 01	436050.	7012000.	65.000
G06153		290950.	7079400.	39.000
G06145	DU 01	428350.	7013650.	26.000
G03572	DU 01	436100.	7008150.	26.000
G06364	WL 02	294000.	7061100.	25.000
G03532		446200.	6933300.	22.000
G03582	WL 01	275400.	7066650.	22.000

Table 7: Ranked Samples > 95th Percentile
Wiluna "R/F2/F3" Samples
(Wiluna, Kingston, Duketon, Sir Samuel)
Ferricretes MF FF PF PE RC

Element		Lab	Method	L.L.D.	#Samples
SiO2	Wt%	Csiro	ICP-FS	0.5	72

Sample	Anomaly	Easting	Northing	Value
G06282	WL 01	260850.	7073750.	28.820
G06308	WL 01	262400.	7071200.	27.520
G06337	WL 01	260950.	7075600.	25.920
G06290	WL 01	263450.	7075800.	25.650
G06296	WL 01	262850.	7077500.	25.380
G06286	WL 01	260400.	7074850.	24.080
G06327	WL 01	269050.	7072550.	23.410
G06295	WL 01	261900.	7077200.	21.990
G06280	WL 01	263750.	7073650.	21.170
G06949	WL 01	274496.	7066321.	20.380

Element		Lab	Method	L.L.D.	#Samples
Al2O3	Wt%	Csiro	ICP-FS	0.5	72

Sample	Anomaly	Easting	Northing	Value
G06381	DU 01	431000.	7009050.	12.670
G06380	DU 01	431950.	7010150.	12.560
G06953	WL 01	275265.	7066643.	9.640
G05362	DU 01	429050.	6966250.	9.560
G06295	WL 01	261900.	7077200.	9.500
G06282	WL 01	260850.	7073750.	9.300
G05365	DU 01	430550.	6967200.	8.390
G06339	WL 02	297150.	7055150.	8.310
G06318	WL 01	267600.	7066800.	8.140
G06320	WL 01	267200.	7066050.	7.490

Element		Lab	Method	L.L.D.	#Samples
Fe2O3	Wt%	Amdel	AAS-HF	0.1	164

Sample	Anomaly	Easting	Northing	Value
G06616		430450.	6960450.	92.070
G06954	WL 01	274961.	7066637.	88.930
G06125		447200.	6923600.	88.780
G06592	WL 02	290800.	7056150.	88.640
G06563	WL 01	281750.	7058150.	87.070
G03528		440950.	6941550.	86.210
G06580	WL 02	291200.	7054900.	86.070
G06558	WL 01	278900.	7061650.	84.780
G06135		419200.	6999450.	84.640
G06615		430000.	6960750.	84.640

Element		Lab	Method	L.L.D.	#Samples
MgO	Wt%	Csrio	ICP-FS	0.05	72

Sample	Anomaly	Easting	Northing	Value
G06312	WL 01	266900.	7068650.	.270
G06316	WL 01	268250.	7069300.	.233
G06329	WL 01	272750.	7067700.	.210
G06283	WL 01	258900.	7073600.	.205
G05696	WL 01	273017.	7066973.	.201
G05695	WL 01	272874.	7067216.	.194
G06285	WL 01	259450.	7074800.	.194
G06360	WL 02	294450.	7059600.	.186
G06333	WL 01	272500.	7065500.	.176
G06946	WL 01	273560.	7065997.	.172

Element		Lab	Method	L.L.D.	#Samples
CaO	Wt%	Csiro	ICP-FS	0.05	72

Sample	Anomaly	Easting	Northing	Value
G06316	WL 01	268250.	7069300.	1.390
G06946	WL 01	273560.	7065997.	1.300
G06945	WL 01	273228.	7065991.	.738
G06331	WL 01	271800.	7066250.	.575
G06332	WL 01	273150.	7066150.	.566
G05698	WL 01	273660.	7066614.	.260
G06312	WL 01	266900.	7068650.	.259
G06283	WL 01	258900.	7073600.	.228
G06367	WL 02	298800.	7055350.	.216
G08092		292490.	6548170.	.207

Element		Lab	Method	L.L.D.	#Samples
TiO2	Wt%	Csiro	ICP-FS	0.003	72

Sample	Anomaly	Easting	Northing	Value
G06342	WL 02	295950.	7060200.	2.660
G05362	DU 01	429050.	6966250.	1.940
G06380	DU 01	431950.	7010150.	1.420
G05365	DU 01	430550.	6967200.	1.120
G06381	DU 01	431000.	7009050.	1.100
G06314	WL 01	267050.	7067750.	.868
G06327	WL 01	269050.	7072550.	.867
G06363	WL 02	294700.	7060200.	.836
G06395	DU 01	432700.	7001500.	.822
G05363	DU 01	430000.	6966600.	.775

Element		Lab	Method	L.L.D.	#Samples
Ag	ppm	Amdel	OES	0.1	164

Sample	Anomaly	Easting	Northing	Value
G06380	DU 01	431950.	7010150.	3.000
G06606	DU 01	434850.	7005700.	2.000
G06381	DU 01	431000.	7009050.	1.000
G06543	WL 01	274150.	7064150.	.800
G06295	WL 01	261900.	7077200.	.800
G06556	WL 01	279000.	7057450.	.600
G06558	WL 01	278900.	7061650.	.600
G06557	WL 01	279100.	7059150.	.600
G06342	WL 02	295950.	7060200.	.600
G06613		429050.	6961350.	.600

Element		Lab	Method	L.L.D.	#Samples
Mn	ppm	Amdel	AAS	5.0	164

Sample	Anomaly	Easting	Northing	Value
G08092		292490.	6548170.	9342.000
G06152		290650.	7081700.	5760.000
G06610		431250.	6959500.	5289.000
G06563	WL 01	281750.	7058150.	5209.000
G06370	WL 02	297550.	7057600.	4824.000
G06125		447200.	6923600.	4774.000
G06586	WL 02	292700.	7057700.	4558.000
G06618		430850.	6959800.	4504.000
G06616		430450.	6960450.	4502.000
G03546		431250.	6964300.	4456.000

Element		Lab	Method	L.L.D.	#Samples
Cr	ppm	Amdel	XRF	5.0	164

Sample	Anomaly	Easting	Northing	Value
G03543		419500.	6932950.	9999.000
G05746		305850.	7020350.	7475.000
G05833	WL 01	291533.	7065687.	4167.000
G06597	DU 01	437450.	7010600.	2905.000
G06107		429050.	6916250.	2588.000
G06546	WL 01	277800.	7061600.	2371.000
G06370	WL 02	297550.	7057600.	2164.000
G06545	WL 01	277100.	7062500.	2112.000
G06536	WL 01	273100.	7062900.	2024.000
G06566	WL 01	282950.	7059400.	1963.000

Element		Lab	Method	L.L.D.	#Samples
V	ppm	Amdel	XRF	10.0	164

Sample	Anomaly	Easting	Northing	Value
G06546	WL 01	277800.	7061600.	1755.000
G06380	DU 01	431950.	7010150.	1701.000
G06555	WL 01	279050.	7054850.	1546.000
G06551	WL 01	275200.	7061100.	1536.000
G06606	DU 01	434850.	7005700.	1528.000
G06536	WL 01	273100.	7062900.	1500.000
G06342	WL 02	295950.	7060200.	1482.000
G06107		429050.	6916250.	1459.000
G06545	WL 01	277100.	7062500.	1390.000
G06381	DU 01	431000.	7009050.	1354.000

Element		Lab	Method	L.L.D.	#Samples
Cu	ppm	Amdel	AA-HF	2.0	164

Sample	Anomaly	Easting	Northing	Value
G06302	WL 01	263050.	7073050.	934.000
G06340	WL 02	296700.	7056700.	751.000
G06288	WL 01	262750.	7074900.	731.000
G05746		305850.	7020350.	470.000
G06292	WL 01	265200.	7070300.	444.000
G06563	WL 01	281750.	7058150.	441.000
G05699	WL 01	273300.	7066608.	434.000
G06281	WL 01	262800.	7073800.	416.000
G06283	WL 01	258900.	7073600.	410.000
G06543	WL 01	274150.	7064150.	385.000

Element		Lab	Method	L.L.D.	#Samples
Pb	ppm	Amdel	XRF	4.0	164

Sample	Anomaly	Easting	Northing	Value
G06543	WL 01	274150.	7064150.	189.000
G06337	WL 01	260950.	7075600.	165.000
G06370	WL 02	297550.	7057600.	148.000
G06302	WL 01	263050.	7073050.	143.000
G06283	WL 01	258900.	7073600.	104.000
G06947	WL 01	273864.	7066002.	90.000
G06367	WL 02	298800.	7055350.	74.000
G06548	WL 01	278350.	7063900.	74.000
G06210		340150.	7025000.	73.000
G06360	WL 02	294450.	7059600.	72.000

Element		Lab	Method	L.L.D.	#Samples
Zn	ppm	Amdel	AA-HF	2.0	164

Sample	Anomaly	Easting	Northing	Value
G06333	WL 01	272500.	7065500.	2621.000
G06302	WL 01	263050.	7073050.	1637.000
G06370	WL 02	297550.	7057600.	1274.000
G06540	WL 01	271550.	7064100.	1183.000
G06369	WL 02	297950.	7056250.	1033.000
G06548	WL 01	278350.	7063900.	927.000
G06557	WL 01	279100.	7059150.	919.000
G06563	WL 01	281750.	7058150.	914.000
G06367	WL 02	298800.	7055350.	912.000
G08092		292490.	6548170.	893.000

Element		Lab	Method	L.L.D.	#Samples
Ni	ppm	Amdel	AA-HF	5.0	164

Sample	Anomaly	Easting	Northing	Value
G03543		419500.	6932950.	1728.000
G06556	WL 01	279000.	7057450.	1320.000
G06370	WL 02	297550.	7057600.	1267.000
G06297	WL 01	263800.	7077850.	1078.000
G05746		305850.	7020350.	990.000
G06205		327400.	7016950.	847.000
G08092		292490.	6548170.	847.000
G06369	WL 02	297950.	7056250.	819.000
G05745		307750.	7023150.	768.000
G06319	WL 01	268750.	7066550.	725.000

Element		Lab	Method	L.L.D.	#Samples
Co	ppm	Amdel	AA-HF	5.0	164

Sample	Anomaly	Easting	Northing	Value
G08092		292490.	6548170.	612.000
G06370	WL 02	297550.	7057600.	591.000
G06556	WL 01	279000.	7057450.	487.000
G06369	WL 02	297950.	7056250.	367.000
G06152		290650.	7081700.	362.000
G06563	WL 01	281750.	7058150.	360.000
G06191	WL 01	266450.	7078200.	331.000
G06205		327400.	7016950.	297.000
G06397	DU 01	431700.	7000150.	295.000
G06367	WL 02	298800.	7055350.	284.000

Element		Lab	Method	L.L.D.	#Samples
As	ppm	Analb	XRF	2.0	164

Sample	Anomaly	Easting	Northing	Value
G06109		432550.	6913650.	2232.000
G06332	WL 01	273150.	7066150.	1994.000
G06947	WL 01	273864.	7066002.	1749.000
G06951	WL 01	273261.	7065684.	1715.000
G06283	WL 01	258900.	7073600.	1458.000
G06946	WL 01	273560.	7065997.	1425.000
G06945	WL 01	273228.	7065991.	1247.000
G06950	WL 01	273593.	7065690.	1161.000
G06333	WL 01	272500.	7065500.	690.000
G06948	WL 01	274219.	7066316.	641.000

Table 7 (cont'd)

Element	Lab	Method	L.L.D.	#Samples
Sb	ppm Amdel	XRF	2.0	164

Sample	Anomaly	Easting	Northing	Value
G06309	WL 01	263150.	7070250.	21.000
G06314	WL 01	267050.	7067750.	21.000
G06543	WL 01	274150.	7064150.	20.000
G03543		419500.	6932950.	16.000
G06322	WL 01	269650.	7070250.	15.000
G06536	WL 01	273100.	7062900.	14.000
G06541	WL 01	272500.	7064300.	14.000
G06308	WL 01	262400.	7071200.	11.000
G06547	WL 01	276400.	7063750.	11.000
G06954	WL 01	274961.	7066637.	11.000

Element	Lab	Method	L.L.D.	#Samples
Bi	ppm Amdel	OES	1.0	164

Sample	Anomaly	Easting	Northing	Value
G06613		429050.	6961350.	4.000
G06612		428900.	6959500.	4.000
G06609		429450.	6960400.	3.000
G06611		429500.	6959500.	2.000
G06533	WL 01	270750.	7062250.	1.000
G06337	WL 01	260950.	7075600.	1.000
G06577		293300.	7054300.	.000
G06573		294000.	7053400.	.000
G06569		292100.	7051550.	.000
G06572		292900.	7052450.	.000

Element	Lab	Method	L.L.D.	#Samples
Bi	ppm Amdel	XRF	1.0	164

Sample	Anomaly	Easting	Northing	Value
G06113		441900.	6911250.	6.000
G05712	WL 01	278850.	7065600.	5.000
G06941	WL 01	273527.	7066304.	5.000
G06615		430000.	6960750.	5.000
G03525		438750.	6946300.	4.000
G06945	WL 01	273228.	7065991.	4.000
G05745		307750.	7023150.	4.000
G06133		433350.	6982150.	4.000
G06297	WL 01	263800.	7077850.	4.000
G06613		429050.	6961350.	4.000

Element	Lab	Method	L.L.D.	#Samples
Mo	ppm Amdel	XRF	2.0	164

Sample	Anomaly	Easting	Northing	Value
G03525		438750.	6946300.	16.000
G06613		429050.	6961350.	11.000
G06566	WL 01	282950.	7059400.	8.000
G06337	WL 01	260950.	7075600.	7.000
G03551		429600.	6963350.	7.000
G06370	WL 02	297550.	7057600.	7.000
G06133		433350.	6982150.	6.000
G06565	WL 01	281050.	7059350.	6.000
G06340	WL 02	296700.	7056700.	6.000
G06967		294764.	7074882.	6.000

Element	Lab	Method	L.L.D.	#Samples
Sn	ppm Amdel	OES	1.0	164

Sample	Anomaly	Easting	Northing	Value
G06543	WL 01	274150.	7064150.	3.000
G05836		294182.	7069732.	2.000
G05845		293759.	7071880.	2.000
G05848		292477.	7074106.	2.000
G05846		294277.	7074135.	2.000
G05833	WL 01	291533.	7065687.	1.000
G06309	WL 01	263150.	7070250.	1.000
G05830	WL 01	291689.	7064612.	1.000
G05838		293188.	7072948.	1.000
G05827		292281.	7070778.	1.000

Element	Lab	Method	L.L.D.	#Samples
Sn	ppm Amdel	XRF	1.0	164

Sample	Anomaly	Easting	Northing	Value
G06543	WL 01	274150.	7064150.	32.000
G06557	WL 01	279100.	7059150.	10.000
G05833	WL 01	291533.	7065687.	8.000
G06380	DU 01	431950.	7010150.	8.000
G06552	WL 01	275250.	7059250.	7.000
G06613		429050.	6961350.	7.000
G06560	WL 01	280050.	7060400.	7.000
G06288	WL 01	262750.	7074900.	6.000
G05846		294277.	7074135.	6.000
G06534	WL 01	273800.	7061550.	6.000

Element	Lab	Method	L.L.D.	#Samples
Ge	ppm Amdel	OES	1.0	164

Sample	Anomaly	Easting	Northing	Value
G06380	DU 01	431950.	7010150.	4.000
G06547	WL 01	276400.	7063750.	1.000
G06342	WL 02	295950.	7060200.	1.000
G06314	WL 01	267050.	7067750.	1.000
G06546	WL 01	277800.	7061600.	1.000
G06551	WL 01	275200.	7061100.	1.000
G03539		421350.	6941150.	1.000
G06543	WL 01	274150.	7064150.	1.000
G06308	WL 01	262400.	7071200.	1.000
G06539	WL 01	287200.	7063000.	1.000

Element	Lab	Method	L.L.D.	#Samples
Ga	ppm Amdel	OES	1.0	164

Sample	Anomaly	Easting	Northing	Value
G06342	WL 02	295950.	7060200.	30.000
G06380	DU 01	431950.	7010150.	30.000
G06606	DU 01	434850.	7005700.	30.000
G06539	WL 01	287200.	7063000.	20.000
G06612		428900.	6959500.	20.000
G06381	DU 01	431000.	7009050.	20.000
G06613		429050.	6961350.	20.000
G06545	WL 01	277100.	7062500.	15.000
G05365	DU 01	430550.	6967200.	15.000
G06107		429050.	6916250.	15.000

Element	Lab	Method	L.L.D.	#Samples
W ppm	Amdel	XRF	10.0	164

Sample	Anomaly	Easting	Northing	Value
G05837		294379.	7072967.	32.000
G06615		430000.	6960750.	31.000
G06368	WL 02	297400.	7055600.	30.000
G06342	WL 02	295950.	7060200.	28.000
G06546	WL 01	277800.	7061600.	25.000
G06608		430550.	6959500.	23.000
G06113		441900.	6911250.	23.000
G06592	WL 02	290800.	7056150.	23.000
G06543	WL 01	274150.	7064150.	23.000
G06125		447200.	6923600.	22.000

Element	Lab	Method	L.L.D.	#Samples
Ba ppm	Csiro	ICP	100.0	72

Sample	Anomaly	Easting	Northing	Value
G06369	WL 02	297950.	7056250.	8636.000
G06337	WL 01	260950.	7075600.	5054.000
G06946	WL 01	273560.	7065997.	3332.000
G05698	WL 01	273660.	7066614.	3042.000
G06950	WL 01	273593.	7065690.	2996.000
G06332	WL 01	273150.	7066150.	2862.000
G05695	WL 01	272874.	7067216.	2573.000
G06286	WL 01	260400.	7074850.	2438.000
G06316	WL 01	268250.	7069300.	2140.000
G05696	WL 01	273017.	7066973.	1984.000

Element	Lab	Method	L.L.D.	#Samples
Zr ppm	Csiro	ICP-FS	50.0	72

Sample	Anomaly	Easting	Northing	Value
G06342	WL 02	295950.	7060200.	468.000
G05362	DU 01	429050.	6966250.	324.000
G05365	DU 01	430550.	6967200.	316.000
G06380	DU 01	431950.	7010150.	313.000
G06332	WL 01	273150.	7066150.	289.000
G06340	WL 02	296700.	7056700.	287.000
G06314	WL 01	267050.	7067750.	287.000
G06381	DU 01	431000.	7009050.	280.000
G06295	WL 01	261900.	7077200.	279.000
G06953	WL 01	275265.	7066643.	271.000

Element	Lab	Method	L.L.D.	#Samples
Nb ppm	Amdel	XRF	3.0	164

Sample	Anomaly	Easting	Northing	Value
G06342	WL 02	295950.	7060200.	15.000
G06539	WL 01	287200.	7063000.	9.000
G05833	WL 01	291533.	7065687.	9.000
G06545	WL 01	277100.	7062500.	9.000
G06107		429050.	6916250.	8.000
G06613		429050.	6961350.	8.000
G06536	WL 01	273100.	7062900.	6.000
G06612		428900.	6959500.	6.000
G05362	DU 01	429050.	6966250.	6.000
G06606	DU 01	434850.	7005700.	5.000

Element	Lab	Method	L.L.D.	#Samples
Ta ppm	Amdel	XRF	3.0	164

Sample	Anomaly	Easting	Northing	Value
G06152		290650.	7081700.	7.000
G06368	WL 02	297400.	7055600.	5.000
G05373	DU 01	430150.	6963950.	5.000
G06133		433350.	6982150.	5.000
G06114		438100.	6910300.	4.000
G05836		294182.	7069732.	4.000
G06537	WL 01	274200.	7063250.	4.000
G06566	WL 01	282950.	7059400.	4.000
G06125		447200.	6923600.	4.000
G06565	WL 01	281050.	7059350.	4.000

Element	Lab	Method	L.L.D.	#Samples
Se ppm	Amdel	XRF	1.0	164

Sample	Anomaly	Easting	Northing	Value
G06543	WL 01	274150.	7064150.	23.000
G06302	WL 01	263050.	7073050.	11.000
G06109		432550.	6913650.	10.000
G06312	WL 01	266900.	7068650.	9.000
G06332	WL 01	273150.	7066150.	8.000
G06547	WL 01	276400.	7063750.	8.000
G06610		431250.	6959500.	8.000
G06562	WL 01	283700.	7057550.	8.000
G06545	WL 01	277100.	7062500.	7.000
G06135		419200.	6999450.	7.000

Element	Lab	Method	L.L.D.	#Samples
Be ppm	Amdel	OES	1.0	164

Sample	Anomaly	Easting	Northing	Value
G03581		497100.	6994800.	1.000
G06340	WL 02	296700.	7056700.	1.000
G06288	WL 01	262750.	7074900.	1.000
G06541	WL 01	272500.	7064300.	1.000
G06302	WL 01	263050.	7073050.	1.000
G06572		292900.	7052450.	.000
G06571		291800.	7052450.	.000
G06570		291000.	7051350.	.000
G06575		291800.	7053200.	.000
G06573		294000.	7053400.	.000

Element	Lab	Method	L.L.D.	#Samples
Au ppb	Analb	234	1.0	162

Sample	Anomaly	Easting	Northing	Value
G06332	WL 01	273150.	7066150.	186.000
G05696	WL 01	273017.	7066973.	22.000
G05728		293250.	7031550.	21.000
G05698	WL 01	273660.	7066614.	19.000
G05710	WL 02	287950.	7049900.	17.000
G06329	WL 01	272750.	7067700.	16.000
G06953	WL 01	275265.	7066643.	13.000
G06950	WL 01	273593.	7065690.	13.000
G05363	DU 01	430000.	6966600.	10.000
G06367	WL 02	298800.	7055350.	10.000

Table 8: Regional Anomalies of the Wiluna Area

Anomaly#	Easting	Northing
DU 01	439000	7004300
WL 01	276850	7060500
WL 02	291050	7057350

Area Codes:
DU: Duketon
WL: Wiluna

Table 9: Robust Principal Components Analysis
Wiluna Laterites "R/F2/F3" Samples

Observations: 265 Variables: 19

Robust Means

Fe2O3	55.04	As	33.30
Ag	.30	Sb	2.81
Mn	212.47	Mo	2.61
Cr	909.24	Sn	2.44
V	1029.55	Ga	13.59
Cu	149.82	W	10.85
Pb	18.27	Nb	4.42
Zn	84.53	Se	3.37
Ni	71.93	Au	3.30
Co	17.80		

Robust Correlation Matrix

	Fe2O3	Ag	Mn	Cr	V	Cu	Pb	Zn	Ni	Co
Fe2O3	1.0000	-.2201	.3235	.0540	-.0211	.2959	-.0317	.3278	.1242	.3131
Ag	-.2201	1.0000	.0319	.0400	.1387	-.1732	.1625	-.1151	-.0813	-.0958
Mn	.3235	.0319	1.0000	-.0314	-.0695	.2991	.0173	.6602	.3796	.7241
Cr	.0540	.0400	-.0314	1.0000	.0931	-.0674	.1423	-.0164	.4466	.0500
V	-.0211	.1387	-.0695	.0931	1.0000	-.1244	.2352	-.1734	-.2095	-.1302
Cu	.2959	-.1732	.2991	-.0674	-.1244	1.0000	-.2081	.4452	.3539	.4798
Pb	-.0317	.1625	.0173	.1423	.2352	-.2081	1.0000	-.0075	-.1449	-.1768
Zn	.3278	-.1151	.6602	-.0164	-.1734	.4452	-.0075	1.0000	.5220	.7077
Ni	.1242	-.0813	.3796	.4466	-.2095	.3539	-.1449	.5220	1.0000	.6032
Co	.3131	-.0958	.7241	.0500	-.1302	.4798	-.1768	.7077	.6032	1.0000
As	.1845	.0330	-.0166	-.0154	.1265	.1152	.1407	.1188	.0462	.0176
Sb	-.0896	.0087	-.0763	-.0712	.0443	-.0510	-.0428	-.0028	-.0694	-.0246
Mo	.1946	-.0890	.0703	.2477	-.0587	-.0520	.1922	.0801	.1600	.0704
Sn	-.0954	.1803	.0897	-.0402	.0410	-.0873	.2210	-.0209	-.0993	-.0413
Ga	-.5891	.4769	-.2094	.0038	.2225	-.4051	.0633	-.3320	-.1325	-.3013
W	.0742	-.0167	-.0728	-.0418	.0312	-.0212	-.0147	-.0065	-.0799	-.0800
Nb	-.0735	.1203	.0288	-.0935	.0884	-.1960	.1788	.0244	-.1077	-.0764
Se	.0849	-.0199	-.0850	.0534	.0948	-.0422	.0928	-.0377	.0108	-.1029
Au	-.0649	-.1936	.0445	-.0124	-.0603	-.0586	-.1428	.0077	.0418	.0420

	As	Sb	Mo	Sn	Ga	W	Nb	Se	Au
Fe2O3	.1845	-.0896	.1946	-.0954	-.5891	.0742	-.0735	.0849	-.0649
Ag	.0330	.0087	-.0890	.1803	.4769	-.0167	.1203	-.0199	-.1936
Mn	-.0166	-.0763	.0703	.0897	-.2094	-.0728	.0288	-.0850	.0445
Cr	-.0154	-.0712	.2477	-.0402	.0038	-.0418	-.0935	.0534	-.0124
V	.1265	.0443	-.0587	.0410	.2225	.0312	.0884	.0948	-.0603
Cu	.1152	-.0510	-.0520	-.0873	-.4051	-.0212	-.1960	-.0422	-.0586
Pb	.1407	-.0428	.1922	.2210	.0633	-.0147	.1788	.0928	-.1428
Zn	.1188	-.0028	.0801	-.0209	-.3320	-.0065	.0244	-.0377	.0077
Ni	.0462	-.0694	.1600	-.0993	-.1325	-.0799	-.1077	.0108	.0418
Co	.0176	-.0246	.0704	-.0413	-.3013	-.0800	-.0764	-.1029	.0420
As	1.0000	.1603	.0548	.1163	-.0728	.0987	.1316	.0677	-.0981
Sb	.1603	1.0000	-.1050	.0097	-.0939	.0287	.0548	-.0835	-.0058
Mo	.0548	-.1050	1.0000	-.0069	-.0961	-.0098	.0788	.0717	-.0362
Sn	.1163	.0097	-.0069	1.0000	.0126	.0282	.1788	.0937	-.0681
Ga	-.0728	-.0939	-.0961	.0126	1.0000	-.0238	.1406	.0813	-.0329
W	.0987	.0287	-.0098	.0282	-.0238	1.0000	-.0488	-.0594	-.1623
Nb	.1316	.0548	.0788	.1788	.1406	-.0488	1.0000	-.0218	-.0279
Se	.0677	-.0835	.0717	.0937	.0813	-.0594	-.0218	1.0000	.0070
Au	-.0981	-.0058	-.0362	-.0681	-.0329	-.1623	-.0279	.0070	1.0000

Eigenvalues	% Trace	Σ Trace
3.7264	19.6128	19.6128
1.8756	9.8718	29.4846
1.6097	8.4719	37.9565
1.5327	8.0671	46.0236
1.2166	6.4032	52.4268
1.1062	5.8222	58.2490
1.0715	5.6397	63.8887
.9562	5.0327	68.9214
.8720	4.5896	73.5111
.8607	4.5302	78.0413
.7592	3.9957	82.0369
.6918	3.6413	85.6782
.6720	3.5369	89.2151
.6113	3.2172	92.4324
.4999	2.6311	95.0634
.2776	1.4610	96.5244
.2459	1.2943	97.8187
.2330	1.2263	99.0450
.1815	.9550	100.0000

Principal Component R-Scores

	1	2	3	4	5	6	7	8	9	10
Fe2O3	.5624	.0399	-.5259	.1930	-.0280	.1728	.0620	.1960	.0332	-.0567
Ag	-.3153	.4829	.3527	-.2954	.2833	.1133	.0183	-.0219	-.0186	-.1399
Mn	.7021	.3187	.1930	-.2820	-.1530	.1526	-.0151	.1872	-.0548	.1269
Cr	.1023	.2953	.2514	.6763	.2652	-.2911	-.0370	-.0085	-.2242	.0896
V	-.2865	.3567	-.1412	.0093	.1443	-.0813	.4672	.5882	-.0649	.1695
Cu	.6574	-.1416	-.0989	-.1462	.2124	.0958	.2254	-.0798	-.0257	-.1974
Pb	-.2064	.6306	-.2087	.1539	-.1589	.0598	-.0800	.1726	-.2900	-.0367
Zn	.8048	.2318	.0653	-.2137	-.0460	-.0118	-.0073	.0087	.0910	.0596
Ni	.6634	.1703	.4149	.2463	.2037	-.2334	.0122	-.2090	.0689	.0530
Co	.8455	.1447	.2367	-.1840	.0183	-.0163	.0399	.0758	.0105	.0608
As	.0813	.3535	-.4774	-.1169	.1577	-.3639	.2226	-.1892	.2873	-.0504
Sb	-.0637	-.0581	-.2168	-.3199	.0958	-.7382	.0054	-.0885	-.2072	-.0502
Mo	.1592	.3207	-.1153	.5576	-.1755	-.0312	-.3874	-.0095	.2001	-.0839
Sn	-.1198	.4502	-.1226	-.2544	-.2386	.1513	-.0306	-.4793	-.4425	.2438
Ga	-.5974	.2450	.5440	-.1081	.1517	.0332	.1019	.0031	.2978	.0604
W	-.0496	-.0088	-.3576	-.0798	.5010	.1460	-.2945	-.0571	.2008	.6512
Nb	-.1684	.4265	-.0727	-.2571	-.4122	-.1847	-.2513	.0456	.4235	-.0781
Se	-.0788	.1850	-.1161	.3199	-.1546	.2105	.6220	-.4050	.2109	.0436
Au	.0583	-.3057	.2382	.0884	-.5631	-.2815	.2020	.0882	.0330	.4770

Relative Contributions: Variables

	1	2	3	4	5	6	7	8	9	10
Fe2O3	44.6180	.2244	39.0123	5.2539	.1108	4.2126	.5417	5.4176	.1553	.4535
Ag	15.1089	35.4342	18.9028	13.2628	12.1921	1.9502	.0509	.0731	.0523	2.9727
Mn	60.6782	12.5024	4.5865	9.7925	2.8816	2.8665	.0280	4.3129	.3697	1.9817
Cr	1.2555	10.4676	7.5876	54.9015	8.4448	10.1706	.1644	.0087	6.0351	.9642
V	9.6100	14.8989	2.3340	.0102	2.4376	.7734	25.5559	40.5211	.4927	3.3662
Cu	68.1147	3.1592	1.5408	3.3709	7.1103	1.4460	8.0085	1.0044	.1041	6.1410
Pb	6.4767	60.4349	6.6188	3.6000	3.8397	.5435	.9734	4.5295	12.7789	.2045
Zn	84.6041	7.0191	.5568	5.9632	.2763	.0183	.0070	.0098	1.0807	.4646
Ni	51.8263	3.4156	20.2686	7.1418	4.8842	6.4135	.0174	5.1426	.5589	.3312
Co	85.3649	2.5009	6.6889	4.0433	.0399	.0317	.1900	.6859	.0133	.4414
As	.9428	17.8288	32.5182	1.9499	3.5507	18.8908	7.0681	5.1067	11.7808	.3632
Sb	.5306	.4415	6.1504	13.3909	1.2017	71.3104	.0038	1.0247	5.6162	.3297
Mo	3.7200	15.0890	1.9502	45.6308	4.5210	.1426	22.0226	.0132	5.8784	1.0321
Sn	1.6645	23.5031	1.7435	7.5046	6.6023	2.6530	.1085	26.6322	22.6991	6.8893
Ga	41.9220	7.0474	34.7635	1.3713	2.7020	.1293	1.2201	.0011	10.4152	.4283
W	.2550	.0080	13.2698	.6608	26.0565	2.2123	9.0001	.3381	4.1868	44.0126
Nb	3.8534	24.7085	.7174	8.9740	23.0746	4.6304	8.5757	.2821	24.3552	.8287
Se	.7564	4.1637	1.6416	12.4551	2.9075	5.3907	47.0835	19.9586	5.4119	.2310
Au	.4070	11.1921	6.7946	.9355	37.9771	9.4899	4.8897	.9324	.1307	27.2509

Table 10: Robust Principal Components Analysis

Wiluna Ferricretes "R/F2/F3"

Observations: 162 Variables: 18

Robust Means

Fe2O3	73.51	Co	112.50
Ag	.16	As	156.02
Mn	1879.12	Sb	3.89
Cr	495.88	Mo	2.83
V	512.74	Sn	2.09
Cu	206.68	Ga	3.01
Pb	28.69	W	12.27
Zn	402.85	Se	2.53
Ni	222.85	Au	3.15

Robust Correlation Matrix

	Fe2O3	Ag	Mn	Cr	V	Cu	Pb	Zn	Ni	Co
Fe2O3	1.0000	-.2229	.5821	-.2217	-.1722	.0082	-.0771	.3537	.2543	.4623
Ag	-.2229	1.0000	-.1340	.3259	.3759	-.1658	.0576	-.1511	-.0962	-.1253
Mn	.5821	-.1340	1.0000	-.1337	-.0216	.0921	-.2271	.4560	.4393	.8006
Cr	-.2217	.3259	-.1337	1.0000	.6012	-.1107	-.0917	-.1316	.2060	-.0149
V	-.1722	.3759	-.0216	.6012	1.0000	-.0942	-.1871	-.2886	-.1820	-.0996
Cu	.0082	-.1658	.0921	-.1107	-.0942	1.0000	.1476	.2501	.1024	.1641
Pb	-.0771	.0576	-.2271	-.0917	-.1871	.1476	1.0000	.3159	-.0449	-.0648
Zn	.3537	-.1511	.4560	-.1316	-.2886	.2501	.3159	1.0000	.5404	.7143
Ni	.2543	-.0962	.4393	.2060	-.1820	.1024	-.0449	.5404	1.0000	.7012
Co	.4623	-.1253	.8006	-.0149	-.0996	.1641	-.0648	.7143	.7012	1.0000
As	-.0362	-.0909	-.3605	-.1869	-.2707	.1856	.3834	-.0491	-.2026	-.3203
Sb	-.0955	-.0905	-.2925	-.0348	-.1848	.1358	.1867	-.0532	-.1153	-.2296
Mo	-.0751	-.0510	.0192	-.0895	-.0494	.0524	.0735	-.0027	-.0254	.0116
Sn	-.0677	.1550	-.1110	.1691	.2103	.1082	.0413	.0067	-.0581	-.0512
Ga	-.4511	.5404	-.3392	.4894	.5792	-.2750	.0078	-.4026	-.2346	-.3445
W	.1013	-.0531	.0940	-.0247	.0618	-.0831	-.2152	-.0654	-.0674	-.0041
Se	.0966	.0642	.0970	.1230	.0313	-.0297	.0362	.0075	.0663	.0453
Au	.0529	-.0648	-.1018	-.1573	-.1204	.1166	.2306	.0214	-.0862	-.0449

	As	Sb	Mo	Sn	Ga	W	Se	Au
Fe2O3	-.0362	-.0955	-.0751	-.0677	-.4511	.1013	.0966	.0529
Ag	-.0909	-.0905	-.0510	.1550	.5404	-.0531	.0642	-.0648
Mn	-.3605	-.2925	.0192	-.1110	-.3392	.0940	.0970	-.1018
Cr	-.1869	-.0348	-.0895	.1691	.4894	-.0247	.1230	-.1573
V	-.2707	-.1848	-.0494	.2103	.5792	.0618	.0313	-.1204
Cu	.1856	.1358	.0524	.1082	-.2750	-.0831	-.0297	.1166
Pb	.3834	.1867	.0735	.0413	.0078	-.2152	.0362	.2306
Zn	-.0491	-.0532	-.0027	.0067	-.4026	-.0654	.0075	.0214
Ni	-.2026	-.1153	-.0254	-.0581	-.2346	-.0674	.0663	-.0862
Co	-.3203	-.2296	.0116	-.0512	-.3445	-.0041	.0453	-.0449
As	1.0000	.4143	.0349	-.0730	-.0919	-.1476	.0687	.1434
Sb	.4143	1.0000	.1493	-.0877	-.0556	-.0425	.1052	.0761
Mo	.0349	.1493	1.0000	-.0180	.0224	.0663	-.0237	-.0364
Sn	-.0730	-.0877	-.0180	1.0000	.0836	.0331	-.0667	-.0969
Ga	-.0919	-.0556	.0224	.0836	1.0000	.0494	.0366	-.0418
W	-.1476	-.0425	.0663	.0331	.0494	1.0000	-.0365	-.0879
Se	.0687	.1052	-.0237	-.0667	.0366	-.0365	1.0000	.0315
Au	.1434	.0761	-.0364	-.0969	-.0418	-.0879	.0315	1.0000

Eigenvalues	% Trace	Σ Trace
3.8484	21.3801	21.3801
2.7462	15.2567	36.6368
1.6787	9.3263	45.9631
1.2167	6.7593	52.7224
1.1462	6.3677	59.0901
1.0196	5.6647	64.7548
.9984	5.5468	70.3016
.8938	4.9655	75.2671
.8164	4.5353	79.8024
.7070	3.9279	83.7304
.6730	3.7389	87.4693
.5999	3.3327	90.8020
.5023	2.7907	93.5927
.3535	1.9639	95.5566
.2820	1.5664	97.1230
.2422	1.3455	98.4685
.1891	1.0506	99.5191
.0866	.4809	100.0000

Principal Component R-Scores

	1	2	3	4	5	6	7	8	9	10
Fe2O3	.6566	.0610	-.1635	-.2118	.0653	.3320	.1790	-.1899	-.0476	.2324
Ag	-.4371	.3875	.3620	-.0826	.1075	-.0830	.2451	-.2475	-.0768	.2877
Mn	.7616	.4152	-.0895	-.0959	-.0515	.0704	.1627	.0447	-.1658	.2056
Cr	-.3585	.5807	.4284	-.0948	-.1667	.0747	-.2300	.1486	.2214	-.0755
V	-.4652	.6362	.1560	.0367	-.0439	.2263	.1118	.2119	-.0563	.2231
Cu	.2637	-.2741	.3246	.4185	-.1339	.3527	-.0718	.4645	-.0886	.2331
Pb	-.0100	-.4658	.6125	.0490	.1297	-.1278	.2956	-.2771	.0837	-.0044
Zn	.7472	.0023	.4317	.1189	.0133	-.0994	.0819	-.1677	.1521	-.0008
Ni	.6301	.3144	.3493	-.0701	-.1198	-.2064	-.2498	.0531	.2372	-.1969
Co	.8342	.3803	.2225	-.0013	-.0490	-.0775	.0617	.0509	.0318	.0421
As	-.1516	-.7051	.2360	-.1179	-.0876	.1594	-.0784	-.1617	.0505	.2729
Sb	-.1481	-.5311	.1902	-.1799	-.4843	.1170	-.1632	.0407	.2110	.1091
Mo	.0019	-.1298	-.0036	.1660	-.6774	-.3601	.4338	.1105	-.3251	-.1101
Sn	-.1549	.1864	.2266	.6131	.0178	.4461	.0171	-.3149	-.1594	-.3324
Ga	-.7143	.3962	.2202	-.1112	-.0343	-.1315	.2036	.0229	.0985	.0801
W	.0043	.1845	-.4466	.0958	-.3570	.2813	.3598	-.1600	.5681	-.0414
Se	.0303	.0430	.2294	-.6688	-.2224	.4003	.0127	-.0852	-.3054	-.3136
Au	.0221	-.3446	.1516	-.1741	.4084	.1312	.5066	.4783	.1714	-.2493

Relative Contributions: Variables

	1	2	3	4	5	6	7	8	9	10
Fe2O3	57.8410	.4989	3.5862	6.0203	.5721	14.7900	4.2976	4.8411	.3045	7.2482
Ag	27.0074	21.2227	18.5198	.9645	1.6324	.9747	8.4913	8.6579	.8329	11.6963
Mn	66.2535	19.6901	.9150	1.0509	.3030	.5656	3.0231	.2286	3.1420	4.8281
Cr	15.6489	41.0559	22.3423	1.0951	3.3846	.6797	6.4411	2.6878	5.9711	.6935
V	26.7090	49.9456	3.0022	.1660	.2374	6.3201	1.5423	5.5420	.3912	6.1442
Cu	8.1758	8.8344	12.3875	20.5892	2.1072	14.6217	.6055	25.3701	.9223	6.3863
Pb	.0126	27.1554	46.9528	.3009	2.1063	2.0436	10.9365	9.6132	.8764	.0025
Zn	67.5230	.0006	22.5400	1.7111	.0215	1.1941	.8106	3.3997	2.7993	.0001
Ni	47.2651	11.7658	14.5237	.5854	1.7091	5.0740	7.4268	.3360	6.7004	4.6138
Co	76.6673	15.9385	5.4566	.0002	.2648	.6618	.4191	.2850	.1111	.1956
As	3.1381	67.9078	7.6061	1.8985	1.0471	3.4709	.8404	3.5719	.3489	10.1703
Sb	3.1096	39.9814	5.1283	4.5882	33.2492	1.9397	3.7745	.2343	6.3087	1.6860
Mo	.0004	1.7709	.0014	2.8979	48.2450	13.6301	19.7853	1.2845	11.1097	1.2749
Sn	2.6046	3.7732	5.5758	40.8282	.0343	21.6170	.0316	10.7714	2.7594	12.0045
Ga	63.4111	19.5121	6.0241	1.5355	.1459	2.1496	5.1531	.0653	1.2053	.7979
W	.0020	3.6654	21.4773	.9883	13.7210	8.5187	13.9399	2.7566	34.7465	.1842
Se	.1007	.2026	5.7762	49.0768	5.4284	17.5773	.0178	.7960	10.2308	10.7935
Au	.0524	12.7244	2.4612	3.2462	17.8627	1.8428	27.4967	24.5094	3.1478	6.6565

Table 11a: Ranked Wiluna Laterite Principal Component Scores

Robust Principal Components
"R/F2/F3" Samples

Component 2

< 5th Percentile

Sample	Type	Easting	Northing	Score
G06211	MS	340250.	7027000.	-.9043
G06971	LN	294104.	7060803.	-.5474
G03547	MS	429850.	6964600.	-.4669
G06599	LN	436050.	7012000.	-.2138
G06204	MS	346200.	7026150.	-.1926
G03537	MS	438900.	6940800.	-.1893
G06153	MS	290950.	7079400.	-.1588
G06118	MS	442100.	6929550.	-.1525
G05741	LN	302900.	7032300.	-.1492
G06544	LN	275550.	7065700.	-.1447
G06145	MS	428350.	7013650.	-.1418
G03553	LN	430550.	6959500.	-.1405
G06127	LN	445300.	6923250.	-.1327

> 95th Percentile

Sample	Type	Easting	Northing	Score
G06138	LN	425200.	7007000.	.5176
G06194	LN	269550.	7075450.	.5207
G03527	MS	442200.	6943400.	.5504
G06382	PN	430450.	7007950.	.6242
G06181	MS	253350.	7074700.	.6289
G06199	MS	349350.	7013550.	.6618
G06195	LN	261800.	7073950.	.6861
G03563	LN	436100.	7011250.	.7752
G06200	MS	349350.	7015400.	.7972
G06163	LN	276000.	7070500.	.8602
G06141	PN	421100.	7005600.	1.0004
G03554	LN	430650.	6969500.	1.0802
G05735	LN	293900.	7025700.	1.3792

Table 11b: Wiluna Laterites

Component 5

< 5th Percentile

Sample	Type	Easting	Northing	Score
G06211	MS	340250.	7027000.	-1.9858
G06971	LN	294104.	7060803.	-1.4474
G06141	PN	421100.	7005600.	-1.3605
G03554	LN	430650.	6969500.	-1.1347
G03547	MS	429850.	6964600.	-.9618
G06138	LN	425200.	7007000.	-.7860
G03527	MS	442200.	6943400.	-.6213
G06599	LN	436050.	7012000.	-.4717
G03549	LN	427900.	6969950.	-.4262
G06382	PN	430450.	7007950.	-.3884
G06364	MS	294000.	7061100.	-.3845
G03532	MS	446200.	6933300.	-.3496
G06607	MS	433500.	7005050.	-.2882

> 95th Percentile

Sample	Type	Easting	Northing	Score
G06163	LN	276000.	7070500.	.2638
G06194	LN	269550.	7075450.	.2764
G05709	MS	288500.	7052250.	.3124
G03590	LN	280100.	7059200.	.3203
G06195	LN	261800.	7073950.	.3391
G03553	LN	430550.	6959500.	.3393
G03565	LN	438850.	7011550.	.4092
G05367	MS	431100.	6965500.	.4305
G03563	LN	436100.	7011250.	.4352
G06171	MS	250450.	7087750.	.5220
G06136	MS	419350.	6996350.	.5332
G06137	MS	418400.	6996950.	.5457
G05735	LN	293900.	7025700.	.7942

Table 11c: Wiluna Laterites
Component 6

< 5th Percentile

Sample	Type	Easting	Northing	Score
G05735	LN	293900.	7025700.	-2.1660
G03592	LN	274900.	7056000.	-1.3344
G06174	MS	264250.	7070450.	-1.3160
G06195	LN	261800.	7073950.	-1.3051
G06211	MS	340250.	7027000.	-1.0996
G03586	LN	275300.	7063700.	-.8497
G03563	LN	436100.	7011250.	-.8183
G03590	LN	280100.	7059200.	-.7824
G06137	MS	418400.	6996950.	-.7814
G06136	MS	419350.	6996350.	-.7318
G06335	MS	270150.	7065950.	-.6594
G06971	LN	294104.	7060803.	-.6543
G06171	MS	250450.	7087750.	-.5986

Table 11d: Wiluna Laterites
Component 10

> 95th Percentile

Sample	Type	Easting	Northing	Score
G06364	MS	294000.	7061100.	.3277
G06206	MS	324750.	7019850.	.3320
G06194	LN	269550.	7075450.	.3396
G06132	MS	444200.	6918650.	.3809
G05826	LN	293070.	7070820.	.4385
G03582	LN	275400.	7066650.	.4575
G03538	MS	421500.	6944200.	.4700
G06199	MS	349350.	7013550.	.5283
G06599	LN	436050.	7012000.	.5343
G03553	LN	430550.	6959500.	.7756
G03547	MS	429850.	6964600.	.9402
G06971	LN	294104.	7060803.	1.1412
G06211	MS	340250.	7027000.	2.0434

Table 12a: Ranked Wiluna Ferricrete Principal Component Scores

Robust Principal Components
"R/F2/F3" Samples

Component 2

< 5th Percentile					> 95th Percentile				
Sample	Type	Easting	Northing	Score	Sample	Type	Easting	Northing	Score
G06332	FF	273150.	7066150.	-1.1666	G06546	MF	277800.	7061600.	.3349
G06947	MF	273864.	7066002.	-.4579	G06342	FF	295950.	7060200.	.3606
G06951	MF	273261.	7065684.	-.3908	G06381	FF	431000.	7009050.	.3706
G06283	FF	258900.	7073600.	-.3667	G05833	FF	291533.	7065687.	.3837
G06337	FF	260950.	7075600.	-.3634	G05746	FF	305850.	7020350.	.4976
G06946	MF	273560.	7065997.	-.3413	G06606	FF	434850.	7005700.	.5707
G06309	FF	263150.	7070250.	-.2872	G03543	FF	419500.	6932950.	.6914
G06950	MF	273593.	7065690.	-.2812	G06380	FF	431950.	7010150.	.7330

Table 12b: Wiluna Ferricretes
Component 5

< 5th Percentile					> 95th Percentile				
Sample	Type	Easting	Northing	Score	Sample	Type	Easting	Northing	Score
G03525	FF	438750.	6946300.	-.5861	G05728	FF	293250.	7031550.	.1264
G03543	FF	419500.	6932950.	-.4464	G06369	FF	297950.	7056250.	.1337
G06613	FF	429050.	6961350.	-.3408	G06548	MF	278350.	7063900.	.1394
G06566	MF	282950.	7059400.	-.3357	G06950	MF	273593.	7065690.	.1397
G06302	FF	263050.	7073050.	-.3191	G05698	MF	273660.	7066614.	.1406
G06309	FF	263150.	7070250.	-.2749	G05710	FF	287950.	7049900.	.1603
G06543	MF	274150.	7064150.	-.2705	G05696	MF	273017.	7066973.	.2007
G06370	FF	297550.	7057600.	-.2452	G06332	FF	273150.	7066150.	1.3532

Table 12c: Wiluna Ferricretes
Component 7

> 95th Percentile				
Sample	Type	Easting	Northing	Score
G05728	FF	293250.	7031550.	.2425
G06543	MF	274150.	7064150.	.2679
G06342	FF	295950.	7060200.	.2753
G06606	FF	434850.	7005700.	.3049
G06613	FF	429050.	6961350.	.3609
G03525	FF	438750.	6946300.	.4058
G06380	FF	431950.	7010150.	.4680
G06332	FF	273150.	7066150.	1.7873

Table 12d: Wiluna Ferricretes
Component 8

< 5th Percentile					> 95th Percentile				
Sample	Type	Easting	Northing	Score	Sample	Type	Easting	Northing	Score
G06543	MF	274150.	7064150.	-.8873	G06302	FF	263050.	7073050.	.1862
G06380	FF	431950.	7010150.	-.4789	G06288	FF	262750.	7074900.	.1975
G06557	MF	279100.	7059150.	-.2840	G05710	FF	287950.	7049900.	.2045
G06606	FF	434850.	7005700.	-.2797	G05696	MF	273017.	7066973.	.2424
G06548	MF	278350.	7063900.	-.2259	G06340	FF	296700.	7056700.	.2556
G06337	FF	260950.	7075600.	-.1817	G03543	FF	419500.	6932950.	.3442
G06333	FF	272500.	7065500.	-.1553	G05746	FF	305850.	7020350.	.3545
G06360	FF	294450.	7059600.	-.1543	G06332	FF	273150.	7066150.	1.6560

Table 13a: Ranked CHI-6*X Scores
of the Wiluna Laterites
Chi-6*X Indices > 90th percentile ranking

"R/F2/F3" Samples

Sample	Type	Easting	Northing	Chi-6*X
G05735	LN	293900.	7025700.	2636.6
G03563	LN	436100.	7011250.	1365.0
G06195	LN	261800.	7073950.	1311.2
G03590	LN	280100.	7059200.	1143.3
G06163	LN	276000.	7070500.	1091.5
G06194	LN	269550.	7075450.	767.5
G03586	LN	275300.	7063700.	692.8
G06174	MS	264250.	7070450.	669.7
G05826	LN	293070.	7070820.	602.6
G06377	MS	429600.	7011500.	599.5
G06301	MS	263100.	7072100.	558.5
G03541	LP	418800.	6936500.	549.6
G03554	LN	430650.	6969500.	534.4
G03582	LN	275400.	7066650.	532.1
G05832	LN	290798.	7063273.	519.9
G03553	LN	430550.	6959500.	516.8
G06549	LN	275700.	7064650.	510.0
G06203	MS	344150.	7023500.	491.6
G03549	LN	427900.	6969950.	488.7
G06364	MS	294000.	7061100.	483.0
G05834	LP	290962.	7066755.	470.2
G03569	LN	433450.	7009050.	467.7
G06284	MS	257800.	7074650.	447.7
G03584	LN	270850.	7063650.	445.3
G05360	LN	429050.	6964750.	440.7
G06361	LN	293600.	7060200.	427.7

Table 13b: Ranked PEG-4 Scores
of the Wiluna Laterites
Peg-4 Indices > 90th percentile ranking

"R/F2/F3" Samples

Sample	Type	Easting	Northing	Peg-4
G05735	LN	293900.	7025700.	239.5
G06195	LN	261800.	7073950.	132.1
G03563	LN	436100.	7011250.	108.9
G03590	LN	280100.	7059200.	99.4
G06174	MS	264250.	7070450.	94.4
G06163	LN	276000.	7070500.	90.2
G03592	LN	274900.	7056000.	80.5
G03586	LN	275300.	7063700.	77.5
G03554	LN	430650.	6969500.	54.2
G06377	MS	429600.	7011500.	54.0
G06301	MS	263100.	7072100.	51.1
G06335	MS	270150.	7065950.	51.0
G05826	LN	293070.	7070820.	50.3
G06141	PN	421100.	7005600.	49.8
G03584	LN	270850.	7063650.	49.0
G03541	LP	418800.	6936500.	48.2
G06549	LN	275700.	7064650.	45.8
G06194	LN	269550.	7075450.	45.4
G06364	MS	294000.	7061100.	43.9
G06172	MS	266800.	7066800.	36.7
G06196	MS	262700.	7072100.	36.1
G06192	LN	264800.	7077250.	35.5
G03569	LN	433450.	7009050.	35.4
G06104	MS	427650.	6919800.	35.2
G03582	LN	275400.	7066650.	33.5
G06138	LN	425200.	7007000.	32.4

Table 13c: Ranked NUMCHI Scores of the Wiluna Laterites

NUMCHI Indices > 3.0

"R/F2/F3" Samples

Sample	Type	Easting	Northing	NUMCHI
G05735	LN	293900.	7025700.	3.0
G03578	MS	427550.	7005950.	3.0
G06190	LN	270550.	7073950.	3.0
G05369	MS	429450.	6964100.	3.0
G05375	MS	430700.	6963800.	3.0
G05826	LN	293070.	7070820.	3.0
G06206	MS	324750.	7019850.	3.0
G05832	LN	290798.	7063273.	3.0
G05834	LP	290962.	7066755.	3.0
G06298	LN	265650.	7076150.	3.0
G06317	MS	268850.	7068050.	3.0
G06338	LN	298000.	7054100.	3.0
G06377	MS	429600.	7011500.	3.0
G06364	MS	294000.	7061100.	3.0
G06390	MS	430350.	7003500.	3.0
G06550	LN	276900.	7065450.	3.0

Table 14a: Ranked CHI-6*X Scores of the Wiluna Ferricretes

Chi-6*X Indices > 90th percentile ranking

"R/F2/F3" Samples

Sample	Type	Easting	Northing	Chi-6*X
G06332	FF	273150.	7066150.	2148.1
G06947	MF	273864.	7066002.	1851.2
G06543	MF	274150.	7064150.	1845.7
G06951	MF	273261.	7065684.	1831.8
G06283	FF	258900.	7073600.	1608.1
G06946	MF	273560.	7065997.	1514.0
G06945	MF	273228.	7065991.	1356.3
G06950	MF	273593.	7065690.	1307.6
G06333	FF	272500.	7065500.	942.7
G06288	FF	262750.	7074900.	884.0
G06948	MF	274219.	7066316.	868.5
G06281	FF	262800.	7073800.	743.2
G06319	FF	268750.	7066550.	668.2
G06308	FF	262400.	7071200.	638.3
G06280	FF	263750.	7073650.	633.1
G06954	MF	274961.	7066637.	630.0

Table 14b: Ranked PEG-4 Scores of the Wiluna Ferricretes

Peg-4 Indices > 90th percentile ranking

"R/F2/F3" Samples

Sample	Type	Easting	Northing	Peg-4
G06332	FF	273150.	7066150.	195.1
G06947	MF	273864.	7066002.	172.7
G06951	MF	273261.	7065684.	172.3
G06283	FF	258900.	7073600.	146.9
G06946	MF	273560.	7065997.	139.5
G06945	MF	273228.	7065991.	122.2
G06950	MF	273593.	7065690.	117.1
G06543	MF	274150.	7064150.	111.2
G06333	FF	272500.	7065500.	82.1
G06948	MF	274219.	7066316.	76.7
G06288	FF	262750.	7074900.	72.6
G06309	FF	263150.	7070250.	66.7
G06322	FF	269650.	7070250.	66.5
G06954	MF	274961.	7066637.	65.6
G06308	FF	262400.	7071200.	56.9
G06280	FF	263750.	7073650.	56.9

Table 14c: Ranked NUMCHI Scores of the Wiluna Ferricretes

Chi-6*X Indices > 90th percentile ranking
"R/F2/F3" Samples

Sample	Type	Easting	Northing	NUMCHI
G06543	MF	274150.	7064150.	9.0
G06333	FF	272500.	7065500.	6.0
G06302	FF	263050.	7073050.	5.0
G06557	MF	279100.	7059150.	5.0
G06283	FF	258900.	7073600.	5.0
G06329	FF	272750.	7067700.	5.0
G06332	FF	273150.	7066150.	4.0
G06337	FF	260950.	7075600.	4.0
G06342	FF	295950.	7060200.	4.0
G06290	FF	263450.	7075800.	4.0
G06308	FF	262400.	7071200.	4.0
G06547	MF	276400.	7063750.	4.0
G06558	MF	278900.	7061650.	4.0
G06563	MF	281750.	7058150.	4.0
G06941	MF	273527.	7066304.	4.0
G06947	MF	273864.	7066002.	4.0

Table 15: X^2 Values for Multi-element Group (Laterites)

Cu Pb Zn As Sb Bi Mo Ag Sn W Se Ga Nb Ta

15% Trim (40 samples)

Sample	Type	Easting	Northing	Mahalanobis Distance Observed X^2	Expected X^2
G06103	MS	427650.	6917000.	52.70	19.45
G06335	MS	270150.	7065950.	52.82	19.56
G06104	MS	427650.	6919800.	52.84	19.67
G06301	MS	263100.	7072100.	53.27	19.78
G05834	LP	290962.	7066755.	58.10	19.90
G06392	LN	429200.	7006250.	59.67	20.01
G06605	LN	434850.	7007200.	63.49	20.14
G03538	MS	421500.	6944200.	67.74	20.26
G06132	MS	444200.	6918650.	72.61	20.39
G05727	LN	292800.	7033700.	74.47	20.52
G06182	LN	255200.	7078000.	81.37	20.65
G06183	MS	252850.	7078100.	84.30	20.79
G06130	LN	449000.	6916650.	87.10	20.93
G05737	LN	295450.	7023750.	88.12	21.08
G06206	MS	324750.	7019850.	106.60	21.23
G06377	MS	429600.	7011500.	112.21	21.39
G06385	MS	430300.	7004900.	116.69	21.55
G03586	LN	275300.	7063700.	118.75	21.72
G06181	MS	253350.	7074700.	121.07	21.89
G06201	MS	347400.	7016000.	133.42	22.08
G06203	MS	344150.	7023500.	137.93	22.27
G03553	LN	430550.	6959500.	172.20	22.47
G06200	MS	349350.	7015400.	174.17	22.67
G03590	LN	280100.	7059200.	174.86	22.89
G06199	MS	349350.	7013550.	179.38	23.12
G06192	LN	264800.	7077250.	197.34	23.37
G05701	LN	289500.	7059050.	199.66	23.63
G05826	LN	293070.	7070820.	215.31	23.91
G06174	MS	264250.	7070450.	270.14	24.21
G03563	LN	436100.	7011250.	310.48	24.53
G03527	MS	442200.	6943400.	314.54	24.89
G06138	LN	425200.	7007000.	315.09	25.27
G06195	LN	261800.	7073950.	344.67	25.71
G03592	LN	274900.	7056000.	400.54	26.20
G03554	LN	430650.	6969500.	681.37	26.76
G05360	LN	429050.	6964750.	909.16	27.43
G03549	LN	427900.	6969950.	927.86	28.26
G06163	LN	276000.	7070500.	989.72	29.34
G06141	PN	421100.	7005600.	991.18	30.95
G05735	LN	293900.	7025700.	1472.29	34.28

Table 16: X^2 Values for Multi-element Group (Ferricretes)

Cu Pb Zn As Sb Bi Mo Ag Sn W Se Ga Nb Ta

15% Trim (25 samples)

Sample	Type	Easting	Northing	Mahalanobis Distance Observed X^2	Expected X^2
G06107	FF	429050.	6916250.	44.99	19.42
G06332	FF	273150.	7066150.	46.37	19.60
G06113	FF	441900.	6911250.	47.07	19.78
G06288	FF	262750.	7074900.	52.04	19.97
G06370	FF	297550.	7057600.	58.23	20.17
G06340	FF	296700.	7056700.	59.37	20.37
G06314	FF	267050.	7067750.	59.64	20.58
G06615	MF	430000.	6960750.	60.14	20.81
G05833	FF	291533.	7065687.	65.98	21.04
G06539	FF	287200.	7063000.	67.15	21.29
G06109	FF	432550.	6913650.	72.01	21.55
G06545	FF	277100.	7062500.	89.21	21.82
G06337	FF	260950.	7075600.	95.47	22.12
G05373	FF	430150.	6963950.	112.42	22.43
G06333	FF	272500.	7065500.	113.66	22.78
G06133	FF	433350.	6982150.	117.43	23.15
G06613	FF	429050.	6961350.	120.42	23.55
G06368	FF	297400.	7055600.	141.88	24.01
G06302	FF	263050.	7073050.	142.24	24.52
G06606	FF	434850.	7005700.	165.70	25.11
G03525	FF	438750.	6946300.	193.96	25.80
G06380	FF	431950.	7010150.	397.98	26.65
G06342	FF	295950.	7060200.	403.74	27.77
G06152	MF	290650.	7081700.	427.71	29.43
G06543	MF	274150.	7064150.	541.20	32.83

This page has been left blank.

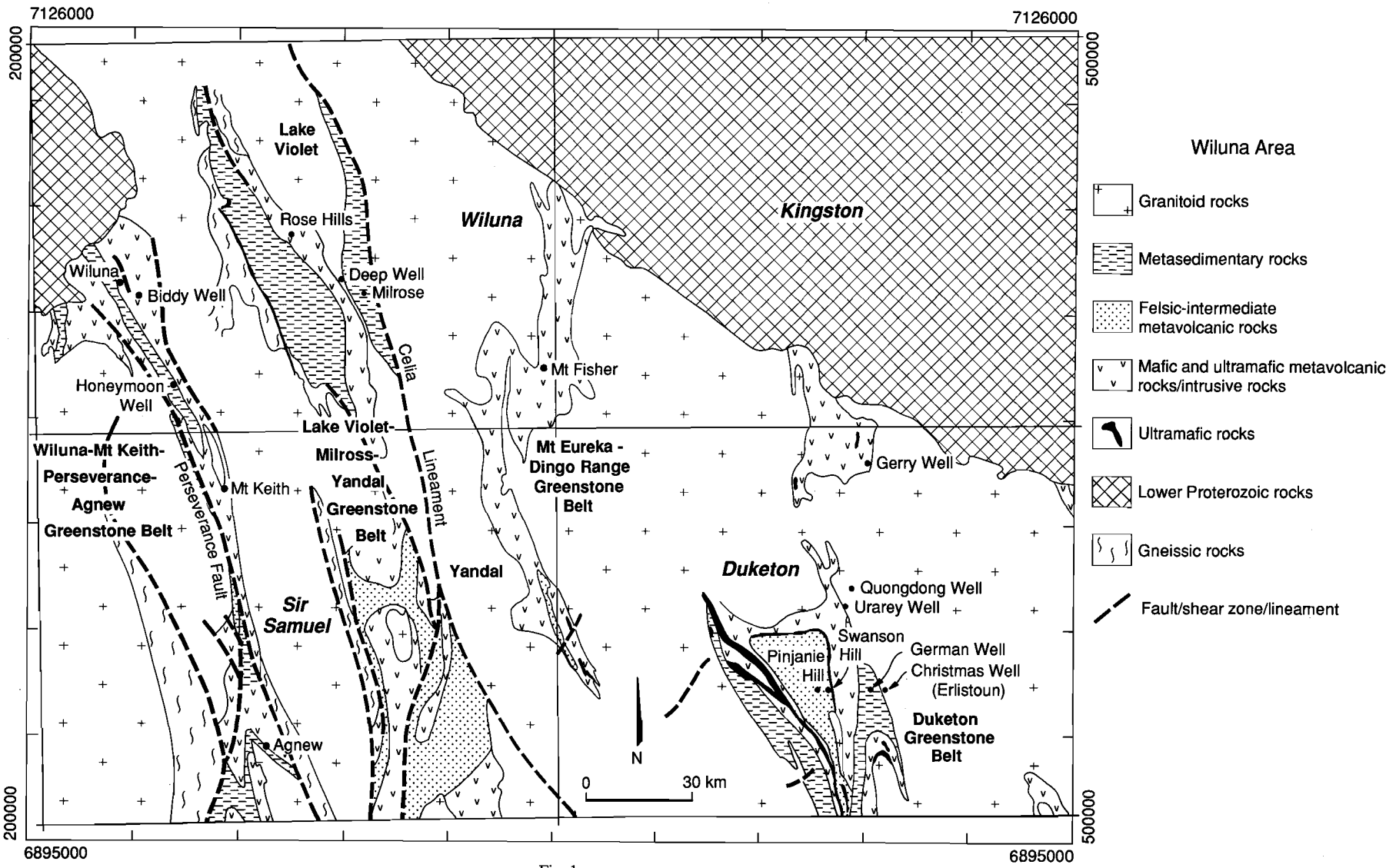
7126000
7126000
200000
500000
Lake Violet
Rose Hills
Wiluna
Deep Well
Milrose
Biddy Well
Wiluna
Celia
Honeymoon Well
Mt Fisher
Lake Violet-
Milross-
Yandal
Greenstone
Belt
Wiluna-Mt Keith-
Perseverance-
Agnew
Greenstone Belt
Perseverance Fault
Mt Keith
Lineament
Mt Eureka -
Dingo Range
Greenstone
Belt
Gerry Well
Yandal
Duketon
Quongdong Well
Urarey Well
Swanson Hill
Pinjanie Hill
German Well
Christmas Well
(Erlistoun)
Duketon
Greenstone
Belt
Sir Samuel
Agnew
N
0
30 km
200000
500000
6895000
6895000
Wiluna Area
Granitoid rocks
Metasedimentary rocks
Felsic-intermediate metavolcanic rocks
Mafic and ultramafic metavolcanic rocks/intrusive rocks
Ultramafic rocks
Lower Proterozoic rocks
Gneissic rocks
Fault/shear zone/lineament

Fig. 1

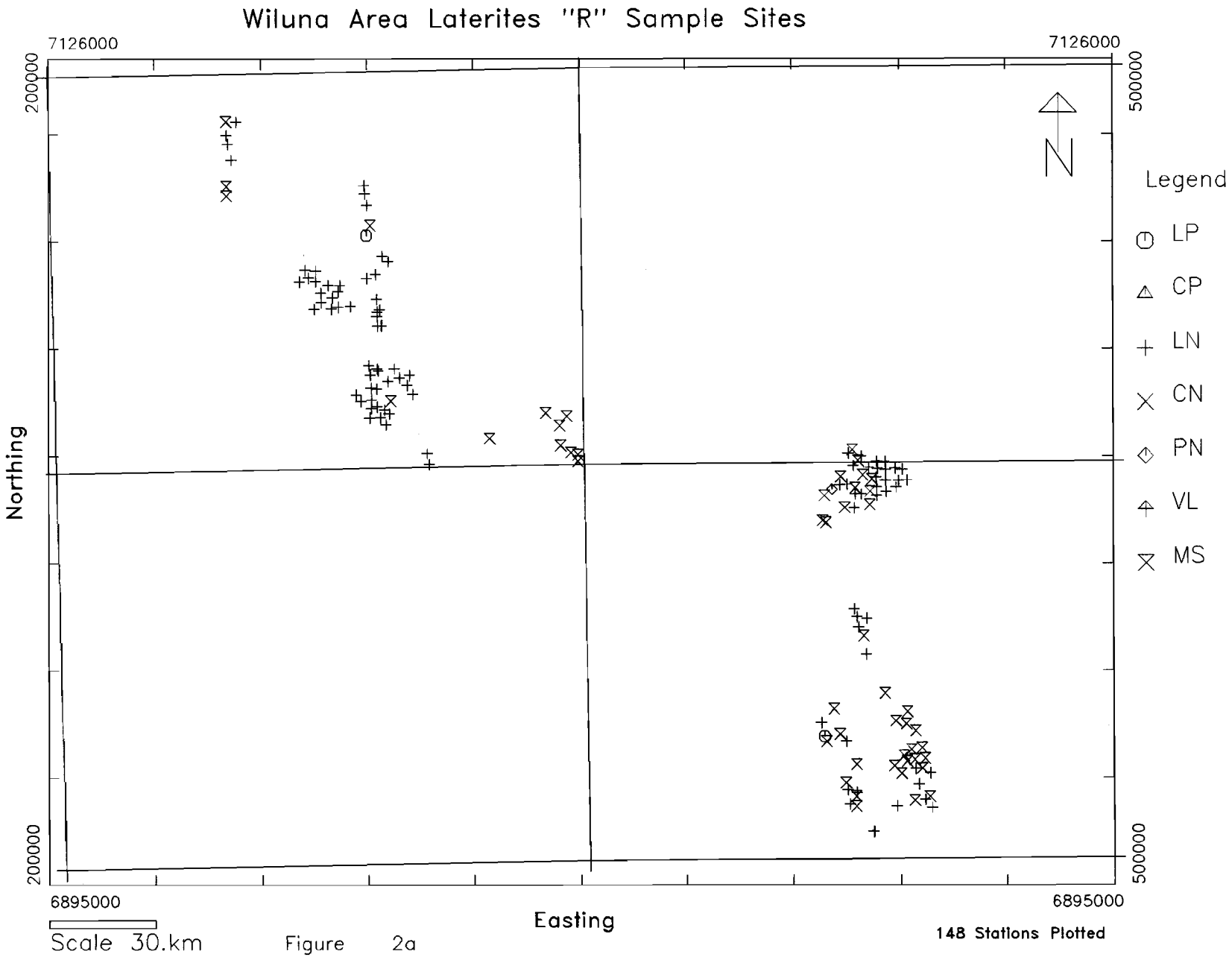
Wiluna Area Laterites "R" Sample Sites
7126000
7126000
200000
500000
N
Legend
LP
CP
LN
CN
PN
VL
MS
Northing
200000
500000
6895000
6895000
Easting
Scale 30.km
148 Stations Plotted

Figure 2a

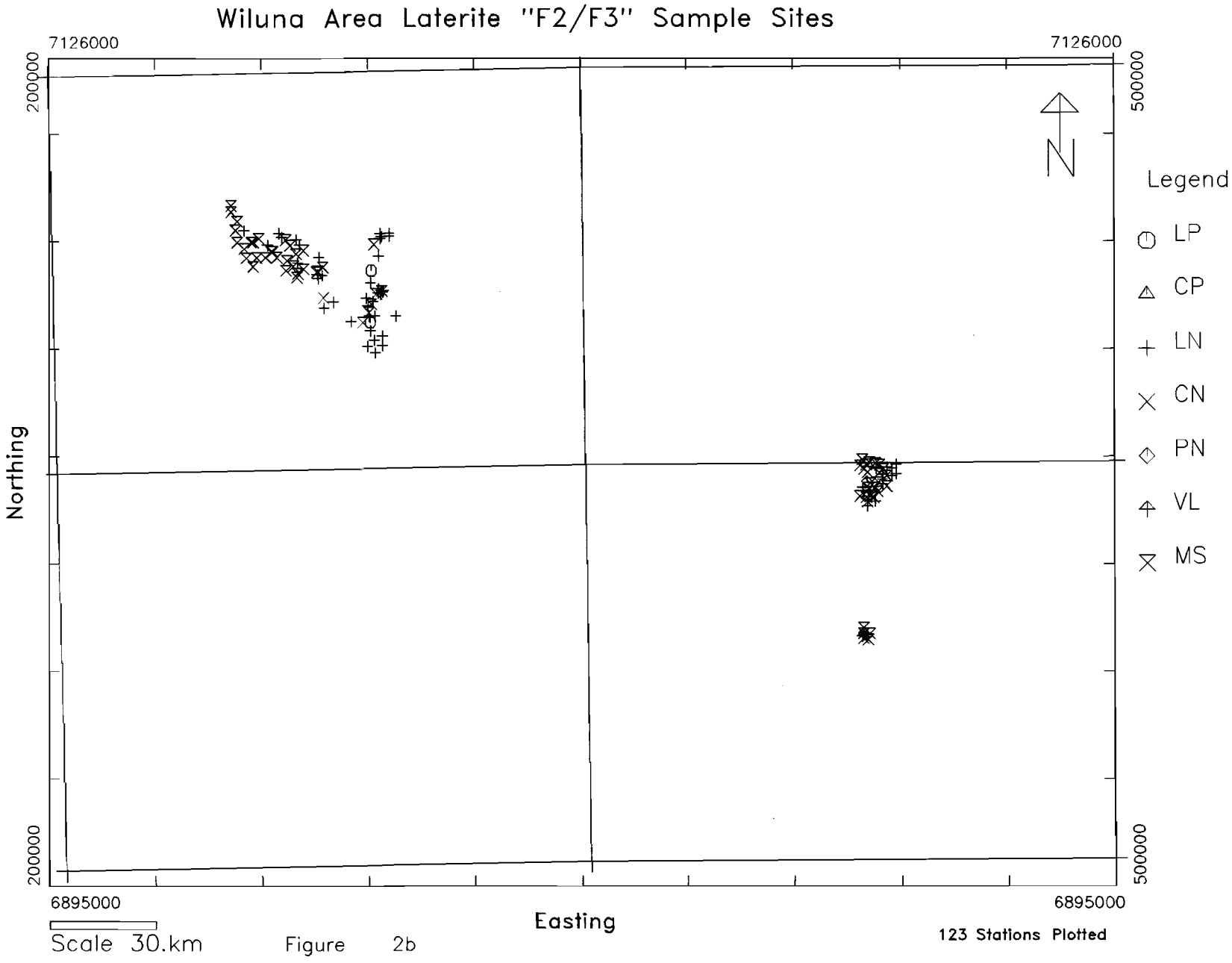
Wiluna Area Laterite "F2/F3" Sample Sites
7126000
7126000
200000
500000
N
Legend
LP
CP
LN
CN
PN
VL
MS
Northing
200000
500000
6895000
6895000
Easting
Scale 30.km
123 Stations Plotted

Figure 2b

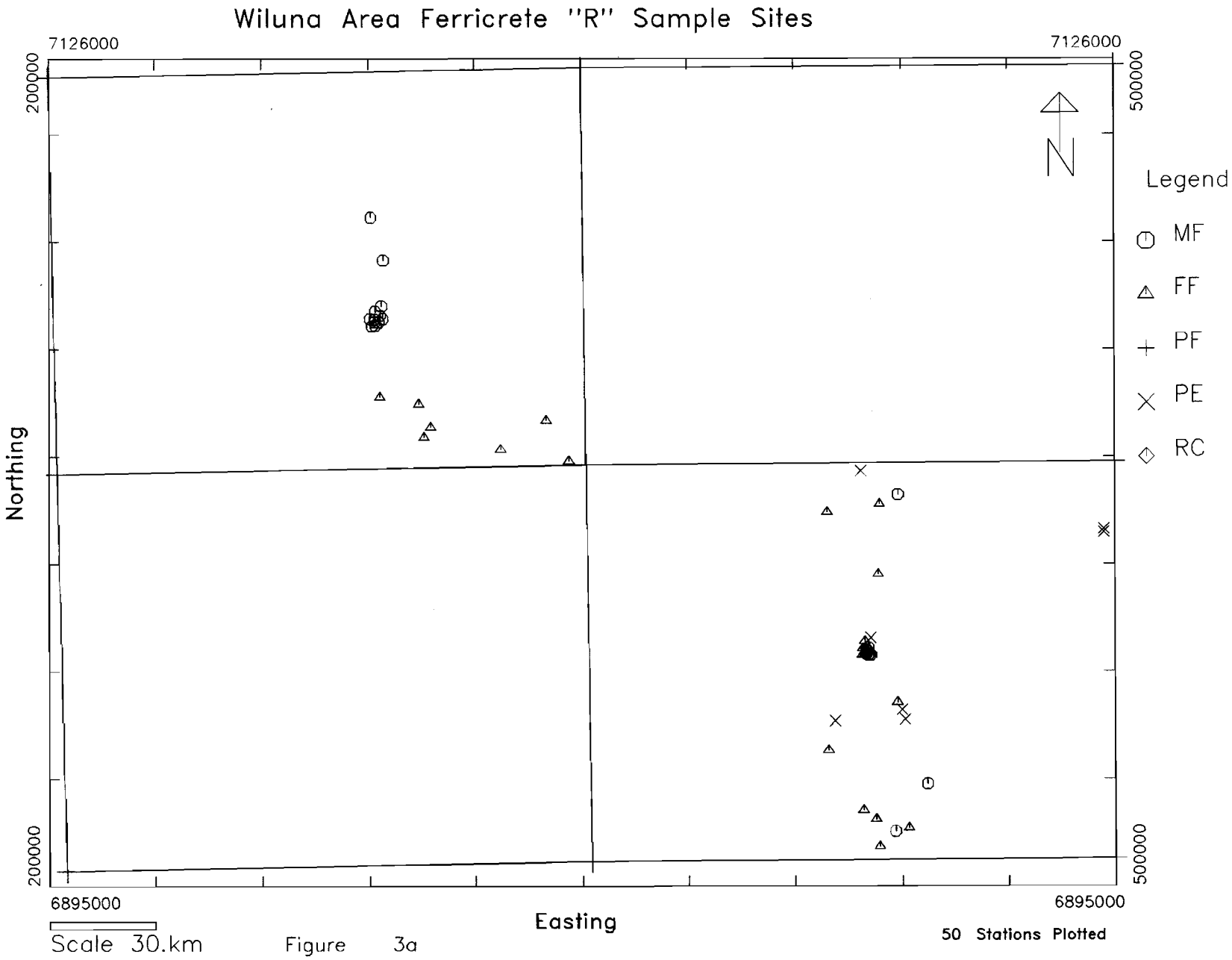
Wiluna Area Ferricrete "R" Sample Sites
7126000
7126000
200000
500000
N
Legend
MF
FF
PF
PE
RC
Northing
200000
500000
6895000
6895000
Easting
Scale 30.km
50 Stations Plotted

Figure 3a

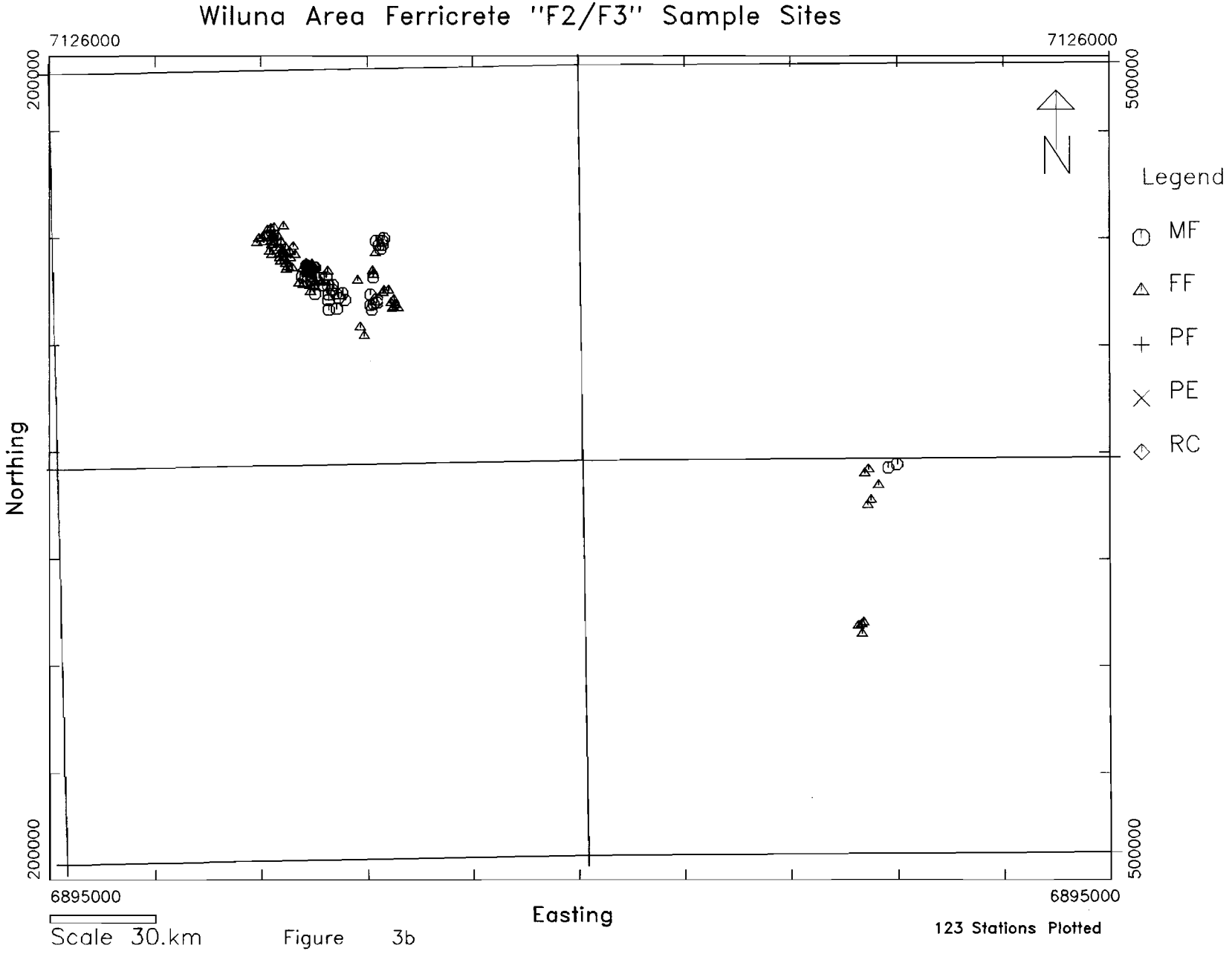
Wiluna Area Ferricrete "F2/F3" Sample Sites
7126000
7126000
200000
500000
N
Legend
MF
FF
PF
PE
RC
Northing
200000
500000
6895000
6895000
Easting
Scale 30.km
123 Stations Plotted

Figure 3b

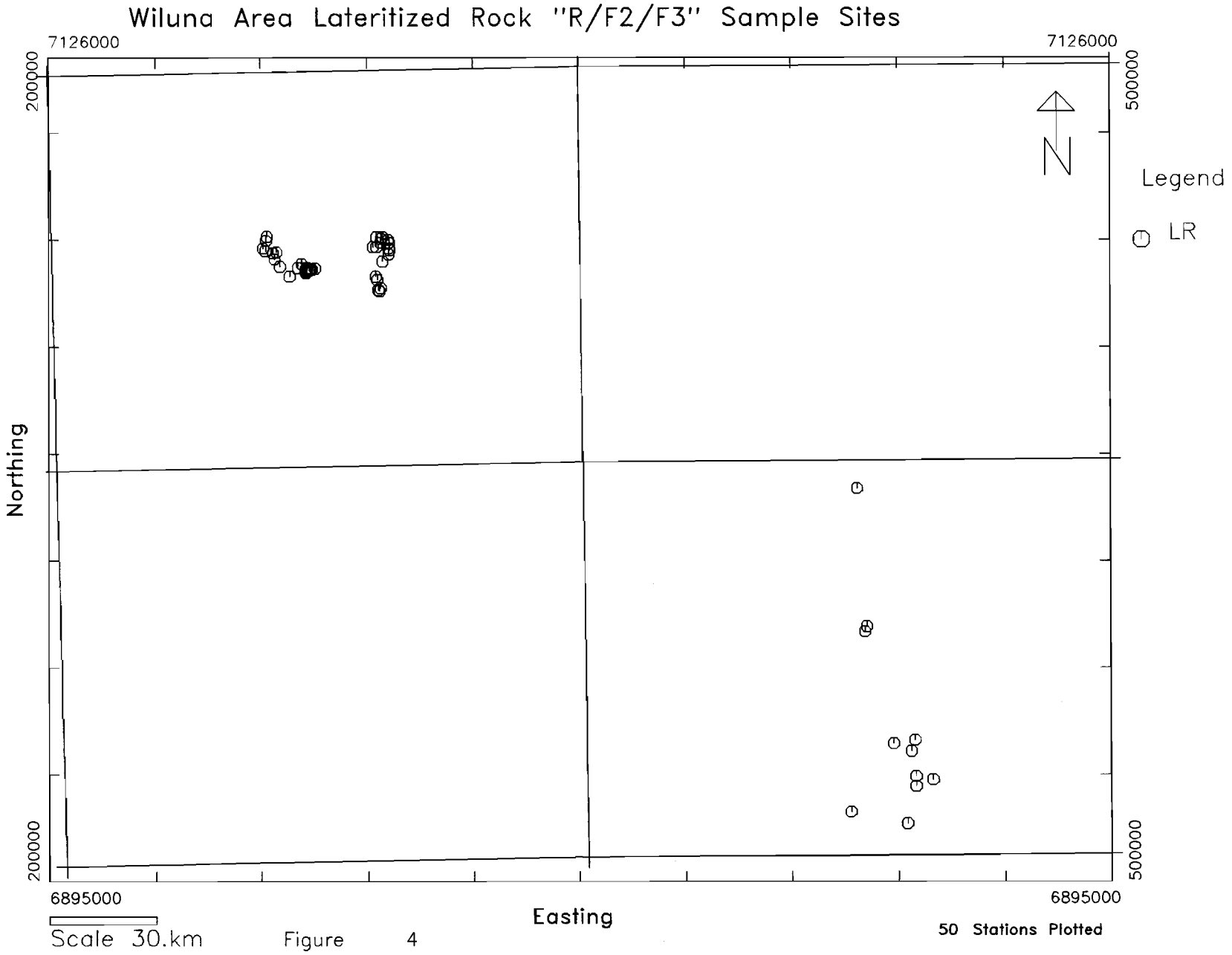
Wiluna Area Lateritized Rock "R/F2/F3" Sample Sites
7126000
7126000
200000
500000
N
Legend
LR
Northing
200000
500000
6895000
6895000
Easting
Scale 30.km
50 Stations Plotted

Figure 4

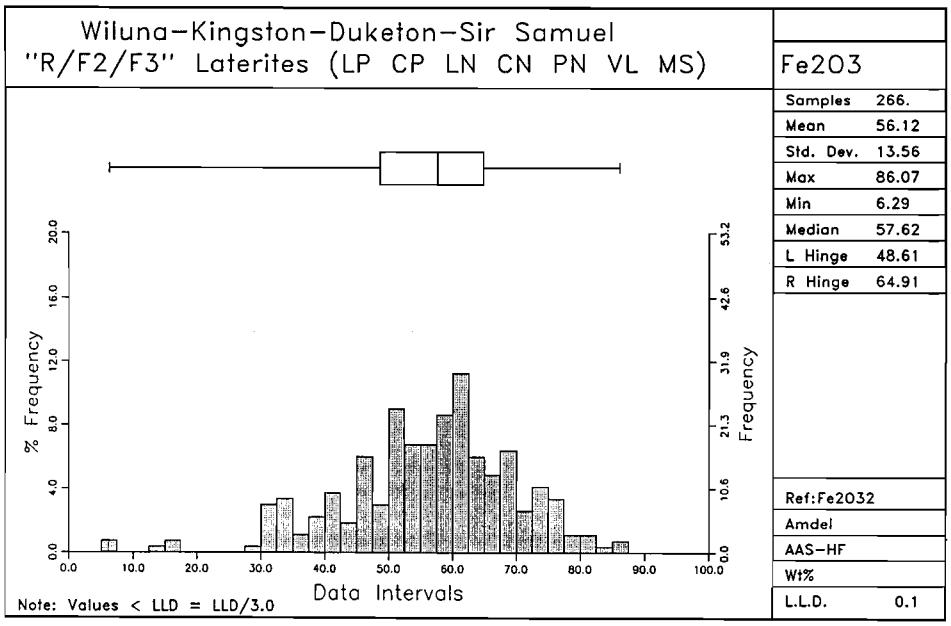

Figure 5a

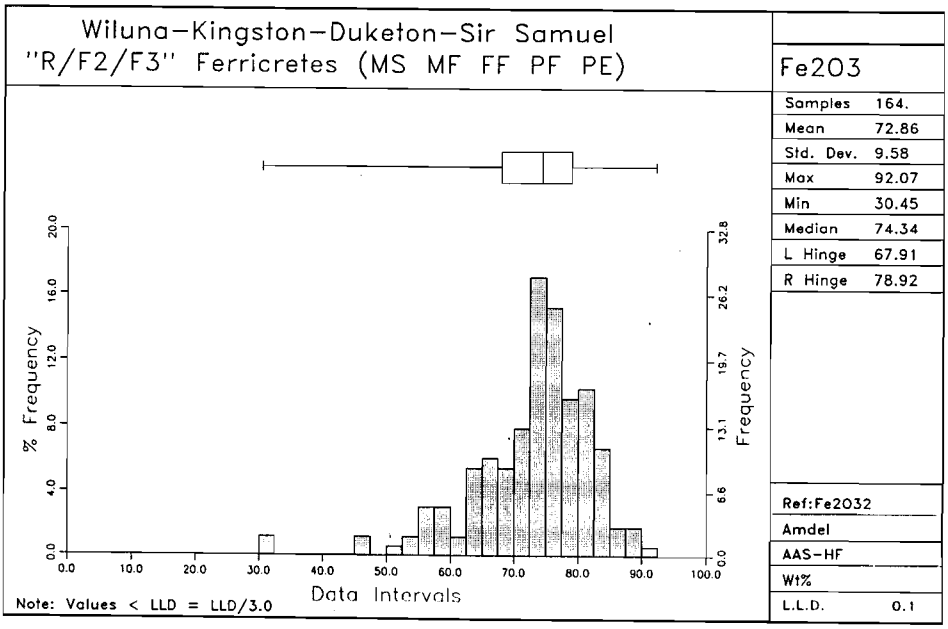

Figure 5b

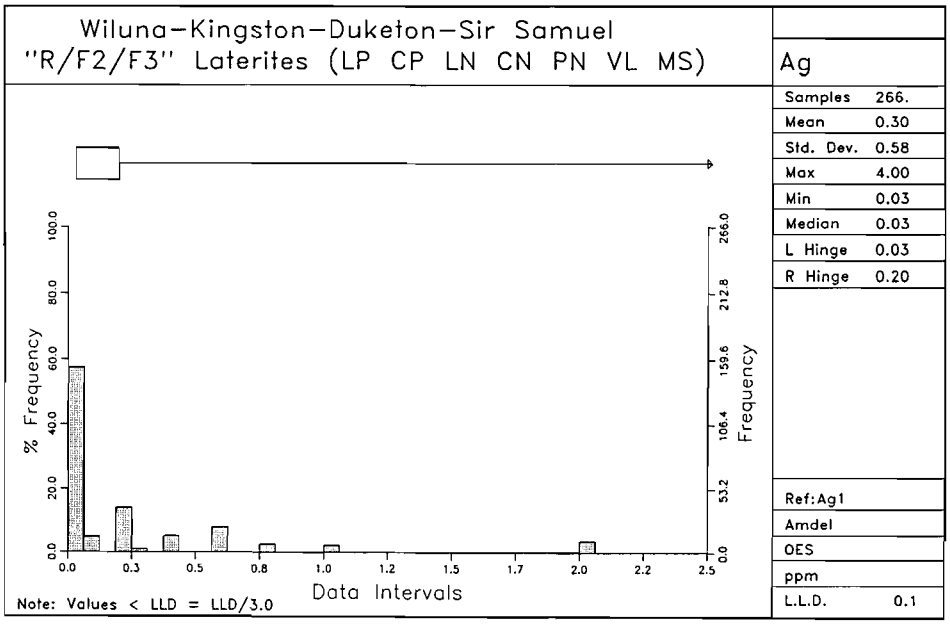

Figure 6a

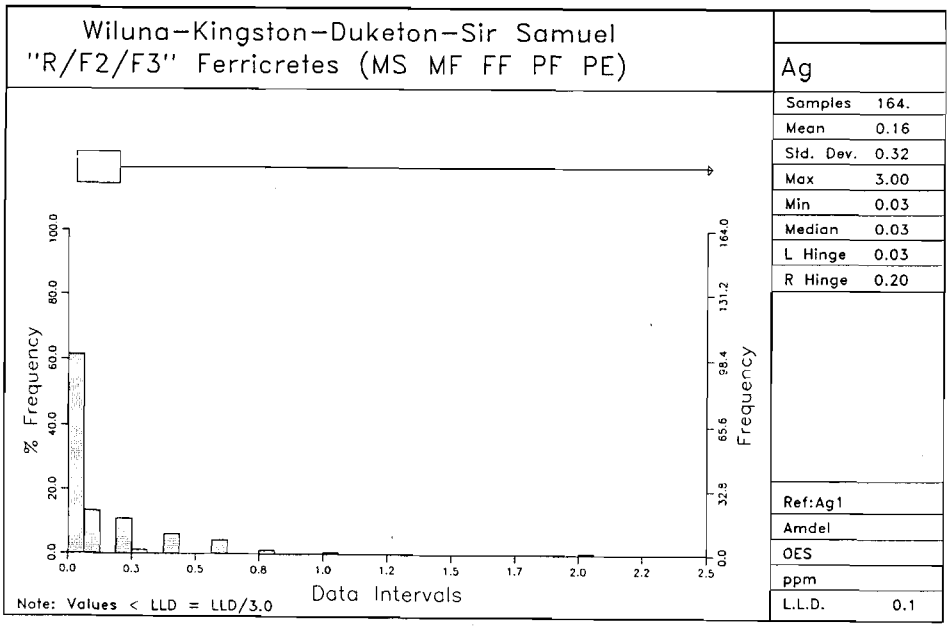

Figure 6b

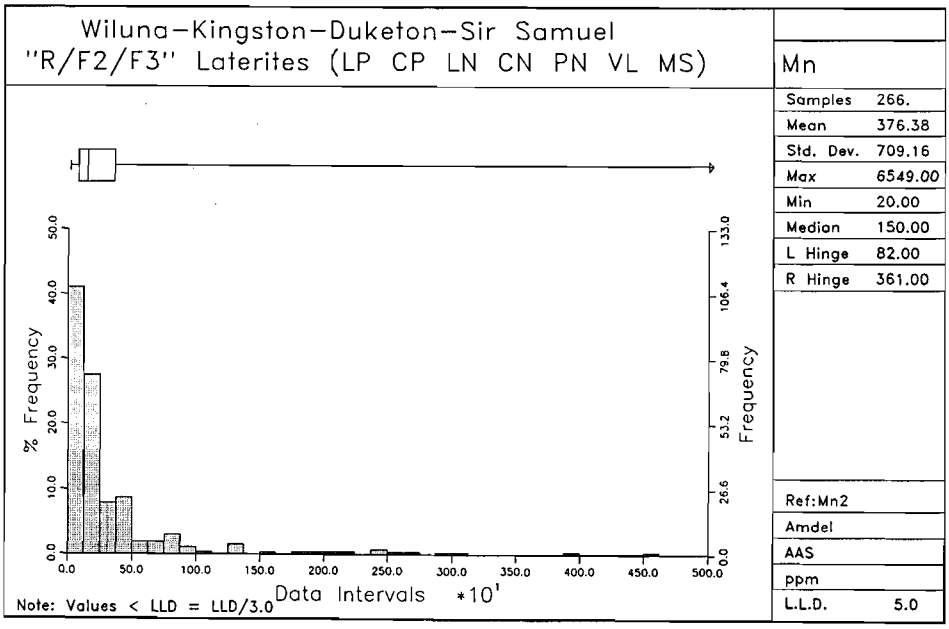

Figure 7a

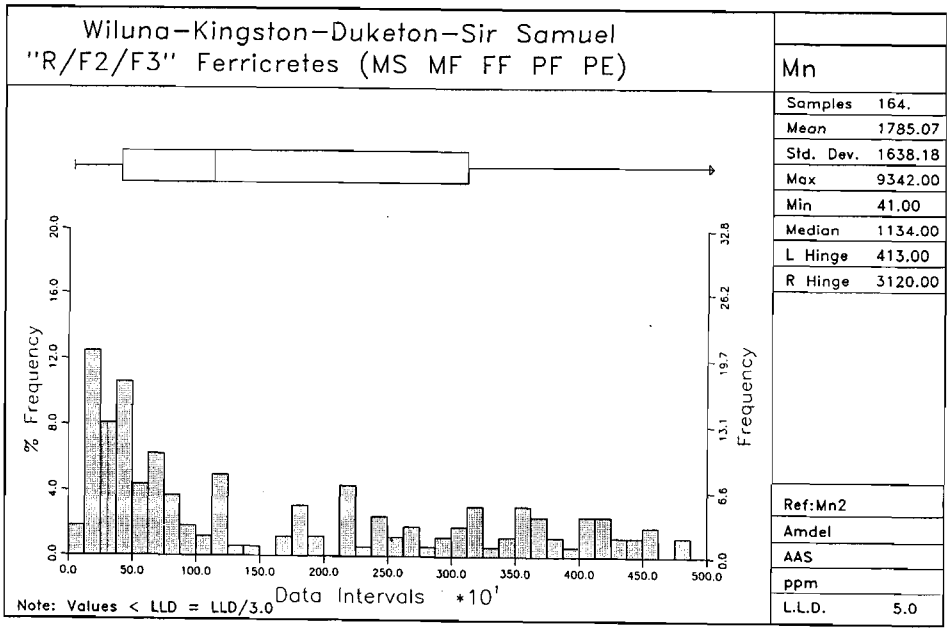

Figure 7b

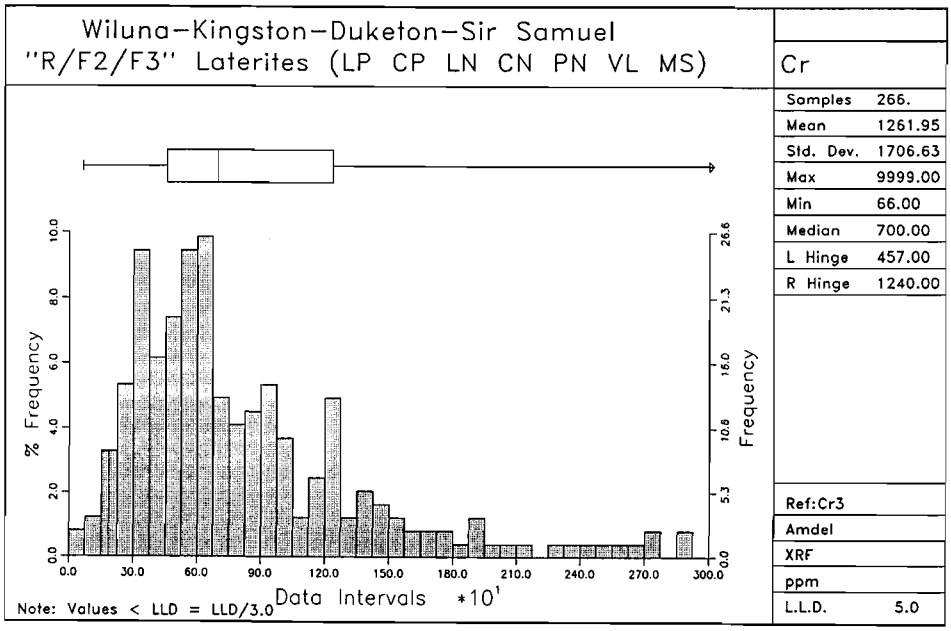

Figure 8a

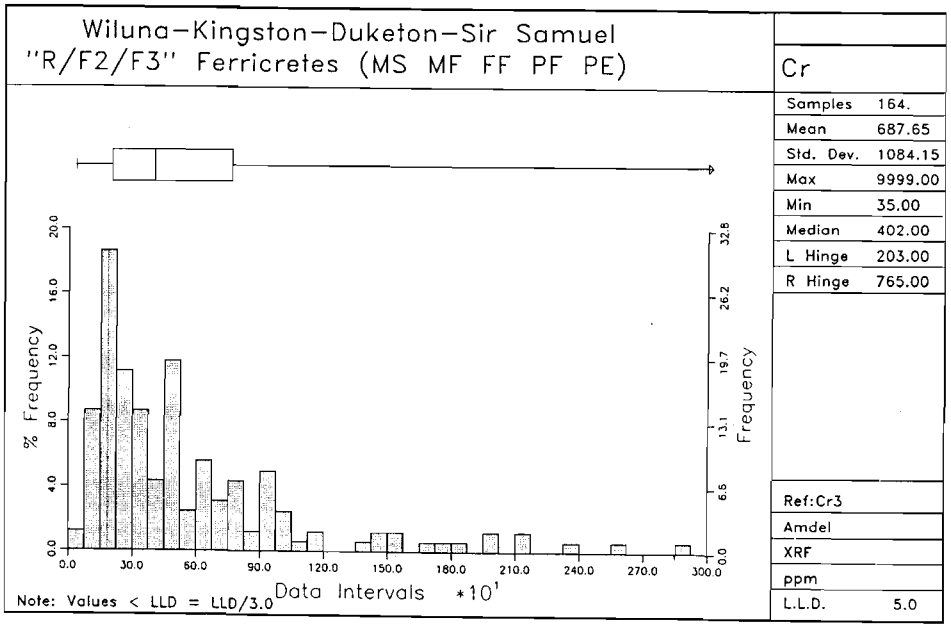

Figure 8b

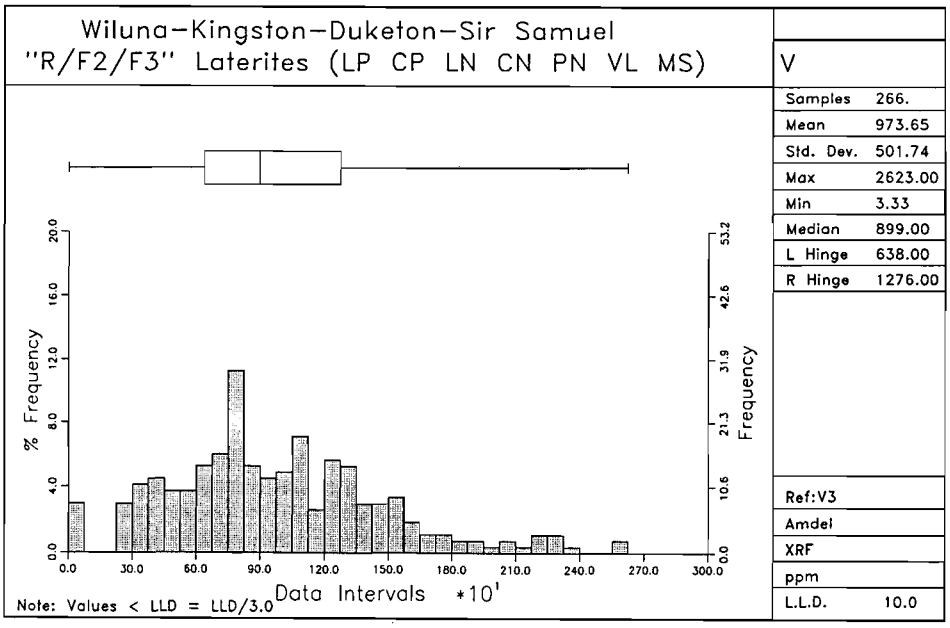

Figure 9a

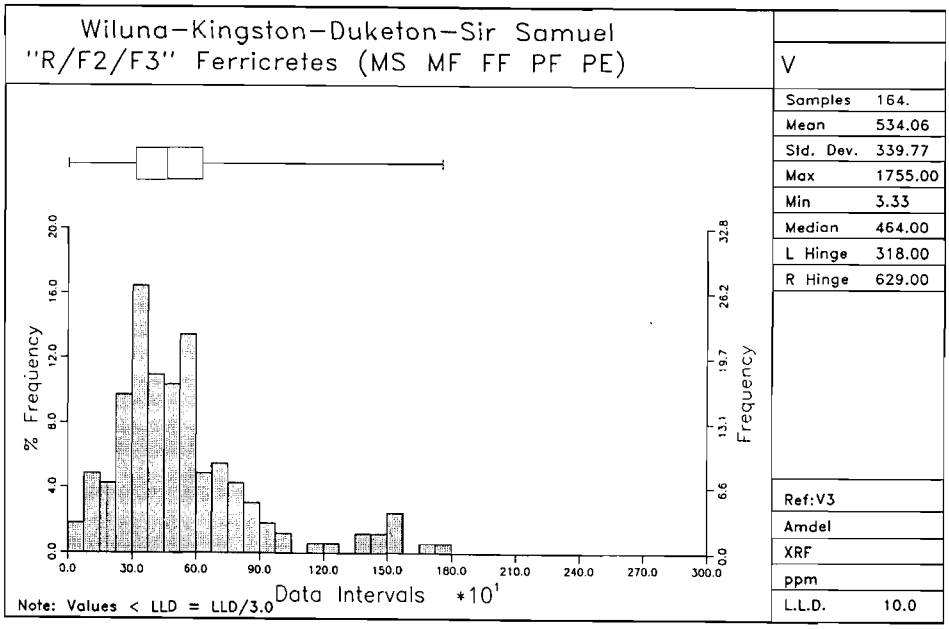

Figure 9b

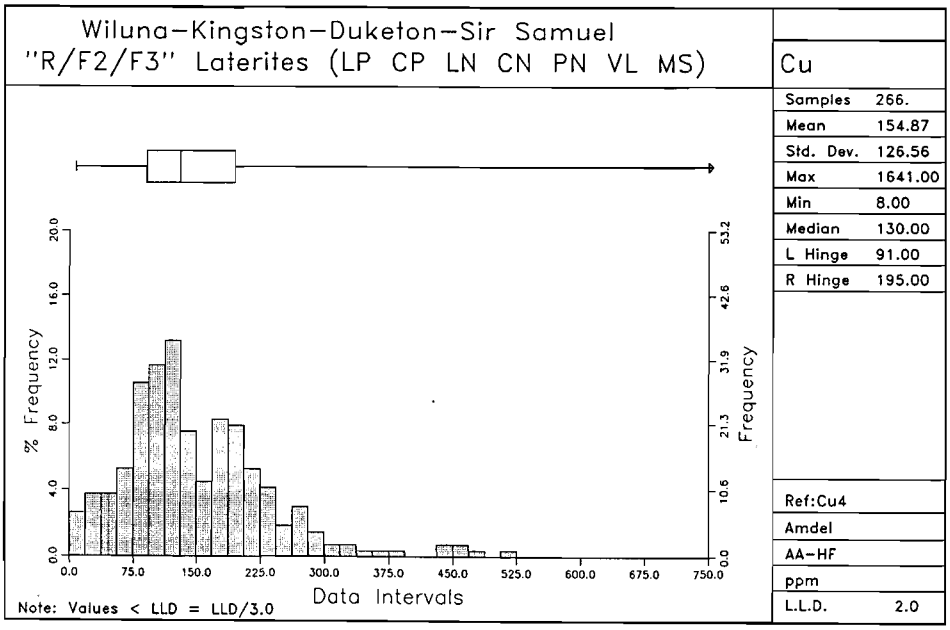

Figure 10a

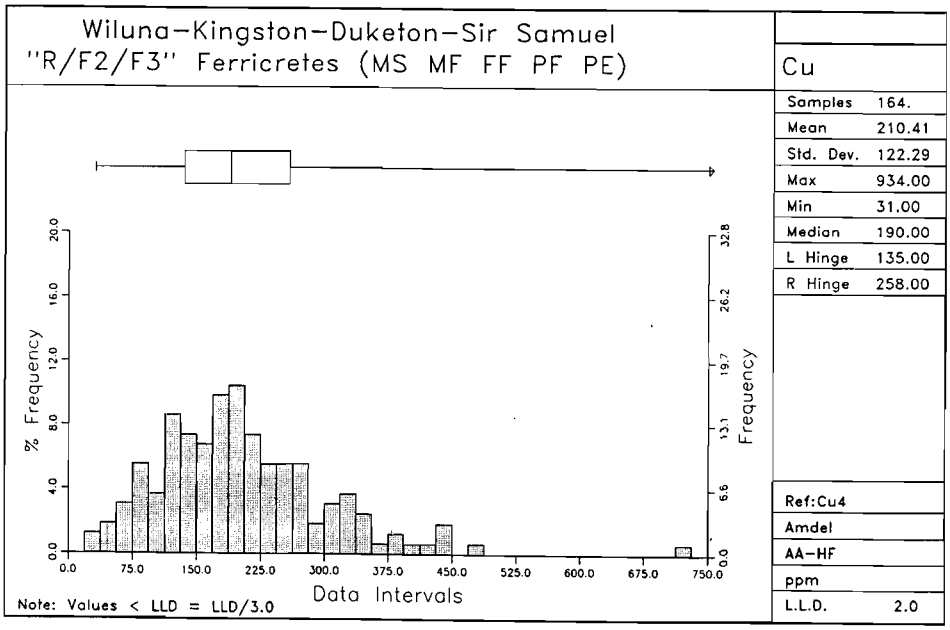

Figure 10b

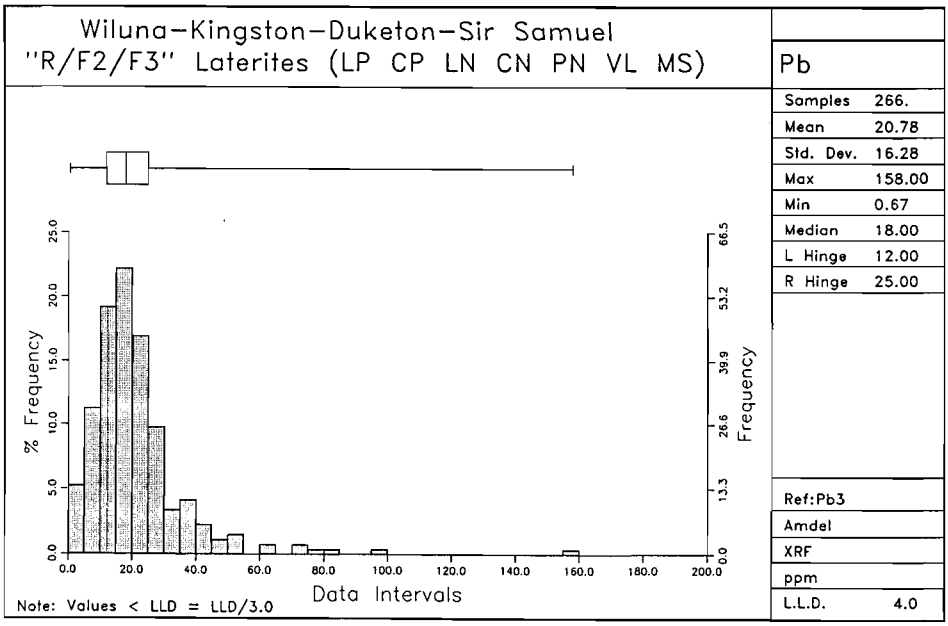

Figure 11a

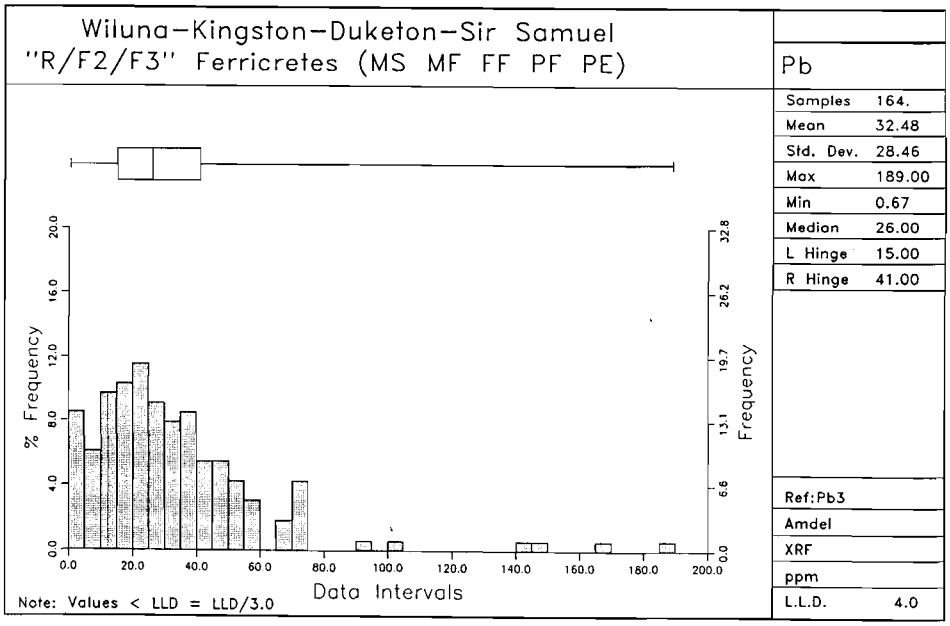

Figure 11b

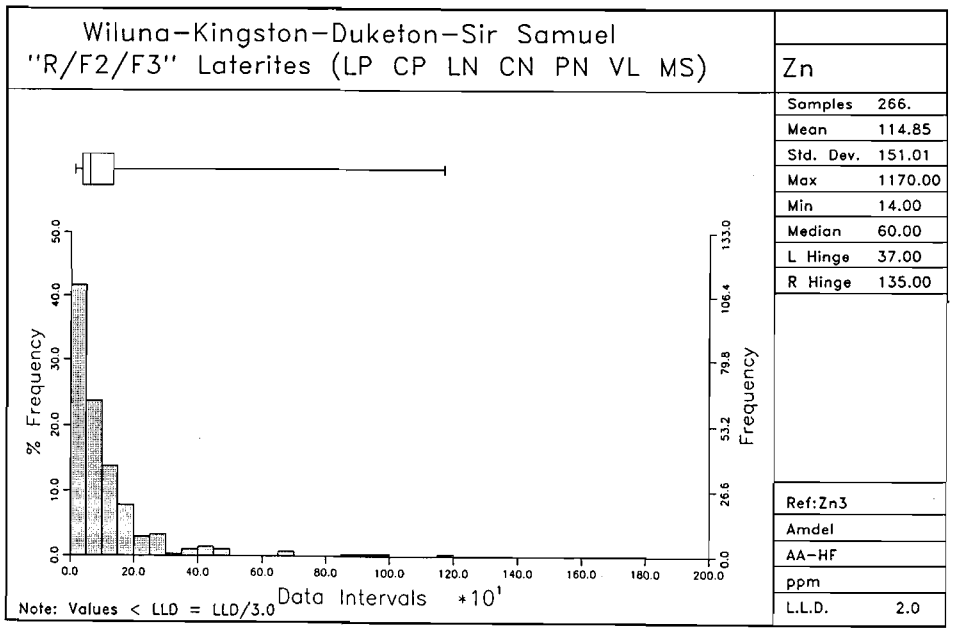

Figure 12a

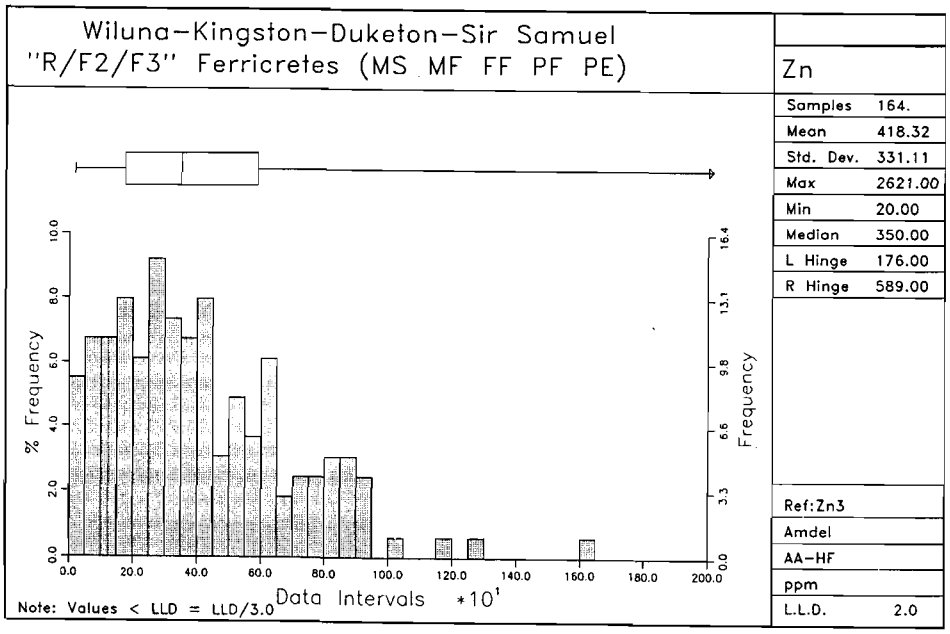

Figure 12b

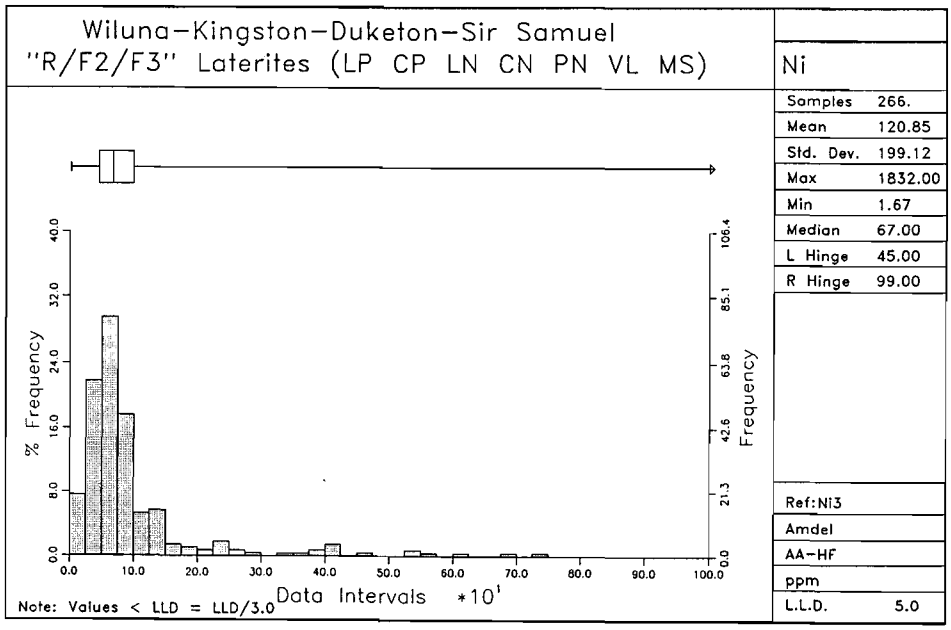

Figure 13a

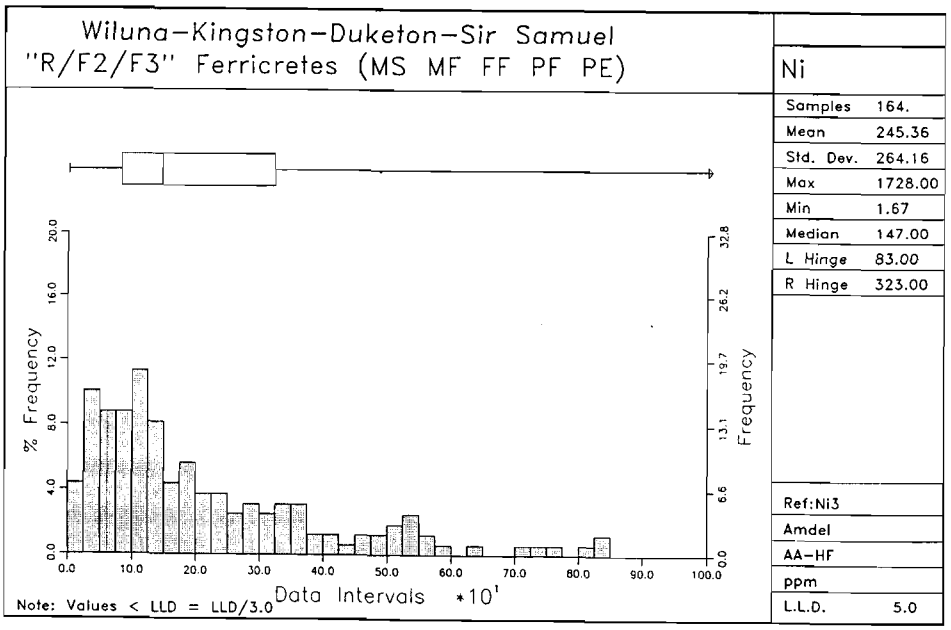

Figure 13b

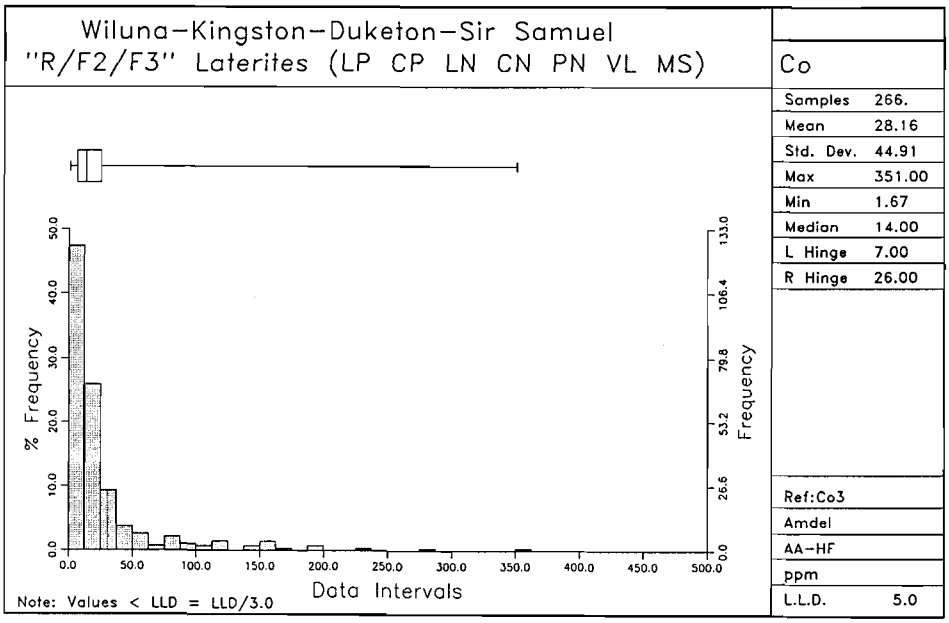

Figure 14a

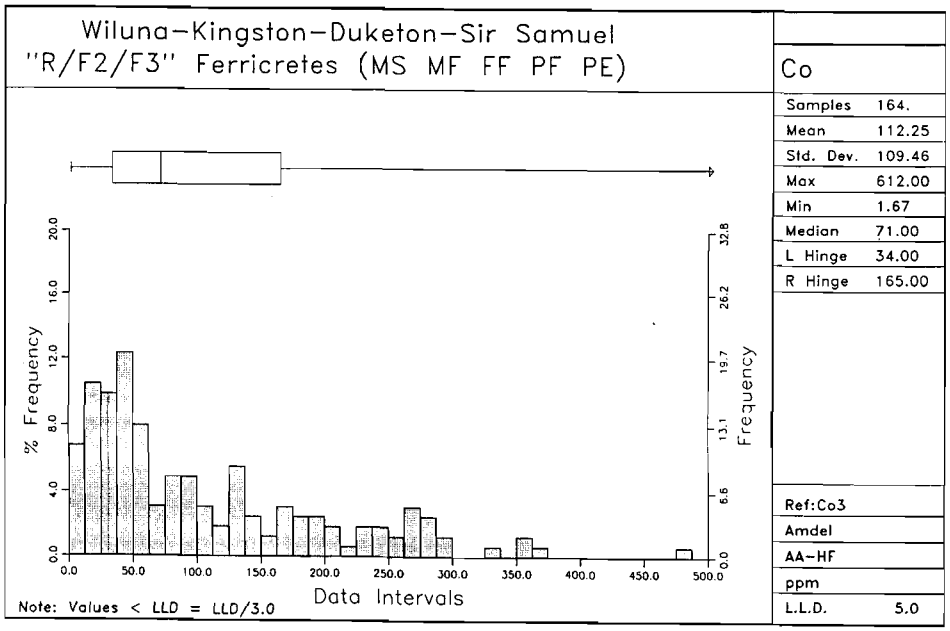

Figure 14b

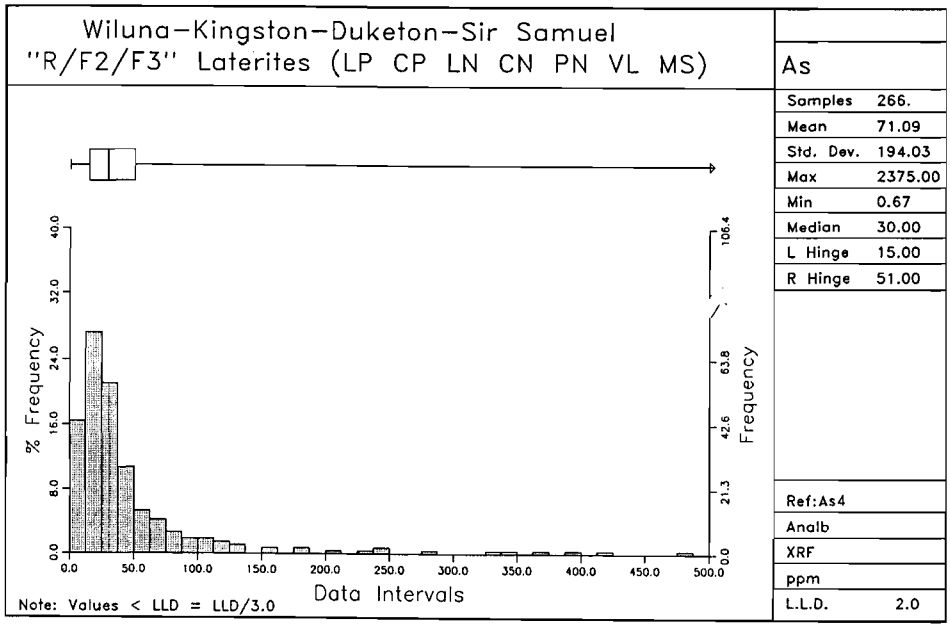

Figure 15a

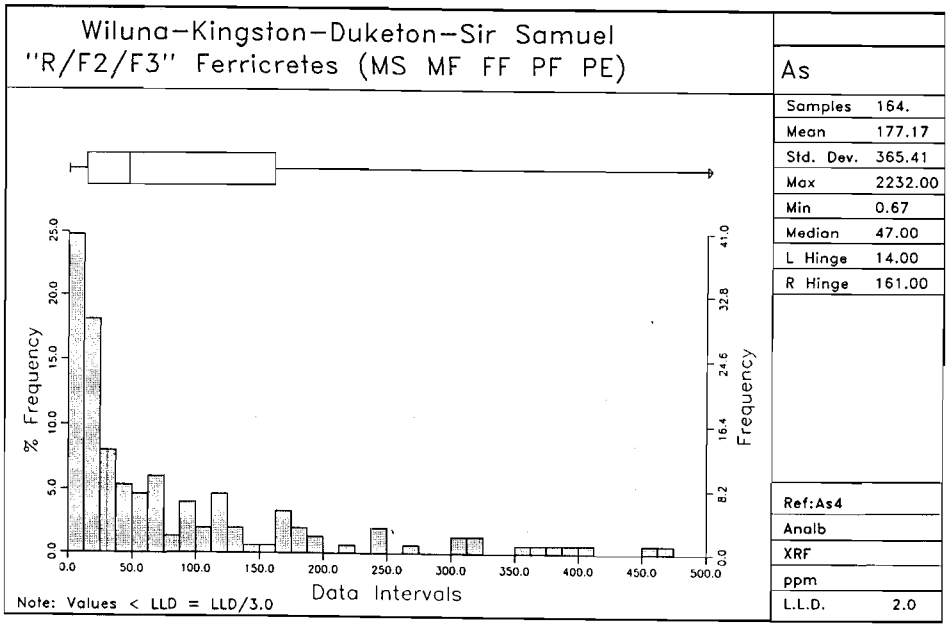

Figure 15b

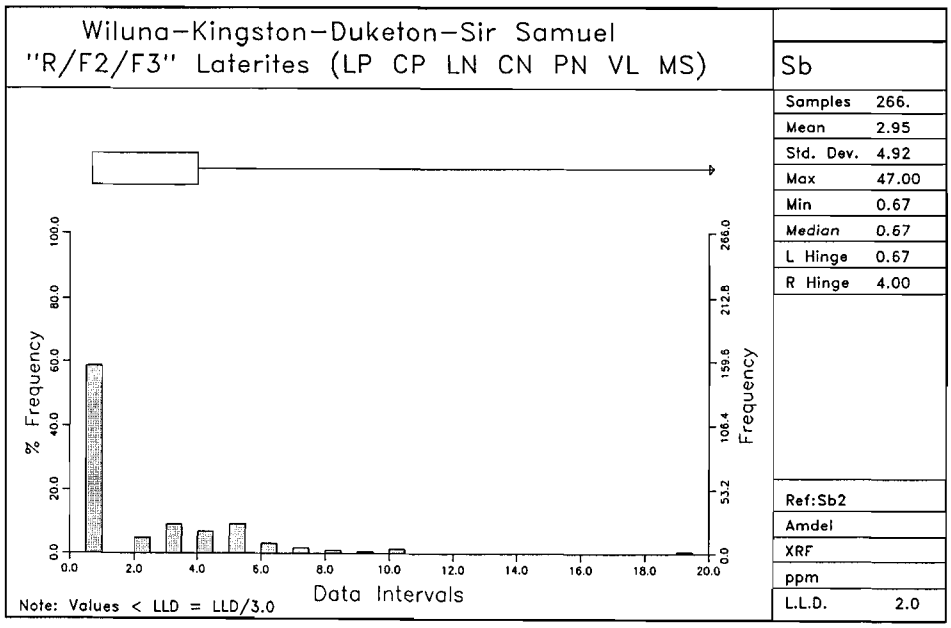

Figure 16a

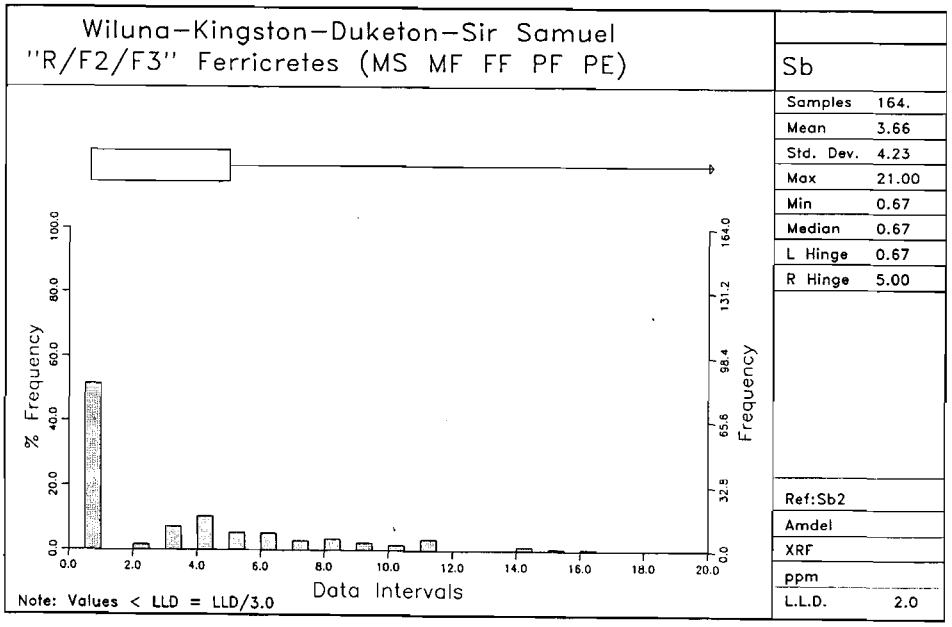

Figure 16b

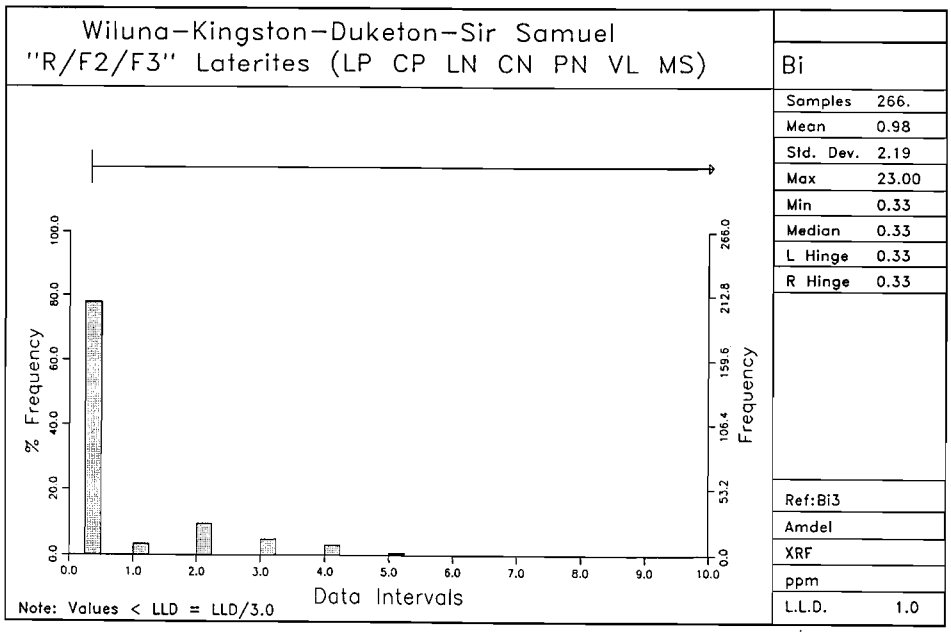

Figure 17a

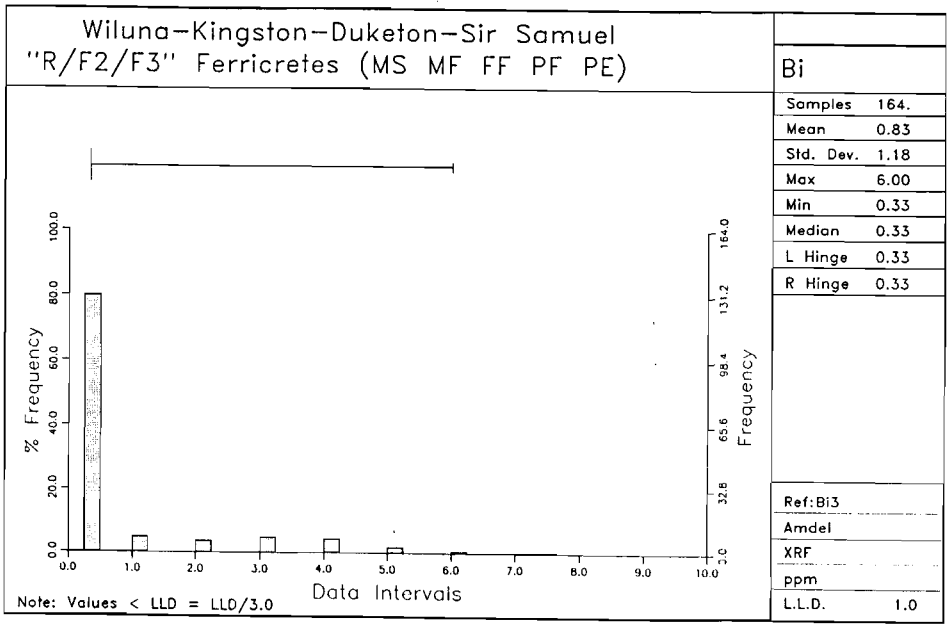

Figure 17b

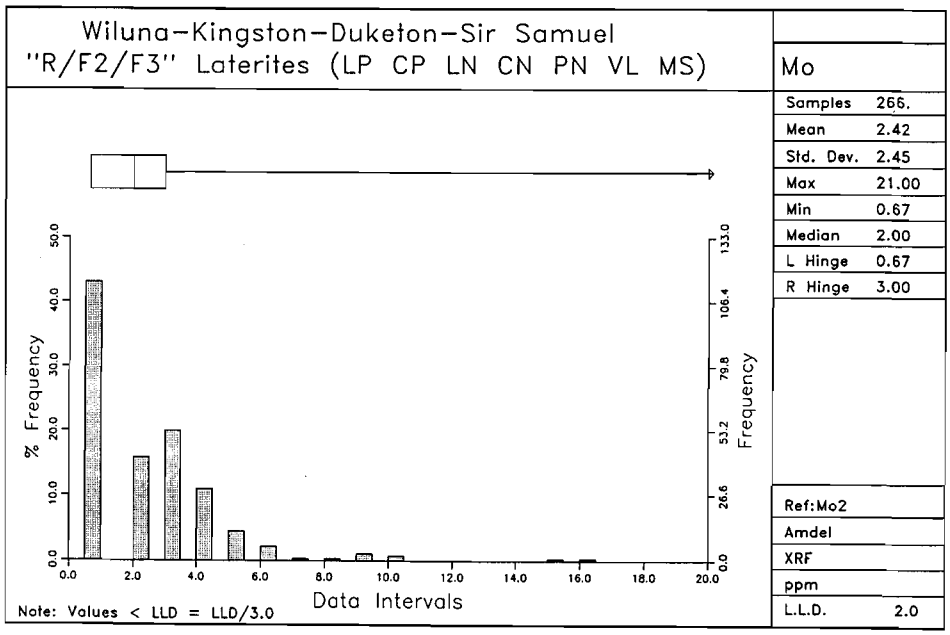

Figure 18a

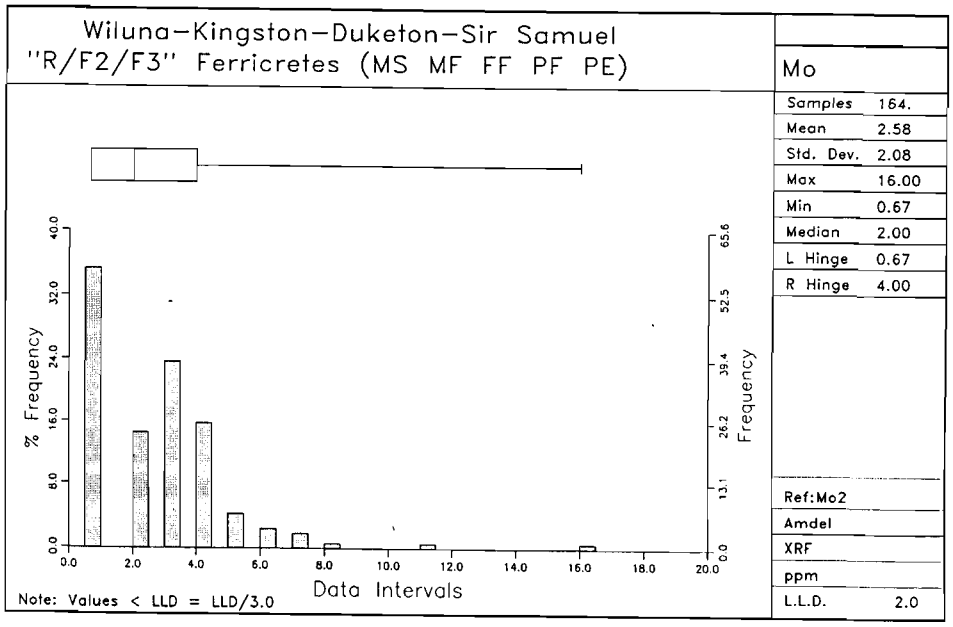

Figure 18b

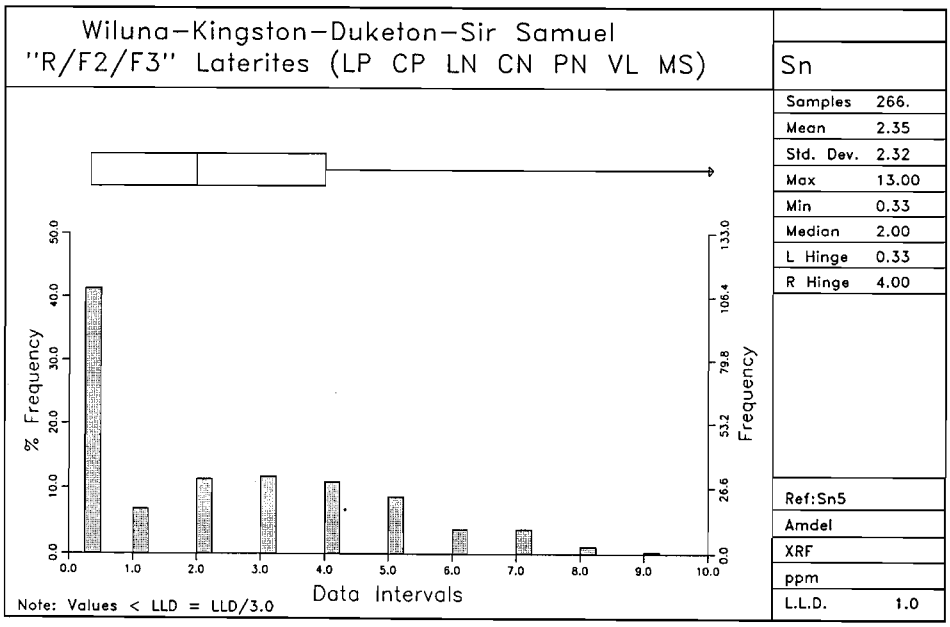

Figure 19a

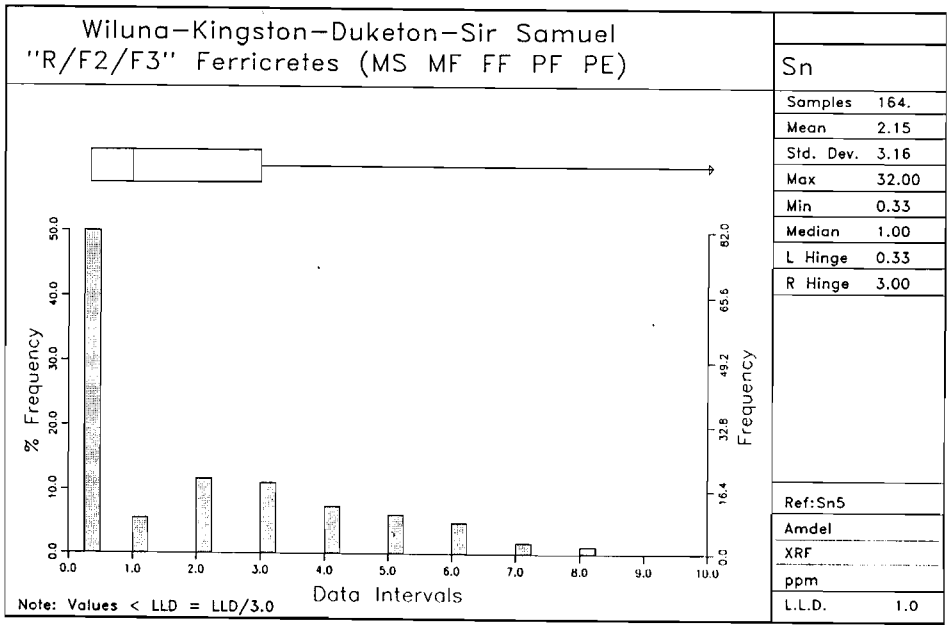

Figure 19b

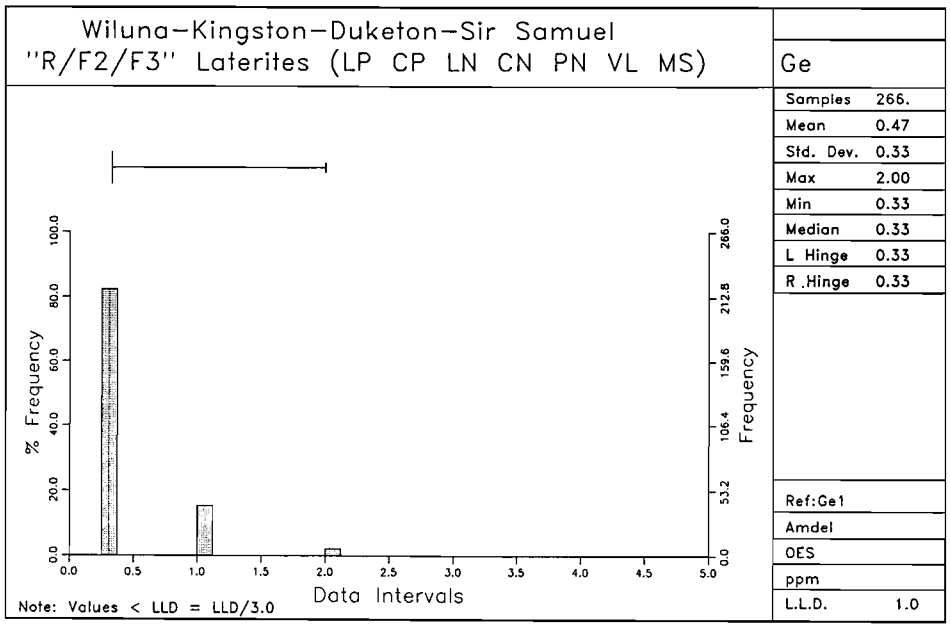

Figure 20a

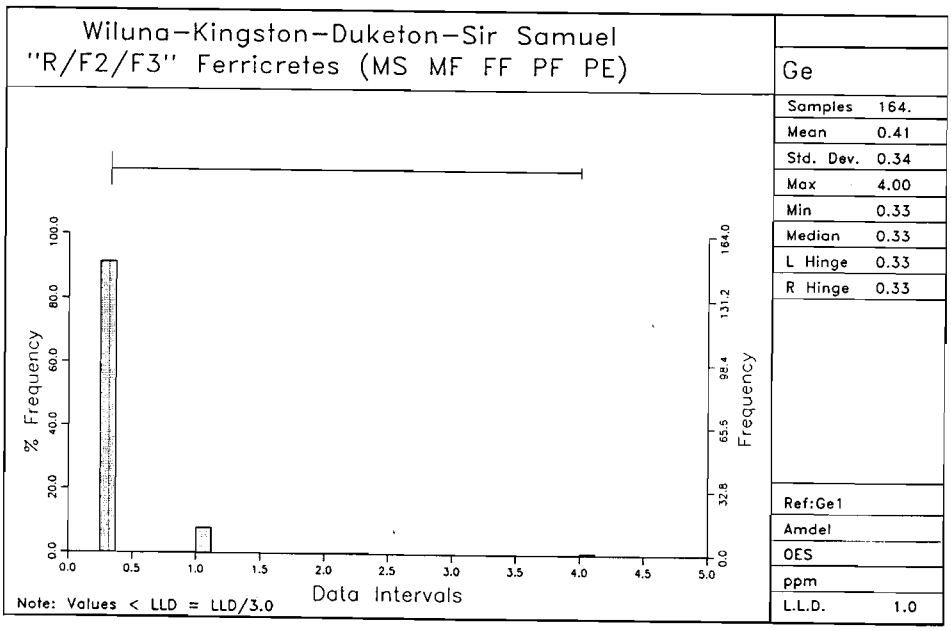

Figure 20b

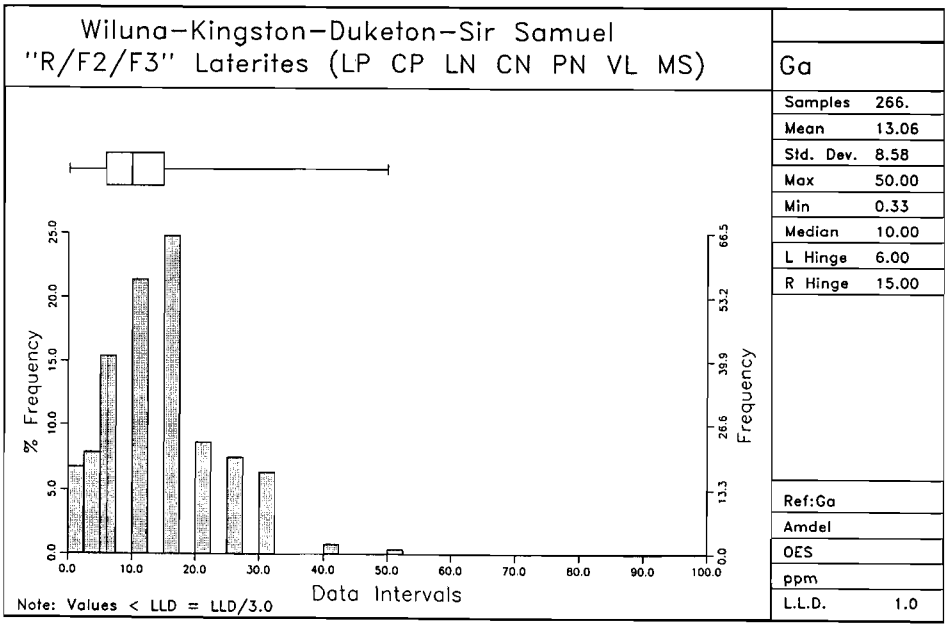

Figure 21a

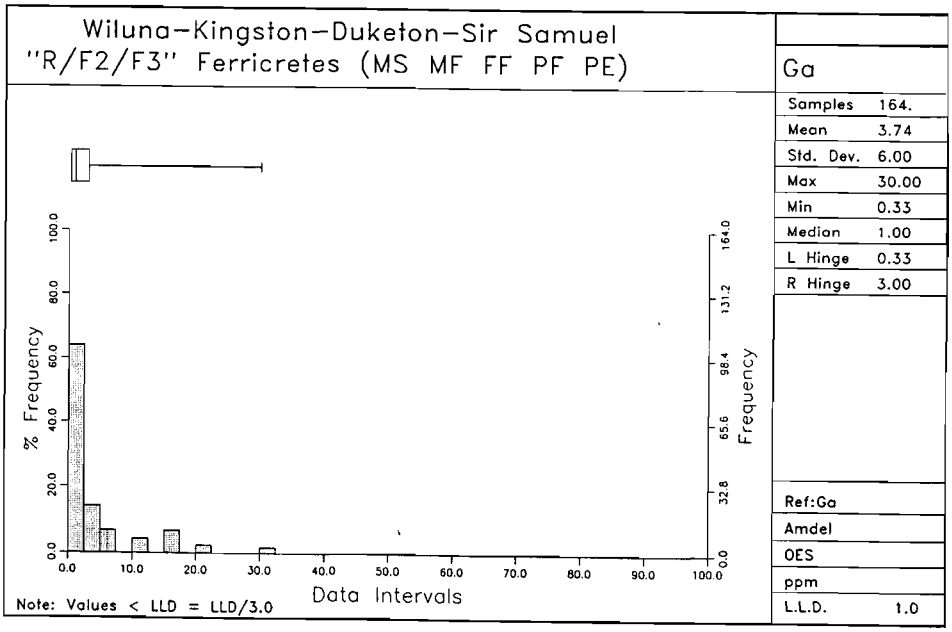

Figure 21b

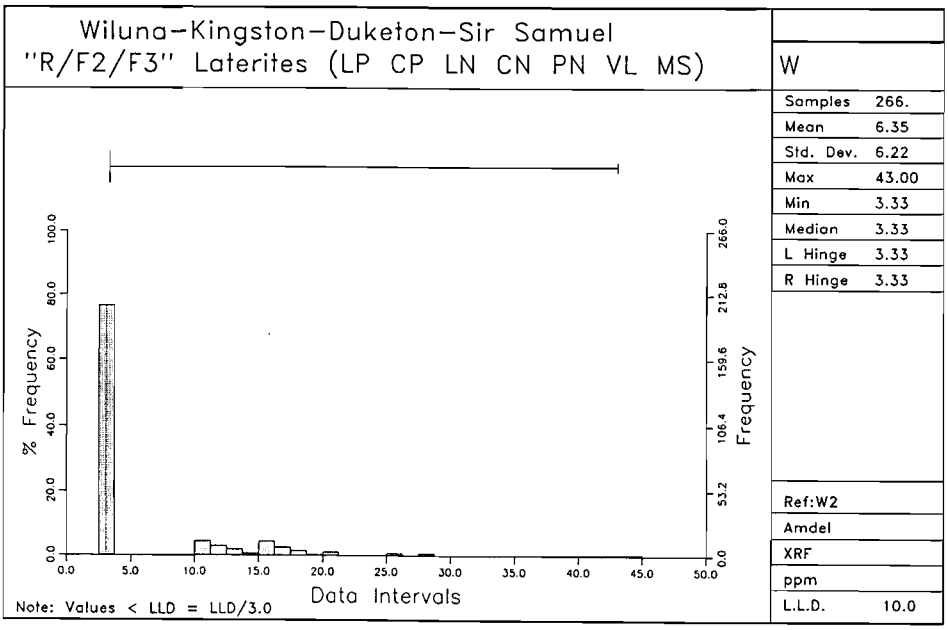

Figure 22a

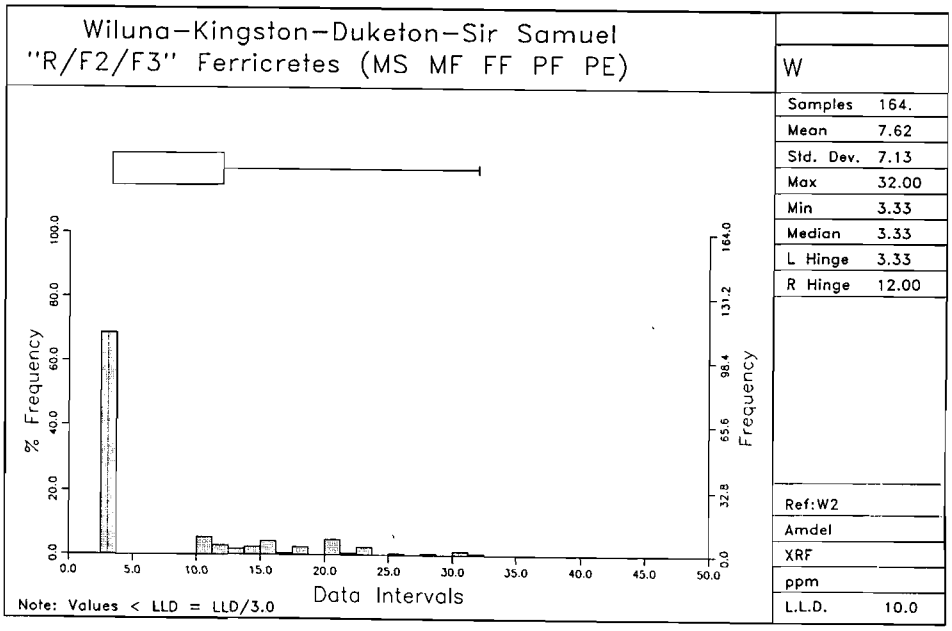

Figure 22b

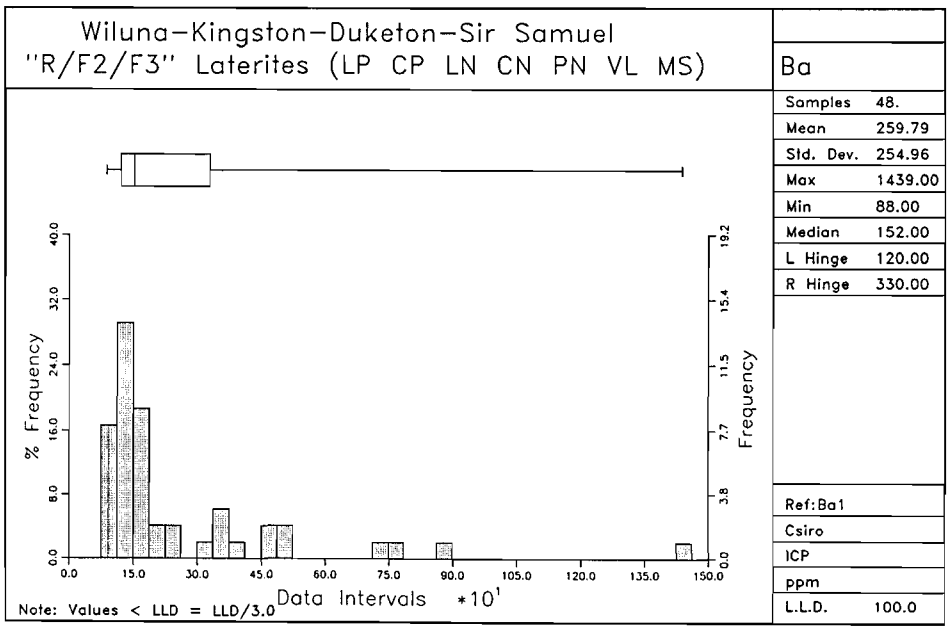

Figure 23a

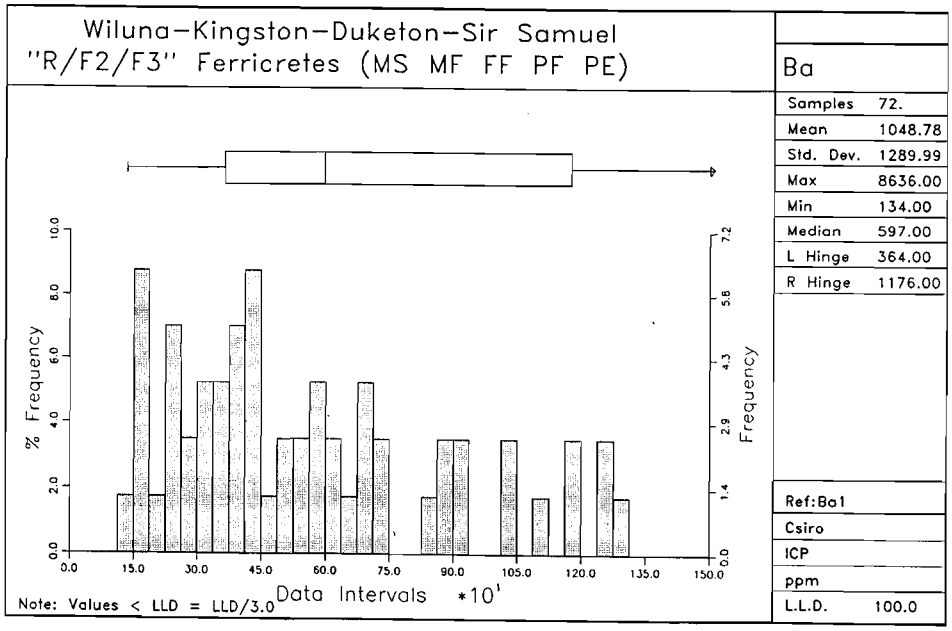

Figure 23b

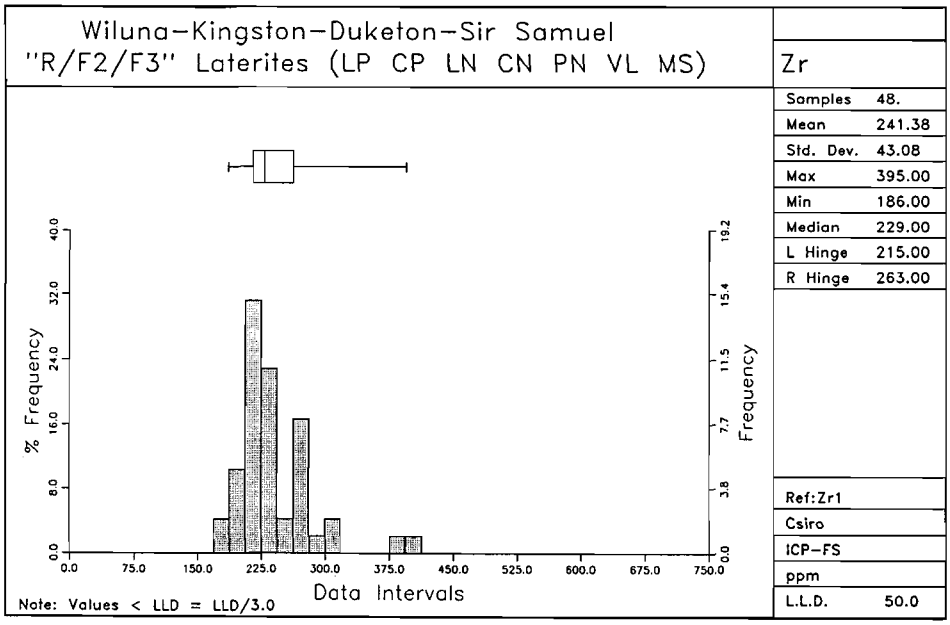

Figure 24a

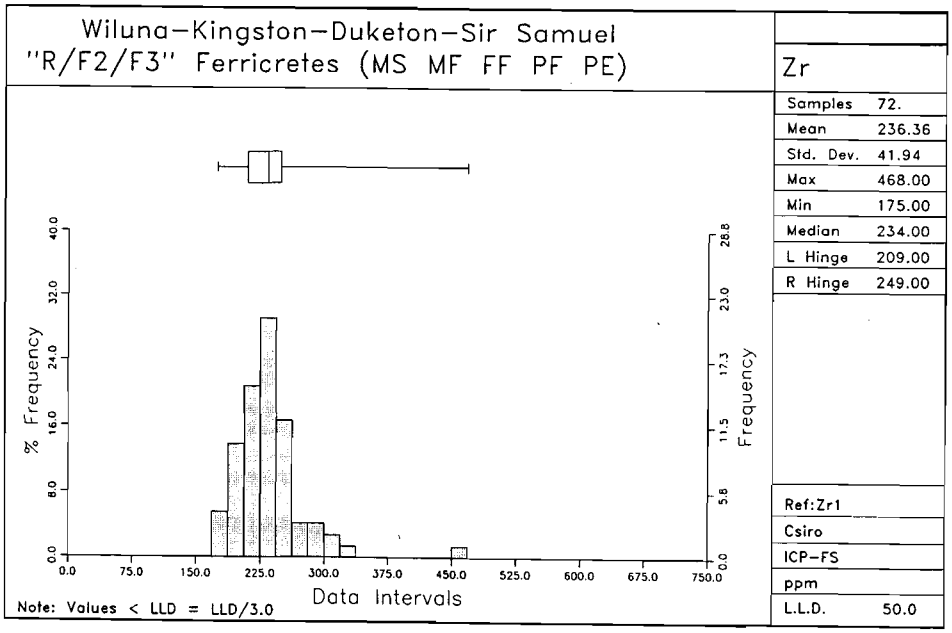

Figure 24b

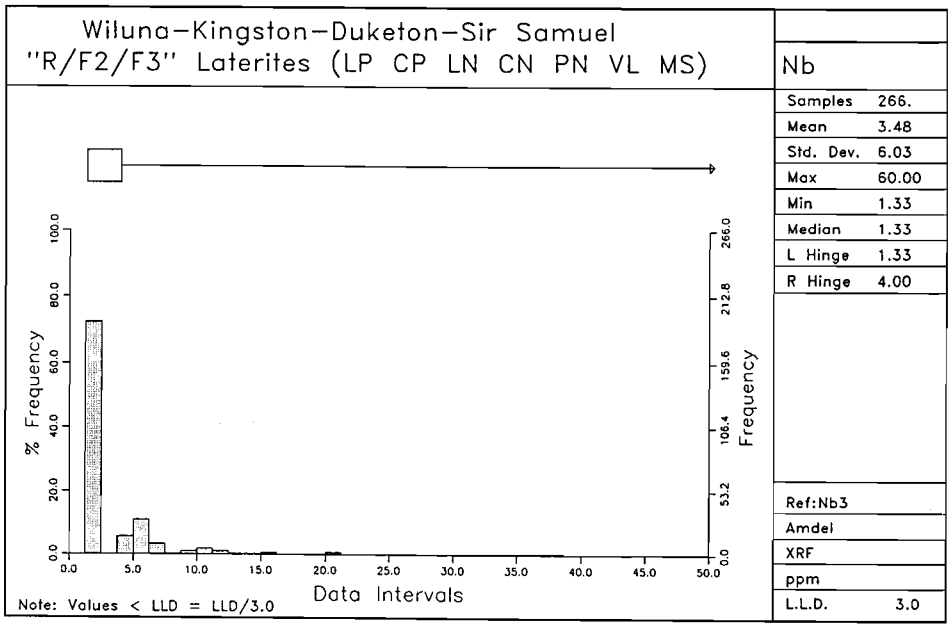

Figure 25a

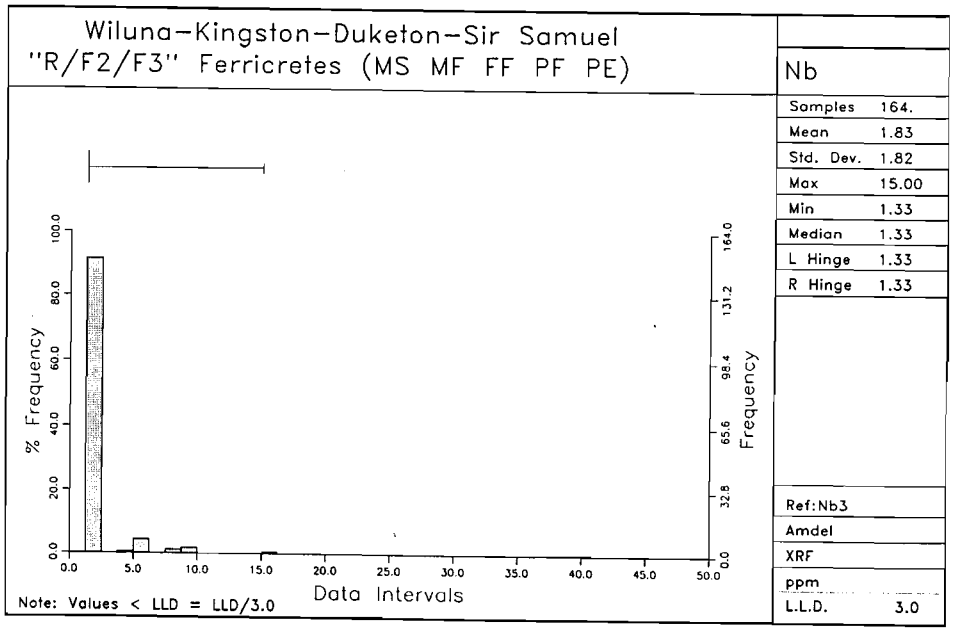

Figure 25b

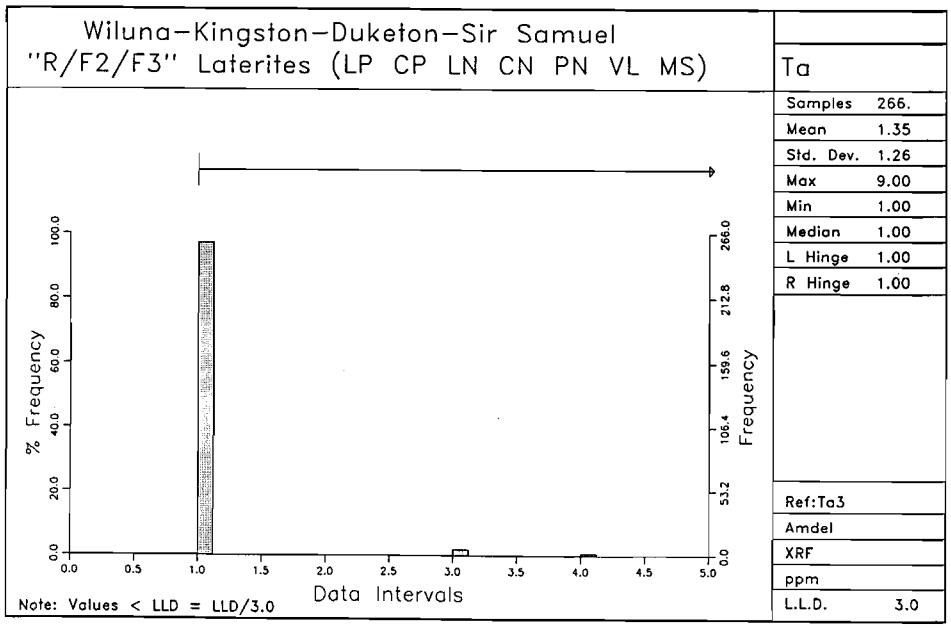

Figure 26a

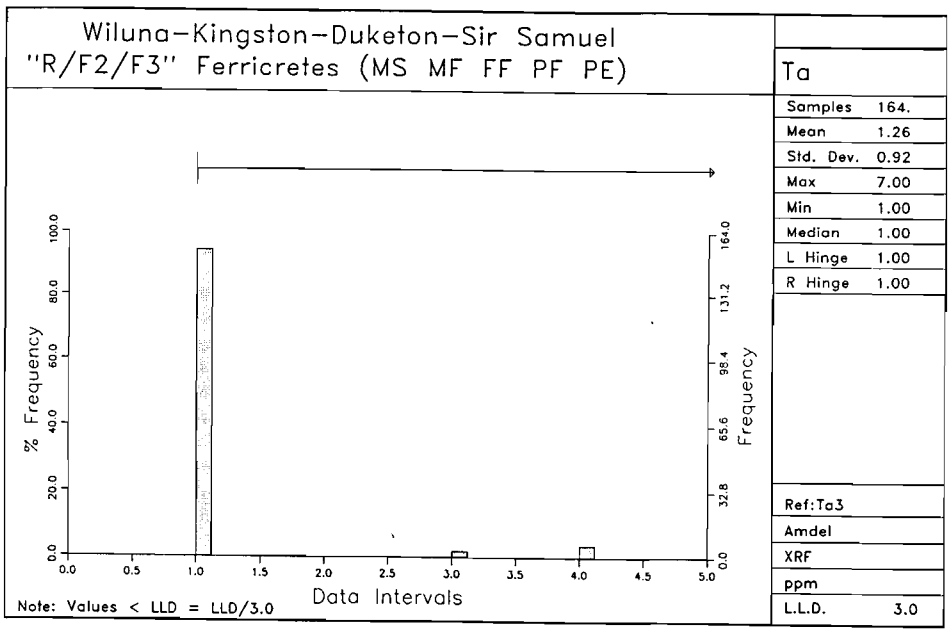

Figure 26b

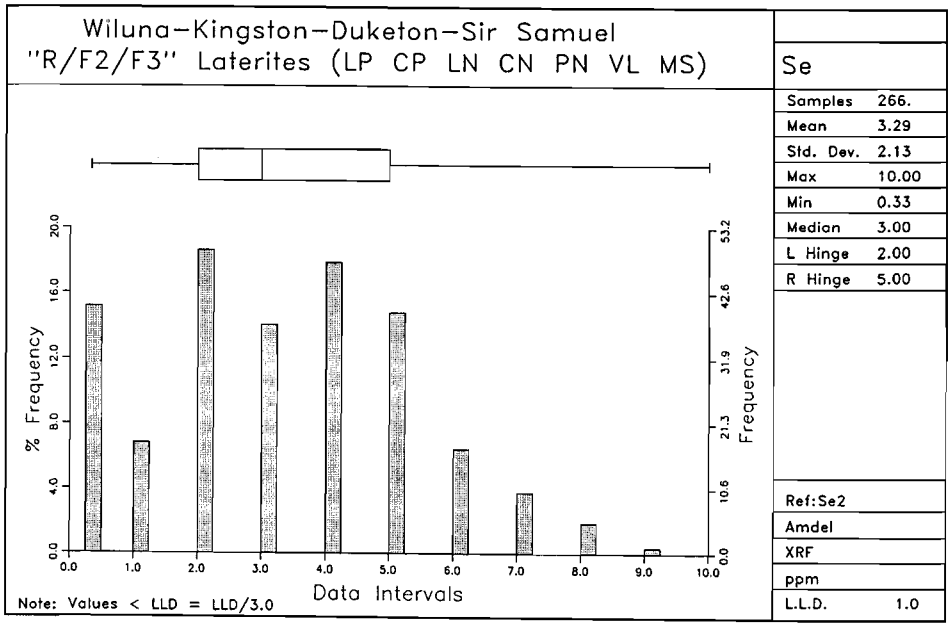

Se	
Samples	266.
Mean	3.29
Std. Dev.	2.13
Max	10.00
Min	0.33
Median	3.00
L Hinge	2.00
R Hinge	5.00
Ref:Se2	
Amdel	
XRF	
ppm	
L.L.D.	1.0

Figure 27a

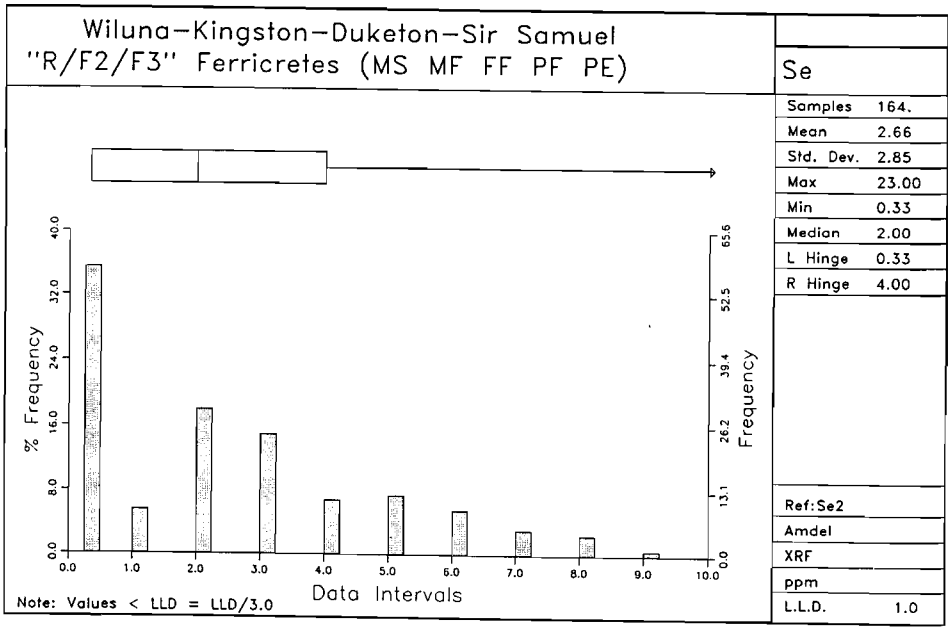

Se	
Samples	164.
Mean	2.66
Std. Dev.	2.85
Max	23.00
Min	0.33
Median	2.00
L Hinge	0.33
R Hinge	4.00
Ref:Se2	
Amdel	
XRF	
ppm	
L.L.D.	1.0

Figure 27b

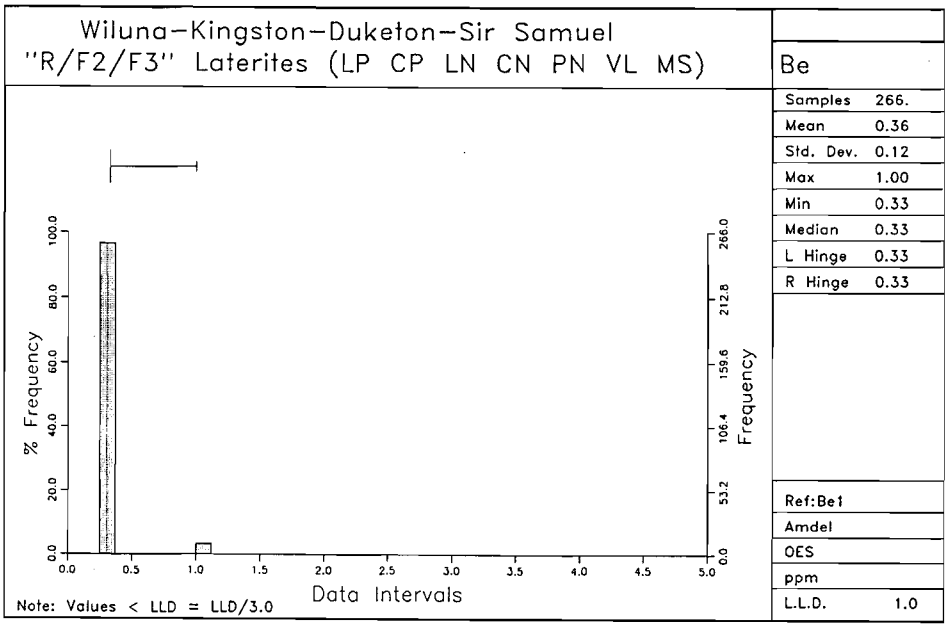

Figure 28a

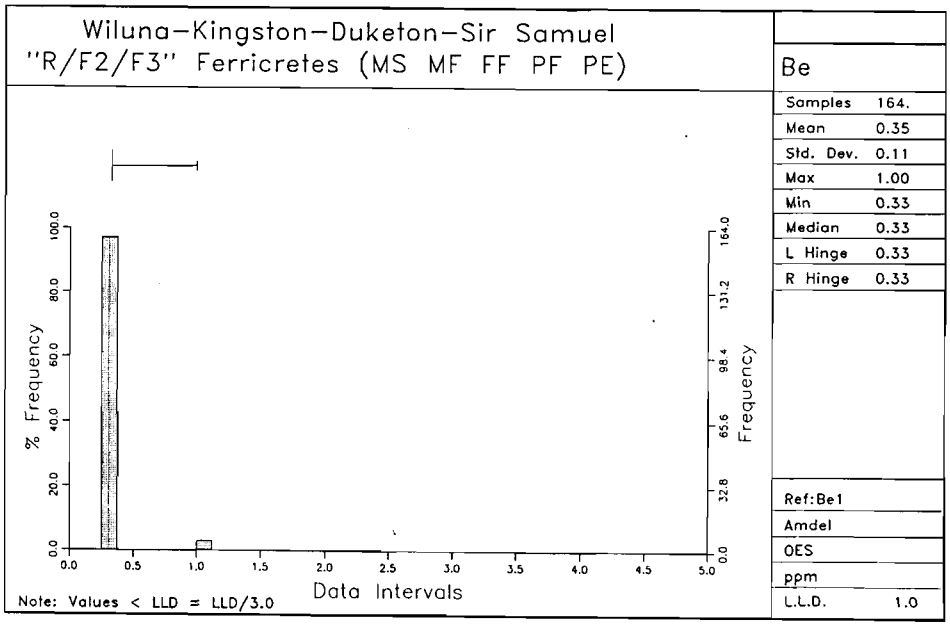

Figure 28b

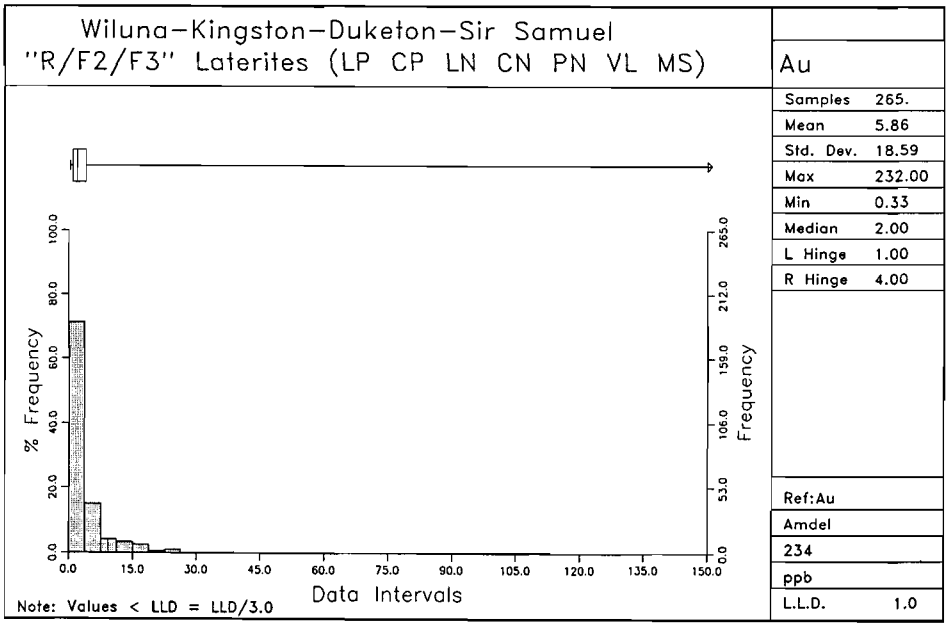

Figure 29a

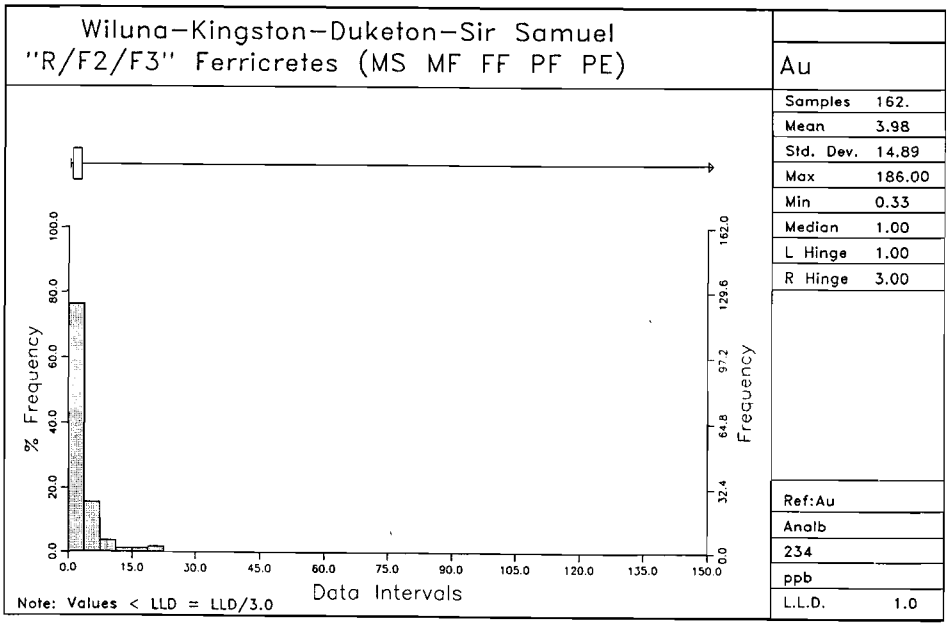

Figure 29b

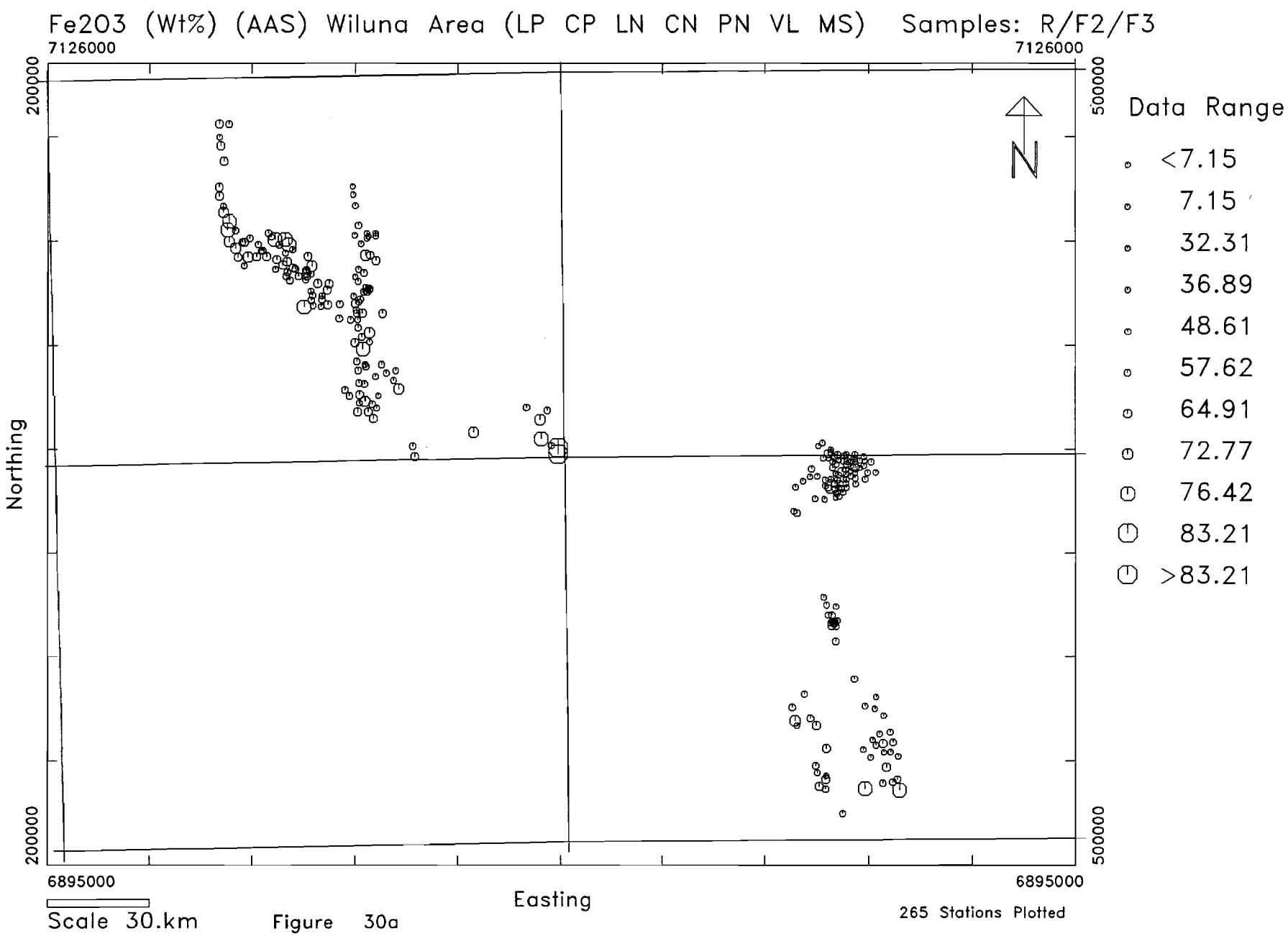
Fe2O3 (Wt%) (AAS) Wiluna Area (LP CP LN CN PN VL MS) Samples: R/F2/F3
7126000
7126000
200000
500000
N
Data Range
<7.15
7.15
32.31
36.89
48.61
57.62
64.91
72.77
76.42
83.21
>83.21
Northing
200000
500000
6895000
6895000
Easting
Scale 30.km
265 Stations Plotted

Figure 30a

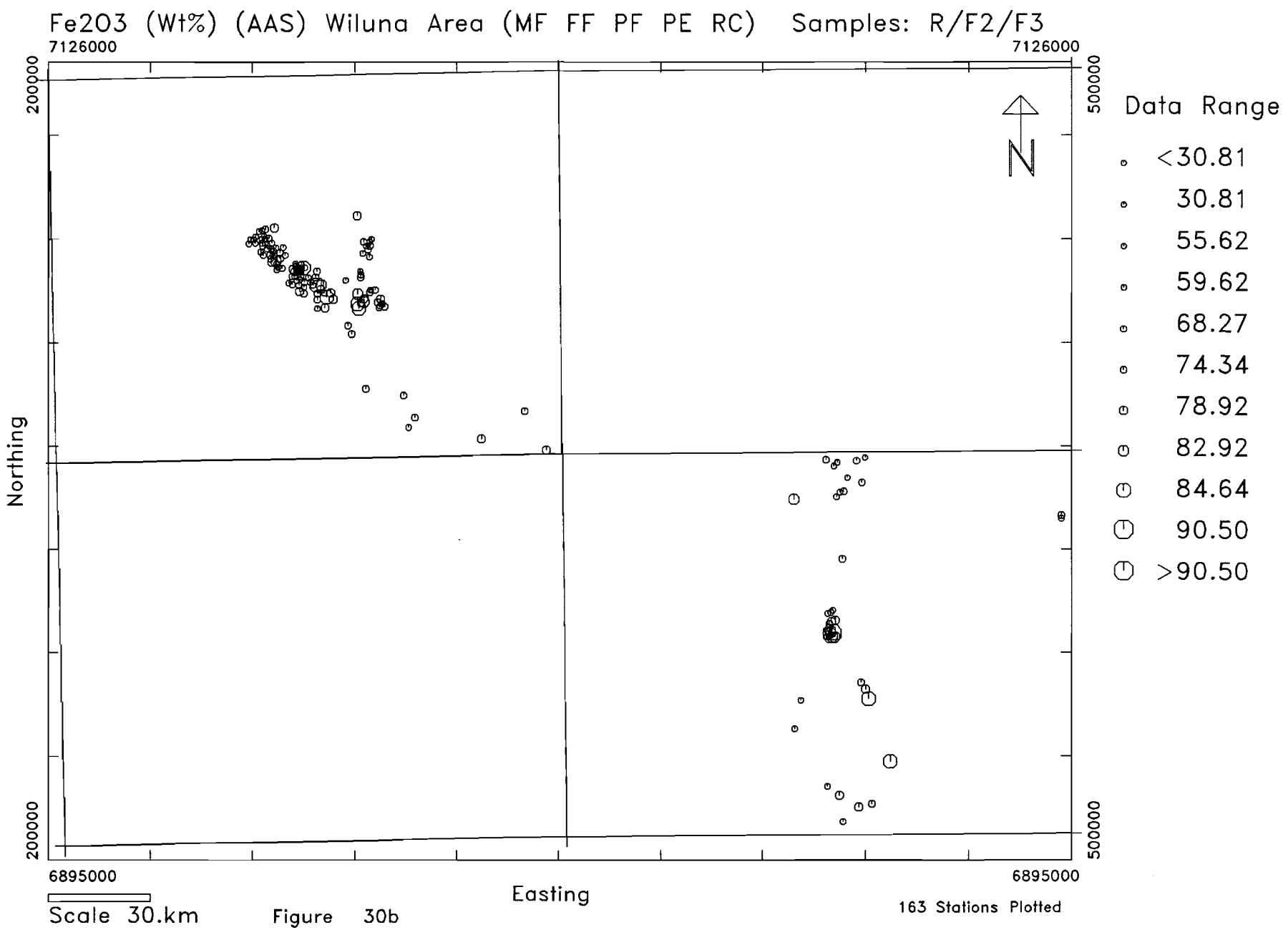
Fe2O3 (Wt%) (AAS) Wiluna Area (MF FF PF PE RC) Samples: R/F2/F3
7126000
7126000
200000
500000
N
Data Range
<30.81
30.81
55.62
59.62
68.27
74.34
78.92
82.92
84.64
90.50
>90.50
Northing
200000
500000
6895000
6895000
Easting
Scale 30.km
163 Stations Plotted

Figure 30b

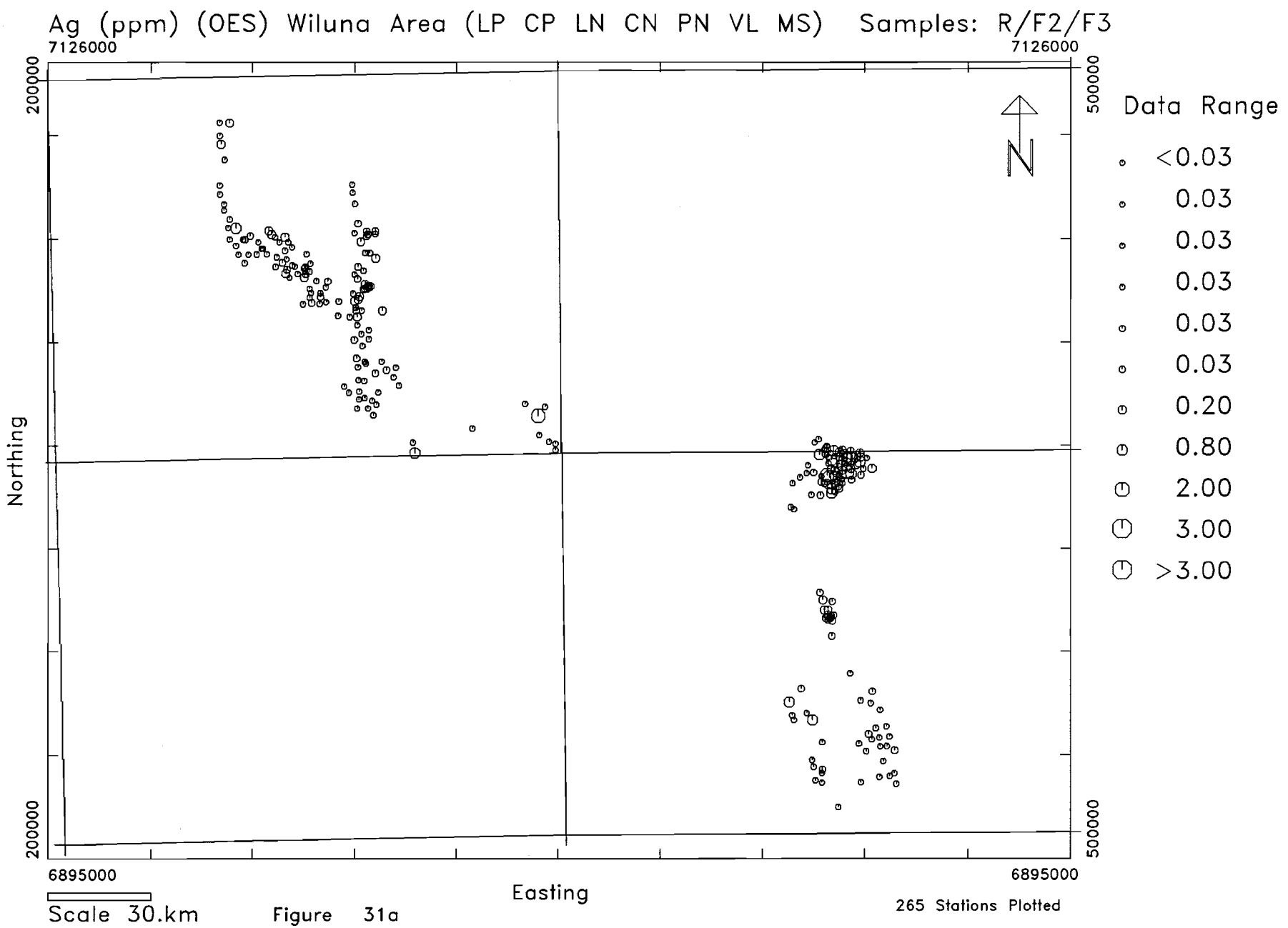
Ag (ppm) (OES) Wiluna Area (LP CP LN CN PN VL MS) Samples: R/F2/F3
7126000
7126000
200000
500000
N
Data Range
<0.03
0.03
0.03
0.03
0.03
0.03
0.20
0.80
2.00
3.00
>3.00
Northing
200000
500000
6895000
6895000
Easting
Scale 30.km
265 Stations Plotted

Figure 31a

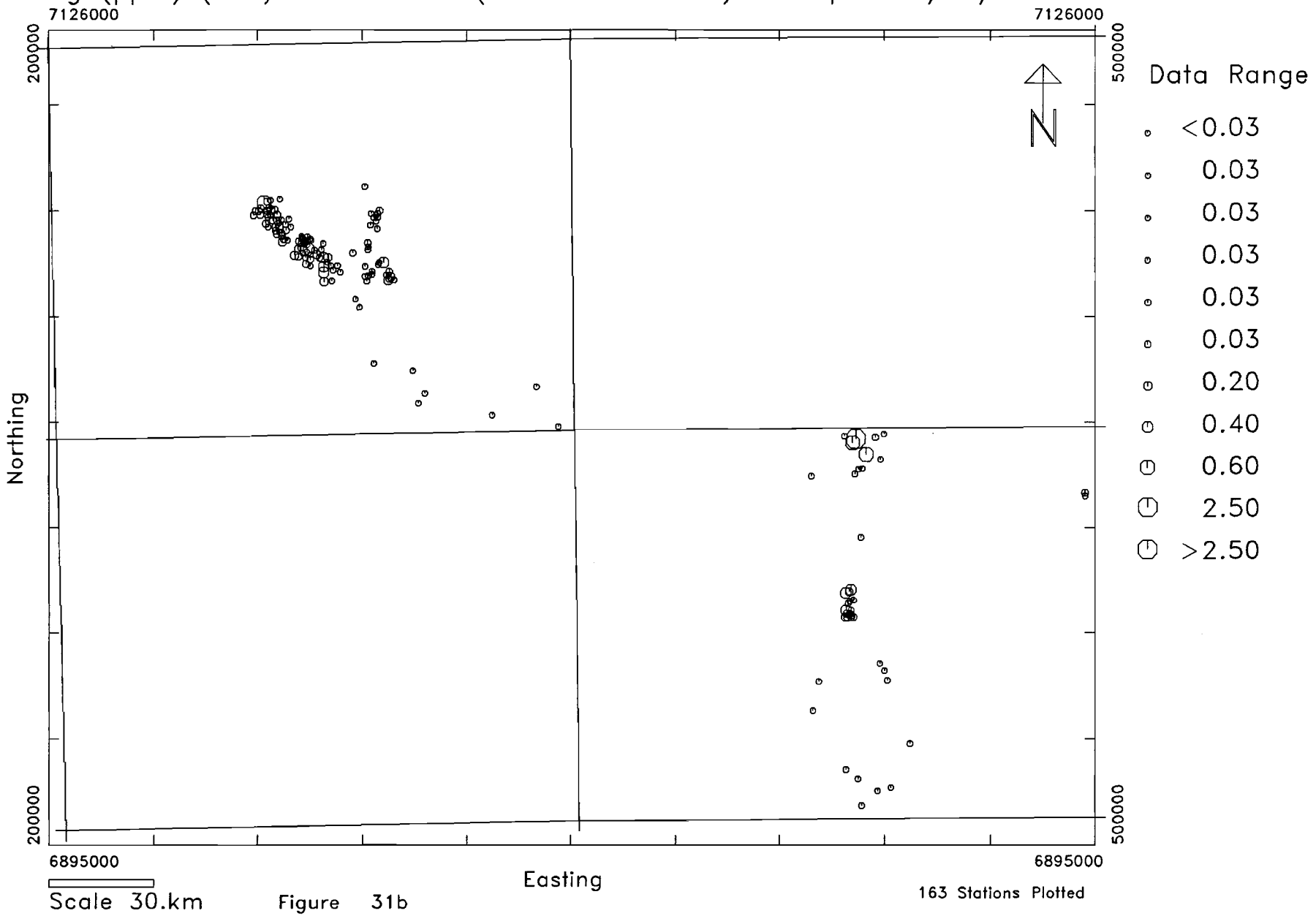
Ag (ppm) (OES) Wiluna Area (MF FF PF PE RC) Samples: R/F2/F3
7126000
7126000
200000
500000
N
Data Range
<0.03
0.03
0.03
0.03
0.03
0.03
0.03
0.20
0.40
0.60
2.50
>2.50
Northing
200000
500000
6895000
6895000
Easting
Scale 30.km
163 Stations Plotted

Figure 31b

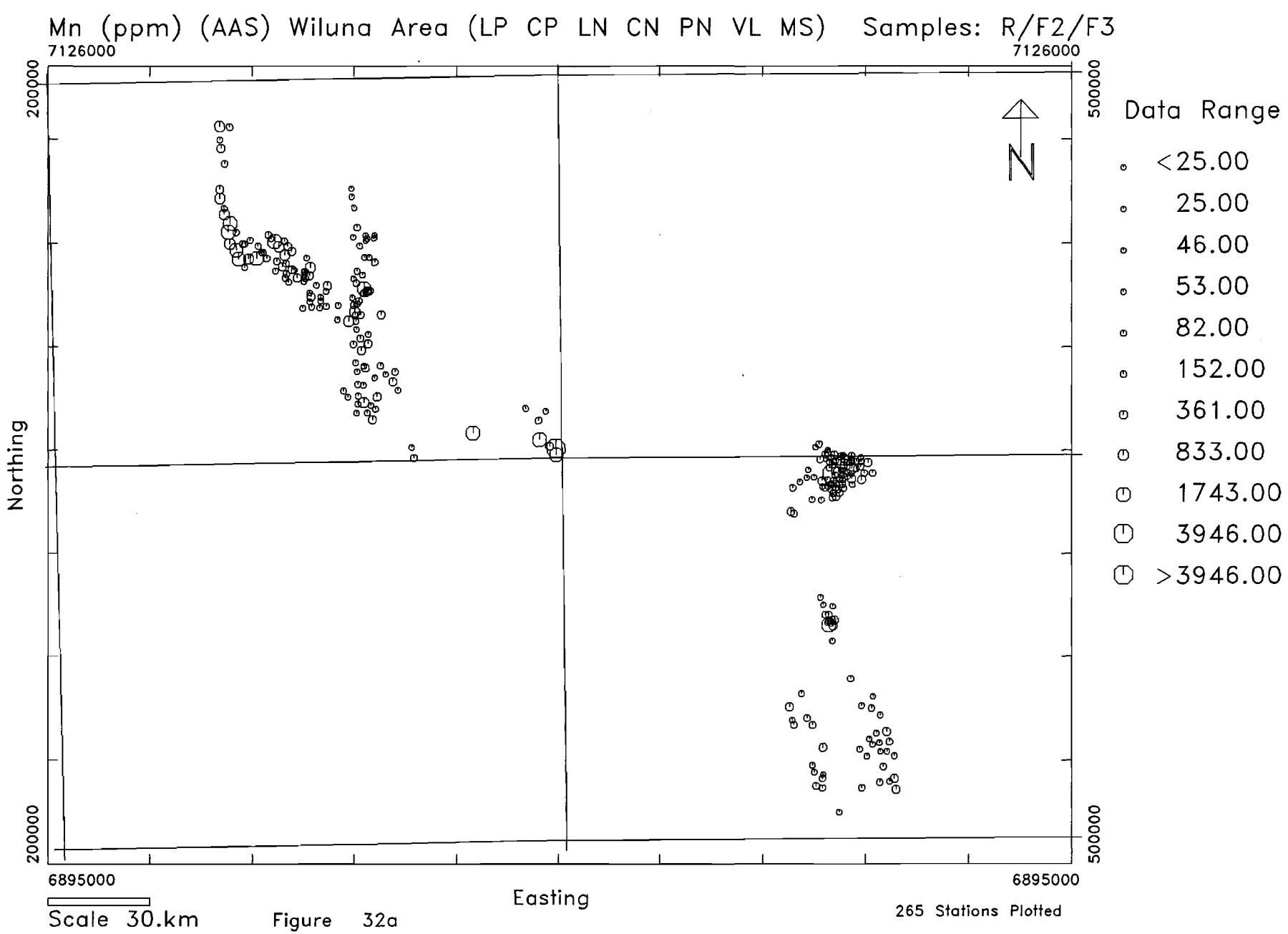
Mn (ppm) (AAS) Wiluna Area (LP CP LN CN PN VL MS) Samples: R/F2/F3
7126000
7126000
200000
500000
Northing
N
Data Range
<25.00
25.00
46.00
53.00
82.00
152.00
361.00
833.00
1743.00
3946.00
>3946.00
200000
500000
6895000
6895000
Easting
Scale 30.km
265 Stations Plotted

Figure 32a

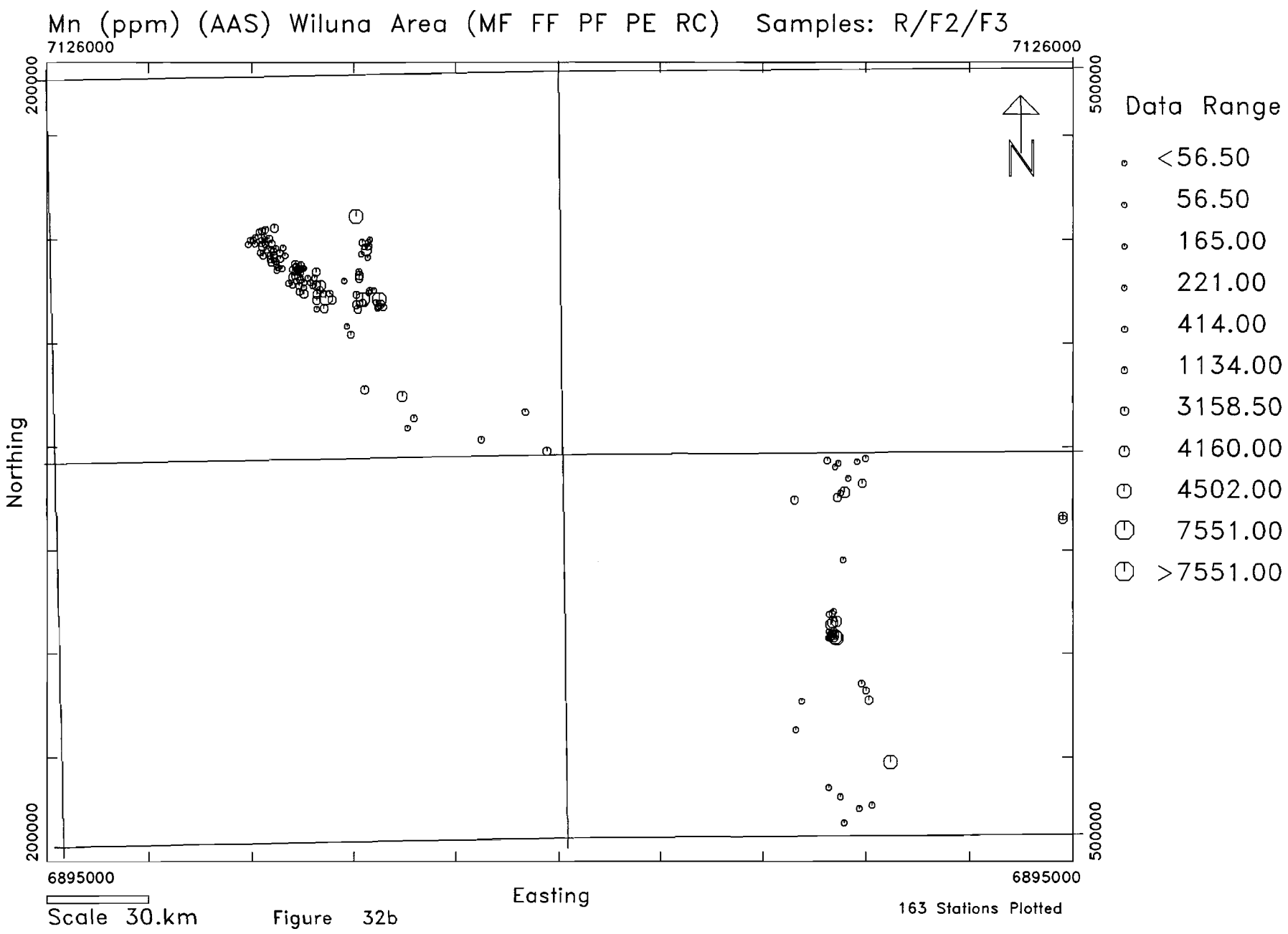
Mn (ppm) (AAS) Wiluna Area (MF FF PF PE RC) Samples: R/F2/F3
7126000
7126000
200000
500000
Data Range
<56.50
56.50
165.00
221.00
414.00
1134.00
3158.50
4160.00
4502.00
7551.00
>7551.00
N
Northing
200000
500000
6895000
6895000
Easting
Scale 30.km
163 Stations Plotted

Figure 32b

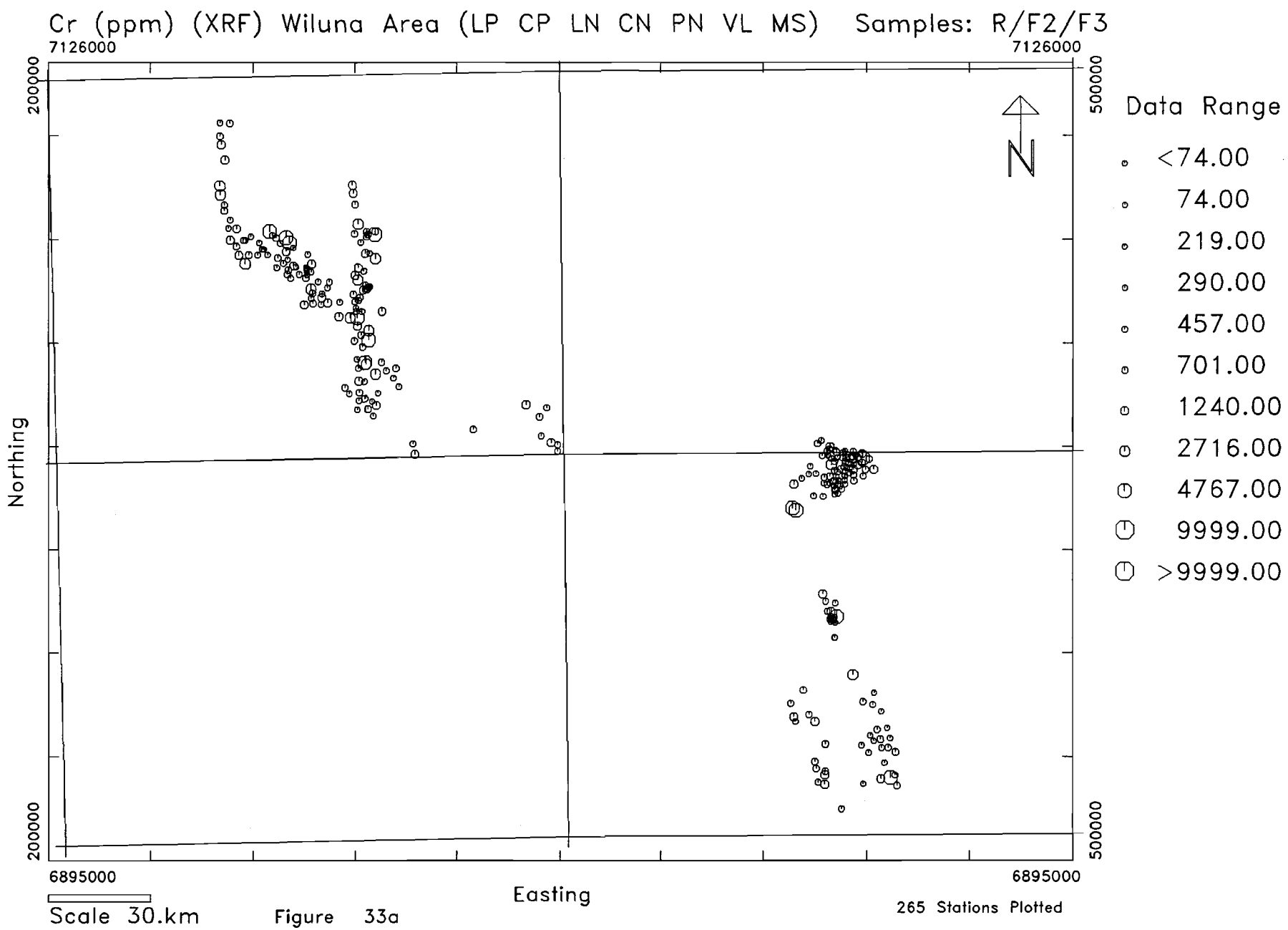
Cr (ppm) (XRF) Wiluna Area (LP CP LN CN PN VL MS) Samples: R/F2/F3
7126000
7126000
200000
500000
Northing
N
Data Range
<74.00
74.00
219.00
290.00
457.00
701.00
1240.00
2716.00
4767.00
9999.00
>9999.00
6895000
6895000
Easting
Scale 30.km
265 Stations Plotted

Figure 33a

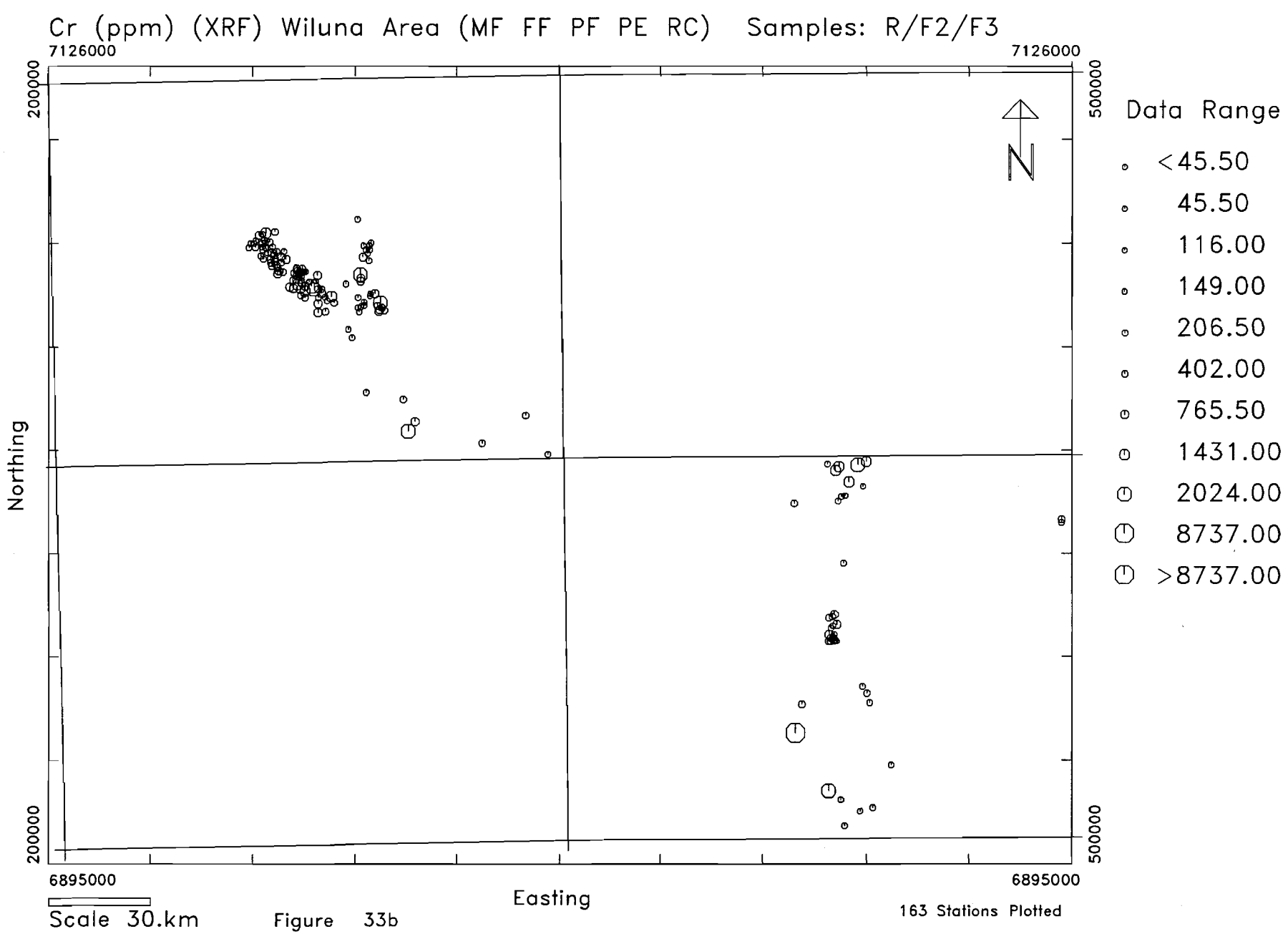
Cr (ppm) (XRF) Wiluna Area (MF FF PF PE RC) Samples: R/F2/F3
7126000
7126000
200000
500000
Data Range
<45.50
45.50
116.00
149.00
206.50
402.00
765.50
1431.00
2024.00
8737.00
>8737.00
N
Northing
200000
500000
6895000
6895000
Easting
Scale 30.km
163 Stations Plotted

Figure 33b

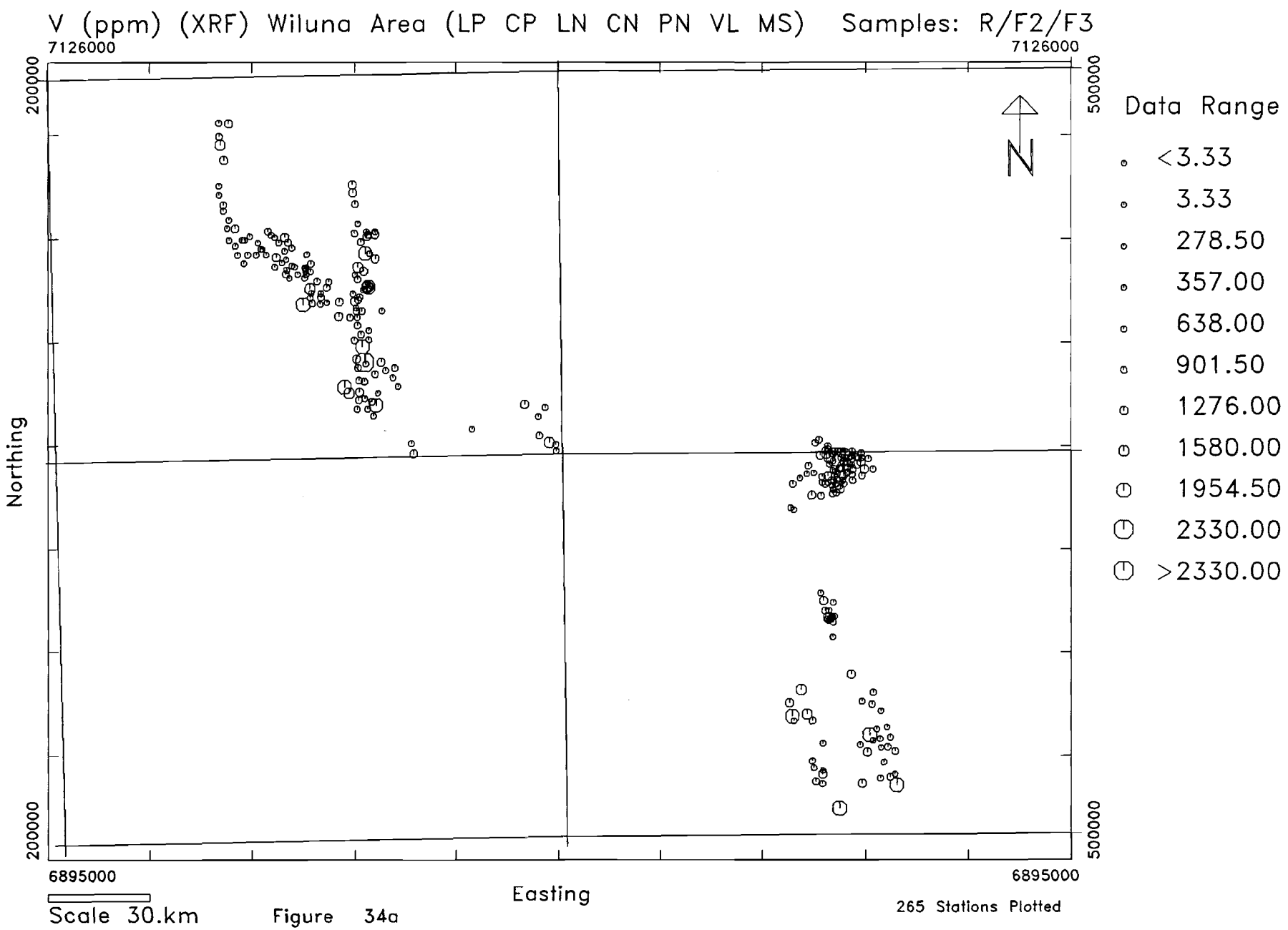
V (ppm) (XRF) Wiluna Area (LP CP LN CN PN VL MS) Samples: R/F2/F3
7126000
7126000
200000
500000
N
Data Range
<3.33
3.33
278.50
357.00
638.00
901.50
1276.00
1580.00
1954.50
2330.00
>2330.00
Northing
200000
500000
6895000
6895000
Easting
Scale 30.km
265 Stations Plotted

Figure 34a

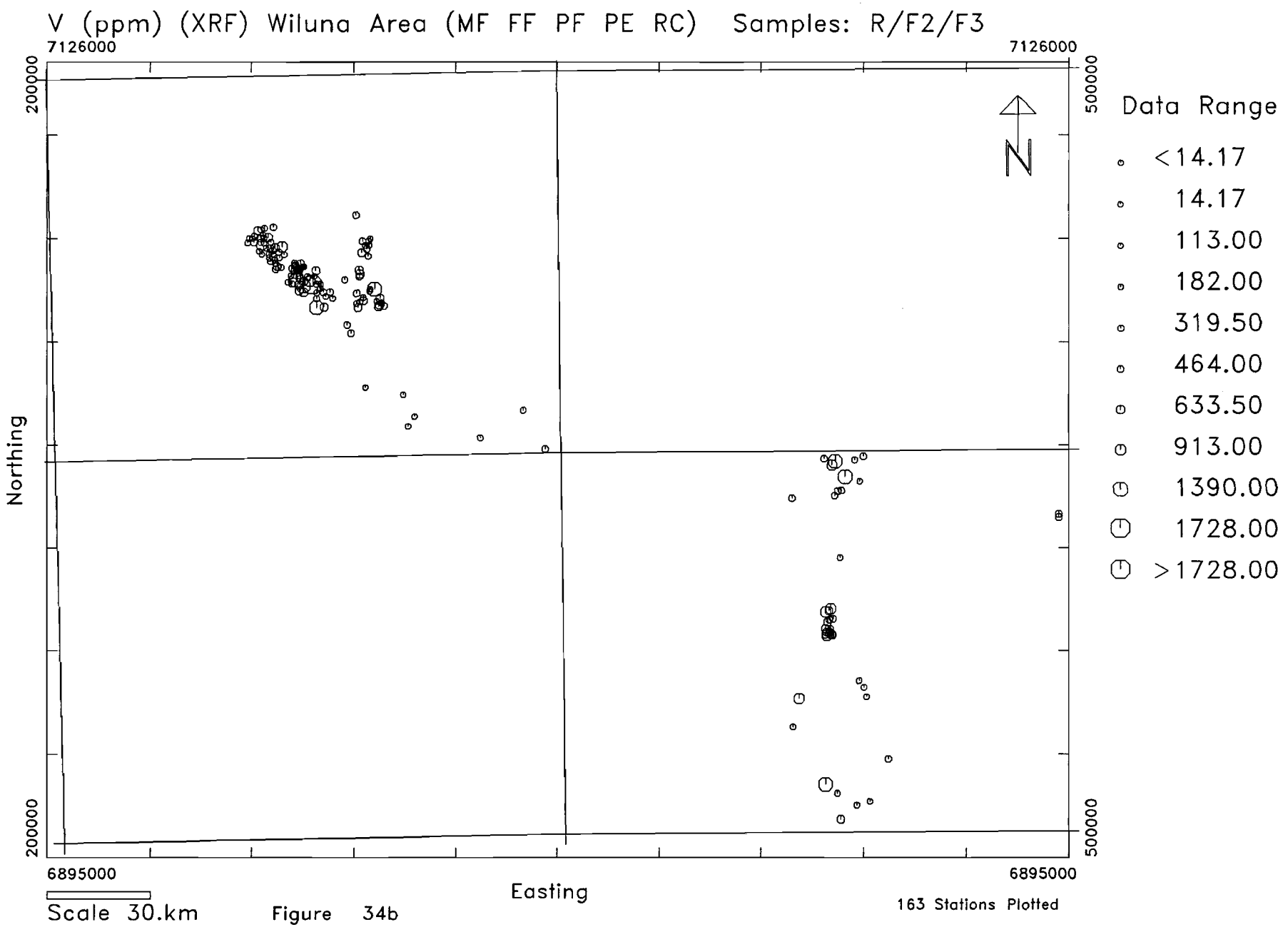
V (ppm) (XRF) Wiluna Area (MF FF PF PE RC) Samples: R/F2/F3
7126000
7126000
200000
500000
N
Data Range
<14.17
14.17
113.00
182.00
319.50
464.00
633.50
913.00
1390.00
1728.00
>1728.00
Northing
200000
500000
6895000
6895000
Easting
Scale 30.km
163 Stations Plotted

Figure 34b

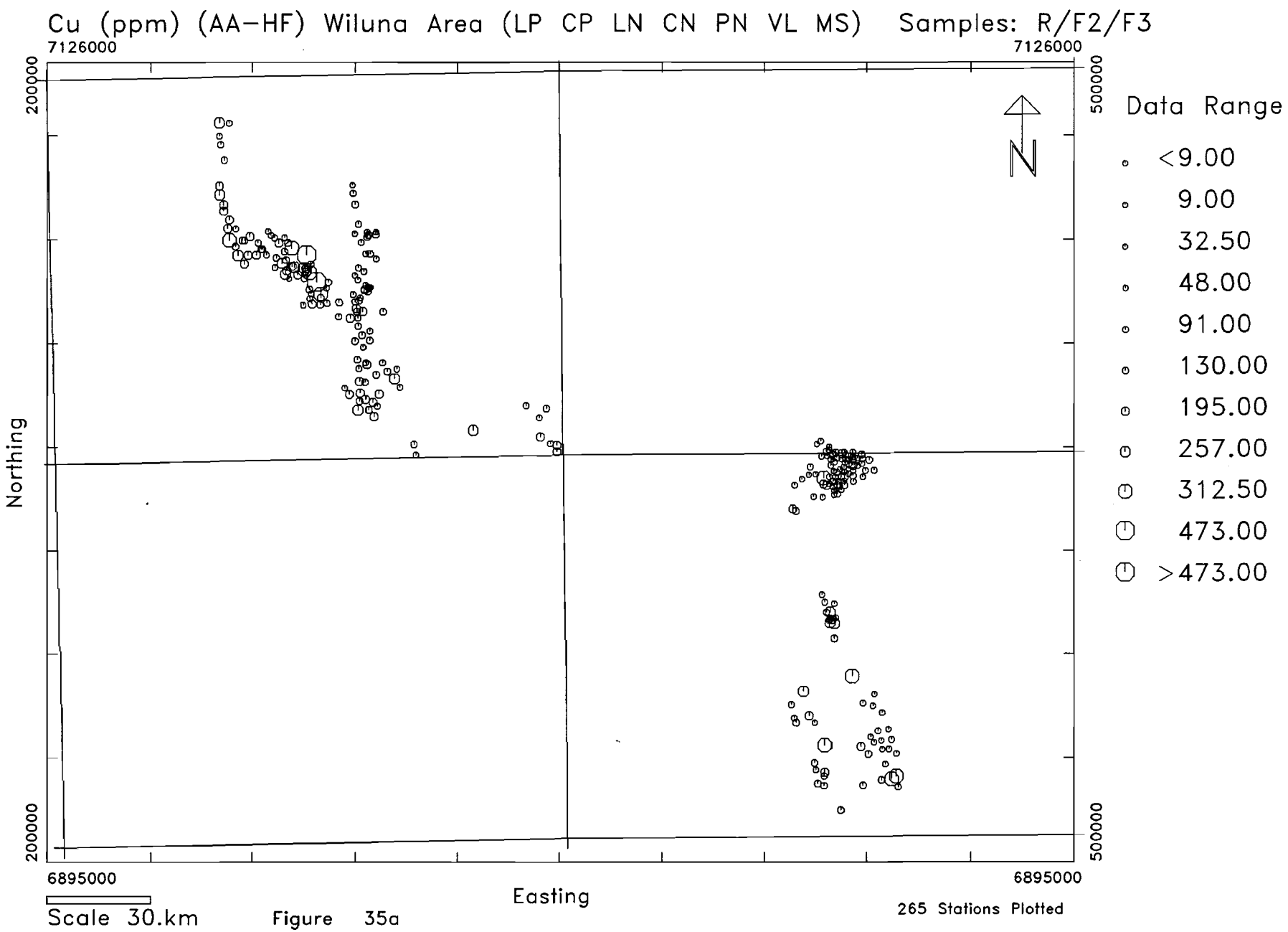
Cu (ppm) (AA-HF) Wiluna Area (LP CP LN CN PN VL MS) Samples: R/F2/F3
7126000
7126000
200000
500000
Data Range
<9.00
9.00
32.50
48.00
91.00
130.00
195.00
257.00
312.50
473.00
>473.00
N
Northing
200000
500000
6895000
6895000
Easting
Scale 30.km
265 Stations Plotted

Figure 35a

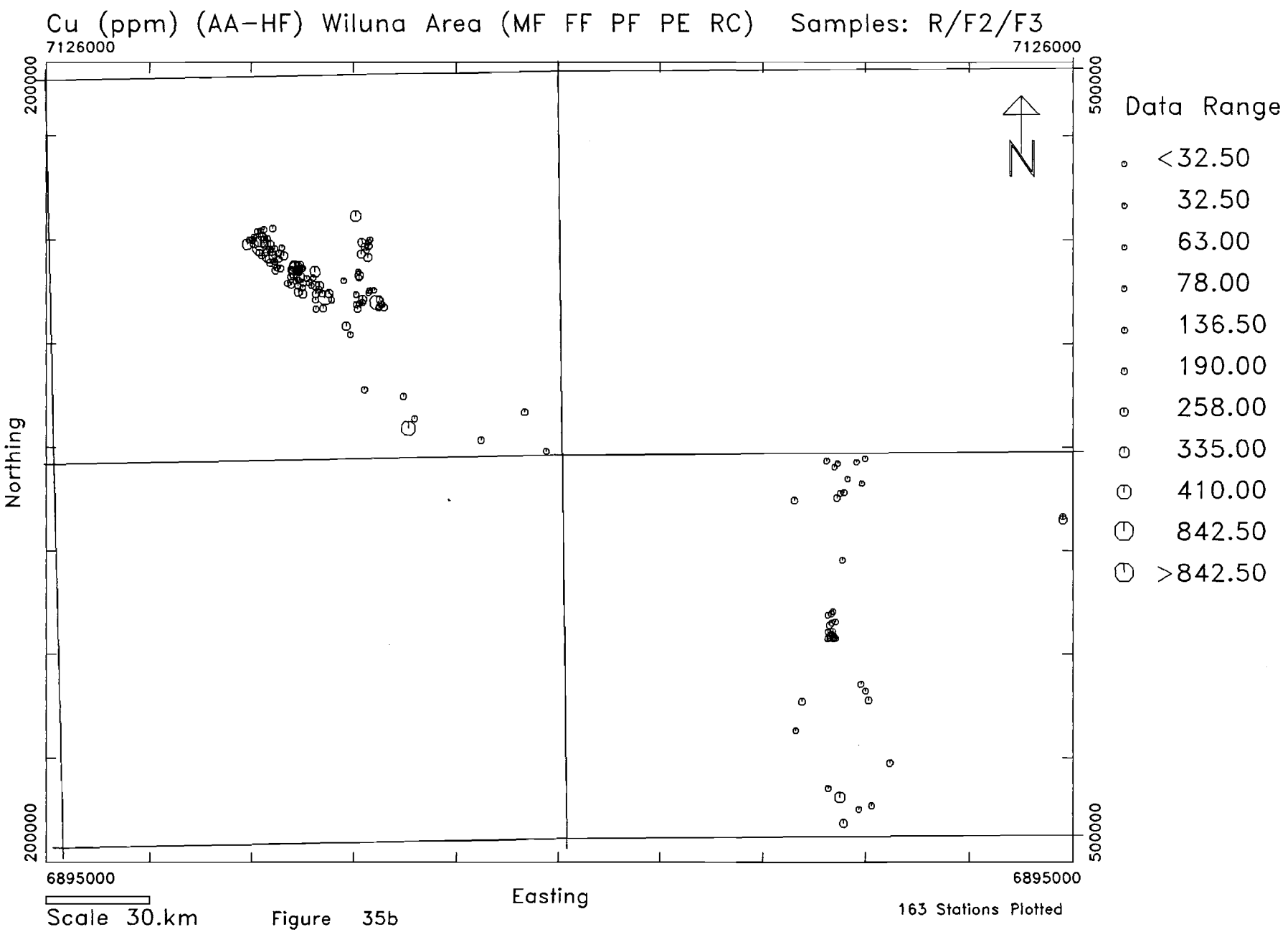
Cu (ppm) (AA-HF) Wiluna Area (MF FF PF PE RC) Samples: R/F2/F3
7126000
7126000
200000
500000
N
Data Range
<32.50
32.50
63.00
78.00
136.50
190.00
258.00
335.00
410.00
842.50
>842.50
Northing
200000
500000
6895000
6895000
Easting
Scale 30.km
163 Stations Plotted

Figure 35b

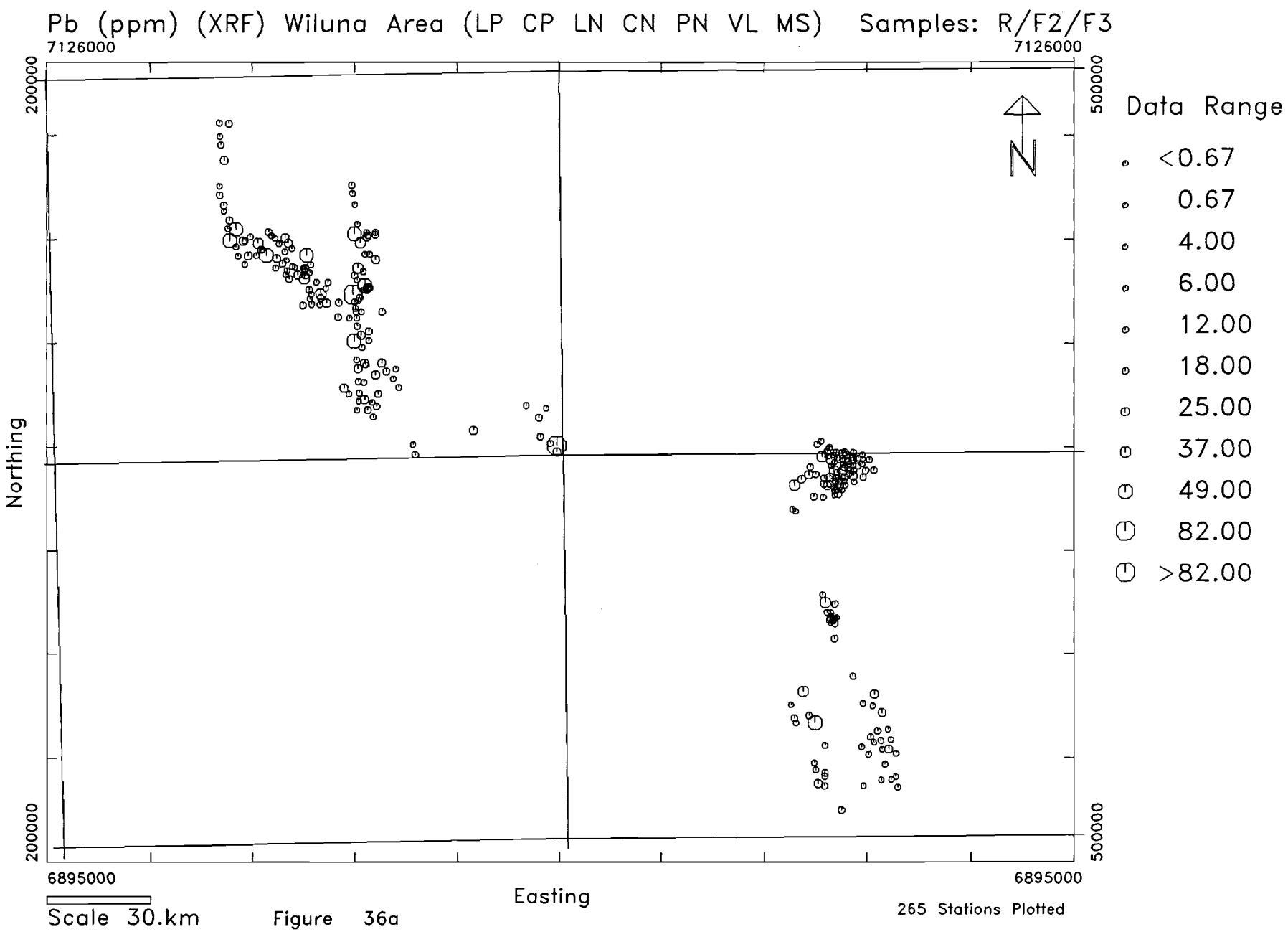
Pb (ppm) (XRF) Wiluna Area (LP CP LN CN PN VL MS) Samples: R/F2/F3
7126000
7126000
200000
500000
N
Data Range
<0.67
0.67
4.00
6.00
12.00
18.00
25.00
37.00
49.00
82.00
>82.00
Northing
200000
500000
6895000
6895000
Easting
Scale 30.km
265 Stations Plotted

Figure 36a

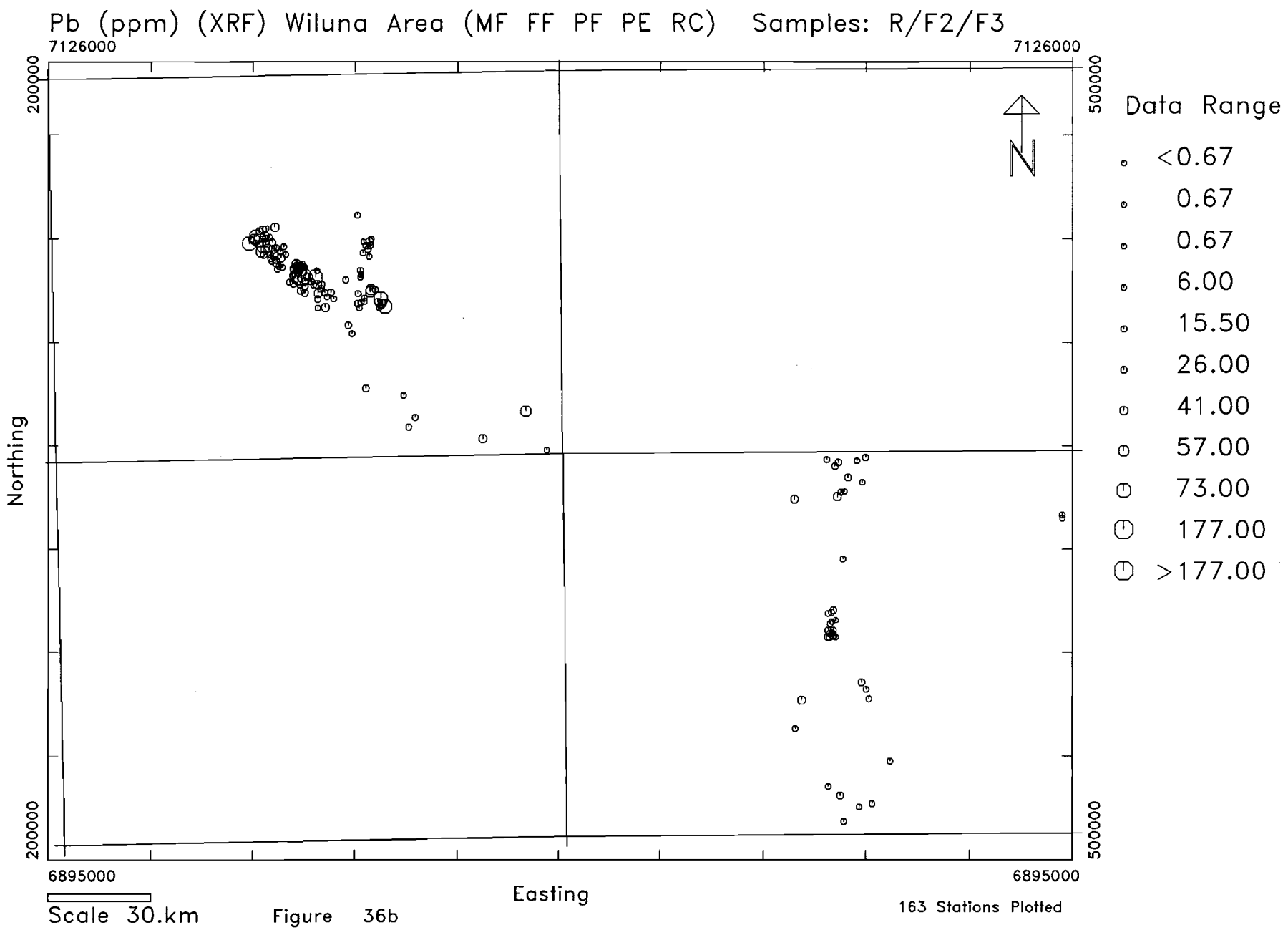
Pb (ppm) (XRF) Wiluna Area (MF FF PF PE RC) Samples: R/F2/F3
7126000
7126000
200000
500000
Northing
N
Data Range
<0.67
0.67
0.67
6.00
15.50
26.00
41.00
57.00
73.00
177.00
>177.00
200000
500000
6895000
6895000
Easting
Scale 30.km
163 Stations Plotted

Figure 36b

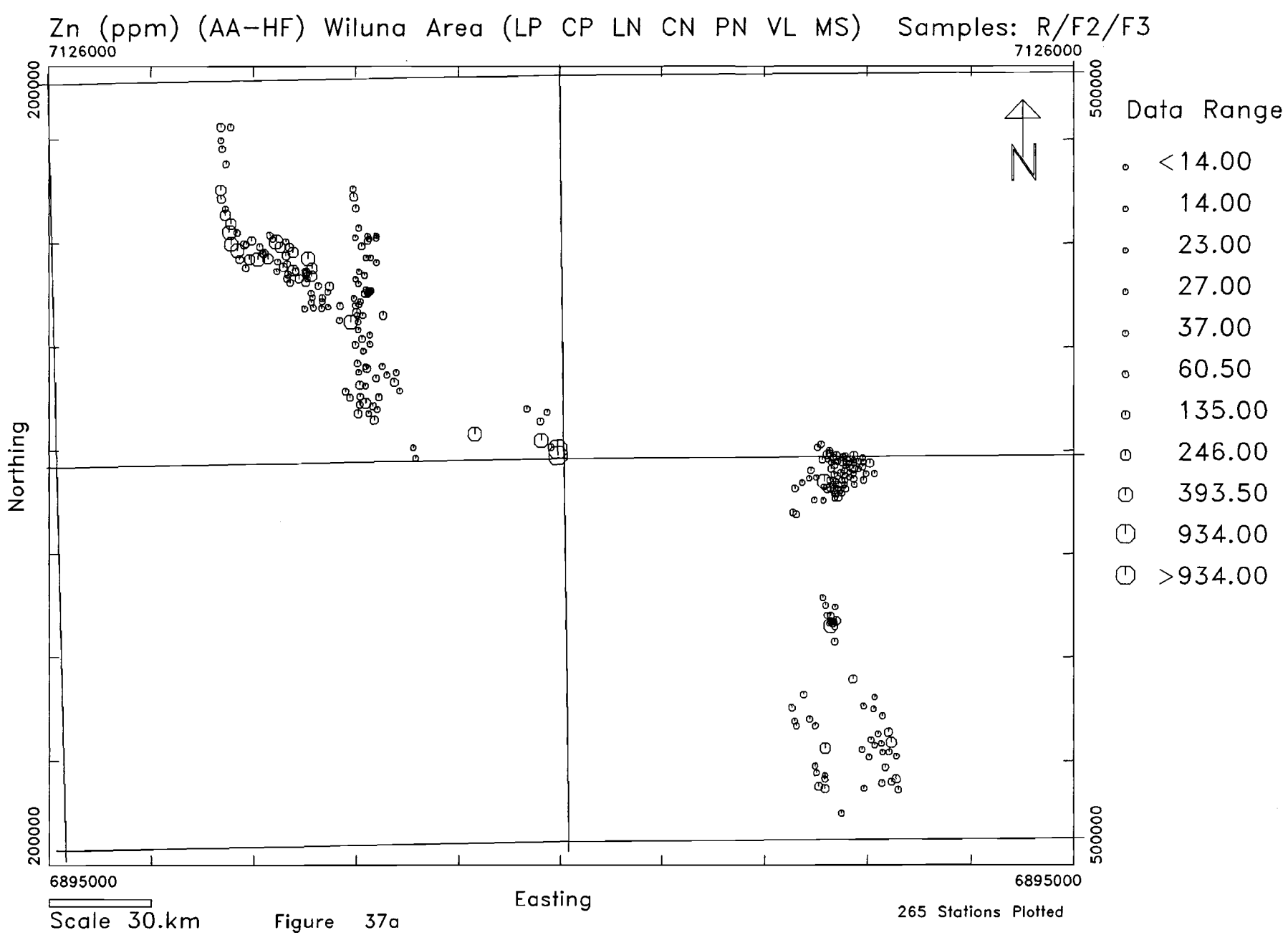
Zn (ppm) (AA-HF) Wiluna Area (LP CP LN CN PN VL MS) Samples: R/F2/F3
7126000
7126000
200000
500000
Northing
N
Data Range
<14.00
14.00
23.00
27.00
37.00
60.50
135.00
246.00
393.50
934.00
>934.00
200000
500000
6895000
6895000
Easting
Scale 30.km
265 Stations Plotted

Figure 37a

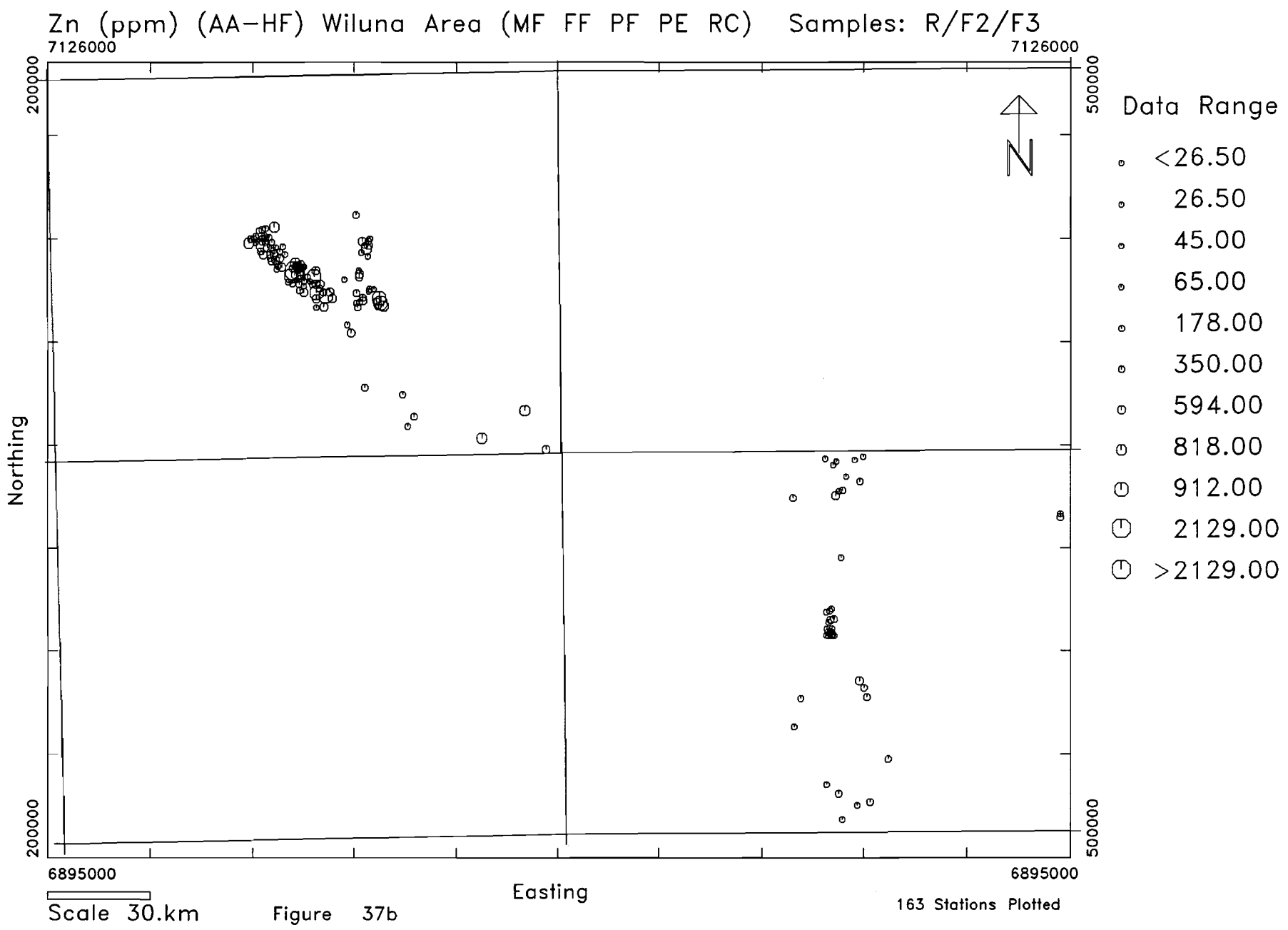
Zn (ppm) (AA-HF) Wiluna Area (MF FF PF PE RC) Samples: R/F2/F3
7126000
7126000
200000
500000
Data Range
<26.50
26.50
45.00
65.00
178.00
350.00
594.00
818.00
912.00
2129.00
>2129.00
N
Northing
200000
500000
6895000
6895000
Easting
Scale 30.km
Figure 37b
163 Stations Plotted

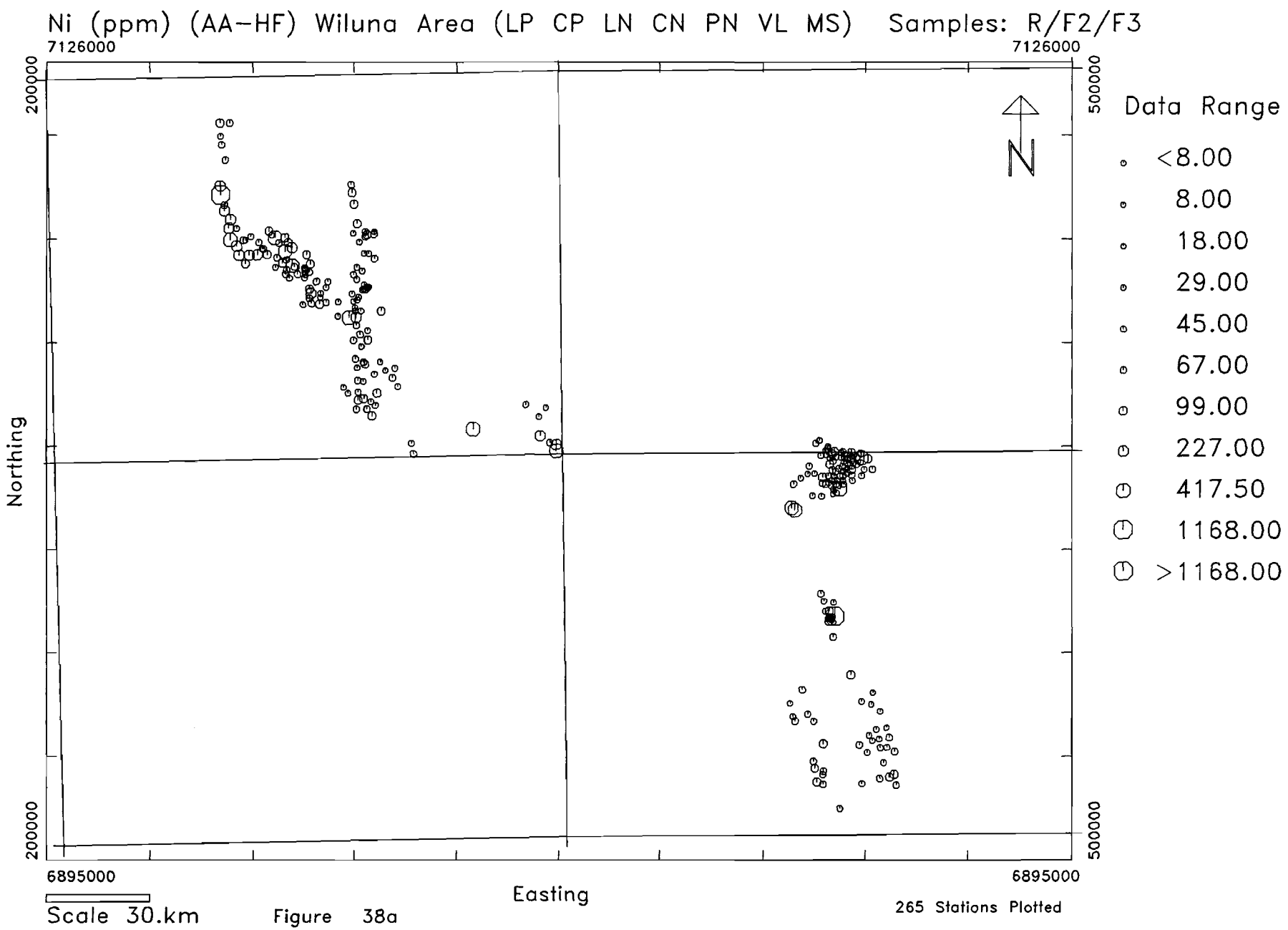
Ni (ppm) (AA-HF) Wiluna Area (LP CP LN CN PN VL MS) Samples: R/F2/F3
7126000
7126000
200000
500000
N
Data Range
<8.00
8.00
18.00
29.00
45.00
67.00
99.00
227.00
417.50
1168.00
>1168.00
Northing
200000
500000
6895000
6895000
Easting
Scale 30.km
265 Stations Plotted

Figure 38a

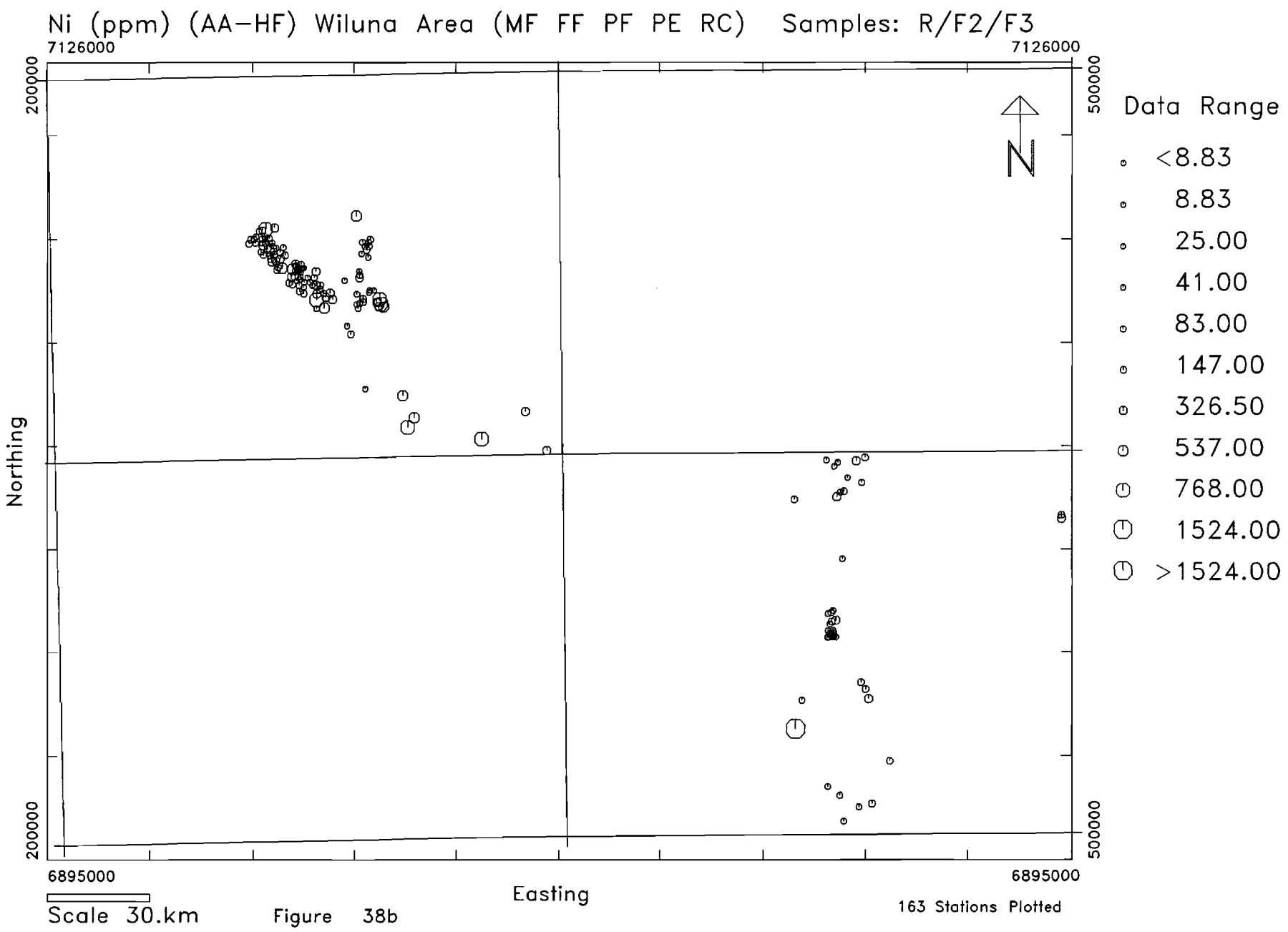
Ni (ppm) (AA–HF) Wiluna Area (MF FF PF PE RC) Samples: R/F2/F3
7126000
7126000
200000
500000
N
Data Range
<8.83
8.83
25.00
41.00
83.00
147.00
326.50
537.00
768.00
1524.00
>1524.00
Northing
200000
500000
6895000
6895000
Easting
Scale 30.km
163 Stations Plotted

Figure 38b

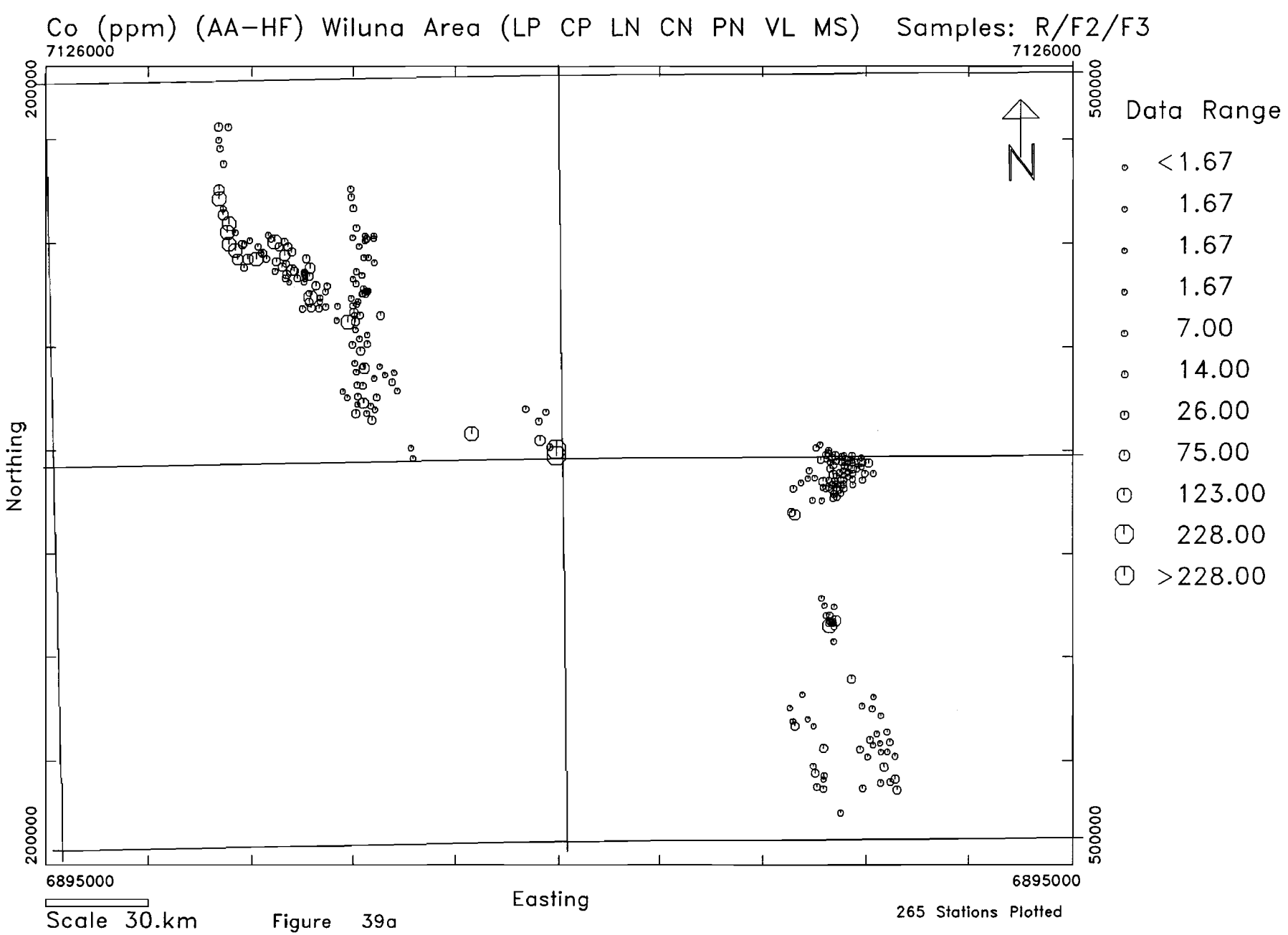
Co (ppm) (AA–HF) Wiluna Area (LP CP LN CN PN VL MS) Samples: R/F2/F3
7126000
7126000
200000
500000
Northing
N
Data Range
<1.67
1.67
1.67
1.67
7.00
14.00
26.00
75.00
123.00
228.00
>228.00
200000
500000
6895000
6895000
Easting
Scale 30.km
265 Stations Plotted

Figure 39a

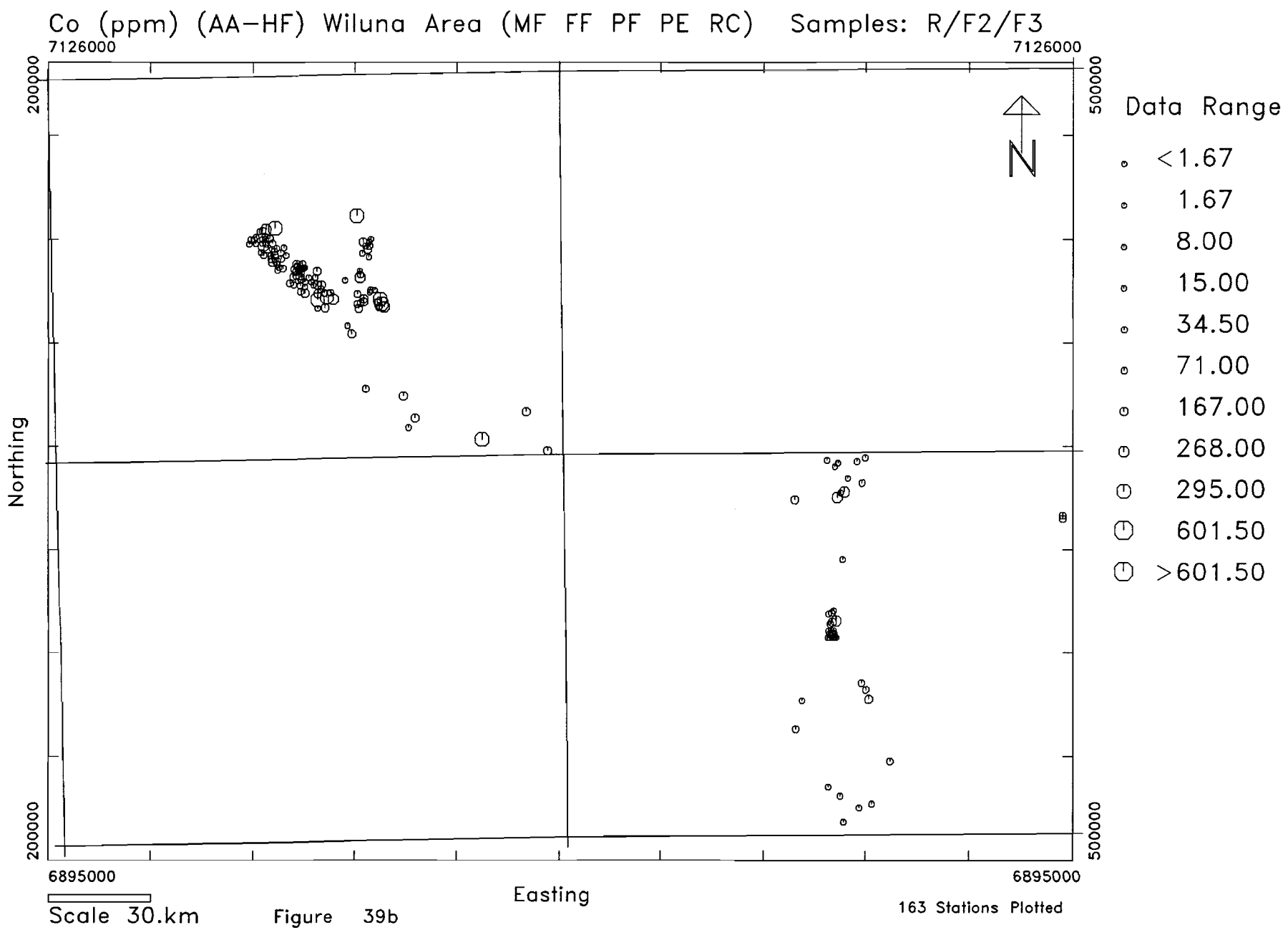
Co (ppm) (AA–HF) Wiluna Area (MF FF PF PE RC) Samples: R/F2/F3
7126000
7126000
200000
500000
N
Data Range
<1.67
1.67
8.00
15.00
34.50
71.00
167.00
268.00
295.00
601.50
>601.50
Northing
200000
500000
6895000
6895000
Easting
Scale 30.km
163 Stations Plotted

Figure 39b

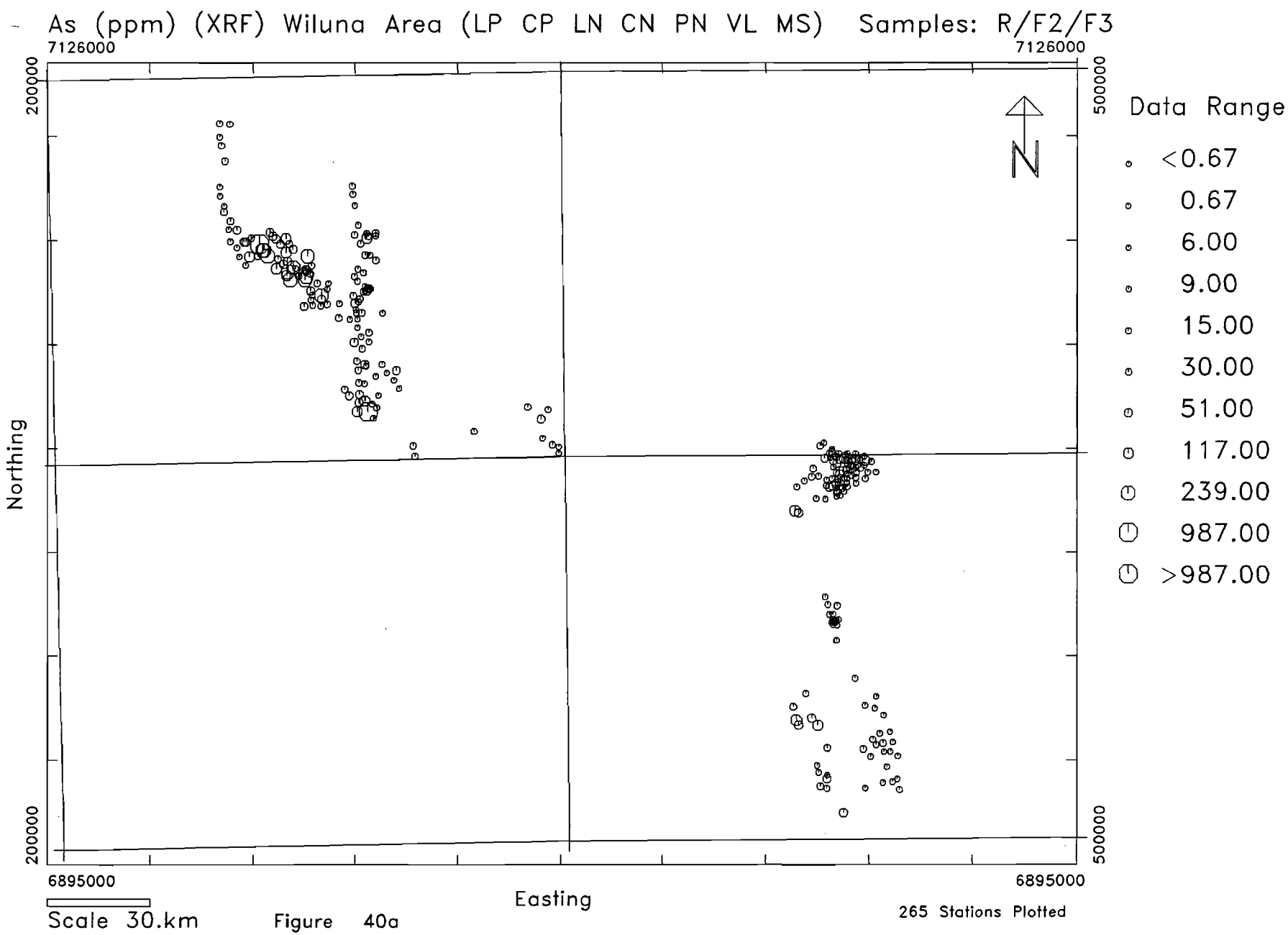
As (ppm) (XRF) Wiluna Area (LP CP LN CN PN VL MS) Samples: R/F2/F3
7126000
7126000
200000
500000
N
Data Range
<0.67
0.67
6.00
9.00
15.00
30.00
51.00
117.00
239.00
987.00
>987.00
Northing
200000
500000
6895000
6895000
Easting
Scale 30.km
265 Stations Plotted

Figure 40a

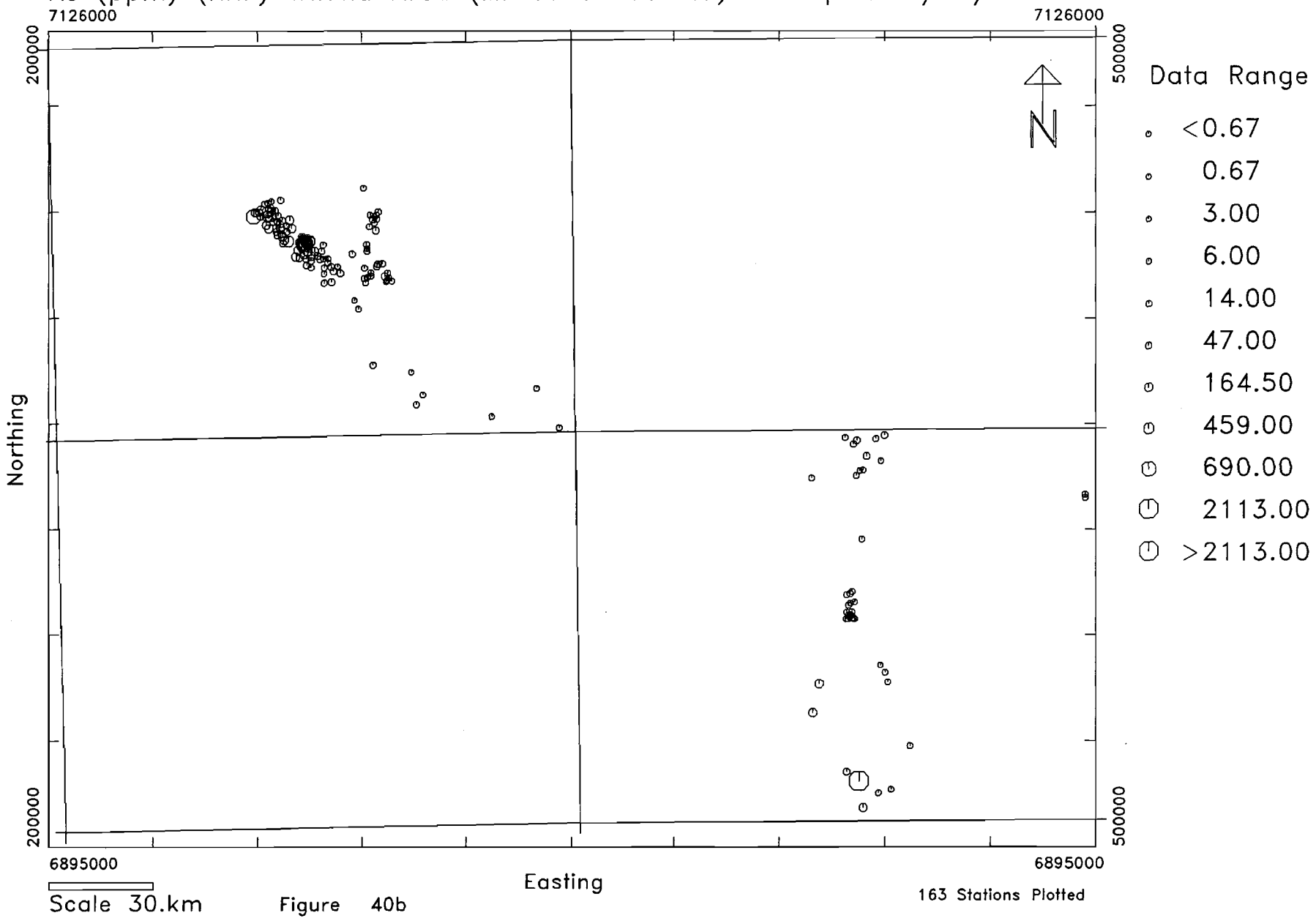
As (ppm) (XRF) Wiluna Area (MF FF PF PE RC) Samples: R/F2/F3
7126000
7126000
200000
500000
N
Data Range
<0.67
0.67
3.00
6.00
14.00
47.00
164.50
459.00
690.00
2113.00
>2113.00
Northing
200000
500000
6895000
6895000
Easting
Scale 30.km
Figure 40b
163 Stations Plotted

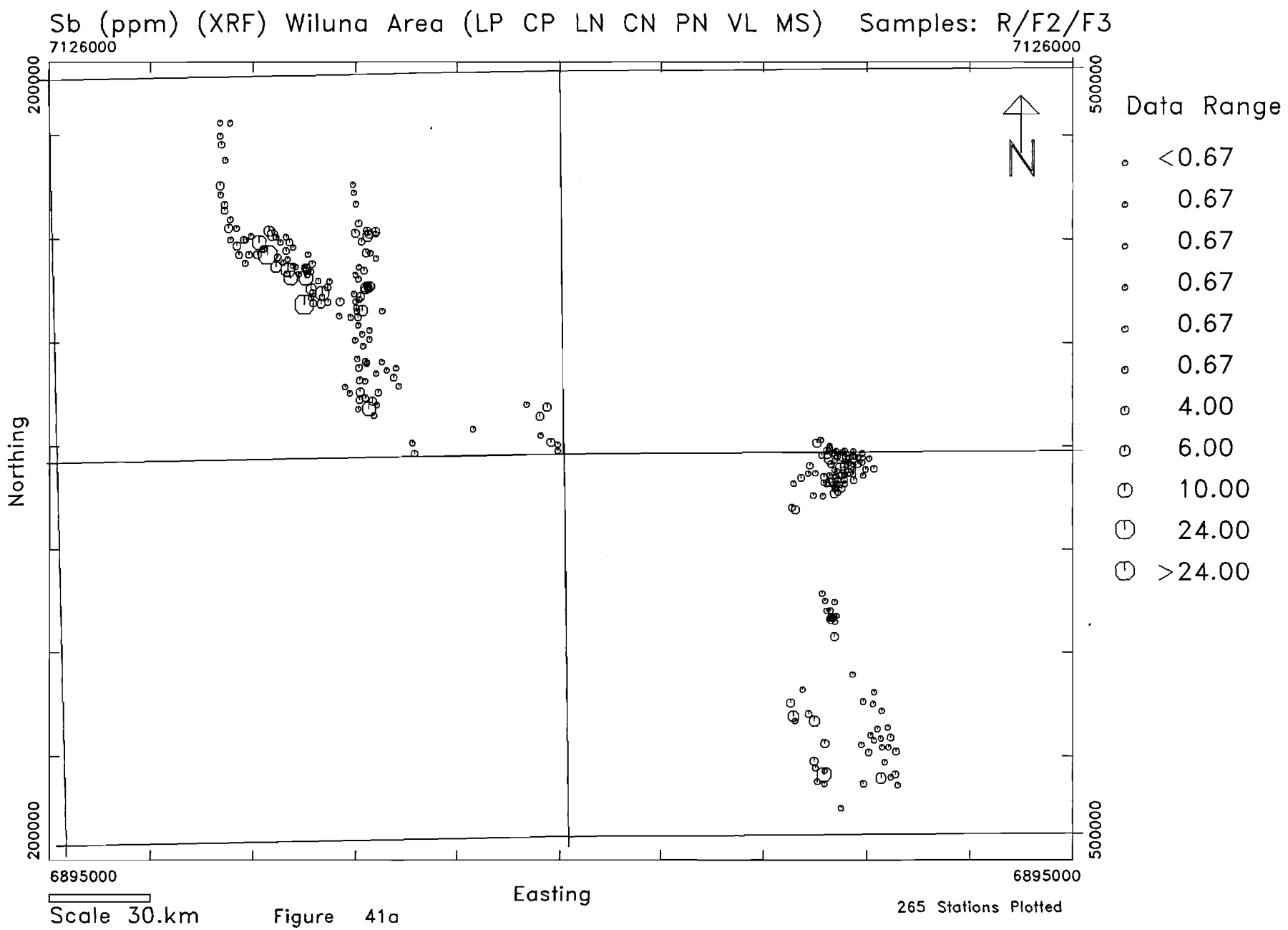
Sb (ppm) (XRF) Wiluna Area (LP CP LN CN PN VL MS) Samples: R/F2/F3
7126000
7126000
200000
500000
Northing
N
Data Range
<0.67
0.67
0.67
0.67
0.67
0.67
4.00
6.00
10.00
24.00
>24.00
200000
500000
6895000
6895000
Easting
Scale 30.km
265 Stations Plotted

Figure 41a

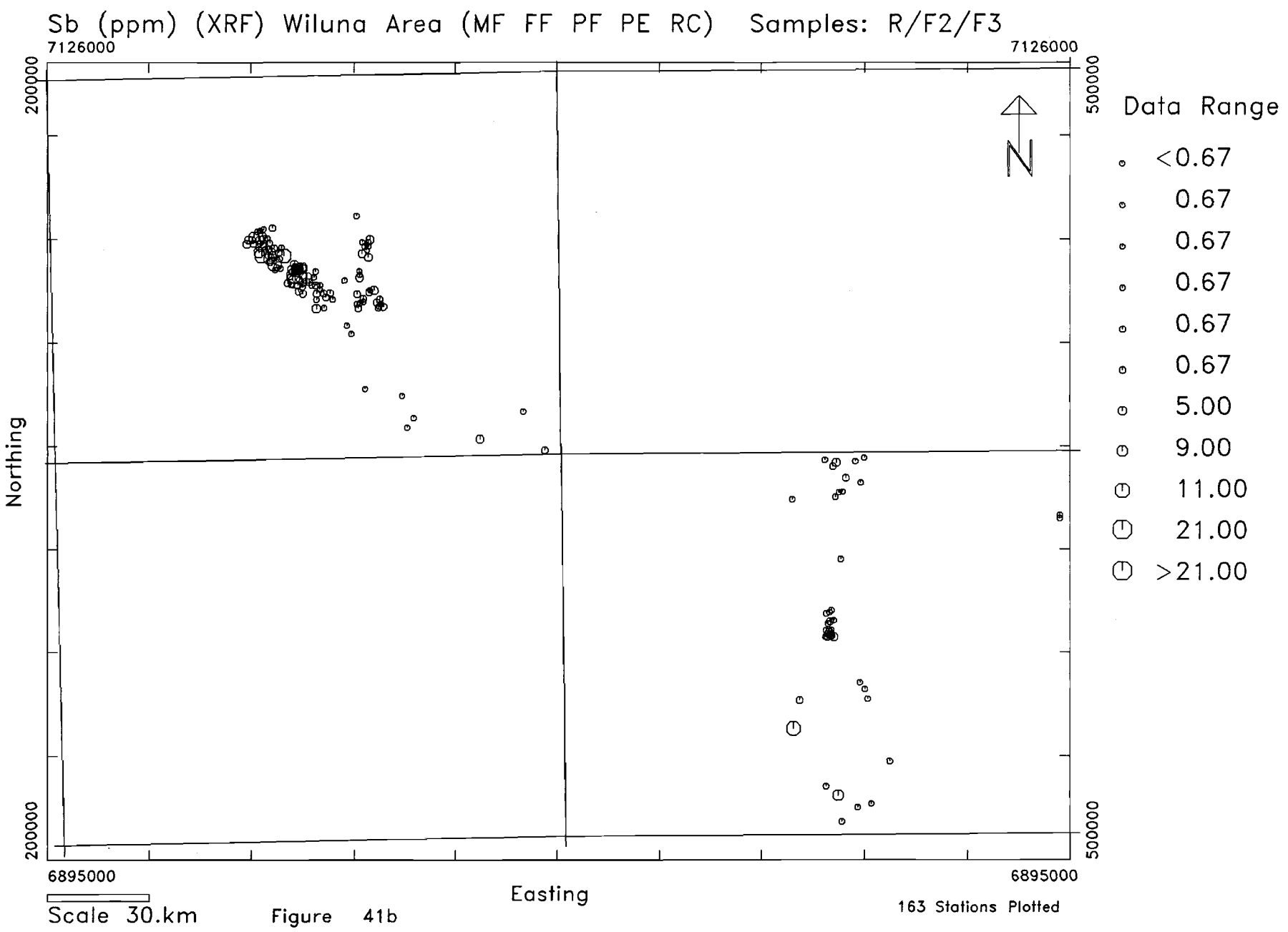
Sb (ppm) (XRF) Wiluna Area (MF FF PF PE RC) Samples: R/F2/F3
7126000
7126000
200000
500000
N
Data Range
<0.67
0.67
0.67
0.67
0.67
0.67
5.00
9.00
11.00
21.00
>21.00
Northing
200000
500000
6895000
6895000
Easting
Scale 30.km
163 Stations Plotted

Figure 41b

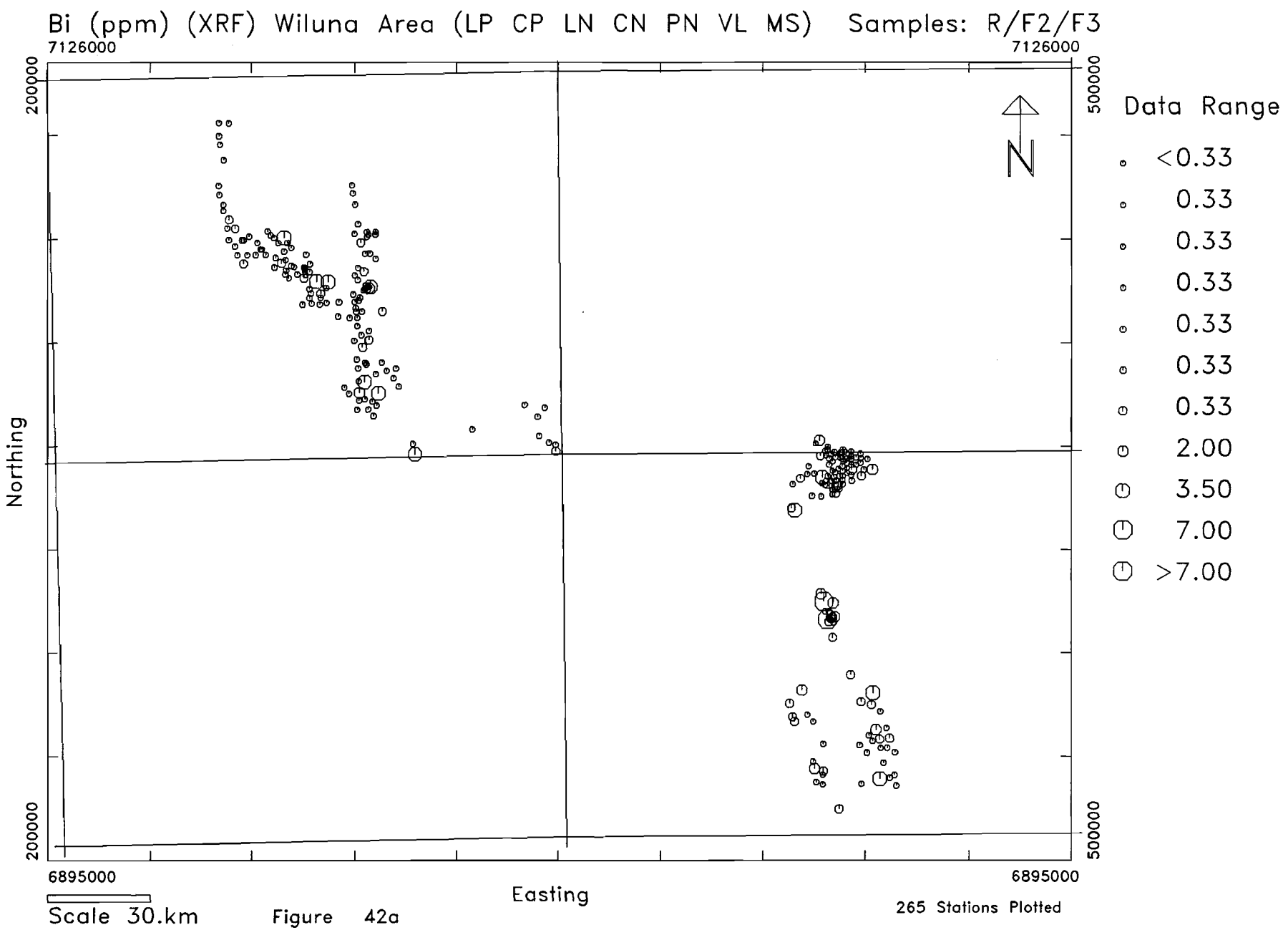
Bi (ppm) (XRF) Wiluna Area (LP CP LN CN PN VL MS) Samples: R/F2/F3
7126000
7126000
200000
500000
Northing
N
Data Range
<0.33
0.33
0.33
0.33
0.33
0.33
0.33
2.00
3.50
7.00
>7.00
200000
500000
6895000
6895000
Easting
Scale 30.km
265 Stations Plotted

Figure 42a

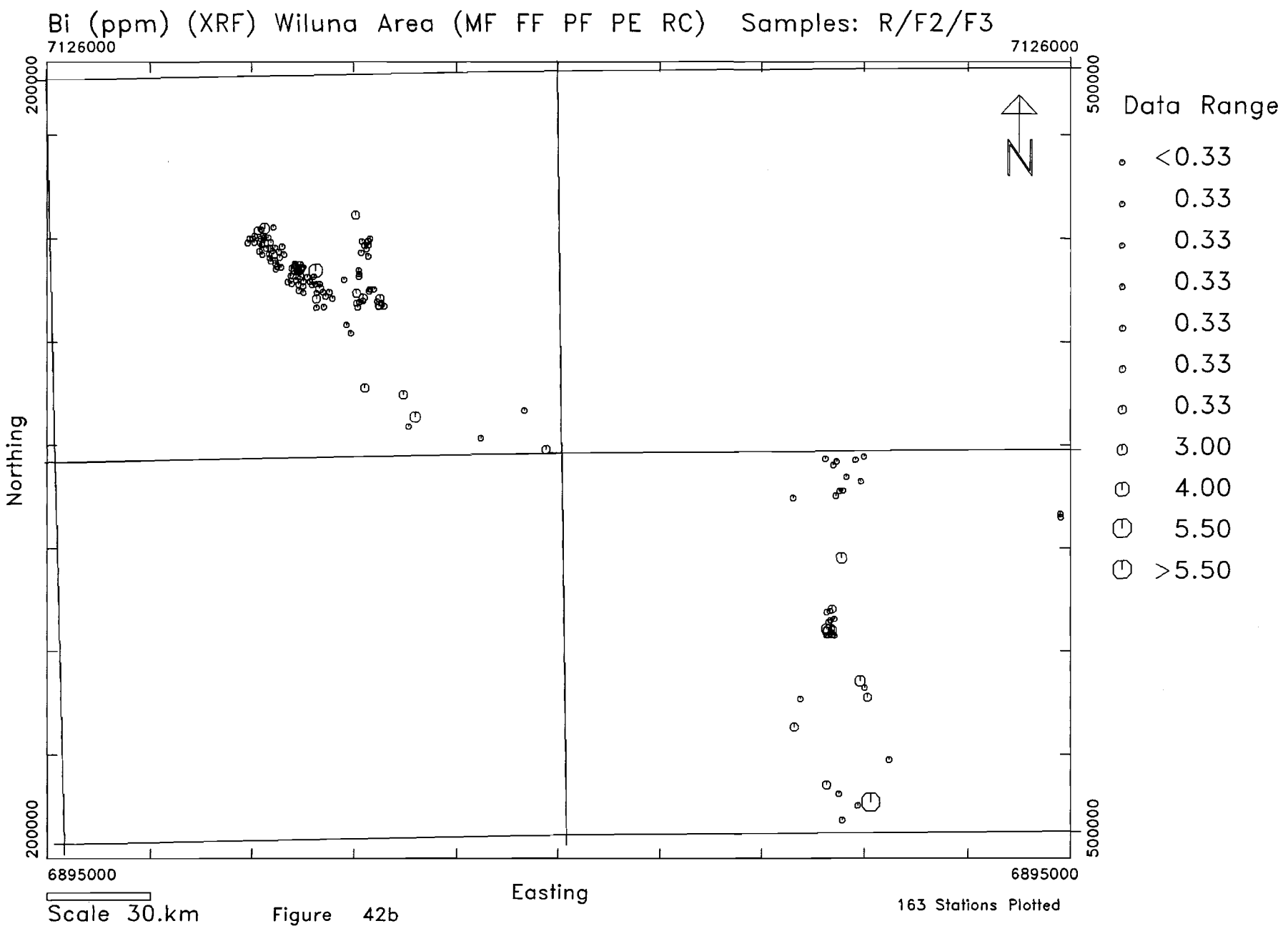
Bi (ppm) (XRF) Wiluna Area (MF FF PF PE RC) Samples: R/F2/F3
7126000
7126000
200000
500000
N
Data Range
<0.33
0.33
0.33
0.33
0.33
0.33
0.33
3.00
4.00
5.50
>5.50
Northing
200000
500000
6895000
6895000
Easting
Scale 30.km
163 Stations Plotted

Figure 42b

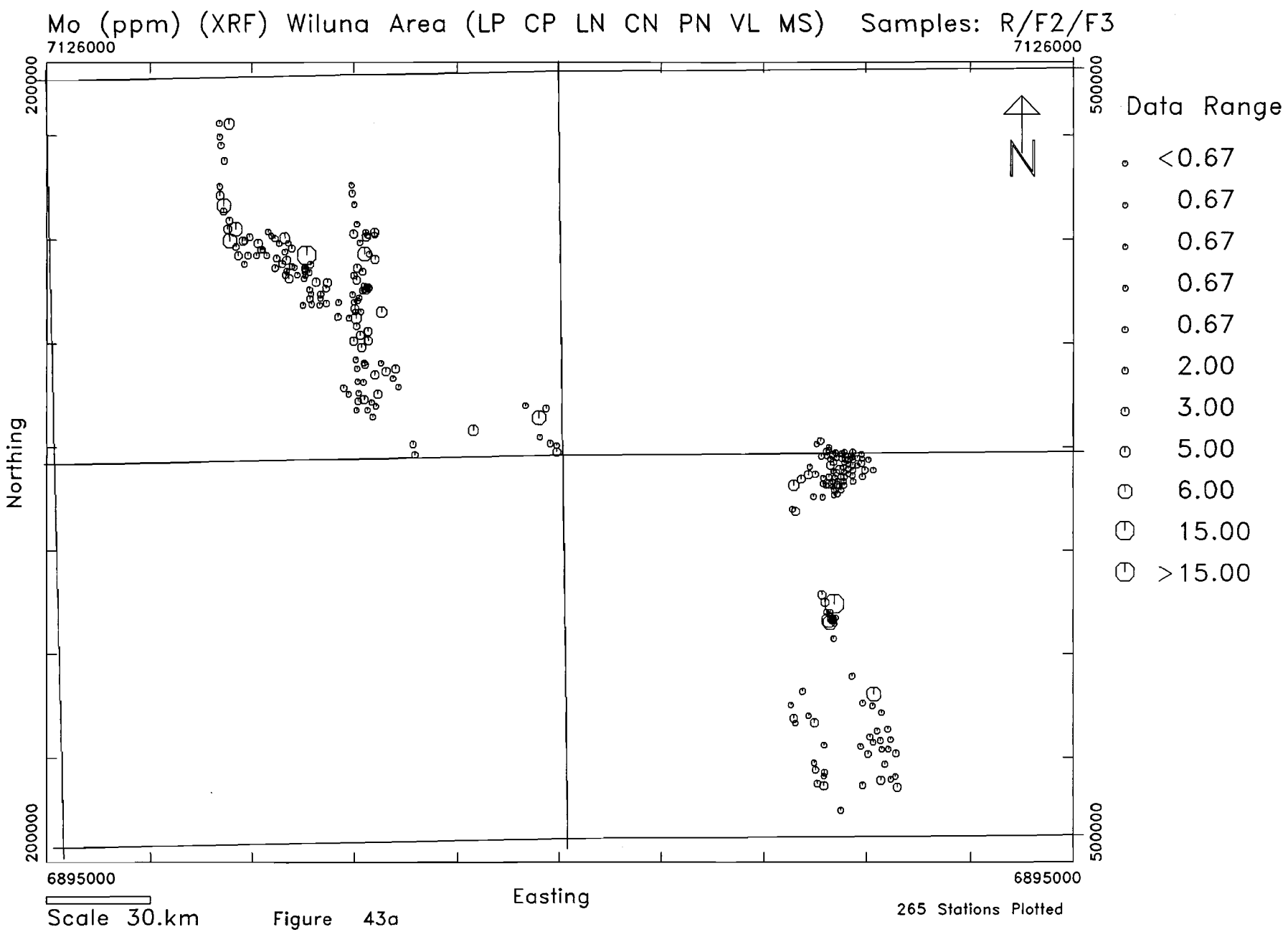
Mo (ppm) (XRF) Wiluna Area (LP CP LN CN PN VL MS) Samples: R/F2/F3
7126000
7126000
200000
500000
N
Data Range
<0.67
0.67
0.67
0.67
0.67
2.00
3.00
5.00
6.00
15.00
>15.00
Northing
200000
500000
6895000
6895000
Easting
Scale 30.km
265 Stations Plotted

Figure 43a

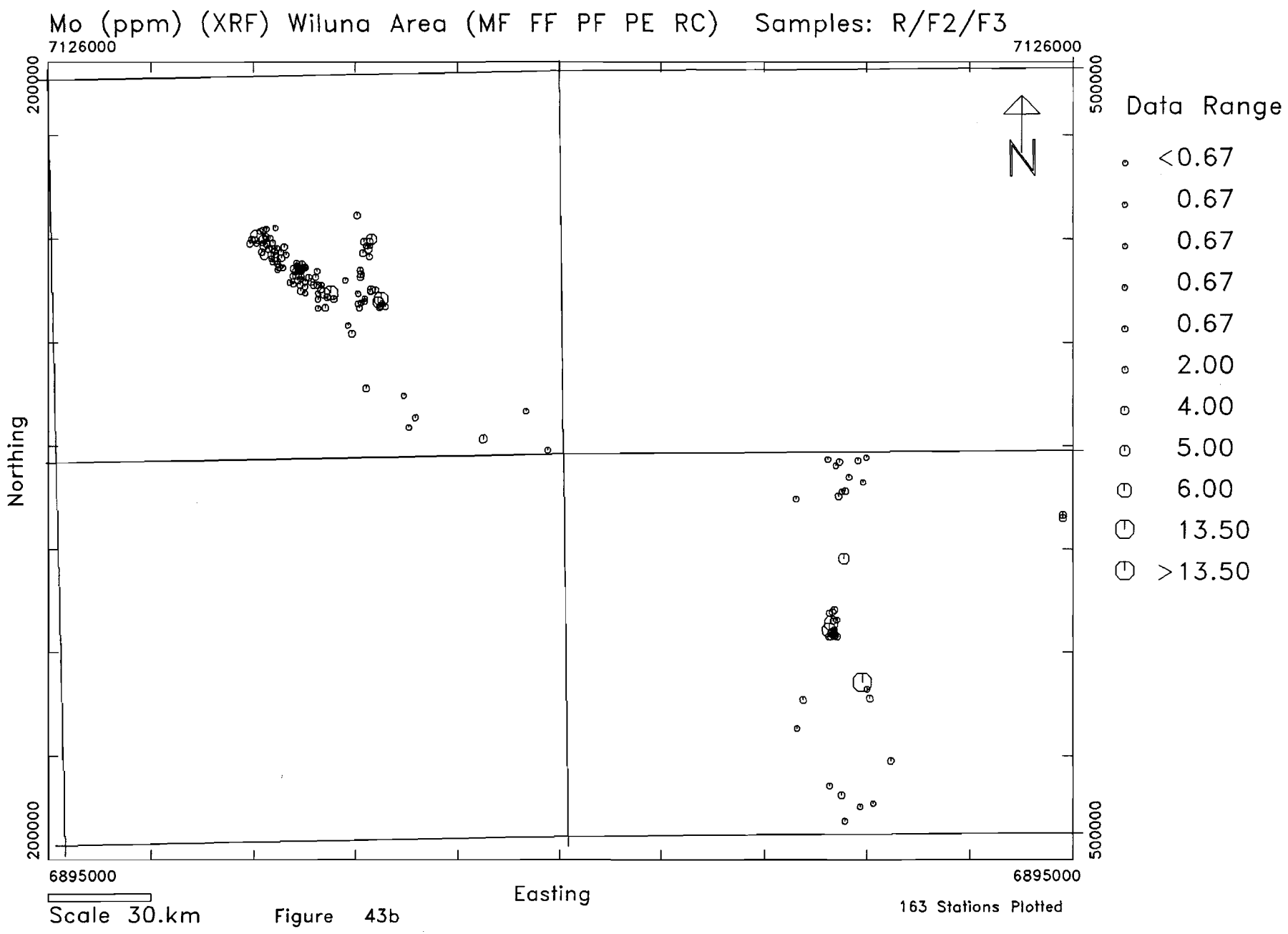
Mo (ppm) (XRF) Wiluna Area (MF FF PF PE RC) Samples: R/F2/F3
7126000
7126000
200000
500000
Northing
N
Data Range
<0.67
0.67
0.67
0.67
0.67
2.00
4.00
5.00
6.00
13.50
>13.50
200000
500000
6895000
6895000
Easting
Scale 30.km
163 Stations Plotted

Figure 43b

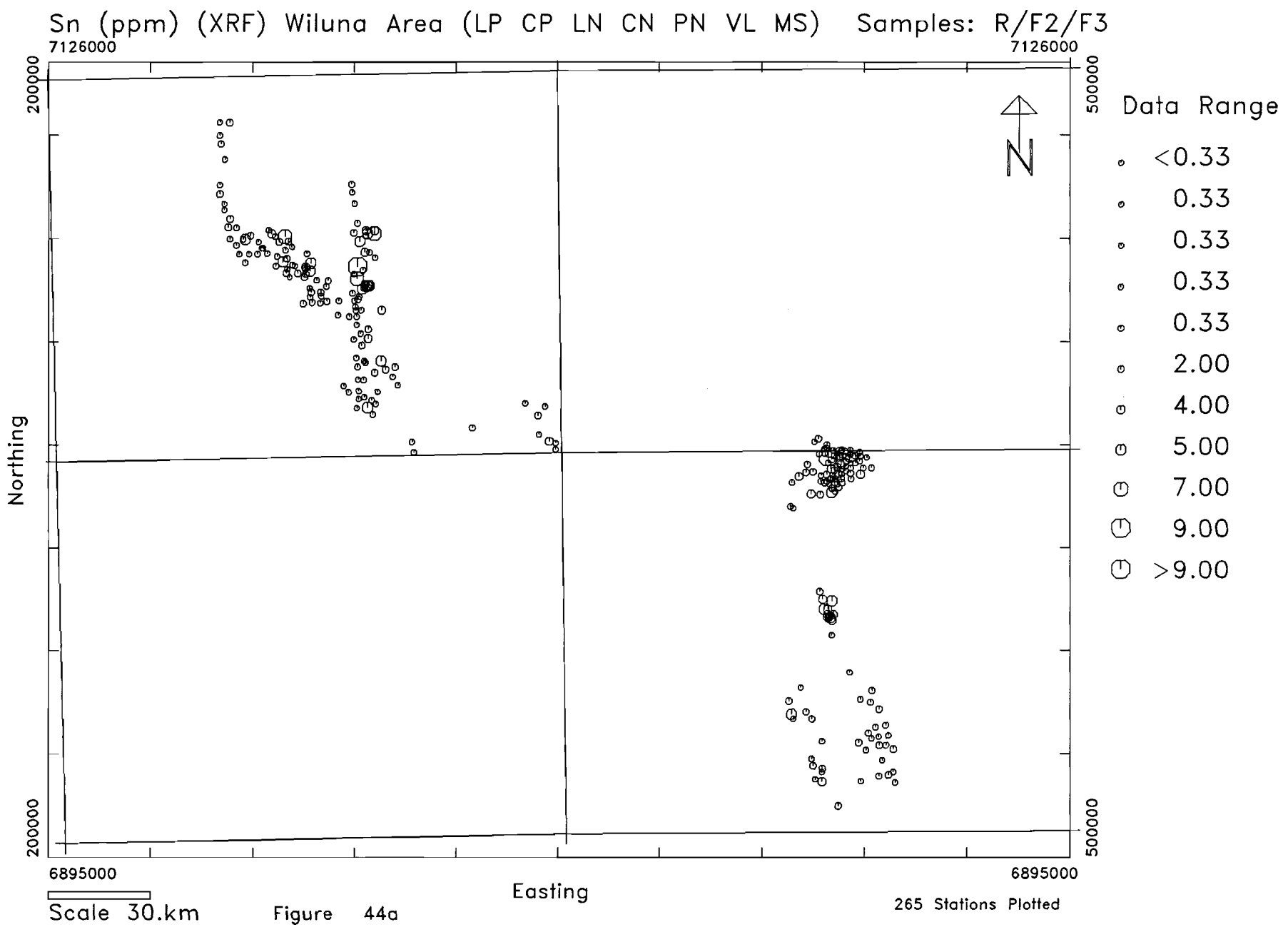
Sn (ppm) (XRF) Wiluna Area (LP CP LN CN PN VL MS) Samples: R/F2/F3
7126000
7126000
200000
500000
N
Data Range
<0.33
0.33
0.33
0.33
0.33
2.00
4.00
5.00
7.00
9.00
>9.00
Northing
200000
500000
6895000
6895000
Easting
Scale 30.km
265 Stations Plotted

Figure 44a

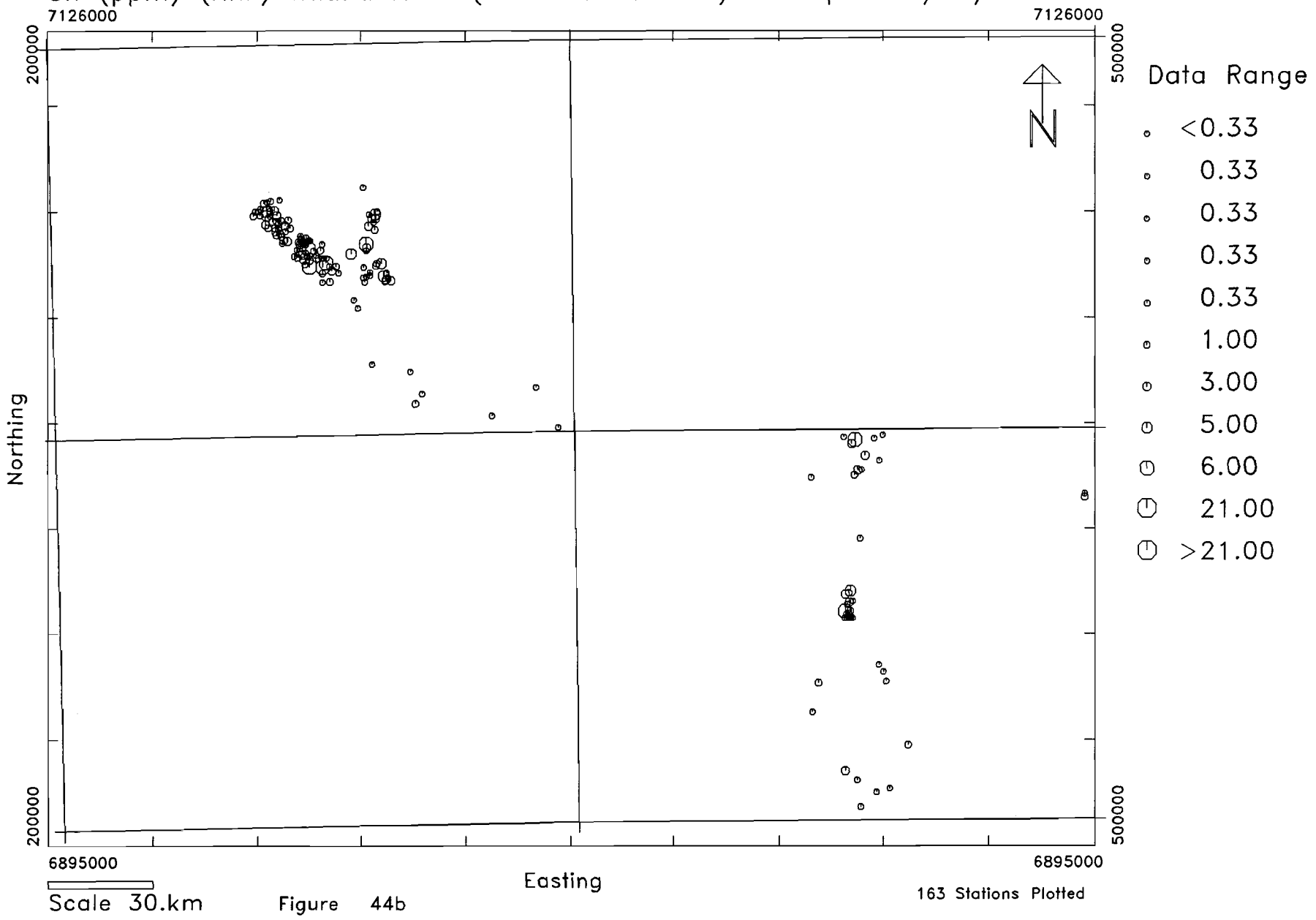
Sn (ppm) (XRF) Wiluna Area (MF FF PF PE RC) Samples: R/F2/F3
7126000
7126000
200000
500000
N
Data Range
<0.33
0.33
0.33
0.33
0.33
1.00
3.00
5.00
6.00
21.00
>21.00
Northing
200000
500000
6895000
6895000
Easting
Scale 30.km
163 Stations Plotted

Figure 44b

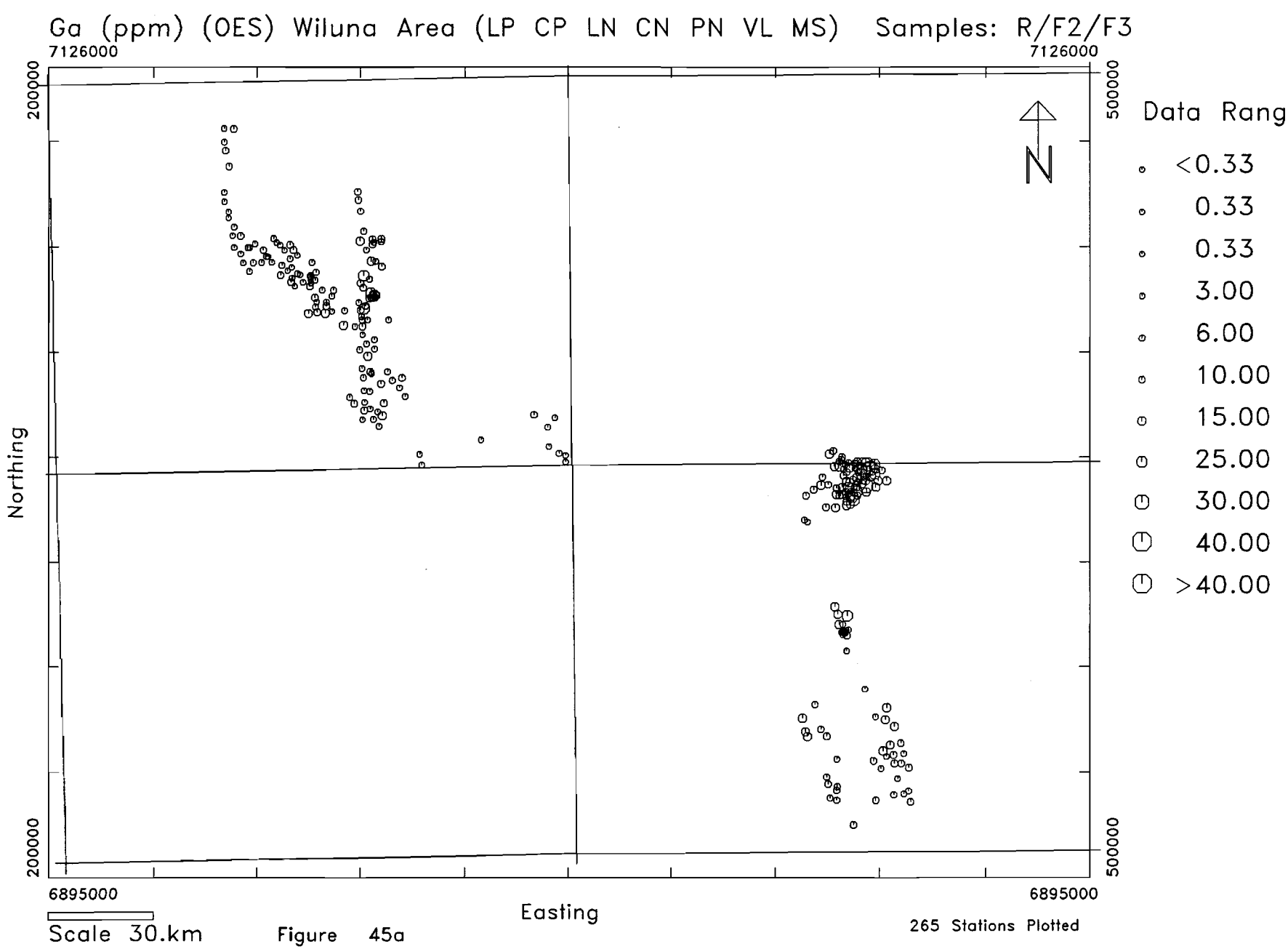
Ga (ppm) (OES) Wiluna Area (LP CP LN CN PN VL MS) Samples: R/F2/F3
7126000
7126000
200000
500000
N
Data Range
<0.33
0.33
0.33
3.00
6.00
10.00
15.00
25.00
30.00
40.00
>40.00
Northing
200000
500000
6895000
6895000
Easting
Scale 30.km
265 Stations Plotted

Figure 45a

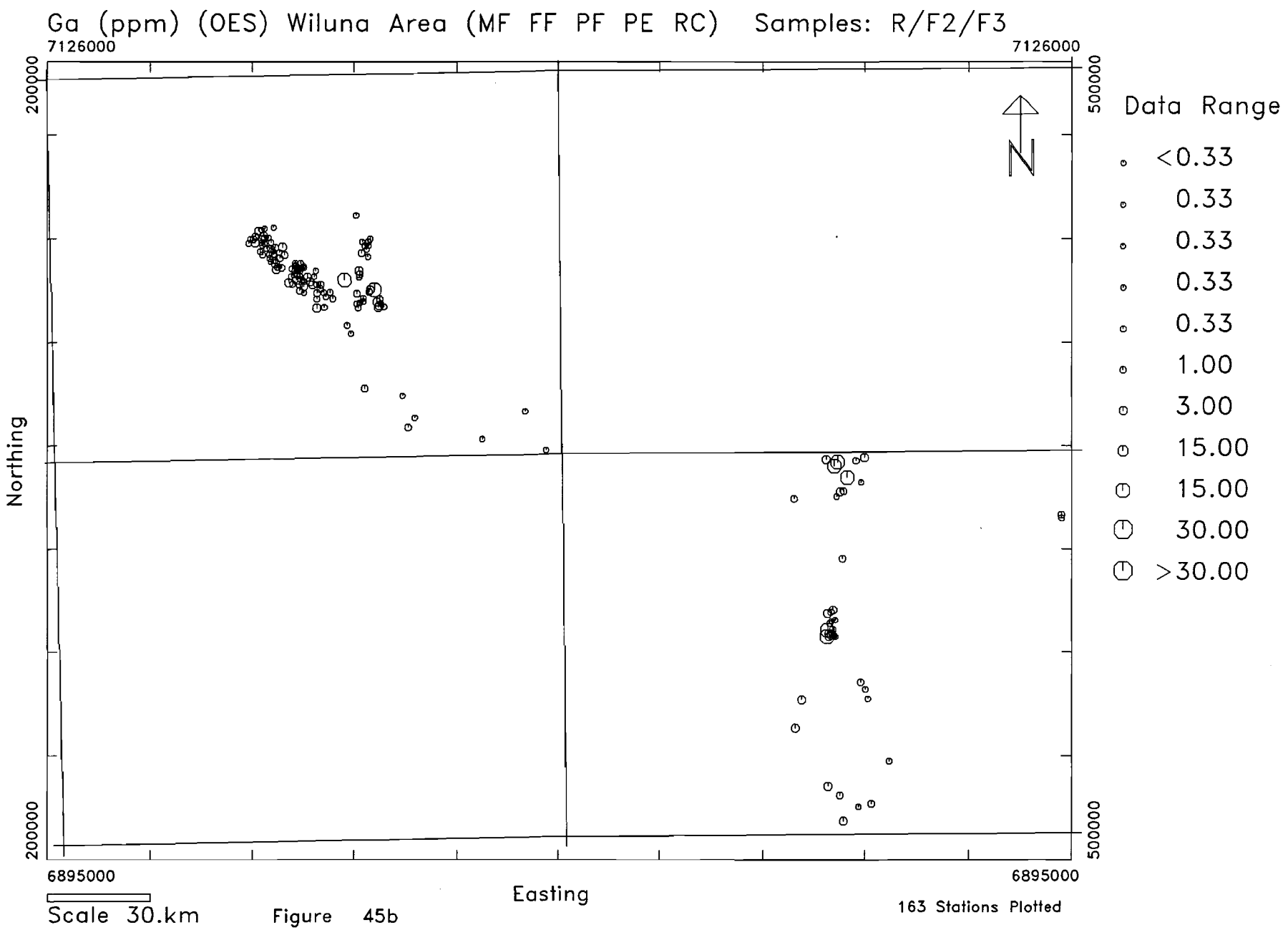
Ga (ppm) (OES) Wiluna Area (MF FF PF PE RC) Samples: R/F2/F3
7126000
7126000
200000
500000
Northing
N
Data Range
<0.33
0.33
0.33
0.33
0.33
1.00
3.00
15.00
15.00
30.00
>30.00
200000
500000
6895000
6895000
Easting
Scale 30.km
163 Stations Plotted

Figure 45b

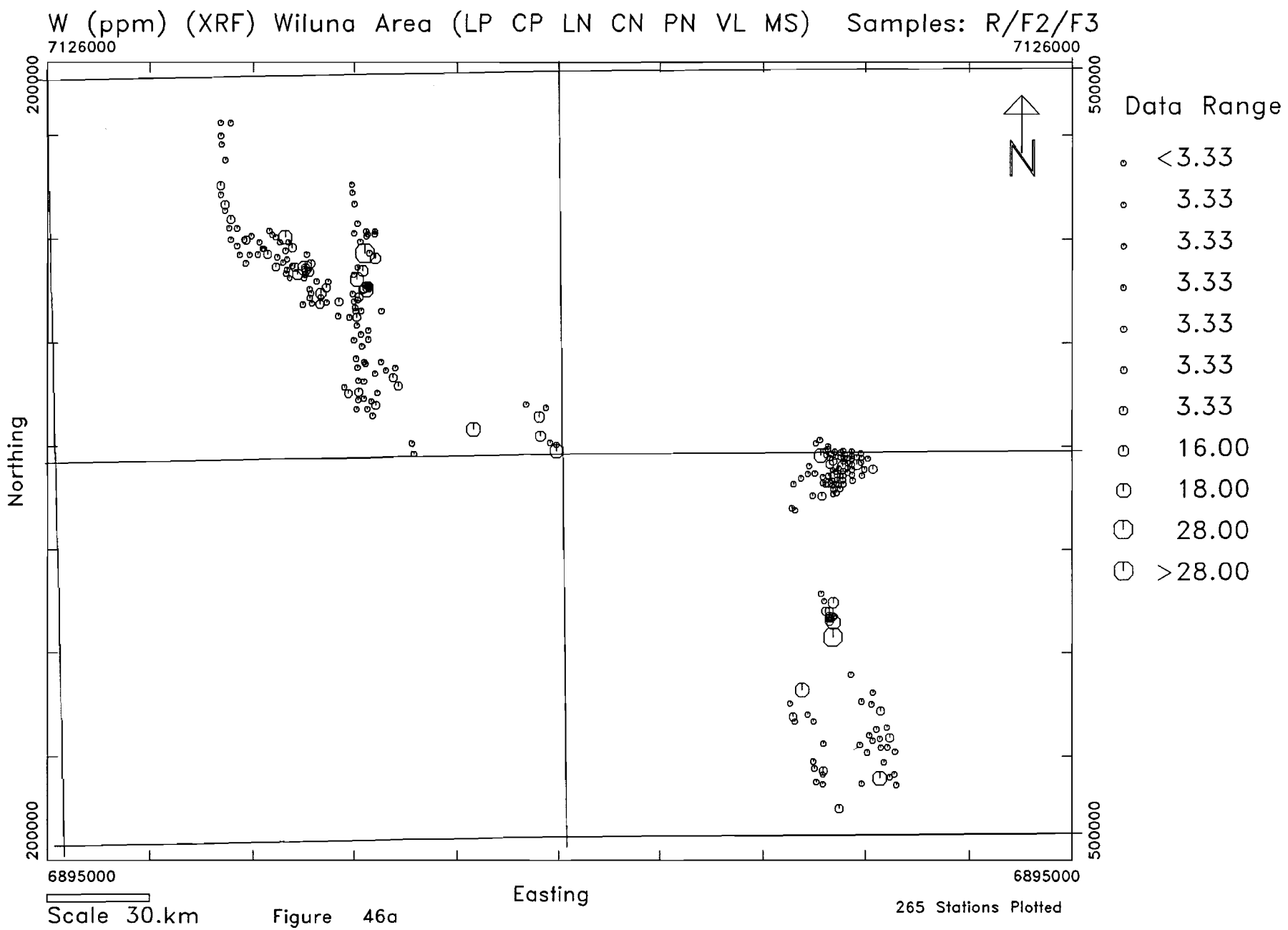
W (ppm) (XRF) Wiluna Area (LP CP LN CN PN VL MS) Samples: R/F2/F3
7126000
7126000
200000
500000
Northing
N
Data Range
<3.33
3.33
3.33
3.33
3.33
3.33
3.33
16.00
18.00
28.00
>28.00
200000
500000
6895000
6895000
Easting
Scale 30.km
265 Stations Plotted

Figure 46a

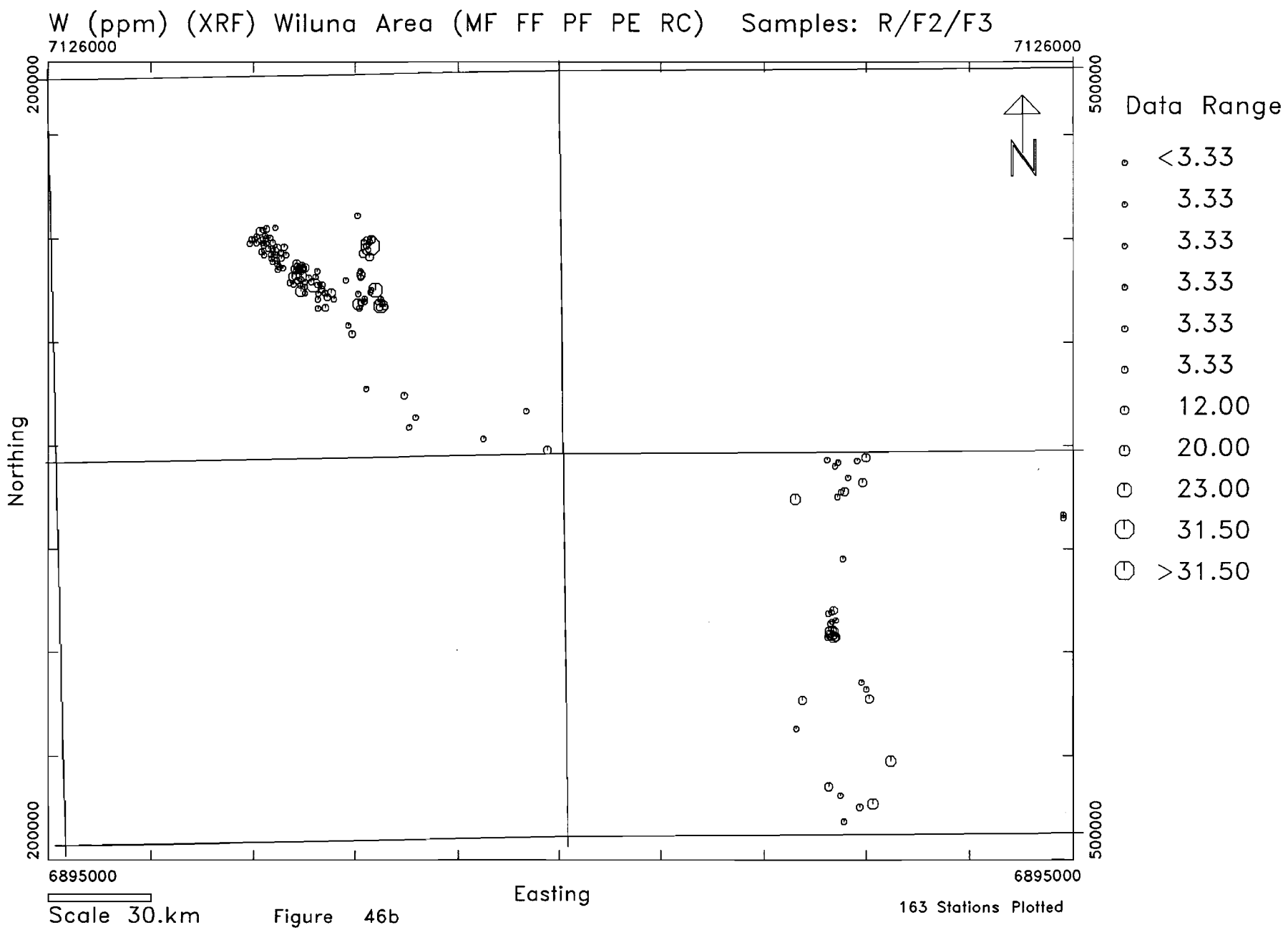
W (ppm) (XRF) Wiluna Area (MF FF PF PE RC) Samples: R/F2/F3
7126000
7126000
200000
500000
Northing
N
Data Range
<3.33
3.33
3.33
3.33
3.33
3.33
12.00
20.00
23.00
31.50
>31.50
200000
500000
6895000
6895000
Easting
Scale 30.km
163 Stations Plotted

Figure 46b

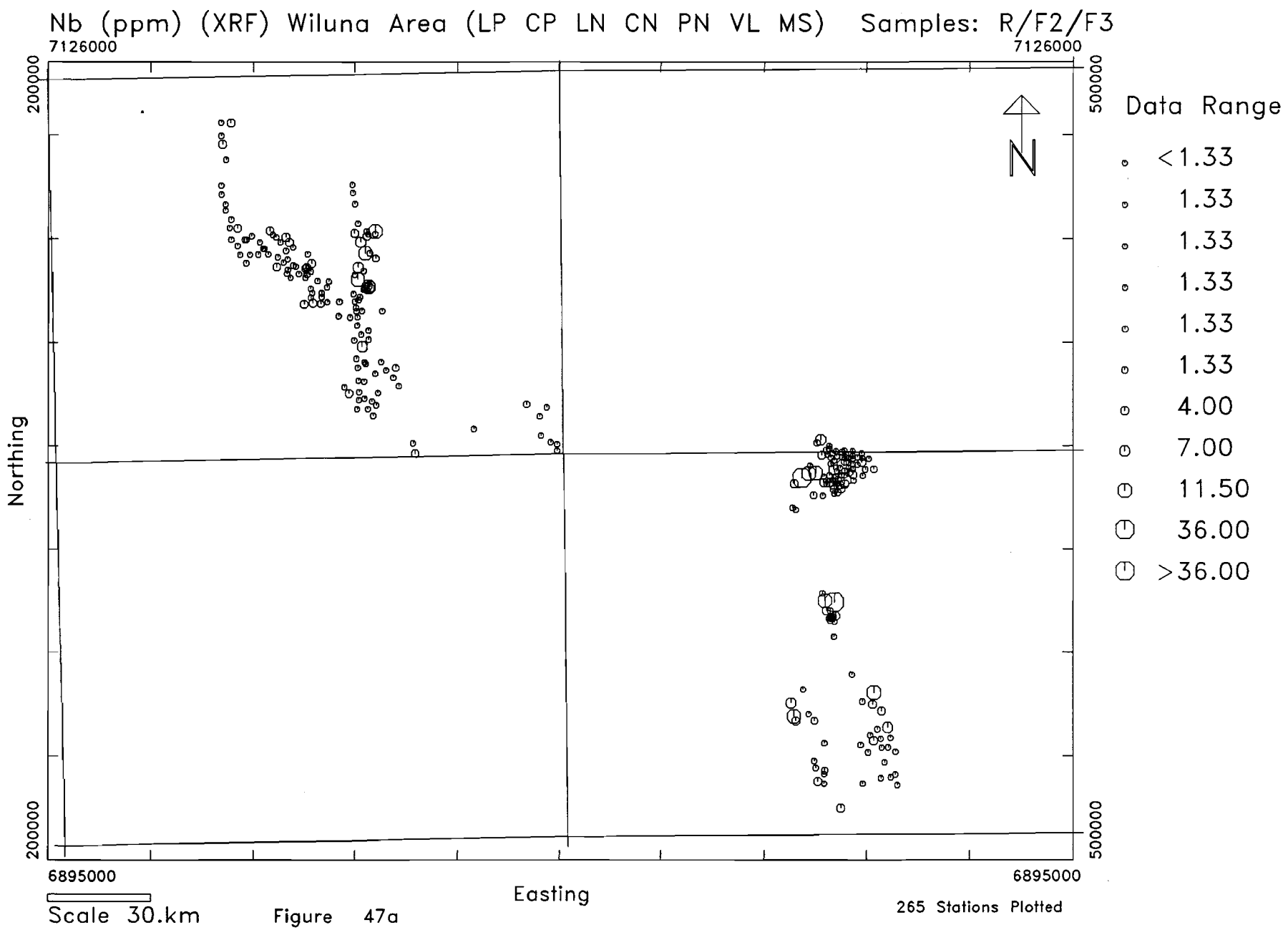
Nb (ppm) (XRF) Wiluna Area (LP CP LN CN PN VL MS) Samples: R/F2/F3
7126000
7126000
200000
500000
Northing
N
Data Range
<1.33
1.33
1.33
1.33
1.33
1.33
4.00
7.00
11.50
36.00
>36.00
200000
500000
6895000
6895000
Easting
Scale 30.km
265 Stations Plotted

Figure 47a

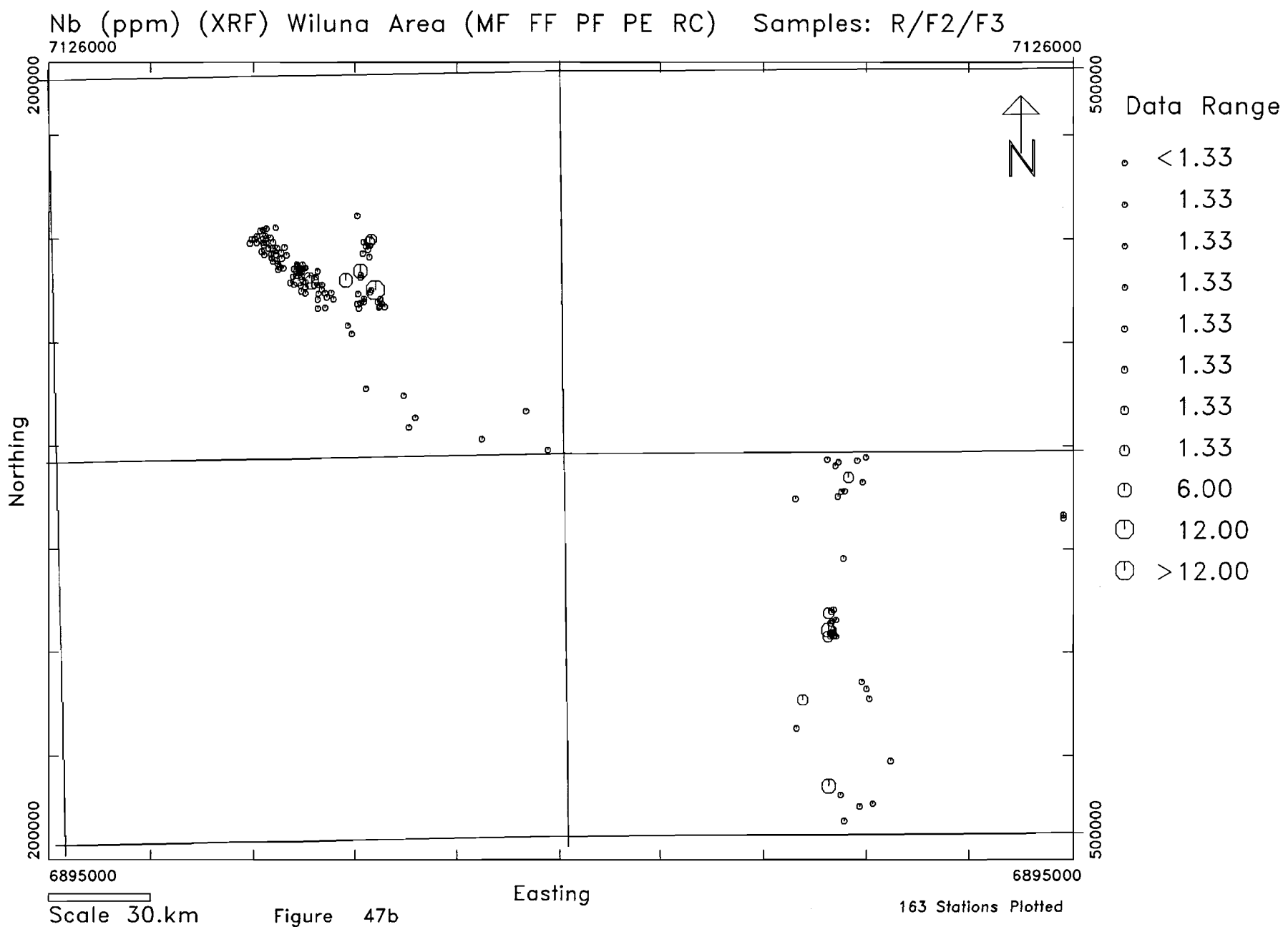
Nb (ppm) (XRF) Wiluna Area (MF FF PF PE RC) Samples: R/F2/F3
7126000
7126000
200000
500000
Northing
N
Data Range
<1.33
1.33
1.33
1.33
1.33
1.33
1.33
1.33
6.00
12.00
>12.00
200000
500000
6895000
6895000
Easting
Scale 30.km
163 Stations Plotted

Figure 47b

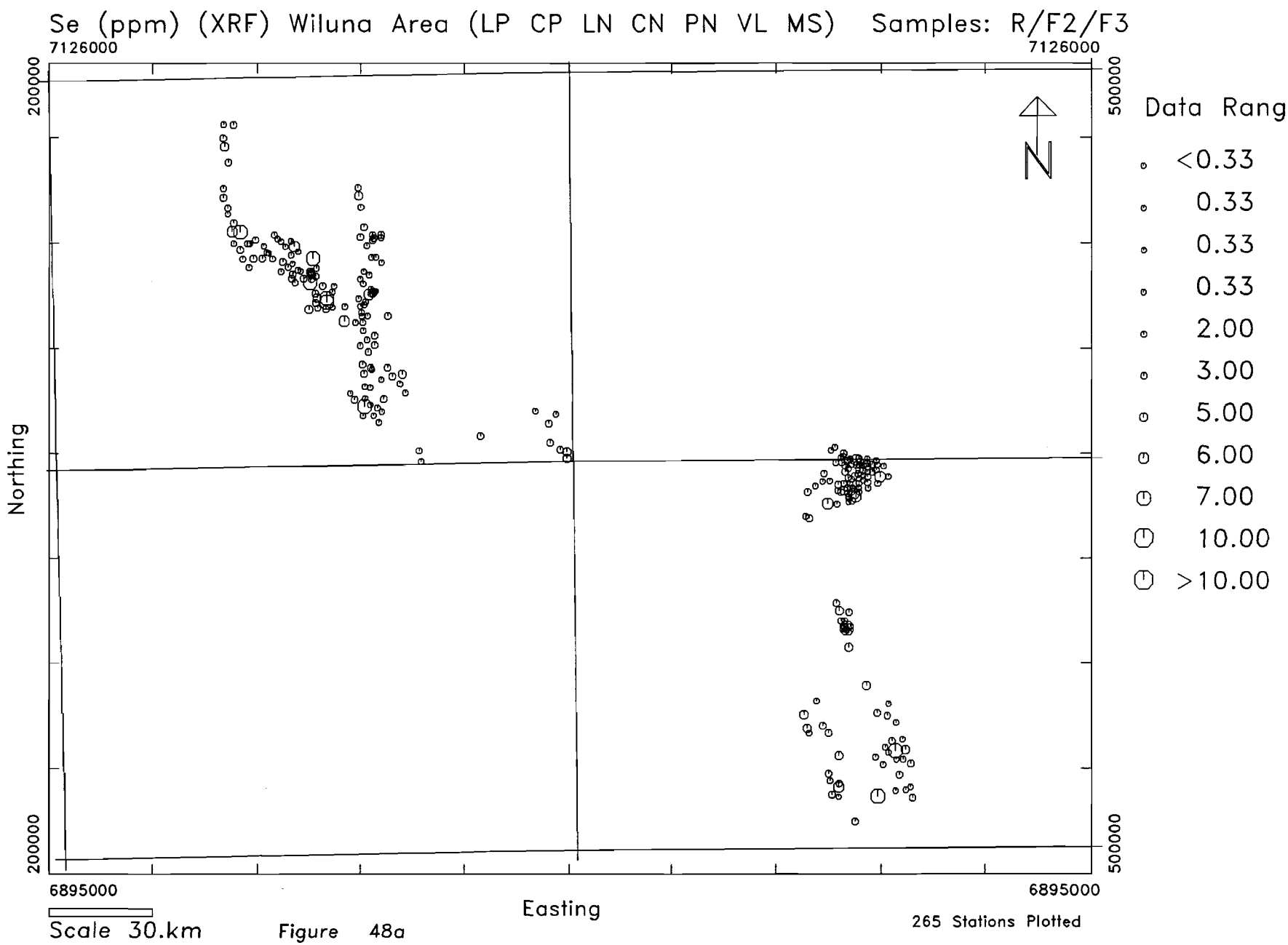
Se (ppm) (XRF) Wiluna Area (LP CP LN CN PN VL MS) Samples: R/F2/F3
7126000
7126000
200000
500000
Northing
N
Data Range
<0.33
0.33
0.33
0.33
2.00
3.00
5.00
6.00
7.00
10.00
>10.00
200000
500000
6895000
6895000
Easting
Scale 30.km
265 Stations Plotted

Figure 48a

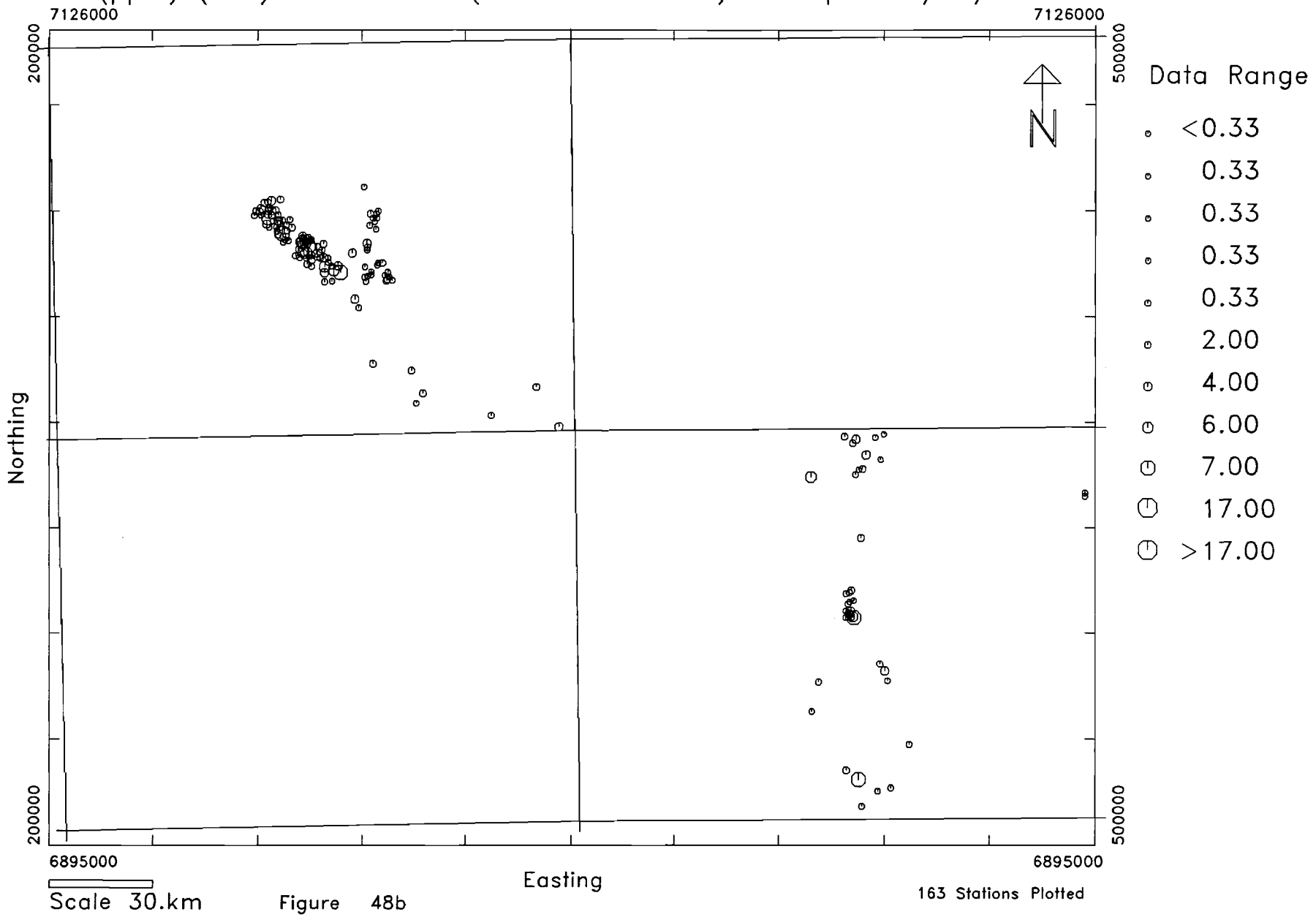
Se (ppm) (XRF) Wiluna Area (MF FF PF PE RC) Samples: R/F2/F3
7126000
7126000
200000
500000
Data Range
<0.33
0.33
0.33
0.33
0.33
2.00
4.00
6.00
7.00
17.00
>17.00
N
Northing
200000
500000
6895000
6895000
Easting
Scale 30.km
163 Stations Plotted

Figure 48b

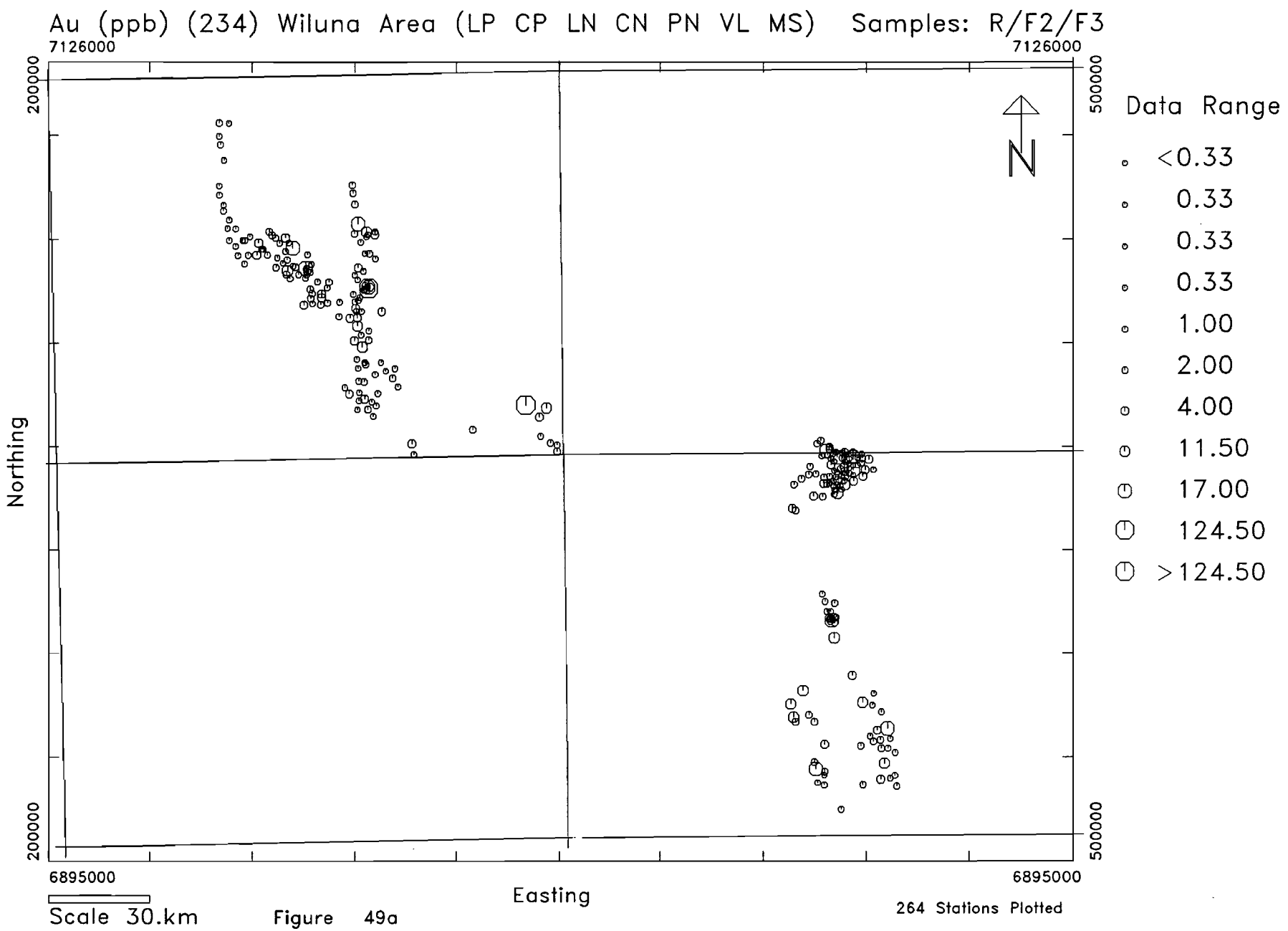
Au (ppb) (234) Wiluna Area (LP CP LN CN PN VL MS) Samples: R/F2/F3
7126000
7126000
200000
500000
Northing
N
Data Range
<0.33
0.33
0.33
0.33
1.00
2.00
4.00
11.50
17.00
124.50
>124.50
200000
500000
6895000
6895000
Easting
Scale 30.km
264 Stations Plotted

Figure 49a

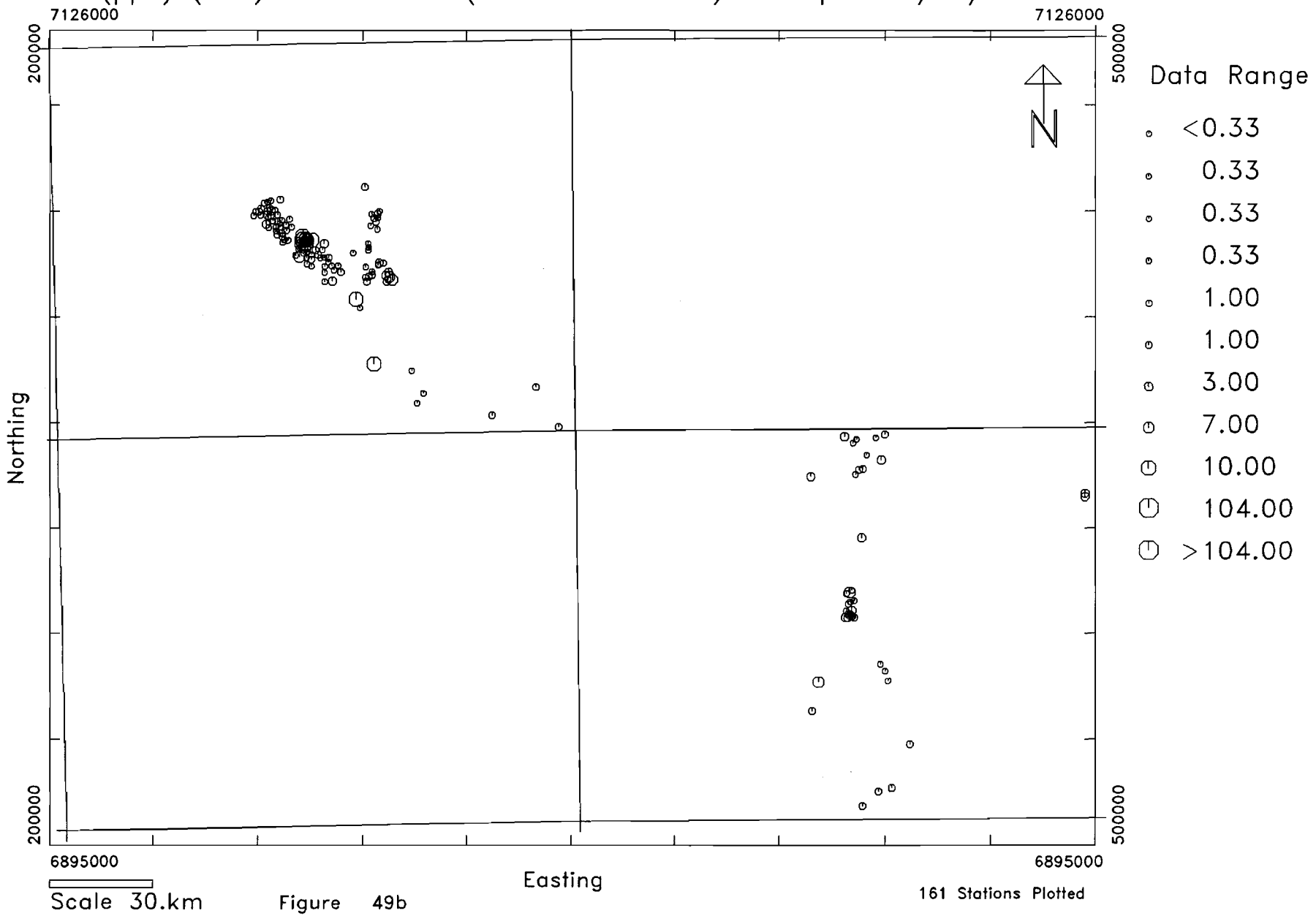
Au (ppb) (234) Wiluna Area (MF FF PF PE RC) Samples: R/F2/F3
7126000
7126000
200000
500000
Data Range
<0.33
0.33
0.33
0.33
1.00
1.00
3.00
7.00
10.00
104.00
>104.00
N
Northing
200000
500000
6895000
6895000
Easting
Scale 30.km
161 Stations Plotted

Figure 49b

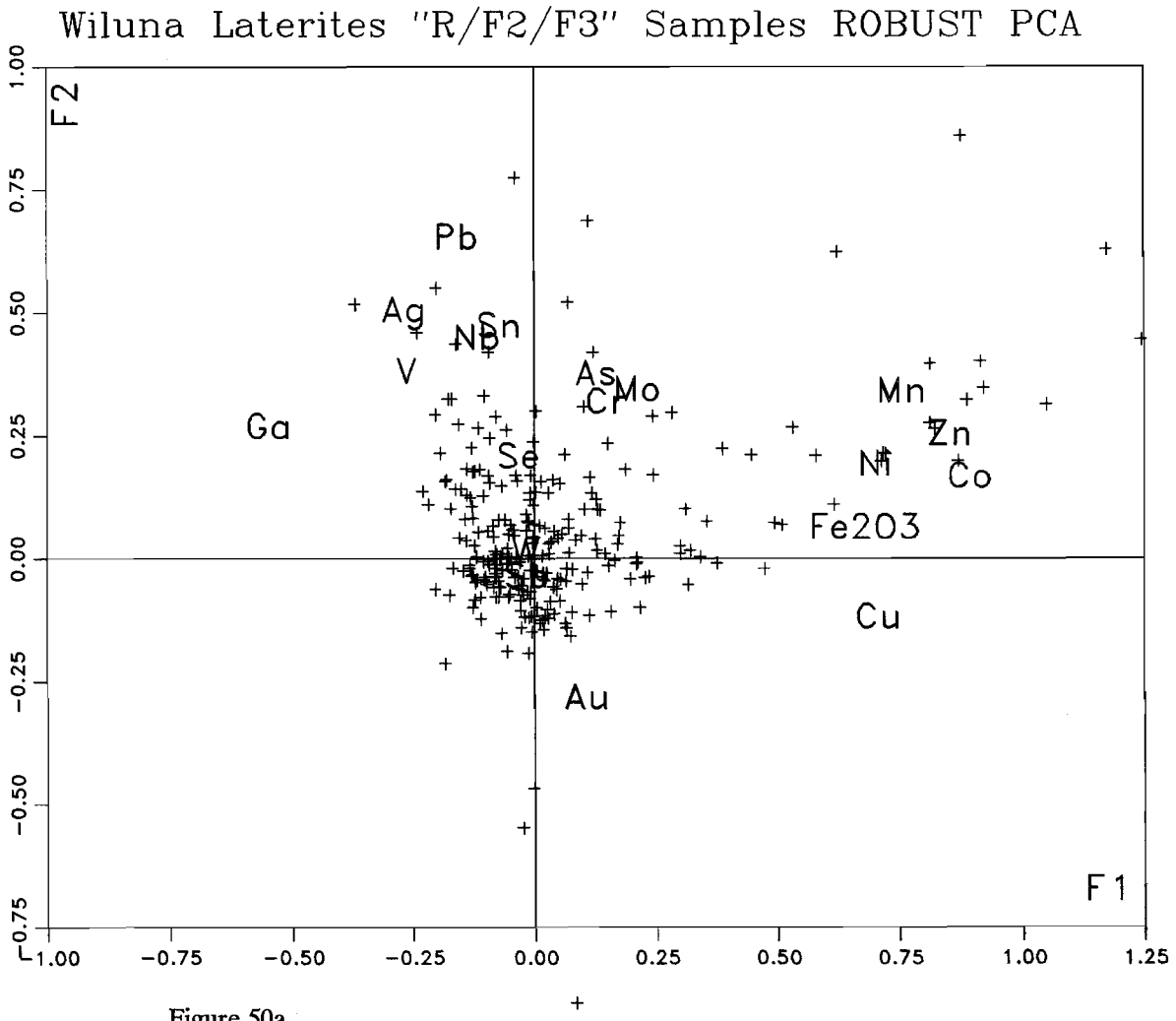
Wiluna Laterites "R/F2/F3" Samples ROBUST PCA
F2
F1
Pb
Ag
Sn
Nb
V
As
Mo
Cr
Mn
Zn
Ni
Co
Ga
Se
Fe203
Cu
Au
1.00
0.75
0.50
0.25
0.00
-0.25
-0.50
-0.75
-1.00
-0.75
-0.50
-0.25
0.00
0.25
0.50
0.75
1.00
1.25

Figure 50a

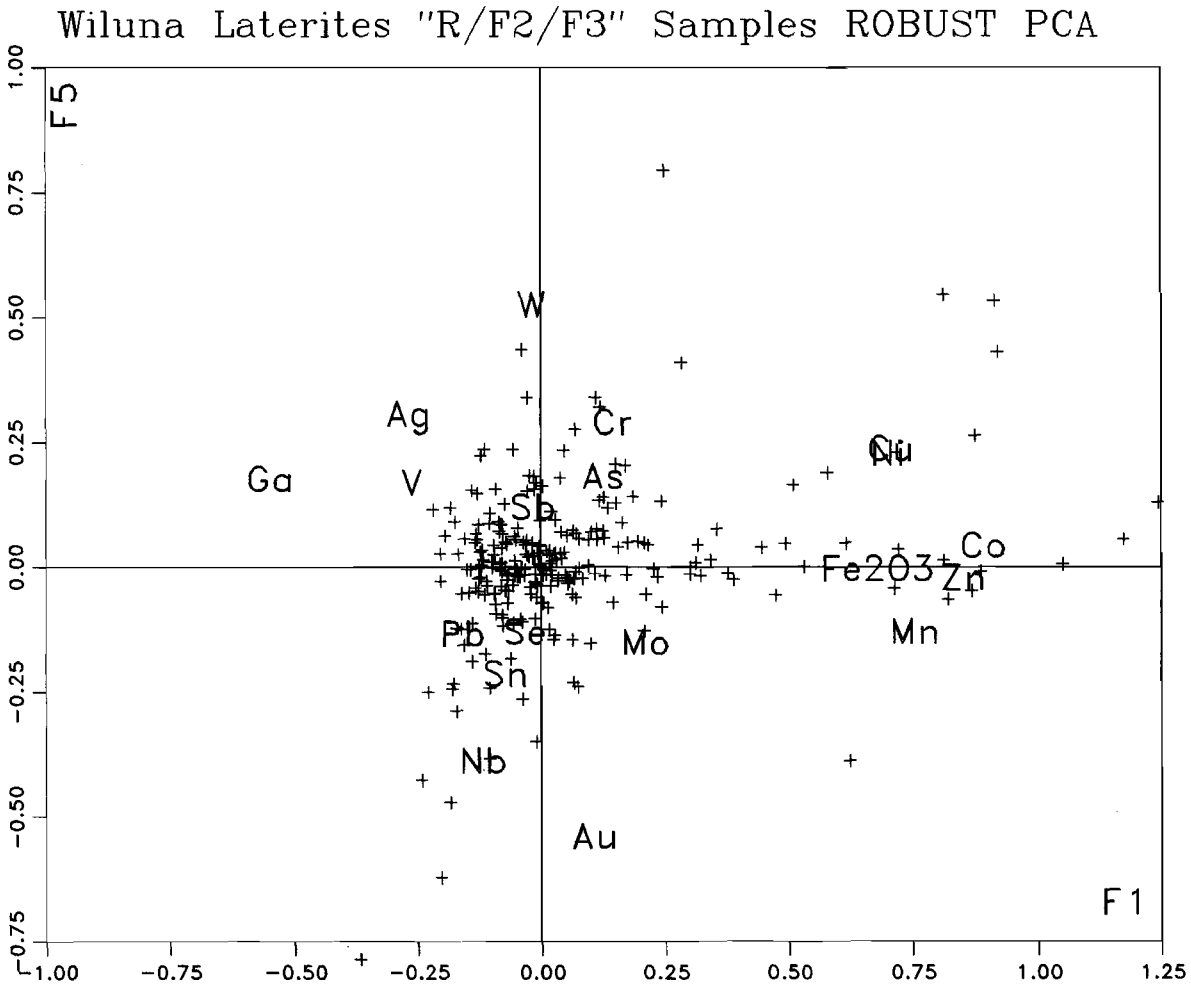
Wiluna Laterites "R/F2/F3" Samples ROBUST PCA
F5
F1
W
Ag
Cr
Cu
Ga
V
As
Sb
Co
Fe2O3
Zn
Pb
Se
Mo
Mn
Sn
Nb
Au
1.00
0.75
0.50
0.25
0.00
-0.25
-0.50
-0.75
-1.00
1.25

Figure 50b

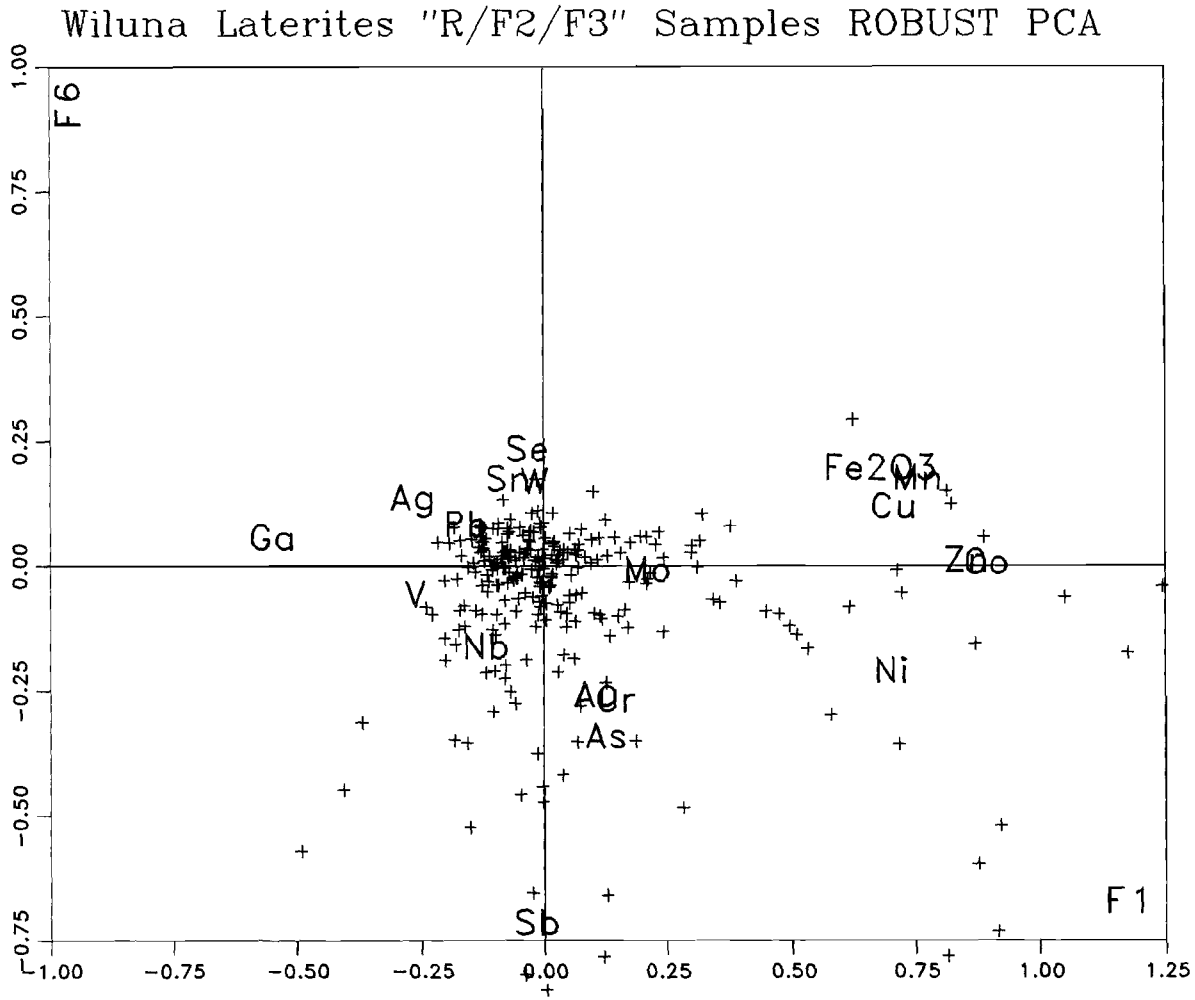
Wiluna Laterites "R/F2/F3" Samples ROBUST PCA
F6
F1
Se
Sn
W
Ag
Pb
Ga
Mo
V
Nb
Cr
As
Sb
Fe2O3
Mn
Cu
Zn
Co
Ni
1.00
0.75
0.50
0.25
0.00
-0.25
-0.50
-0.75
-1.00
1.25

Figure 50c

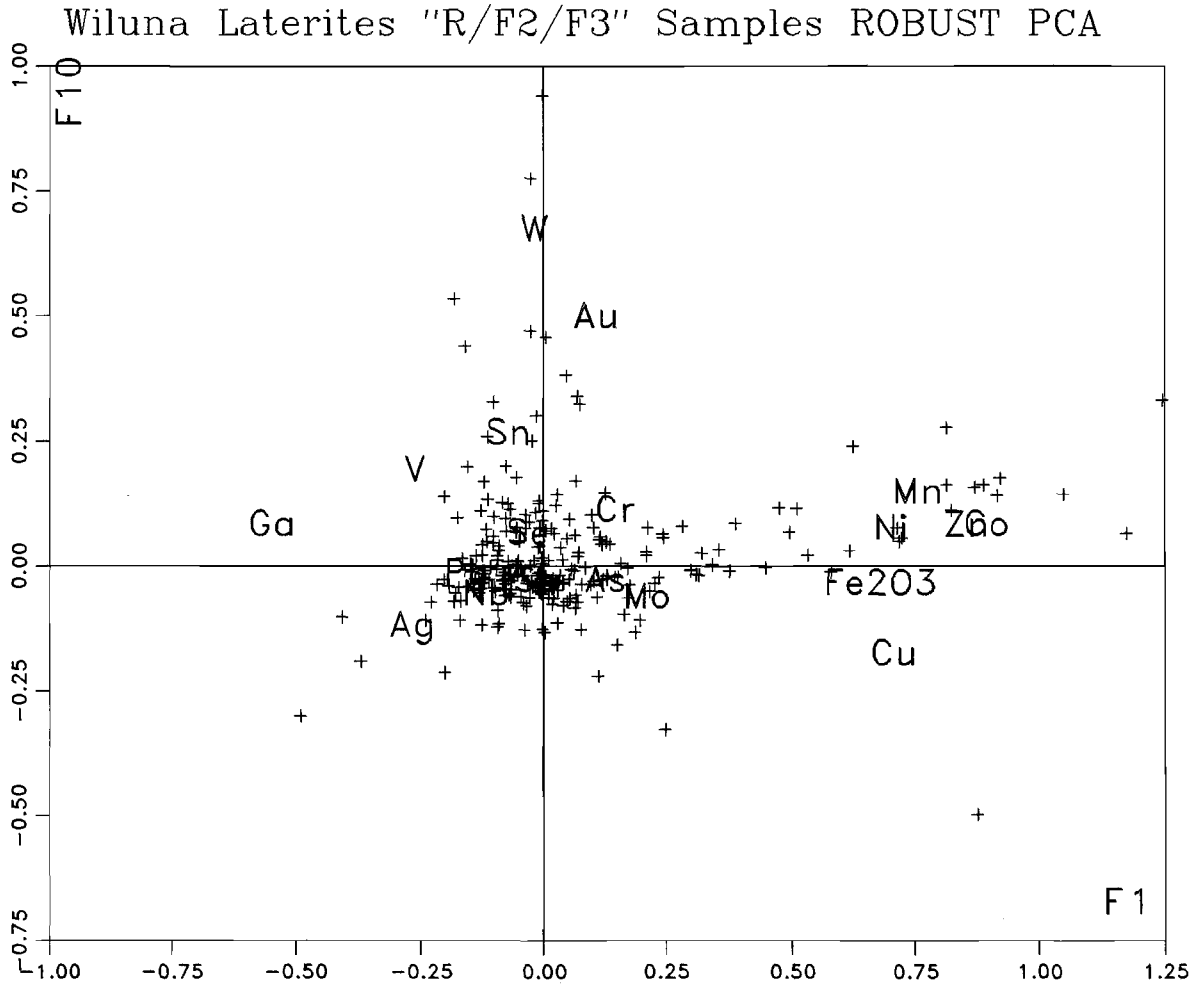
Wiluna Laterites "R/F2/F3" Samples ROBUST PCA
F10
F1
W
Au
Sn
V
Ga
Cr
Mn
Ni
Zn
Co
Mo
Fe203
Ag
Cu
1.00
0.75
0.50
0.25
0.00
-0.25
-0.50
-0.75
-1.00
-0.75
-0.50
-0.25
0.00
0.25
0.50
0.75
1.00
1.25

Figure 50d

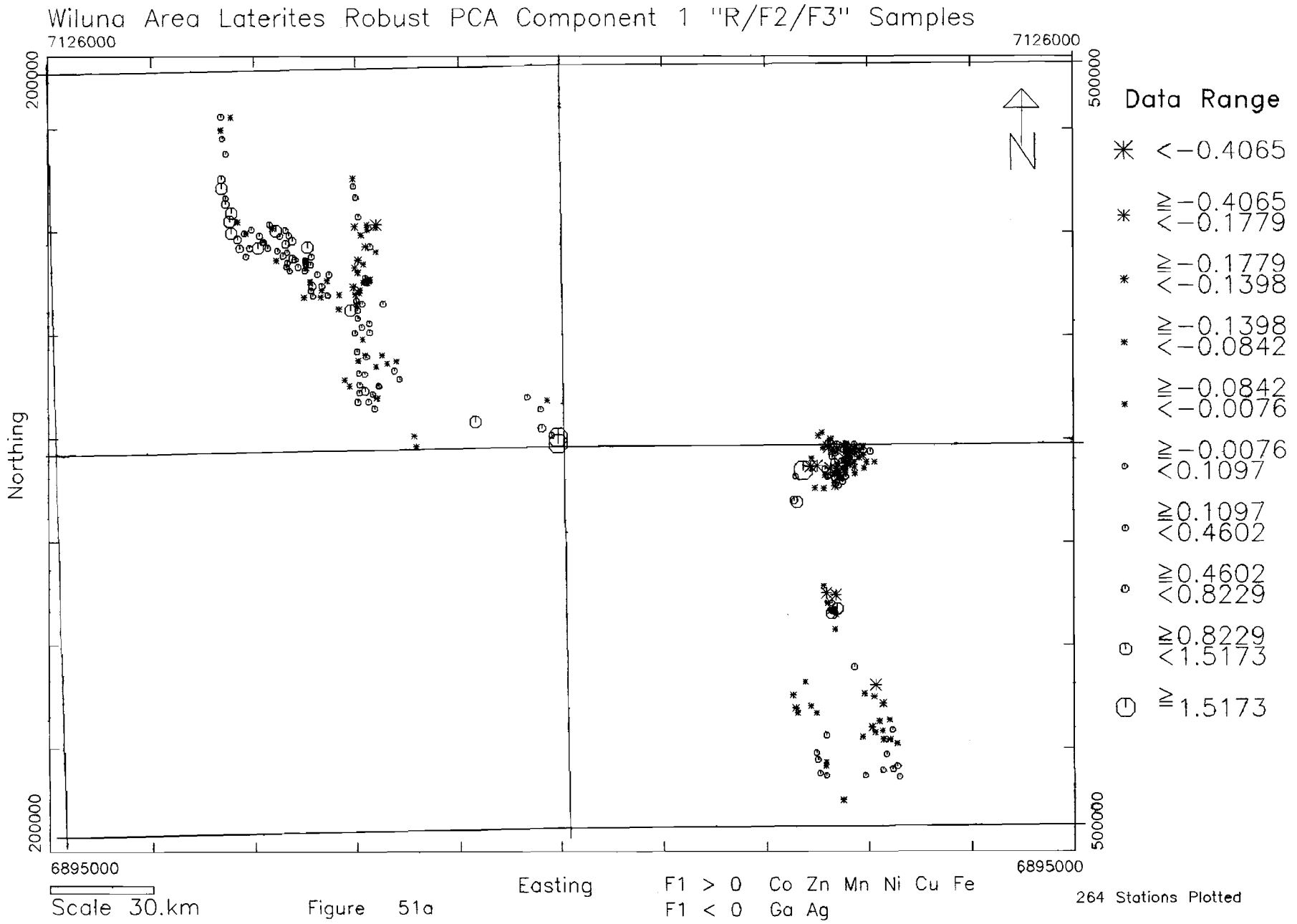
Wiluna Area Laterites Robust PCA Component 1 "R/F2/F3" Samples
7126000
7126000
200000
500000
Northing
Data Range
< −0.4065
≥ −0.4065 < −0.1779
≥ −0.1779 < −0.1398
≥ −0.1398 < −0.0842
≥ −0.0842 < −0.0076
≥ −0.0076 < 0.1097
≥ 0.1097 < 0.4602
≥ 0.4602 < 0.8229
≥ 0.8229 < 1.5173
≥ 1.5173
200000
500000
6895000
6895000
Easting
Scale 30.km
F1 > 0 Co Zn Mn Ni Cu Fe
F1 < 0 Ga Ag
264 Stations Plotted

Figure 51a

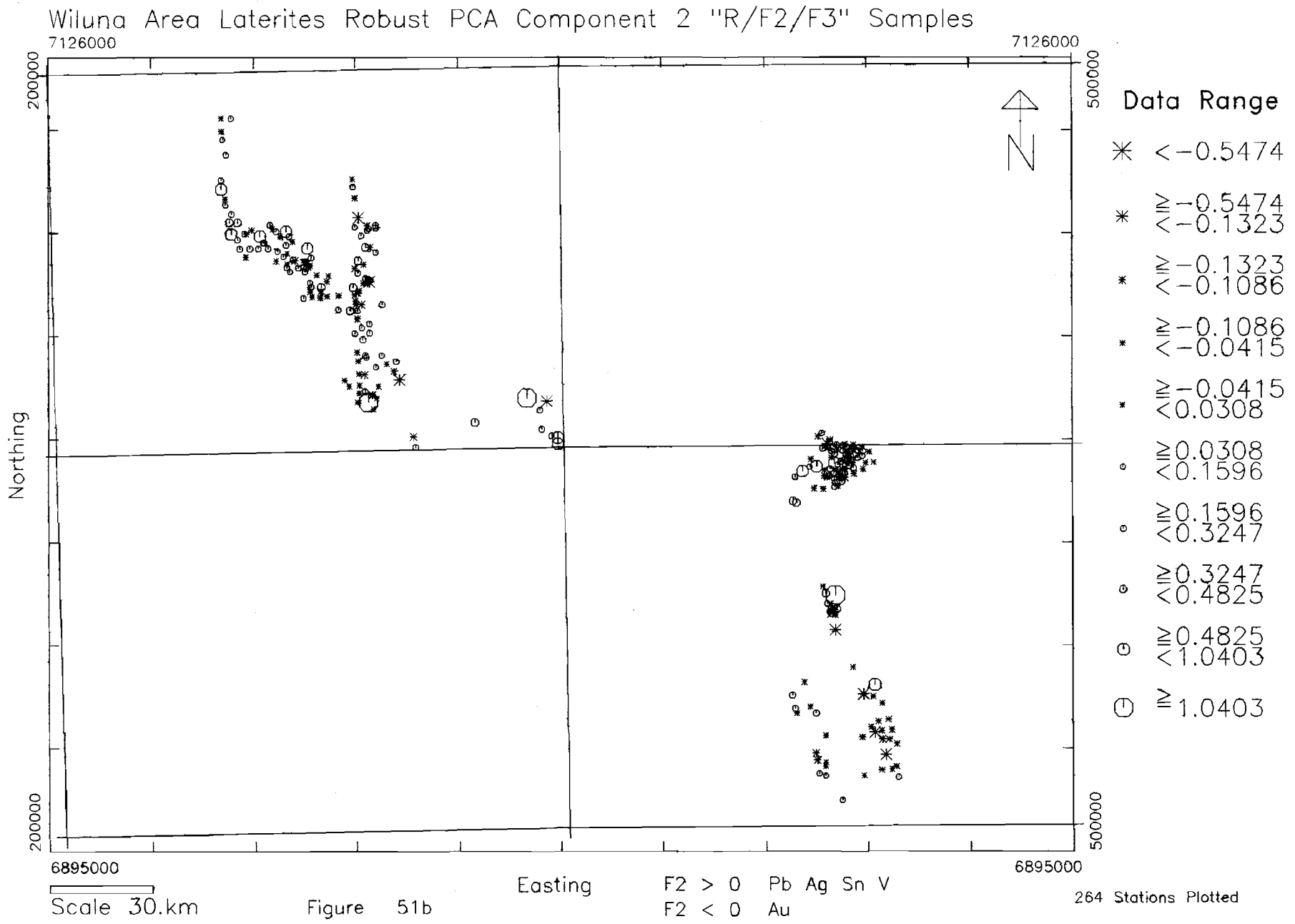
Wiluna Area Laterites Robust PCA Component 2 "R/F2/F3" Samples
7126000
7126000
200000
500000
Northing
N
Data Range
< −0.5474
≧ −0.5474 < −0.1323
≧ −0.1323 < −0.1086
≧ −0.1086 < −0.0415
≧ −0.0415 < 0.0308
≧ 0.0308 < 0.1596
≧ 0.1596 < 0.3247
≧ 0.3247 < 0.4825
≧ 0.4825 < 1.0403
≧ 1.0403
200000
500000
6895000
6895000
Easting
Scale 30.km
F2 > 0 Pb Ag Sn V
F2 < 0 Au
264 Stations Plotted

Figure 51b

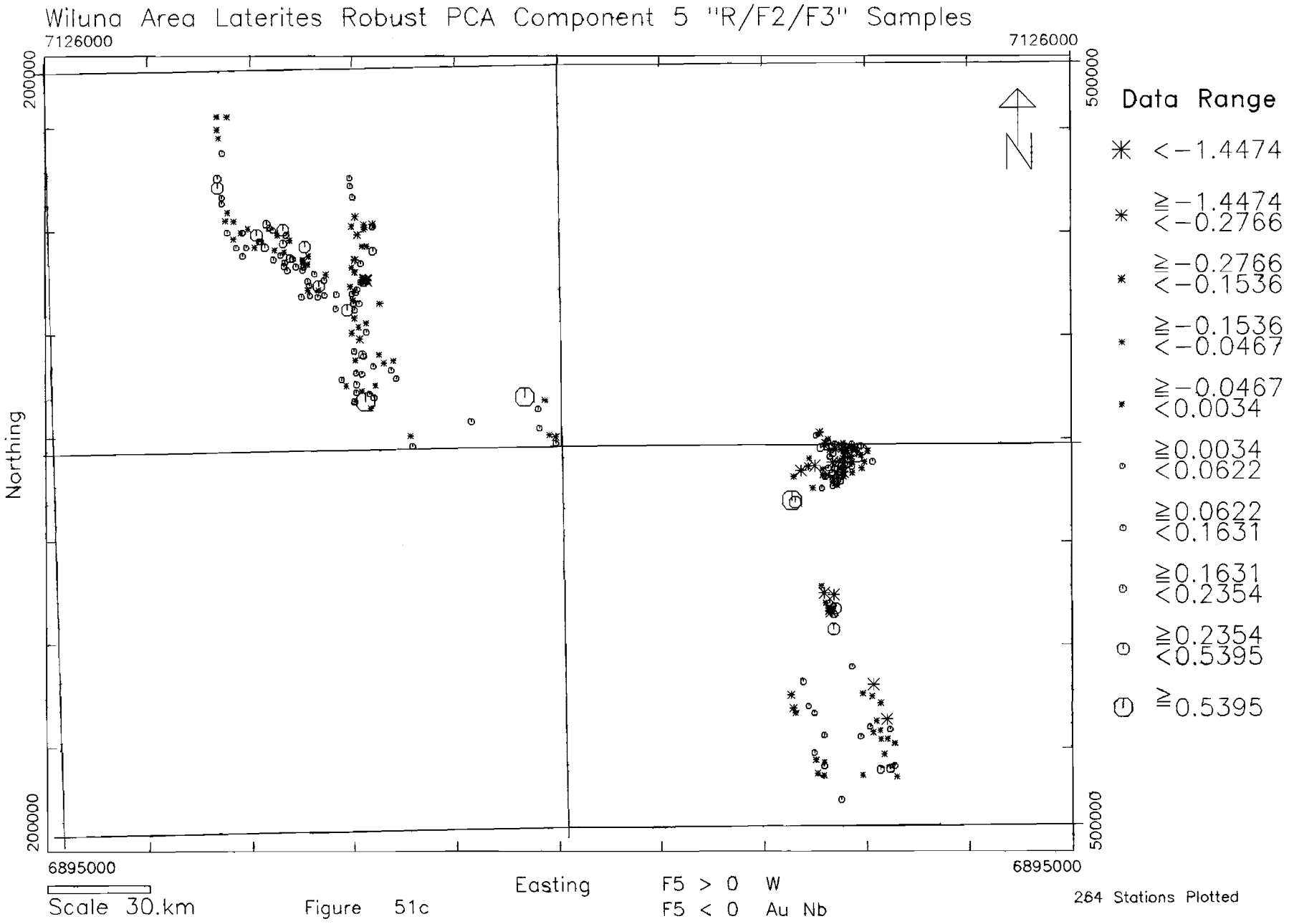
Wiluna Area Laterites Robust PCA Component 5 "R/F2/F3" Samples
7126000
7126000
200000
500000
Northing
Data Range
< −1.4474
≧ −1.4474 < −0.2766
≧ −0.2766 < −0.1536
≧ −0.1536 < −0.0467
≧ −0.0467 < 0.0034
≧ 0.0034 < 0.0622
≧ 0.0622 < 0.1631
≧ 0.1631 < 0.2354
≧ 0.2354 < 0.5395
≧ 0.5395
200000
500000
6895000
6895000
Easting
Scale 30.km
F5 > 0 W
F5 < 0 Au Nb
264 Stations Plotted

Figure 51c

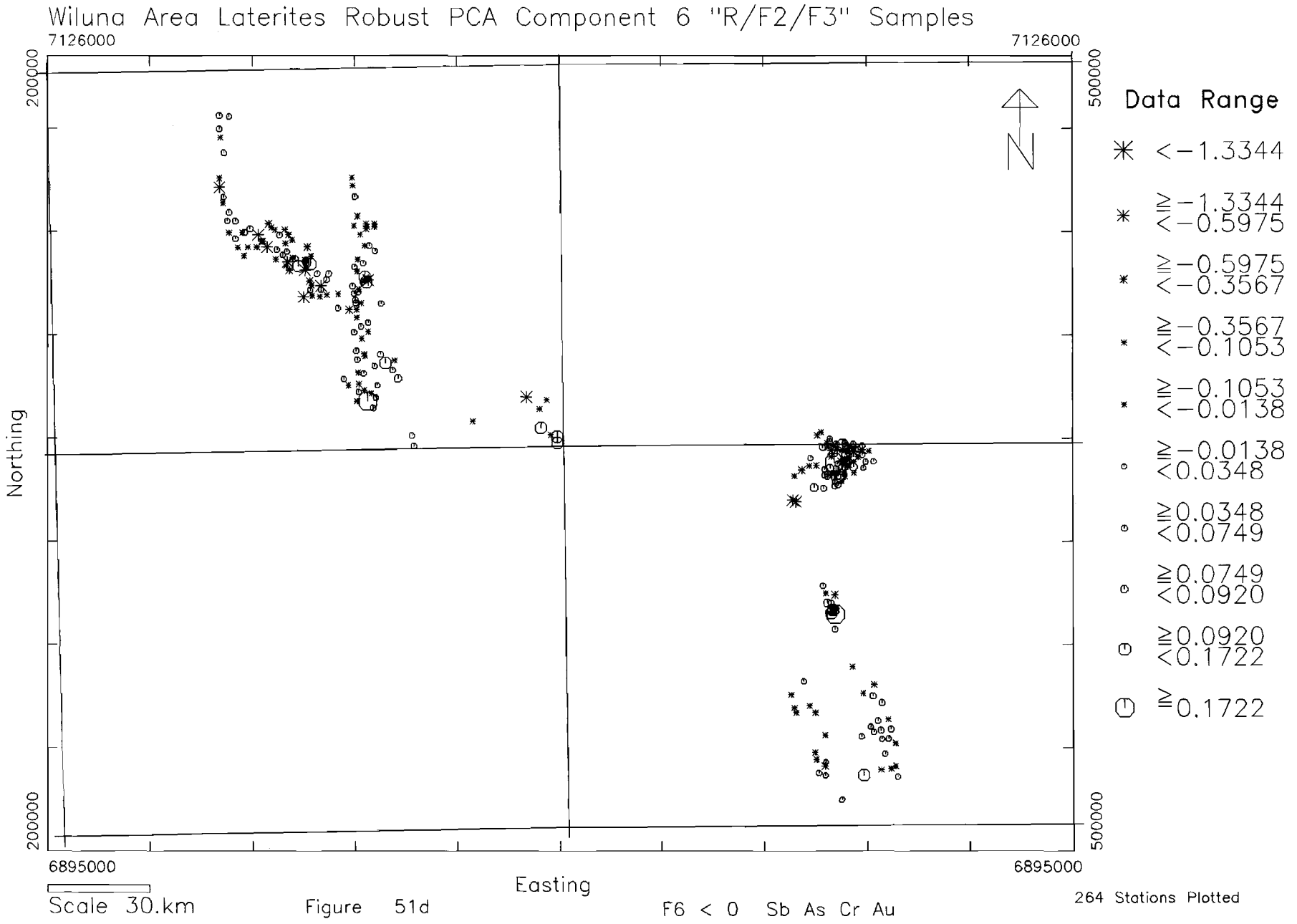
Wiluna Area Laterites Robust PCA Component 6 "R/F2/F3" Samples
7126000
7126000
200000
500000
Northing
N
Data Range
< −1.3344
≥ −1.3344 < −0.5975
≥ −0.5975 < −0.3567
≥ −0.3567 < −0.1053
≥ −0.1053 < −0.0138
≥ −0.0138 < 0.0348
≥ 0.0348 < 0.0749
≥ 0.0749 < 0.0920
≥ 0.0920 < 0.1722
≥ 0.1722
200000
500000
6895000
6895000
Easting
Scale 30.km
Figure 51d
F6 < 0 Sb As Cr Au
264 Stations Plotted

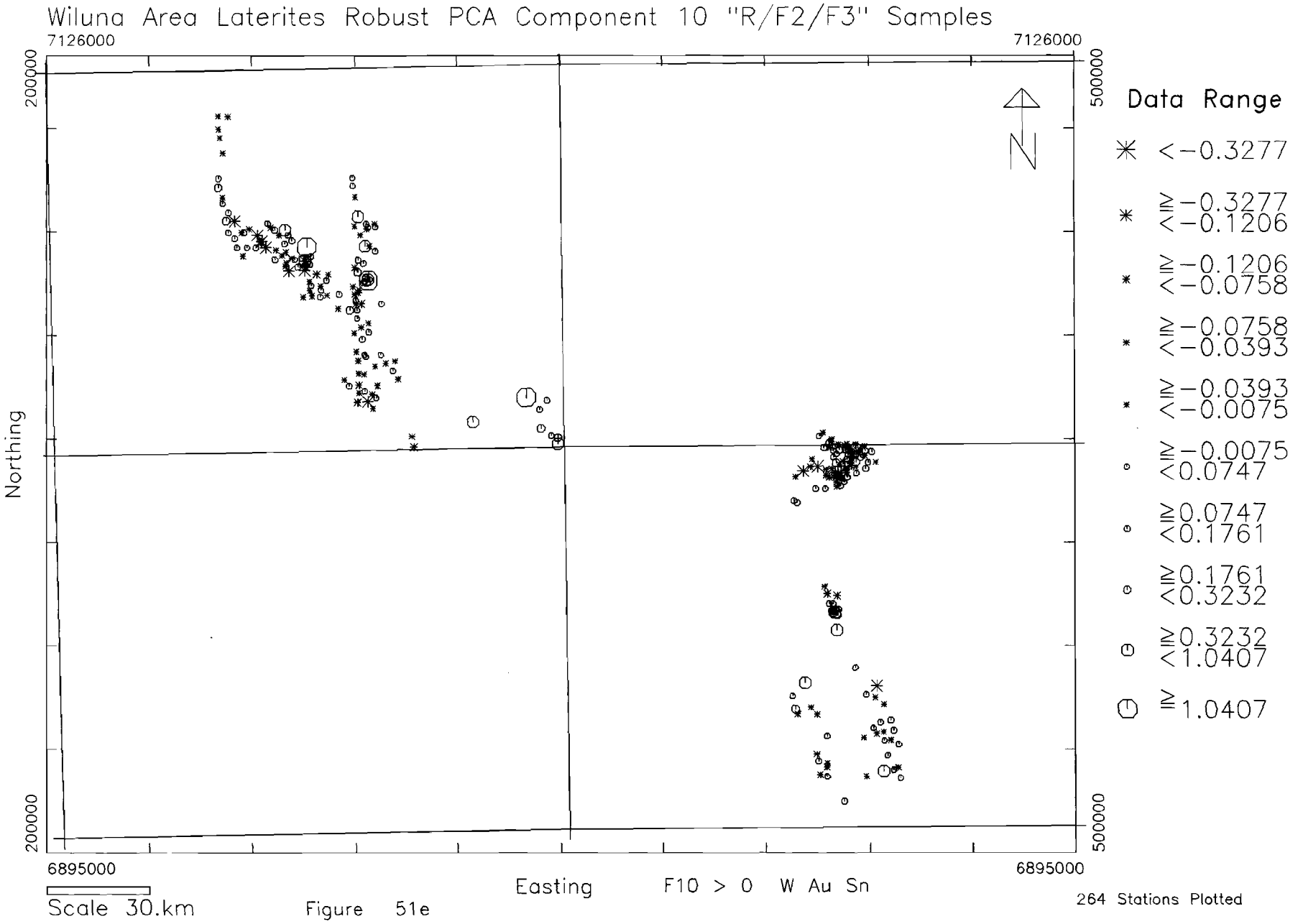
Wiluna Area Laterites Robust PCA Component 10 "R/F2/F3" Samples
7126000
7126000
200000
500000
Northing
Data Range
< −0.3277
≥ −0.3277 < −0.1206
≥ −0.1206 < −0.0758
≥ −0.0758 < −0.0393
≥ −0.0393 < −0.0075
≥ −0.0075 < 0.0747
≥ 0.0747 < 0.1761
≥ 0.1761 < 0.3232
≥ 0.3232 < 1.0407
≥ 1.0407
N
200000
500000
6895000
6895000
Easting
F10 > 0 W Au Sn
Scale 30.km
264 Stations Plotted

Figure 51e

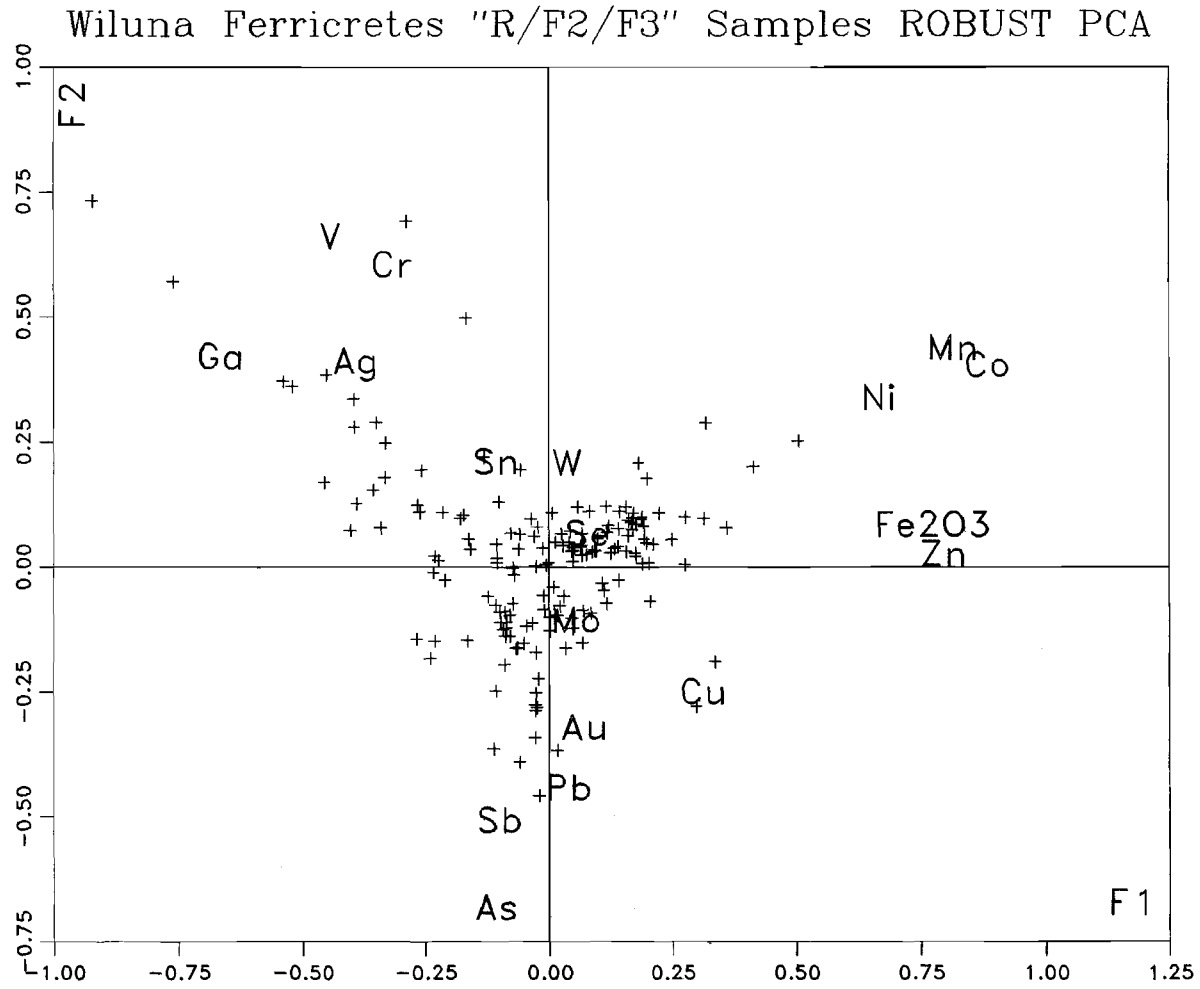
Wiluna Ferricretes "R/F2/F3" Samples ROBUST PCA
F2
F1
V
Cr
Ga
Ag
Mn
Co
Ni
Sn
W
Se
Fe2O3
Zn
Mo
Cu
Au
Pb
Sb
As
1.00
0.75
0.50
0.25
0.00
-0.25
-0.50
-0.75
-1.00
-0.75
-0.50
-0.25
0.00
0.25
0.50
0.75
1.00
1.25

Figure 52a

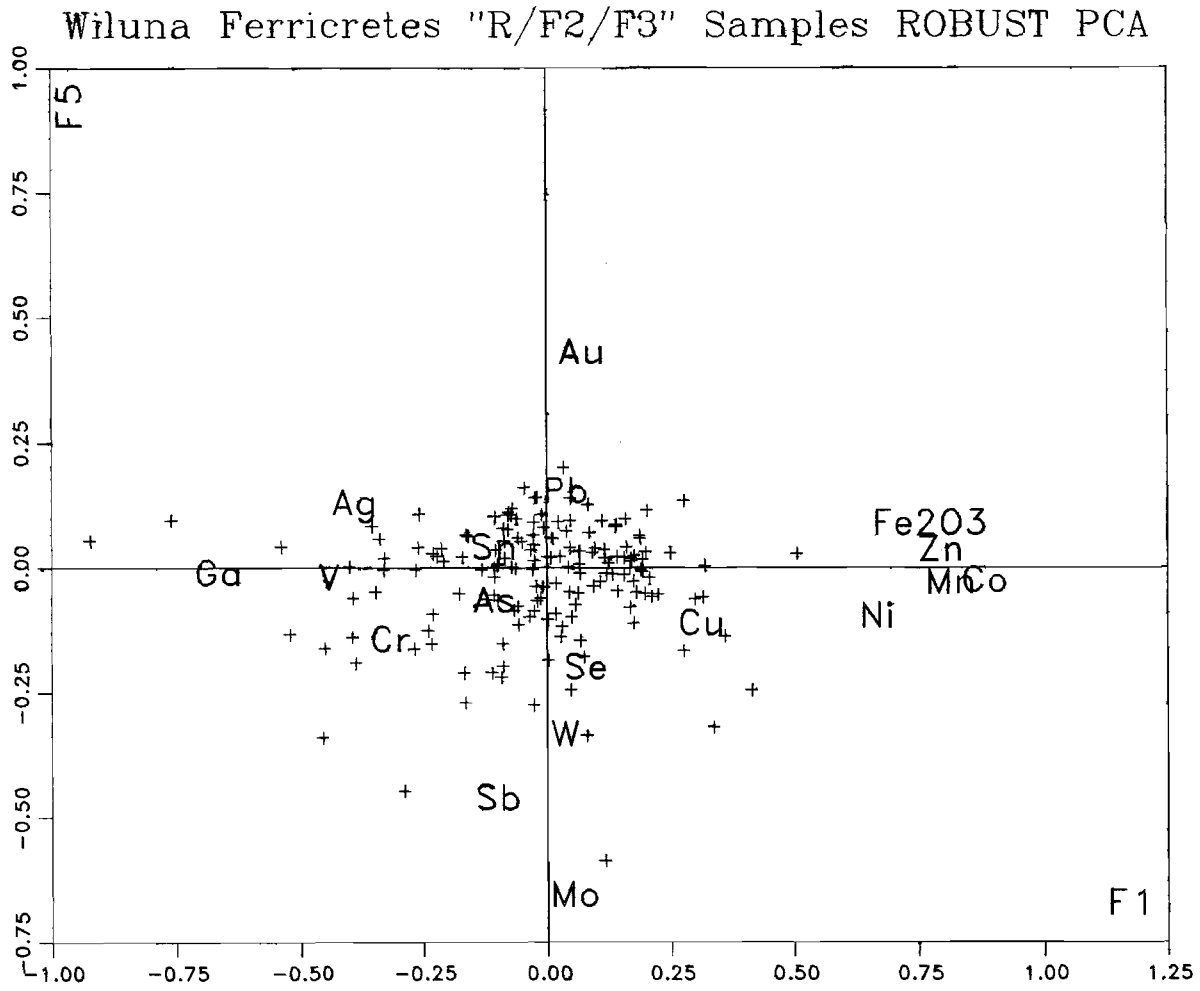
Wiluna Ferricretes "R/F2/F3" Samples ROBUST PCA
F5
F1
Au
Pb
Ag
Sn
Ga
V
As
Cr
Se
W
Sb
Mo
Fe2O3
Zn
Mn
Co
Ni
Cu
1.00
0.75
0.50
0.25
0.00
-0.25
-0.50
-0.75
-1.00
-0.75
-0.50
-0.25
0.00
0.25
0.50
0.75
1.00
1.25

Figure 52b

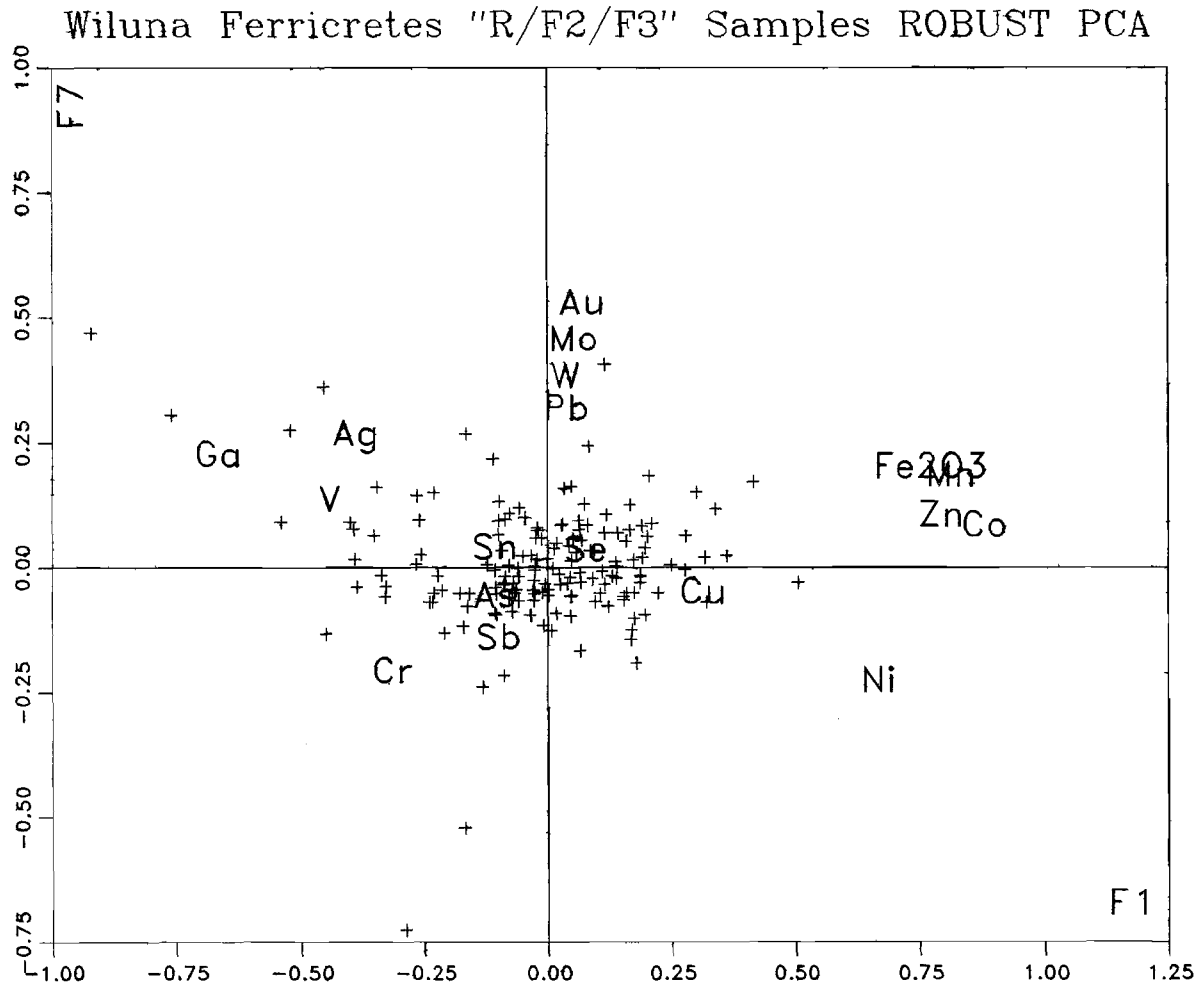
Wiluna Ferricretes "R/F2/F3" Samples ROBUST PCA
F7
F1
Au
Mo
W
Pb
Ag
Ga
V
Fe2O3
Mn
Zn
Co
Sn
Se
Cu
As
Sb
Cr
Ni
1.00
0.75
0.50
0.25
0.00
-0.25
-0.50
-0.75
-1.00
-0.75
-0.50
-0.25
0.00
0.25
0.50
0.75
1.00
1.25

Figure 52c

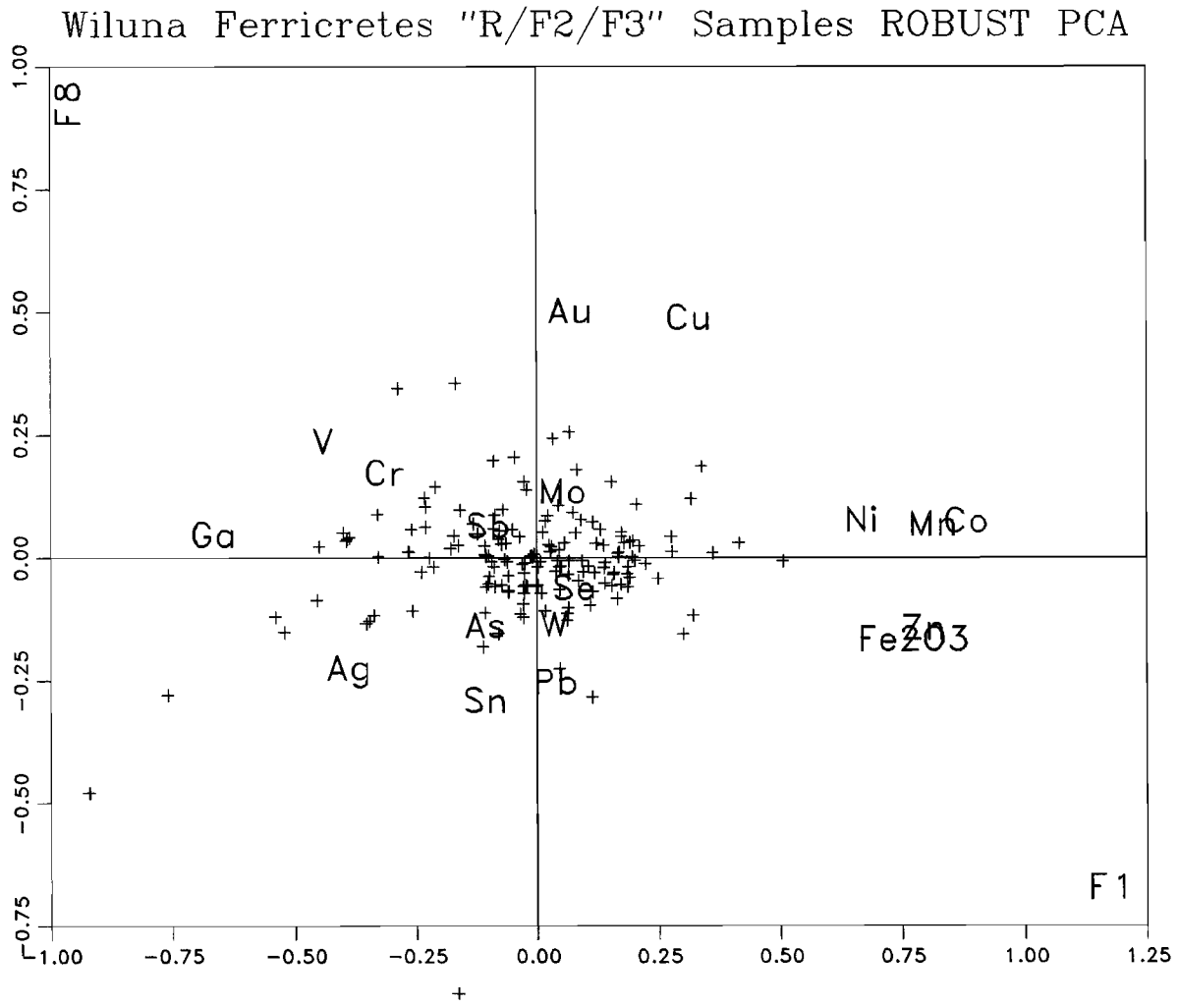
Wiluna Ferricretes "R/F2/F3" Samples ROBUST PCA
F8
F1
Au
Cu
V
Cr
Mo
Ga
Sb
Ni
Mn
Co
Se
As
W
Zn
Fe2O3
Ag
Pb
Sn
1.00
0.75
0.50
0.25
0.00
-0.25
-0.50
-0.75
-1.00
1.25

Figure 52d

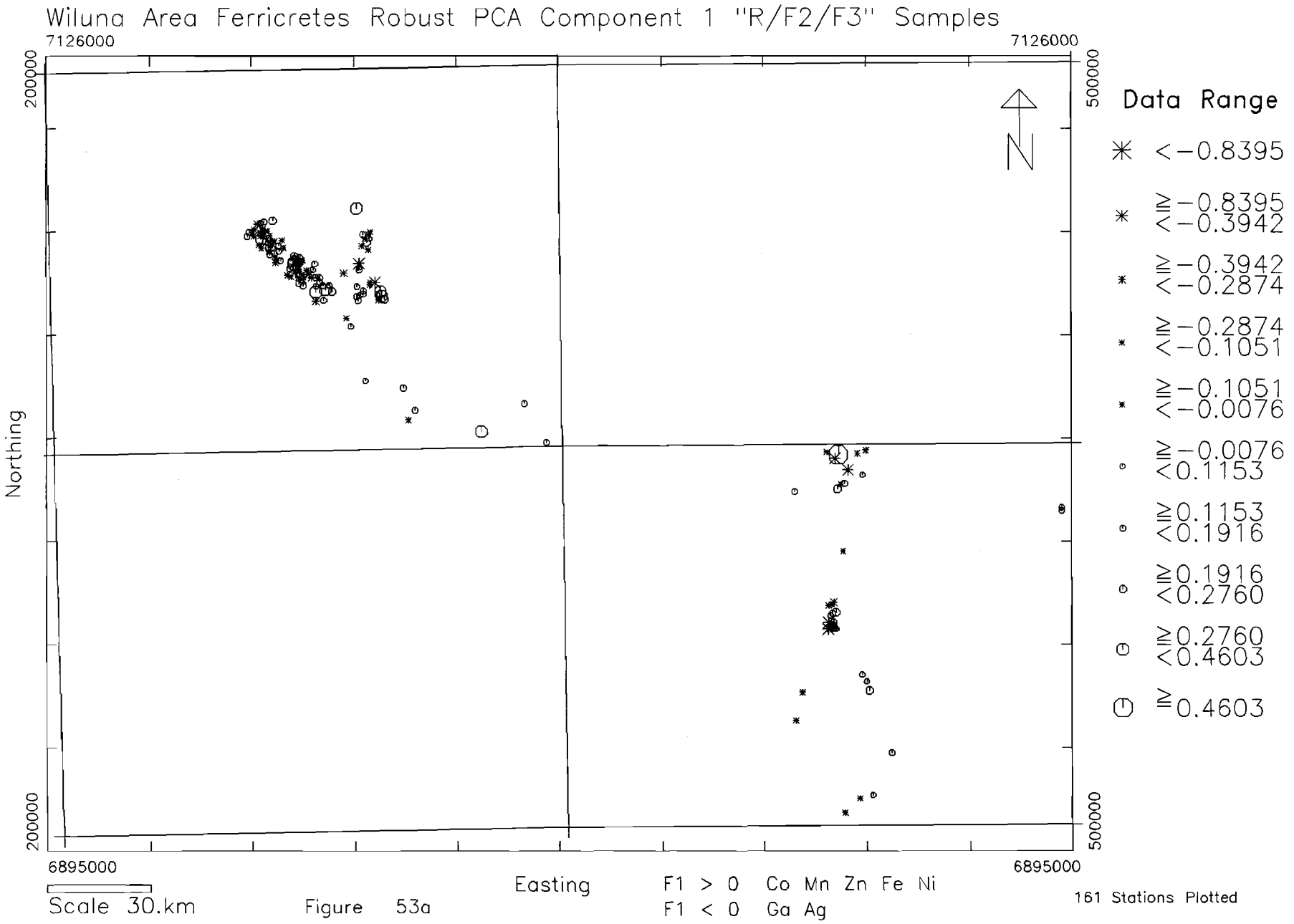
Wiluna Area Ferricretes Robust PCA Component 1 "R/F2/F3" Samples
7126000
7126000
200000
500000
Northing
N
Data Range
< −0.8395
≥ −0.8395 < −0.3942
≥ −0.3942 < −0.2874
≥ −0.2874 < −0.1051
≥ −0.1051 < −0.0076
≥ −0.0076 < 0.1153
≥ 0.1153 < 0.1916
≥ 0.1916 < 0.2760
≥ 0.2760 < 0.4603
≥ 0.4603
200000
500000
6895000
6895000
Easting
Scale 30.km
F1 > 0 Co Mn Zn Fe Ni
F1 < 0 Ga Ag
161 Stations Plotted

Figure 53a

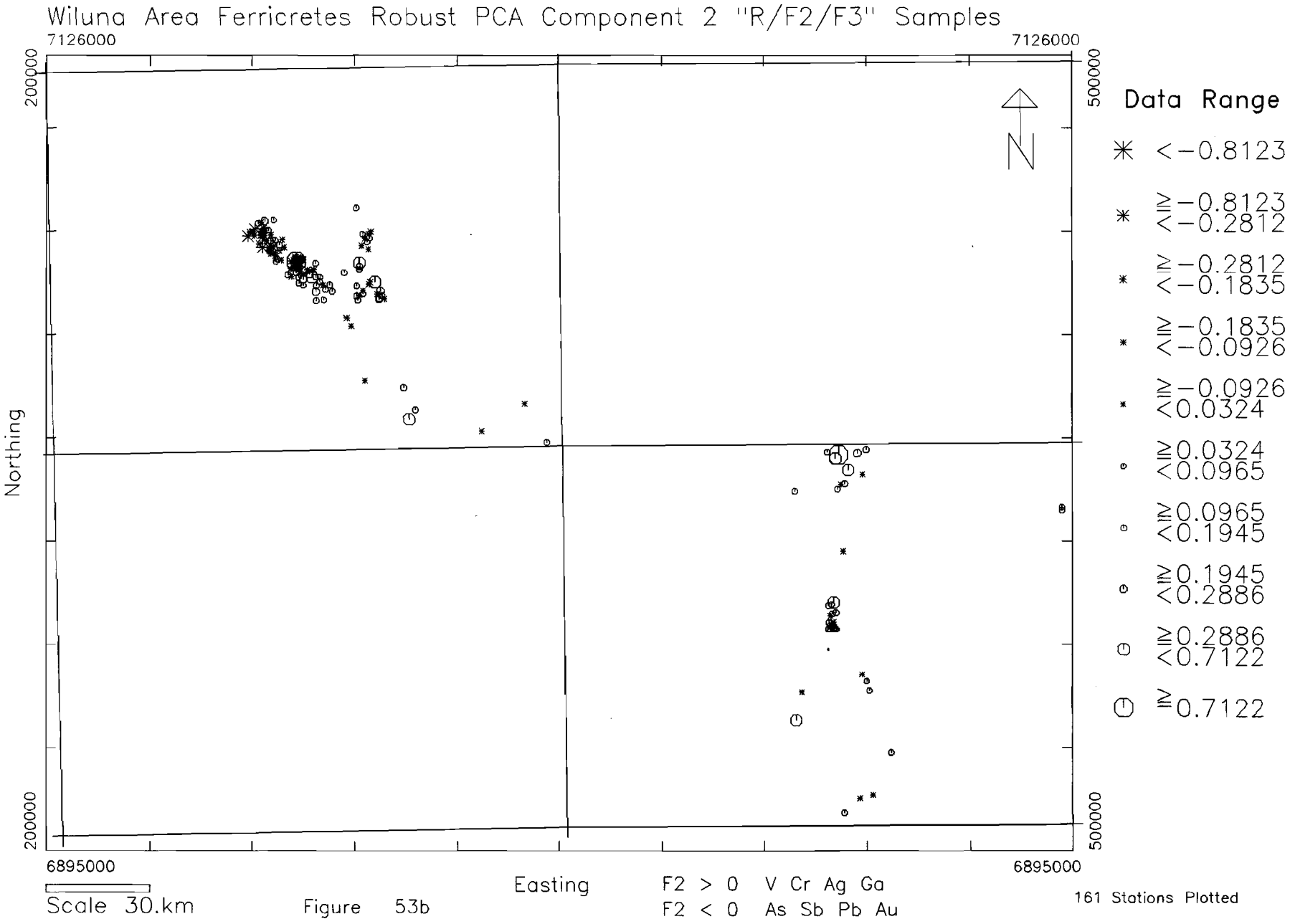
Wiluna Area Ferricretes Robust PCA Component 2 "R/F2/F3" Samples
7126000
7126000
200000
500000
Northing
N
Data Range
< −0.8123
≥ −0.8123 < −0.2812
≥ −0.2812 < −0.1835
≥ −0.1835 < −0.0926
≥ −0.0926 < 0.0324
≥ 0.0324 < 0.0965
≥ 0.0965 < 0.1945
≥ 0.1945 < 0.2886
≥ 0.2886 < 0.7122
≥ 0.7122
200000
500000
6895000
6895000
Easting
Scale 30.km
F2 > 0 V Cr Ag Ga
F2 < 0 As Sb Pb Au
161 Stations Plotted

Figure 53b

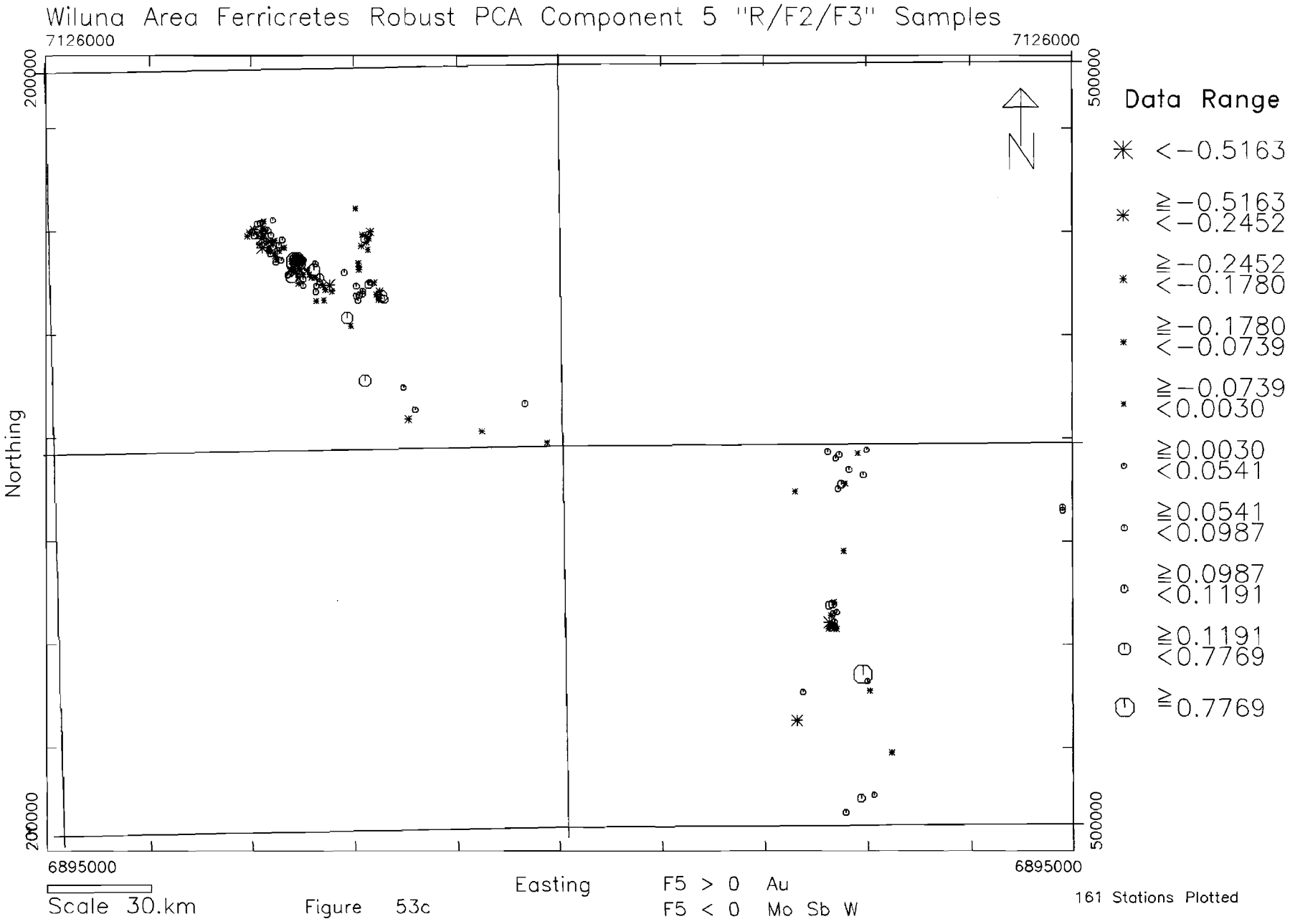
Wiluna Area Ferricretes Robust PCA Component 5 "R/F2/F3" Samples
7126000
7126000
200000
500000
Northing
N
Data Range
* <-0.5163
* ≥-0.5163 <-0.2452
* ≥-0.2452 <-0.1780
* ≥-0.1780 <-0.0739
* ≥-0.0739 <0.0030
• ≥0.0030 <0.0541
• ≥0.0541 <0.0987
• ≥0.0987 <0.1191
⊙ ≥0.1191 <0.7769
⊙ ≥0.7769
200000
500000
6895000
6895000
Easting
Scale 30.km
F5 > 0 Au
F5 < 0 Mo Sb W
161 Stations Plotted

Figure 53c

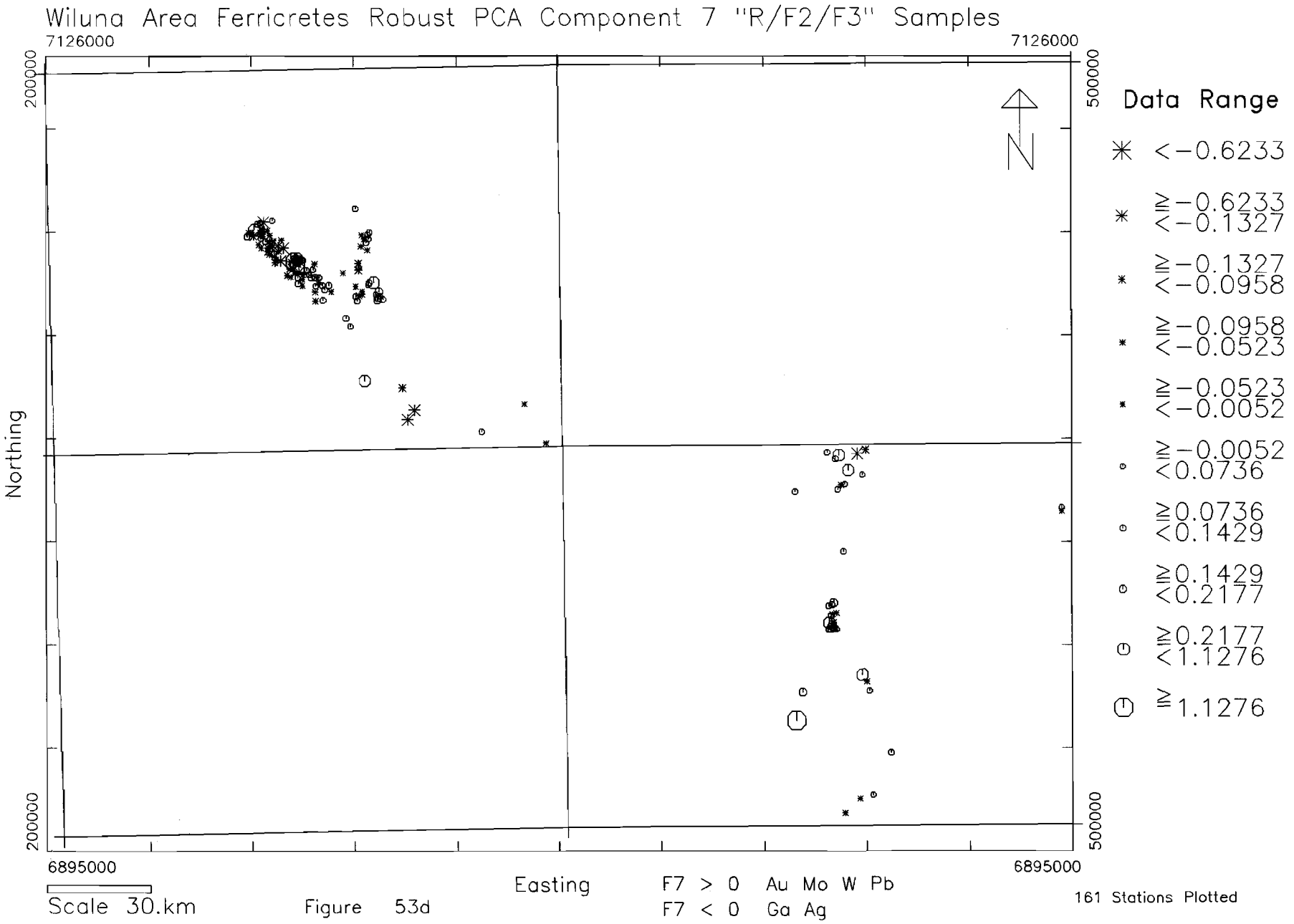
Wiluna Area Ferricretes Robust PCA Component 7 "R/F2/F3" Samples
7126000
7126000
200000
500000
Northing
N
Data Range
< −0.6233
≥ −0.6233 < −0.1327
≥ −0.1327 < −0.0958
≥ −0.0958 < −0.0523
≥ −0.0523 < −0.0052
≥ −0.0052 < 0.0736
≥ 0.0736 < 0.1429
≥ 0.1429 < 0.2177
≥ 0.2177 < 1.1276
≥ 1.1276
200000
500000
6895000
6895000
Easting
Scale 30.km
F7 > 0 Au Mo W Pb
F7 < 0 Ga Ag
161 Stations Plotted

Figure 53d

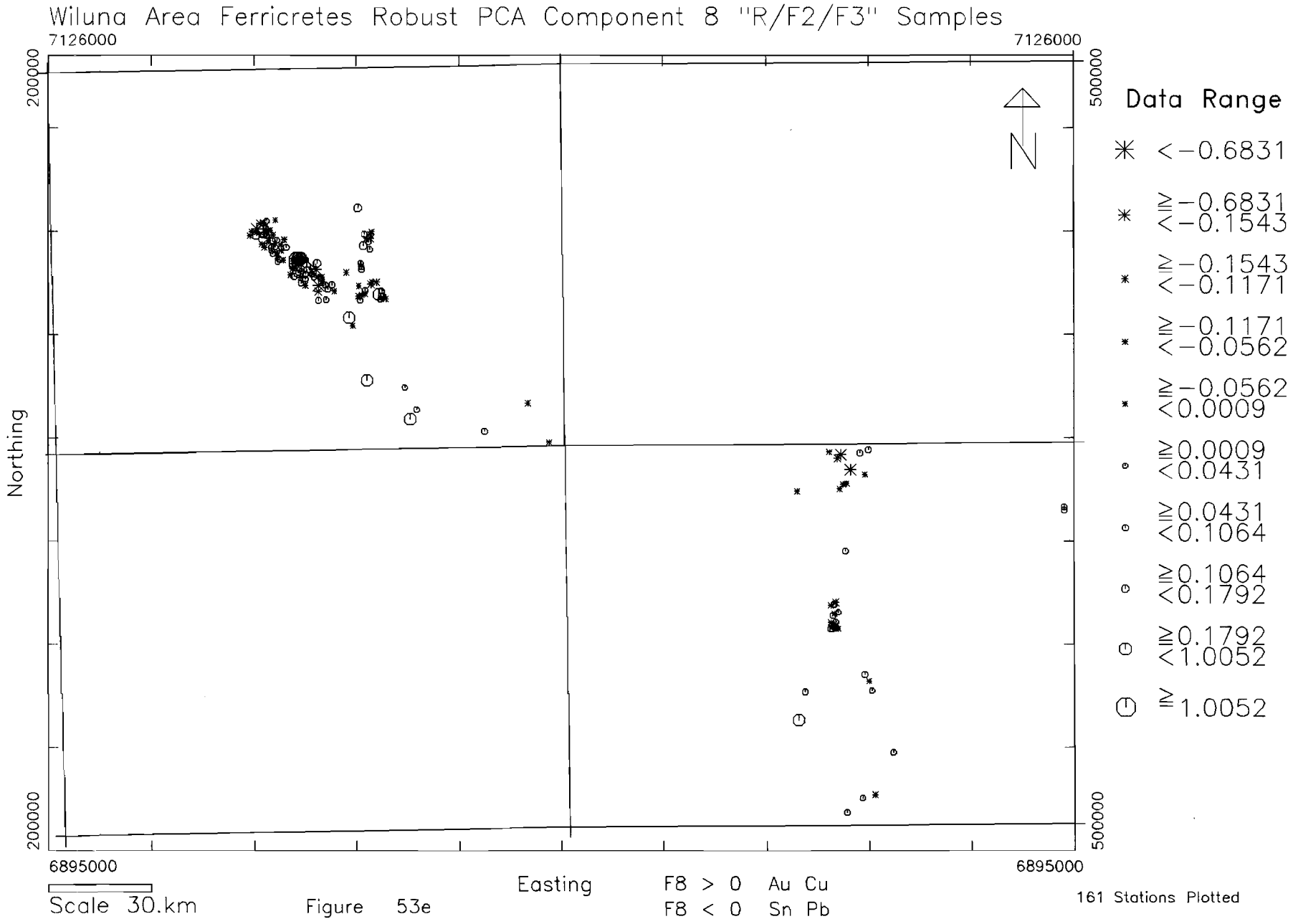
Wiluna Area Ferricretes Robust PCA Component 8 "R/F2/F3" Samples
7126000
7126000
200000
500000
Northing
200000
500000
6895000
6895000
Easting
N
Data Range
< −0.6831
≧ −0.6831 < −0.1543
≧ −0.1543 < −0.1171
≧ −0.1171 < −0.0562
≧ −0.0562 < 0.0009
≧ 0.0009 < 0.0431
≧ 0.0431 < 0.1064
≧ 0.1064 < 0.1792
≧ 0.1792 < 1.0052
≧ 1.0052
Scale 30.km
F8 > 0 Au Cu
F8 < 0 Sn Pb
161 Stations Plotted

Figure 53e

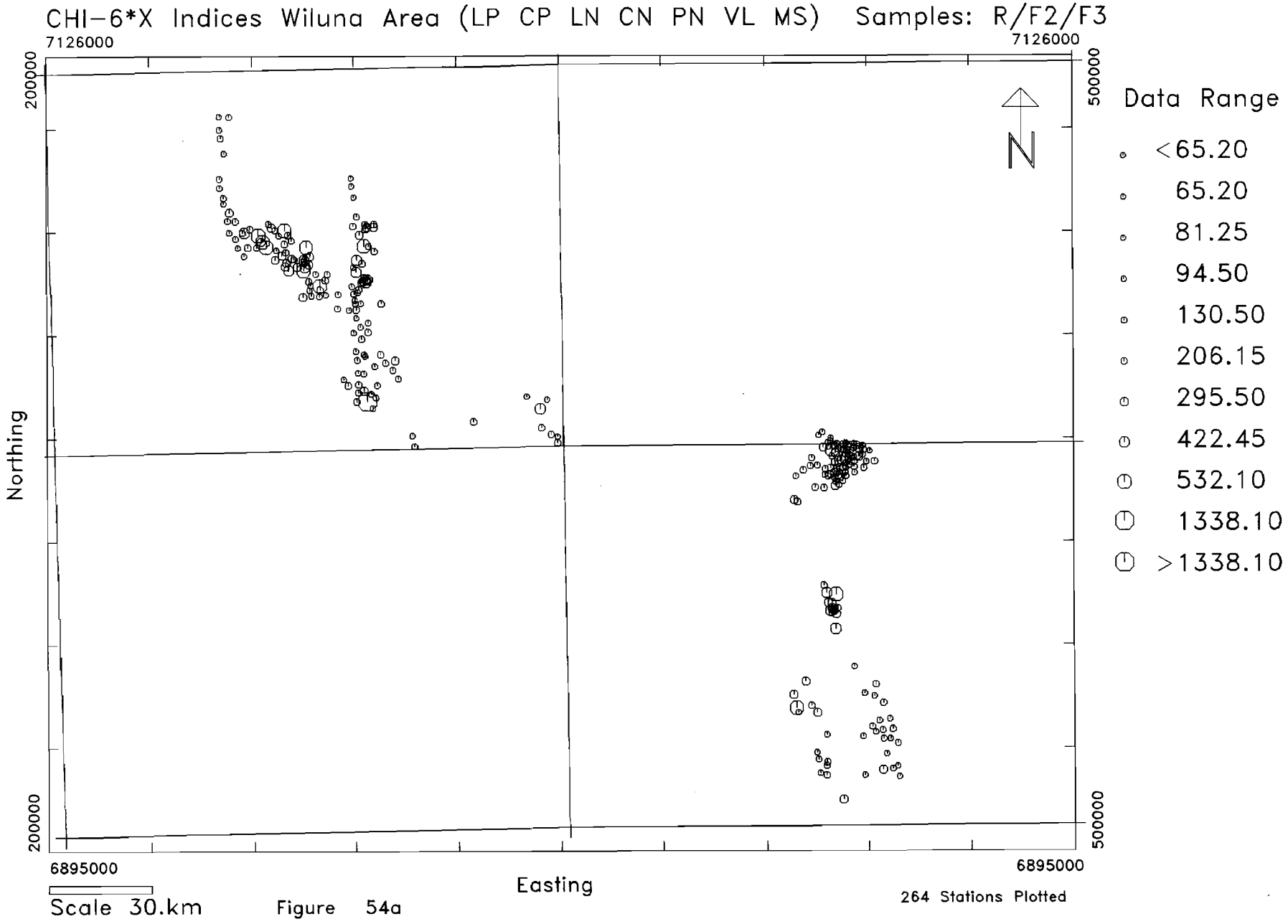
CHI−6*X Indices Wiluna Area (LP CP LN CN PN VL MS) Samples: R/F2/F3
7126000
7126000
200000
500000
Northing
N
Data Range
<65.20
65.20
81.25
94.50
130.50
206.15
295.50
422.45
532.10
1338.10
>1338.10
200000
500000
6895000
6895000
Easting
Scale 30.km
264 Stations Plotted

Figure 54a

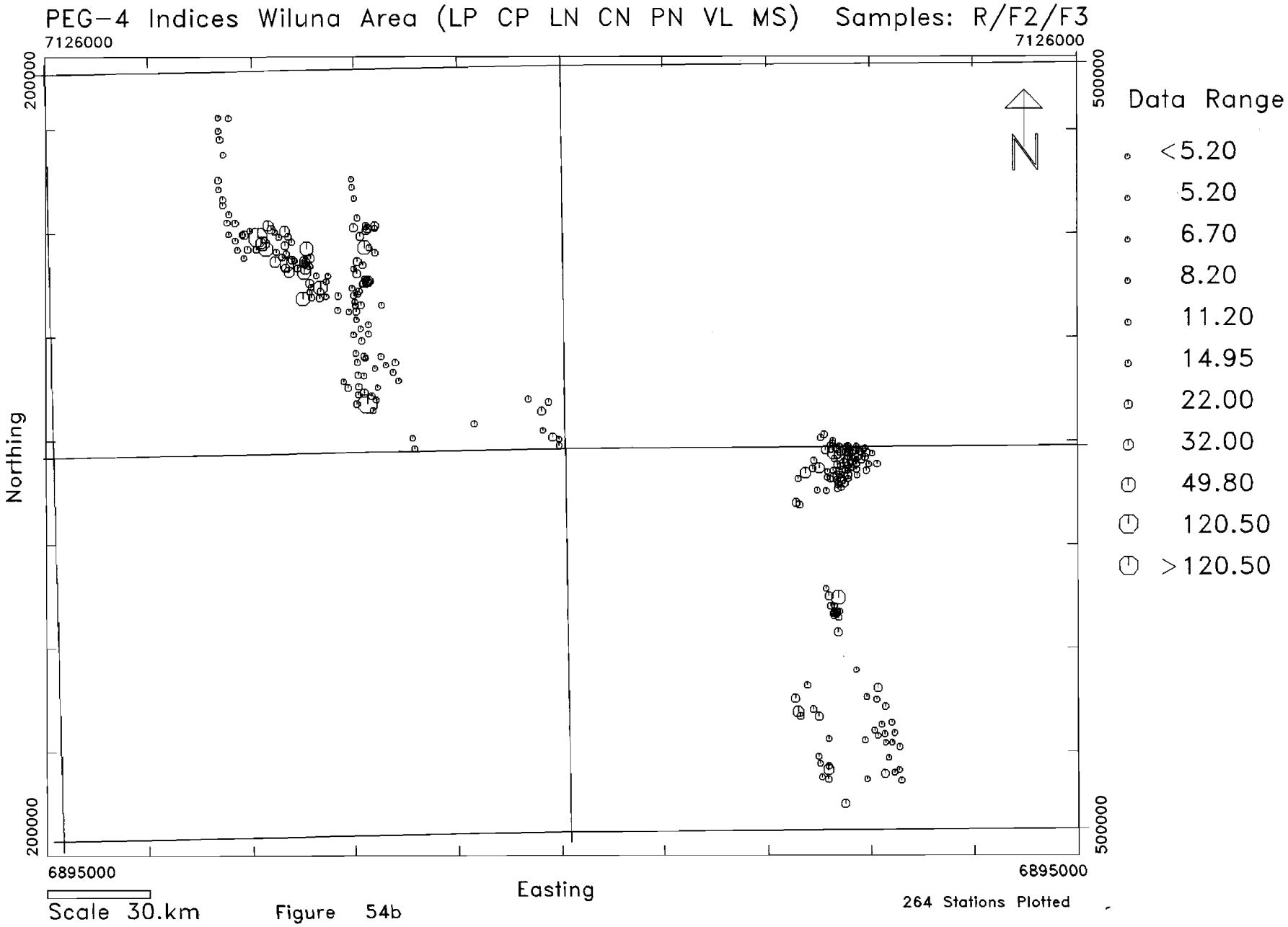
PEG−4 Indices Wiluna Area (LP CP LN CN PN VL MS) Samples: R/F2/F3
7126000
7126000
200000
500000
Northing
N
Data Range
<5.20
5.20
6.70
8.20
11.20
14.95
22.00
32.00
49.80
120.50
>120.50
200000
500000
6895000
6895000
Easting
Scale 30.km
264 Stations Plotted

Figure 54b

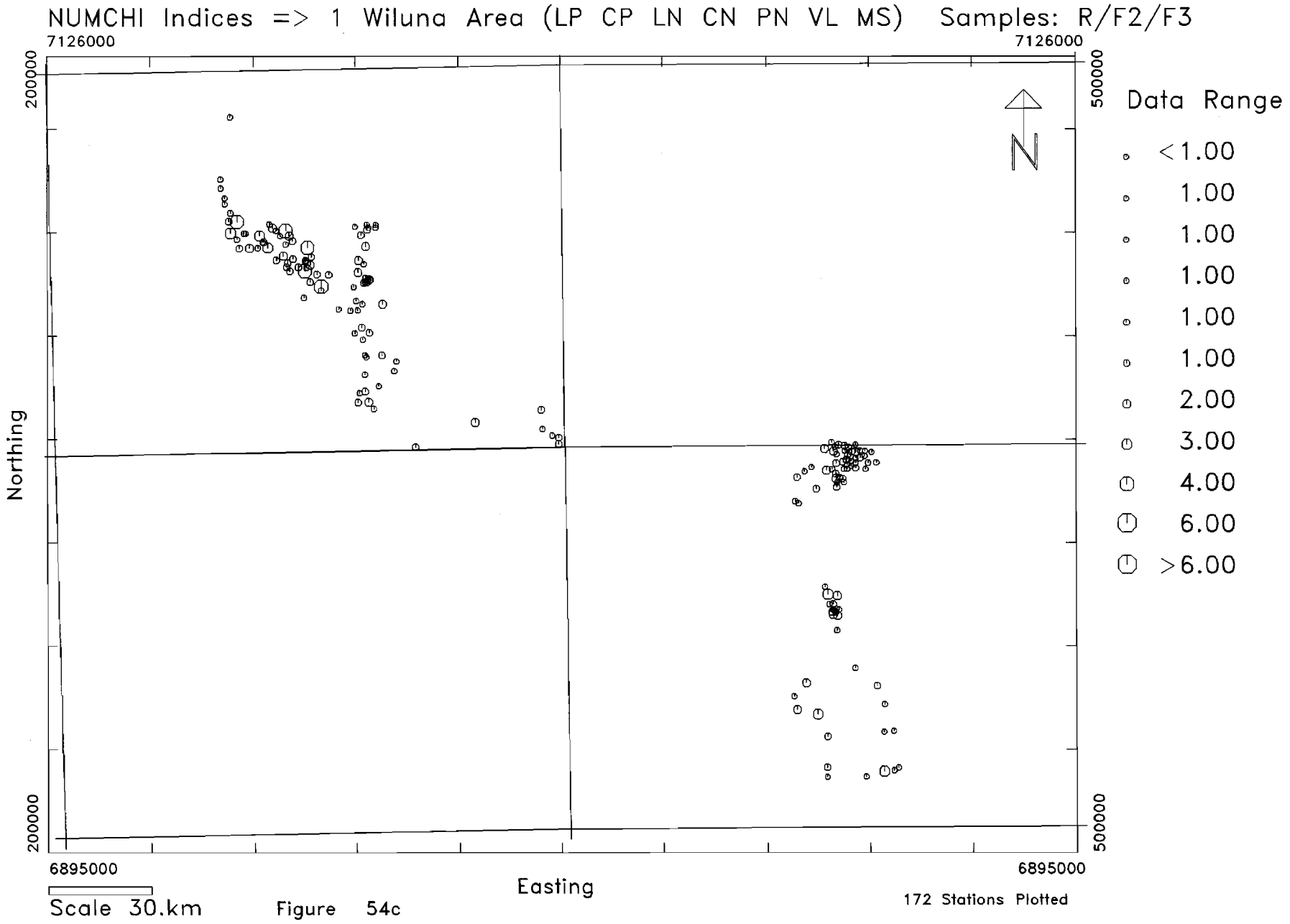
NUMCHI Indices => 1 Wiluna Area (LP CP LN CN PN VL MS) Samples: R/F2/F3
7126000
7126000
200000
500000
Northing
N
Data Range
<1.00
1.00
1.00
1.00
1.00
1.00
2.00
3.00
4.00
6.00
>6.00
200000
500000
6895000
6895000
Easting
Scale 30.km
172 Stations Plotted

Figure 54c

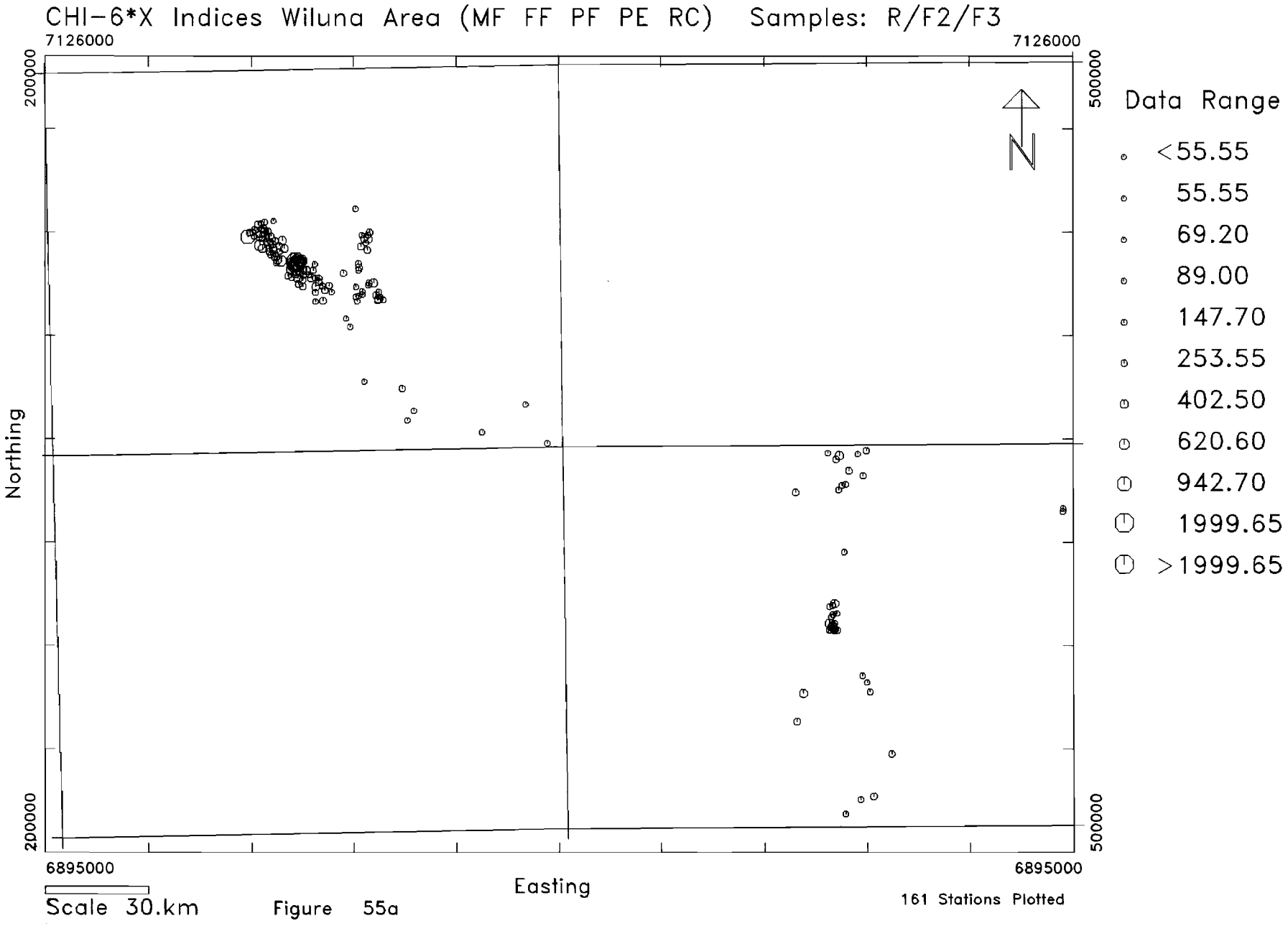
CHI-6*X Indices Wiluna Area (MF FF PF PE RC) Samples: R/F2/F3
7126000
7126000
200000
500000
Northing
Data Range
<55.55
55.55
69.20
89.00
147.70
253.55
402.50
620.60
942.70
1999.65
>1999.65
200000
500000
6895000
6895000
Easting
Scale 30.km
161 Stations Plotted

Figure 55a

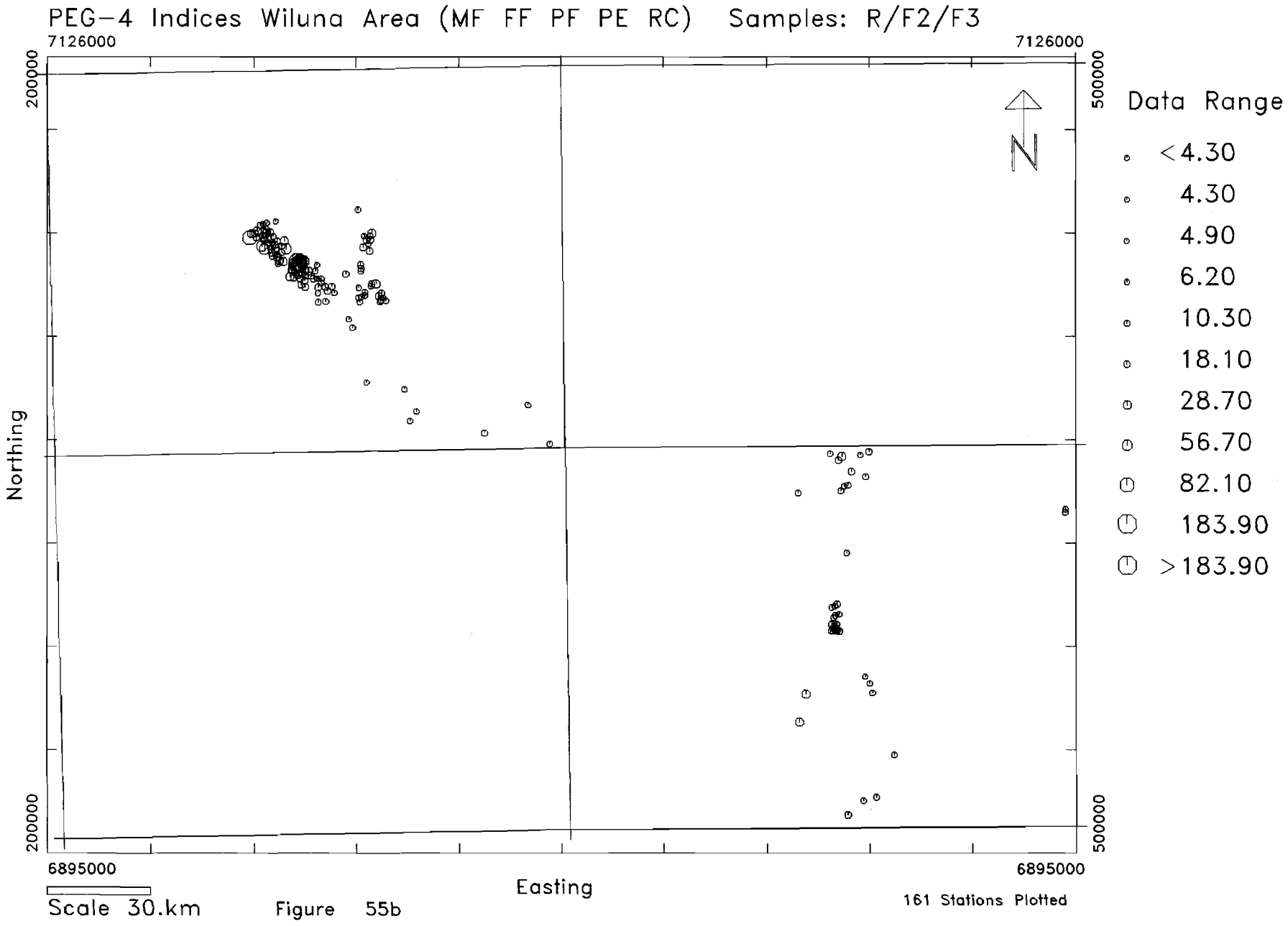
PEG−4 Indices Wiluna Area (MF FF PF PE RC) Samples: R/F2/F3
7126000
7126000
200000
500000
Northing
N
Data Range
< 4.30
4.30
4.90
6.20
10.30
18.10
28.70
56.70
82.10
183.90
> 183.90
6895000
6895000
Easting
Scale 30.km
161 Stations Plotted

Figure 55b

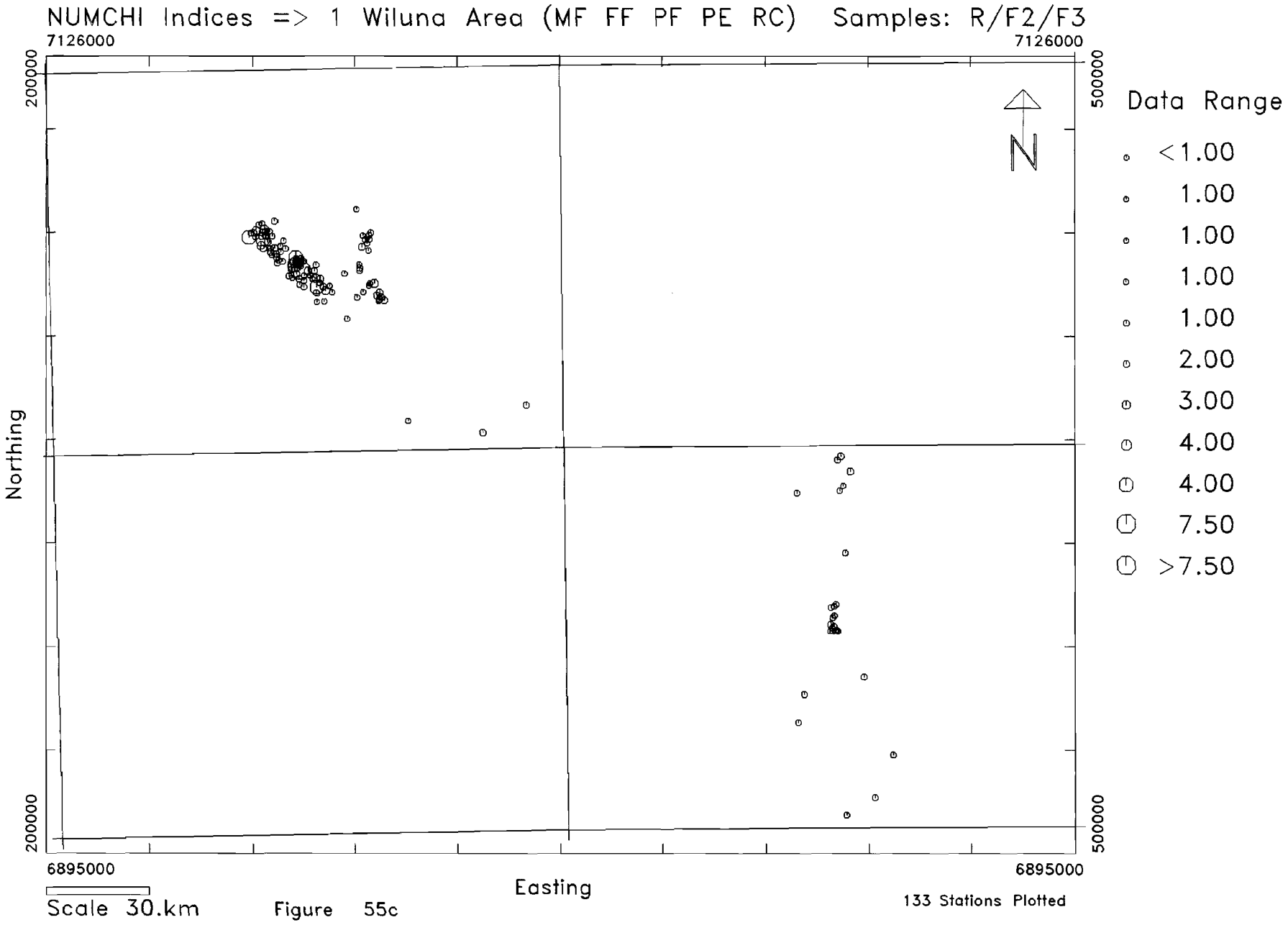
NUMCHI Indices => 1 Wiluna Area (MF FF PF PE RC) Samples: R/F2/F3
7126000
7126000
200000
500000
N
Data Range
<1.00
1.00
1.00
1.00
1.00
2.00
3.00
4.00
4.00
7.50
>7.50
Northing
200000
500000
6895000
6895000
Easting
Scale 30.km
133 Stations Plotted

Figure 55c

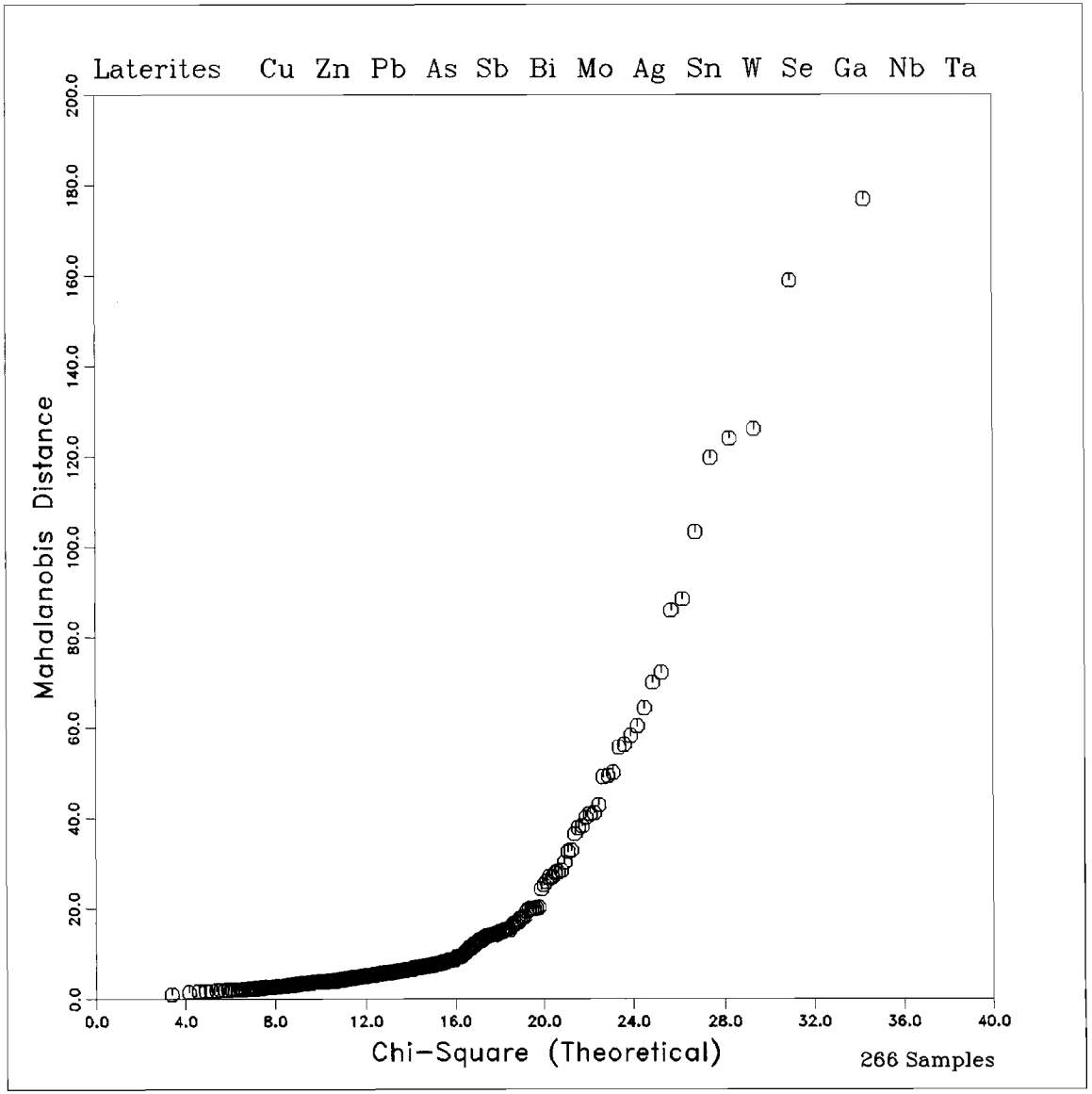
Laterites Cu Zn Pb As Sb Bi Mo Ag Sn W Se Ga Nb Ta
Mahalanobis Distance
0.0
20.0
40.0
60.0
80.0
100.0
120.0
140.0
160.0
180.0
200.0
0.0
4.0
8.0
12.0
16.0
20.0
24.0
28.0
32.0
36.0
40.0
Chi-Square (Theoretical)
266 Samples

Figure: 56a

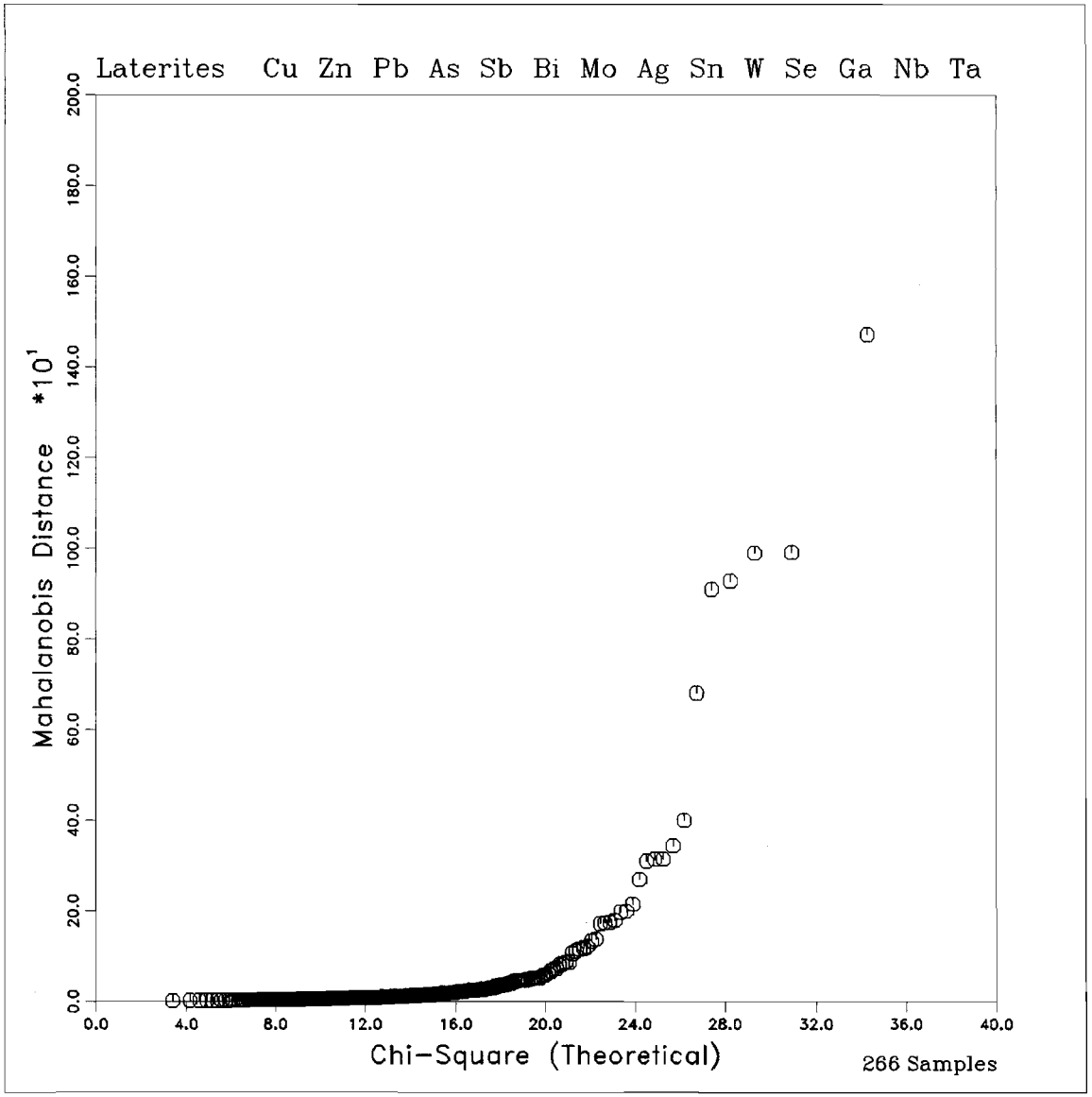
Laterites Cu Zn Pb As Sb Bi Mo Ag Sn W Se Ga Nb Ta
Mahalanobis Distance *10¹
0.0
20.0
40.0
60.0
80.0
100.0
120.0
140.0
160.0
180.0
200.0
0.0
4.0
8.0
12.0
16.0
20.0
24.0
28.0
32.0
36.0
40.0
Chi-Square (Theoretical)
266 Samples

Figure: 56b

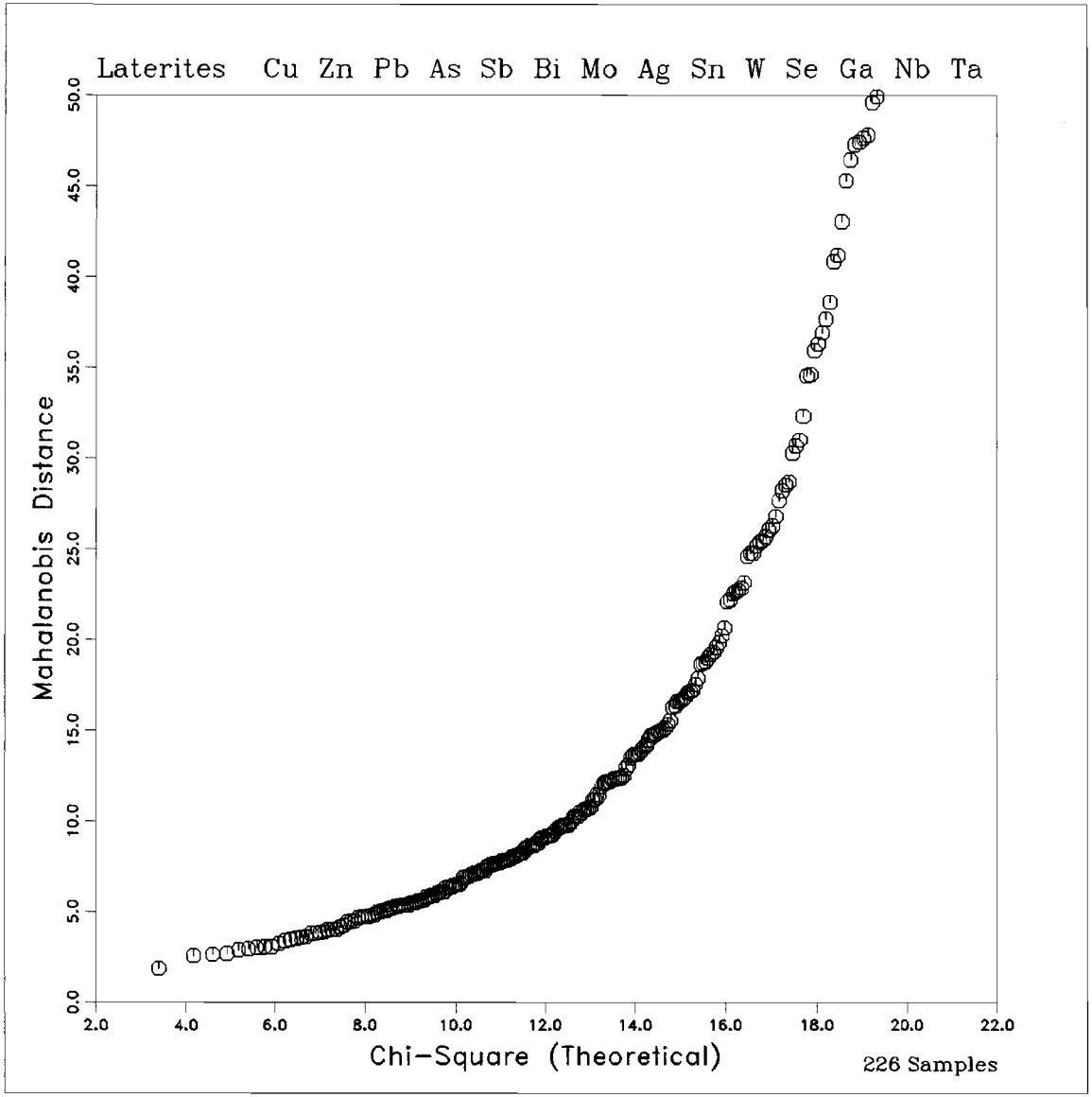
Laterites Cu Zn Pb As Sb Bi Mo Ag Sn W Se Ga Nb Ta
Mahalanobis Distance
0.0
5.0
10.0
15.0
20.0
25.0
30.0
35.0
40.0
45.0
50.0
2.0
4.0
6.0
8.0
10.0
12.0
14.0
16.0
18.0
20.0
22.0
Chi-Square (Theoretical)
226 Samples

Figure: 56c

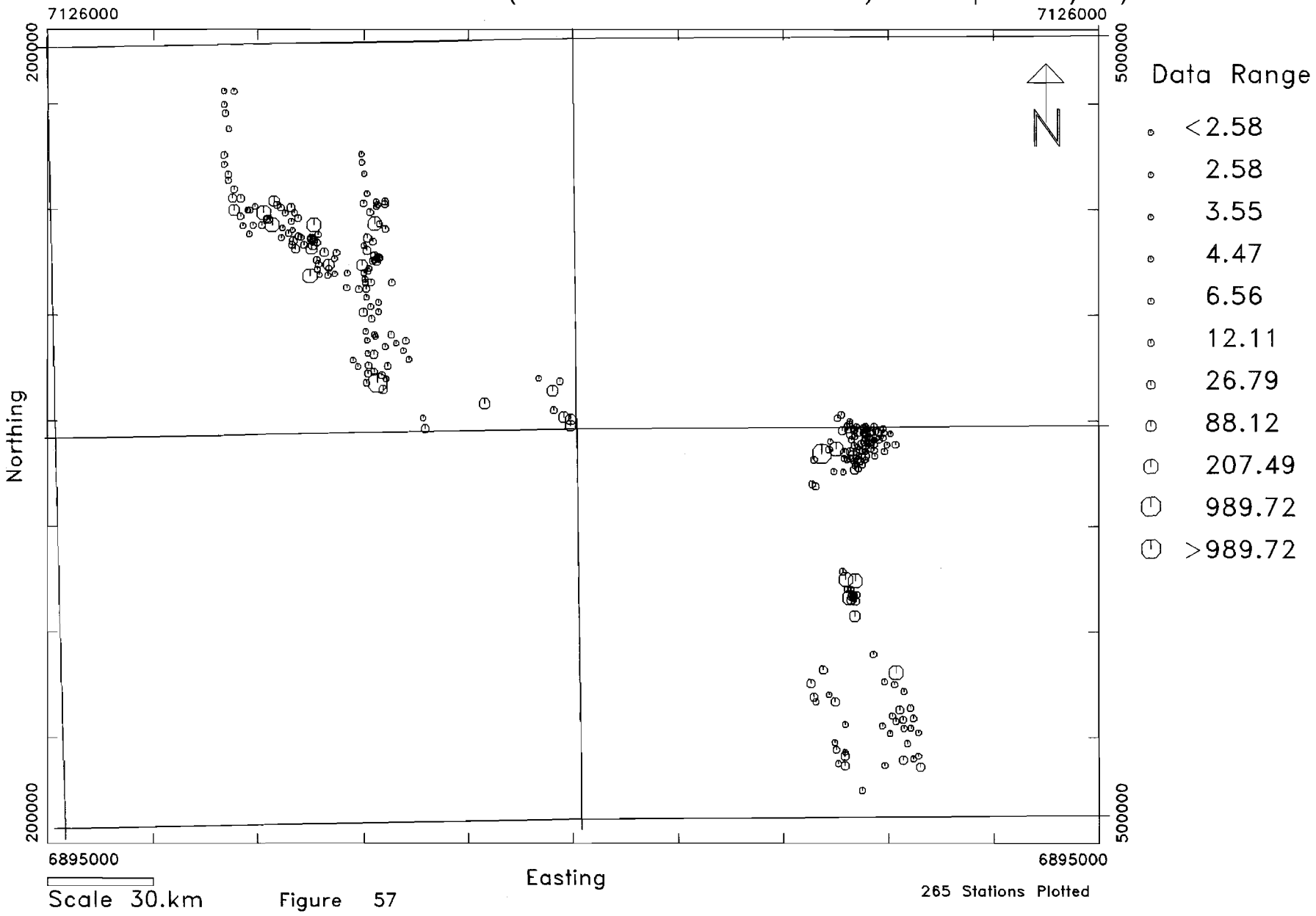
Mahalanobis Distances Laterites (LP CP LN CN PN VL MS) Samples: R/F2/F3
7126000
7126000
200000
500000
N
Data Range
<2.58
2.58
3.55
4.47
6.56
12.11
26.79
88.12
207.49
989.72
>989.72
Northing
200000
500000
6895000
6895000
Easting
Scale 30.km
265 Stations Plotted

Figure 57

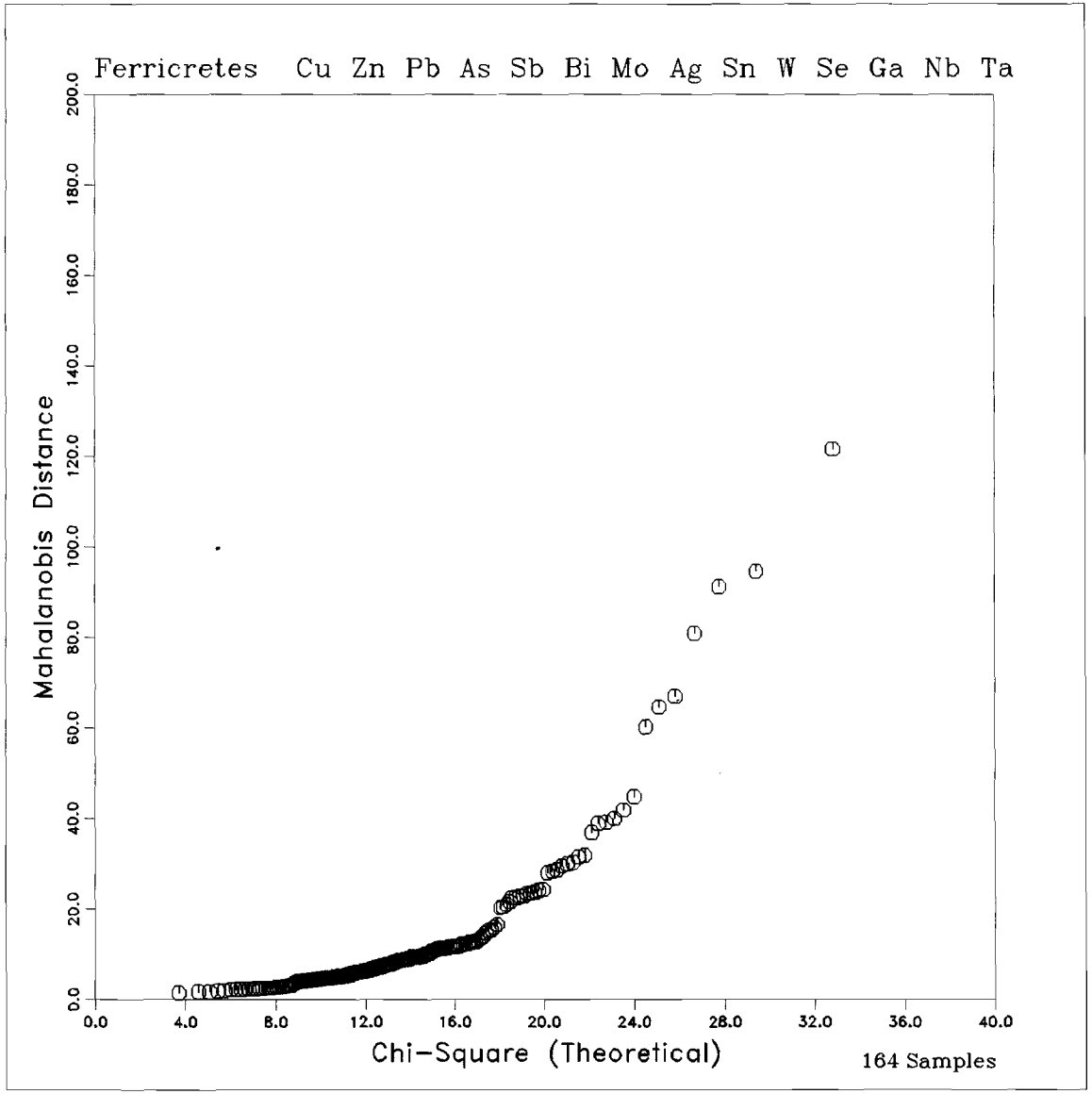
Ferricretes Cu Zn Pb As Sb Bi Mo Ag Sn W Se Ga Nb Ta
Mahalanobis Distance
0.0
20.0
40.0
60.0
80.0
100.0
120.0
140.0
160.0
180.0
200.0
0.0
4.0
8.0
12.0
16.0
20.0
24.0
28.0
32.0
36.0
40.0
Chi-Square (Theoretical)
164 Samples

Figure: 58a

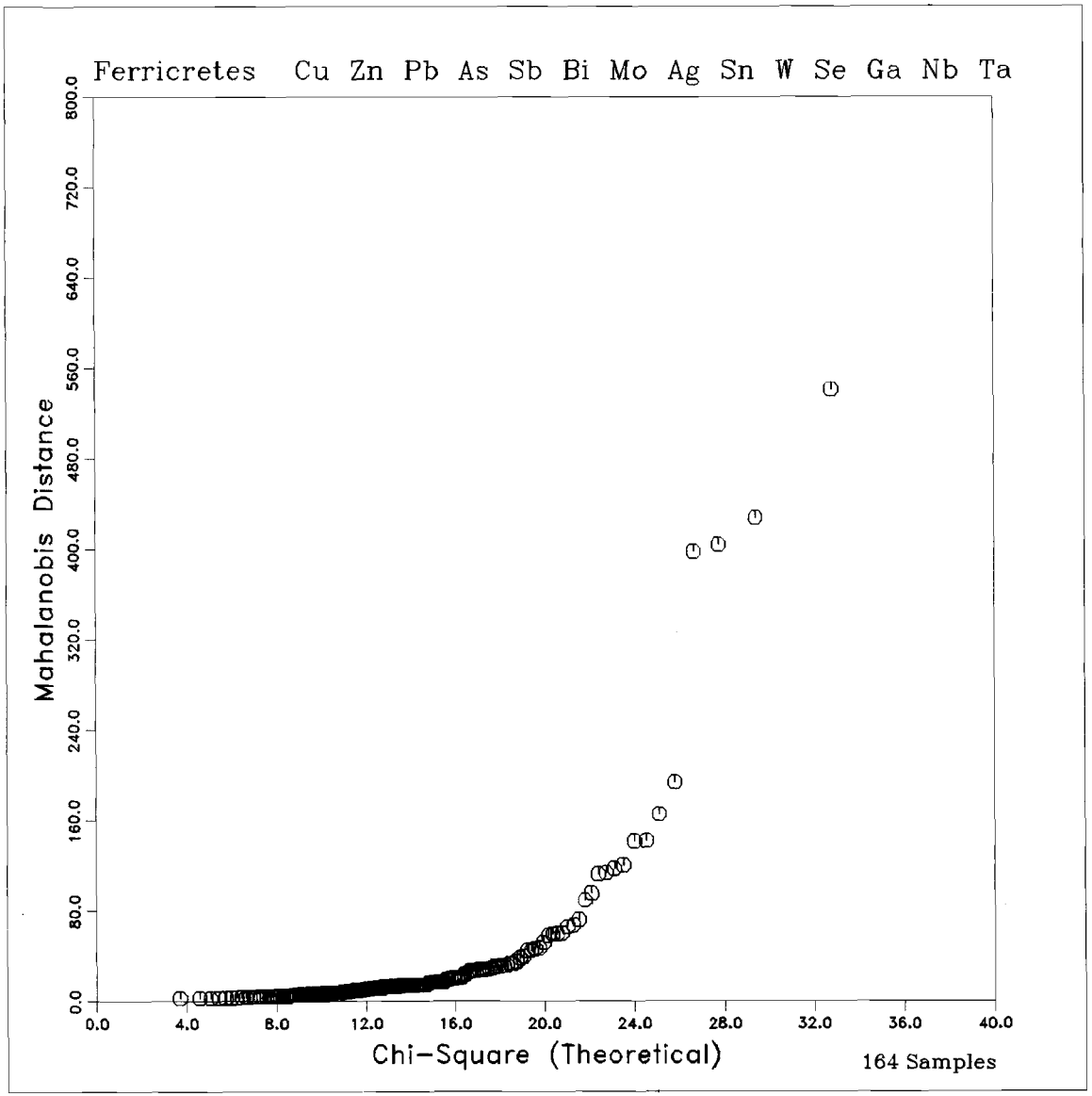
Ferricretes Cu Zn Pb As Sb Bi Mo Ag Sn W Se Ga Nb Ta
Mahalanobis Distance
0.0
80.0
160.0
240.0
320.0
400.0
480.0
560.0
640.0
720.0
800.0
0.0
4.0
8.0
12.0
16.0
20.0
24.0
28.0
32.0
36.0
40.0
Chi-Square (Theoretical)
164 Samples

Figure: 58b

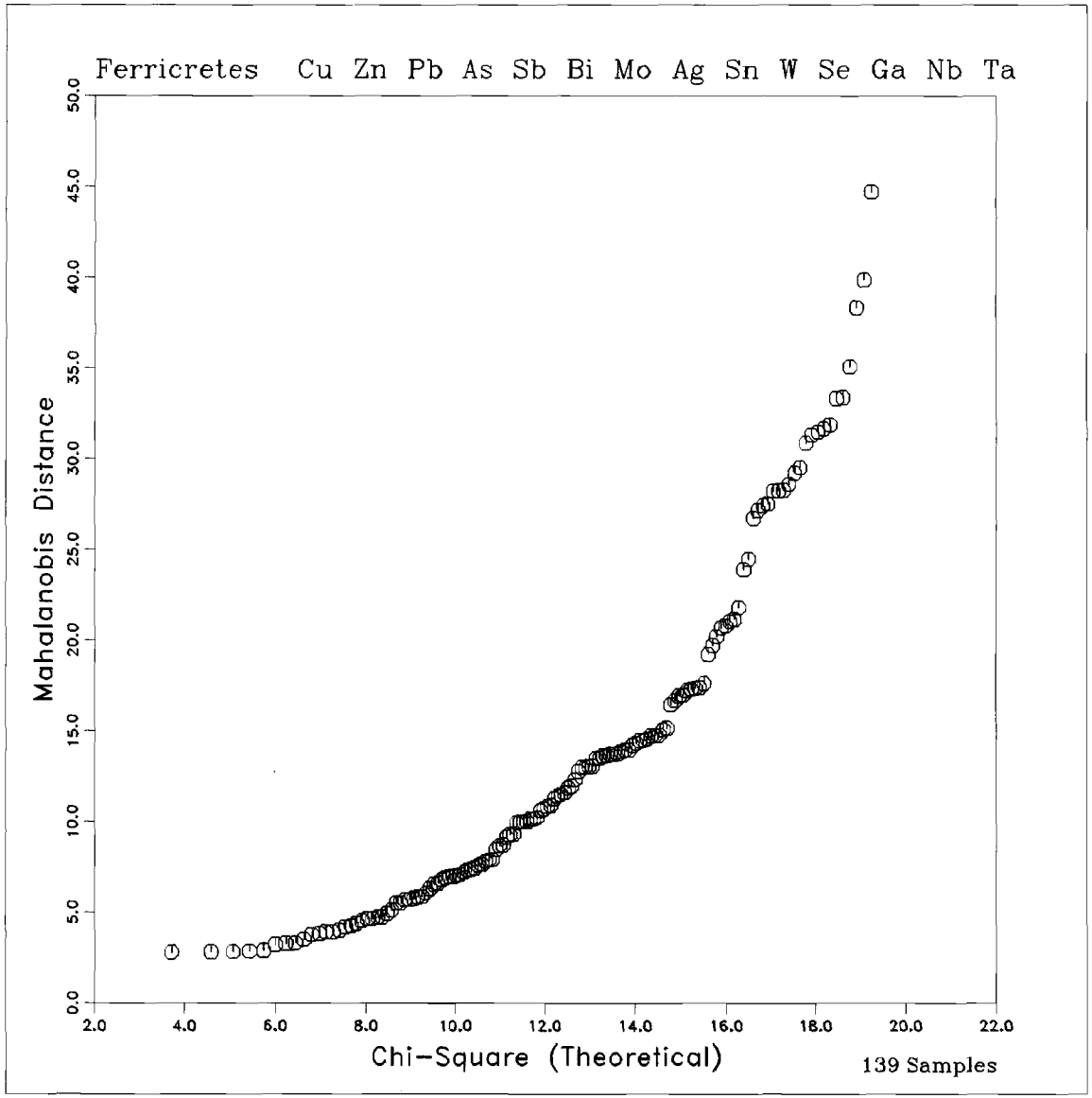
Ferricretes Cu Zn Pb As Sb Bi Mo Ag Sn W Se Ga Nb Ta
Mahalanobis Distance
0.0
5.0
10.0
15.0
20.0
25.0
30.0
35.0
40.0
45.0
50.0
2.0
4.0
6.0
8.0
10.0
12.0
14.0
16.0
18.0
20.0
22.0
Chi-Square (Theoretical)
139 Samples

Figure: 58c

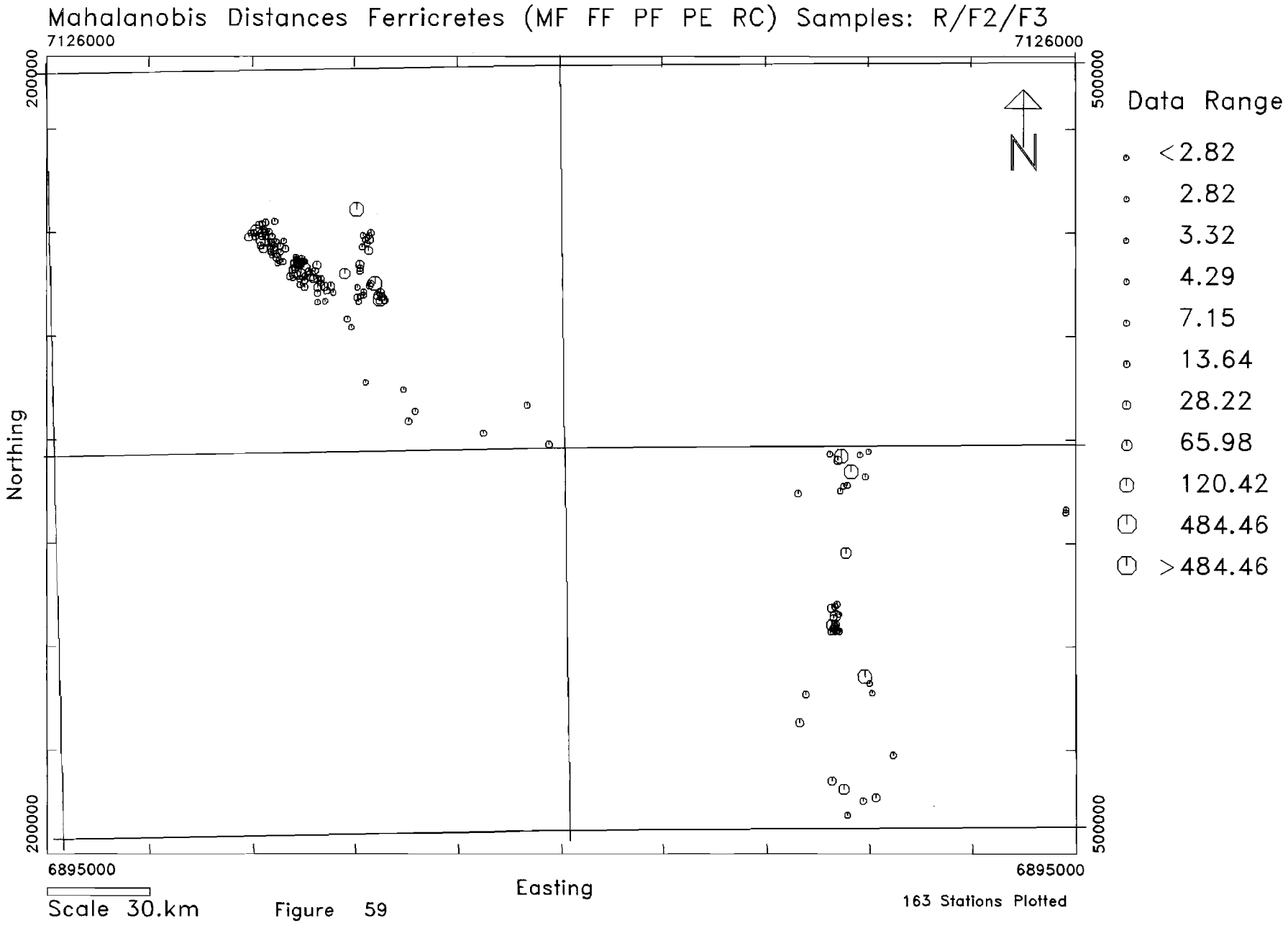
Mahalanobis Distances Ferricretes (MF FF PF PE RC) Samples: R/F2/F3
7126000
7126000
200000
500000
N
Data Range
< 2.82
2.82
3.32
4.29
7.15
13.64
28.22
65.98
120.42
484.46
> 484.46
Northing
200000
500000
6895000
6895000
Easting
Scale 30.km
163 Stations Plotted

Figure 59